NETHERLANDS INDIAN OCEAN PROGRAMME

MONSOONS AND COASTAL ECOSYSTEMS IN KENYA

editors
C.H.R. Heip,
M.A. Hemminga &
M.J.M. de Bie

Leiden 1995

PUBLISERIES VOLUME 5

NETHERLANDS INDIAN OCEAN PROGRAMME

MONSOONS AND COASTAL ECOSYSTEMS IN KENYA

Editors: C.H.R. Heip,
M.A. Hemminga &
M.J.M. de Bie

Published by
National Museum of Natural History
Leiden

on behalf of
Netherlands Geosciences Foundation
The Hague

1995

CRUISE REPORTS VOLUME 5

CIP-GEGEVENS KONINKLIJKE BIBLIOTHEEK, DEN HAAG

Monsoons

Monsoons and coastal ecosystems in Kenya / eds.: C.H.R. Heip,
M.A. Hemminga & M.J.M. de Bie. - Leiden : National Museum of Natural History. -
Ill., with ref. - (Cruise reports Netherlands Indian Ocean Programme,
ISBN 90-73239-29-X ; vol. 5)
Publ. on behalf of the Netherlands Geosciences Foundation (GOA). -
ISBN 90-73239-28-1
Subject headings: monsoons ; Indian Ocean / oceanography ; Kenya / coastal ecosystems

Editing: C.H.R. Heip, M.A. Hemminga & M.J.M. de Bie
Final editing: J. van der Land, National Museum of Natural History, Leiden
Lay-out and cover design: F.J.A. Driessen, National Museum of Natural History, Leiden
NIOP-logo: H. Hobbelink, Netherlands Institute for Sea Research, Texel
Photographs: SOZ (F. Hoogervorst)
Printing: Ridderprint, Ridderkerk

This report was published on behalf of the Netherlands Geosciences Foundation (GOA)
(a merger of the Netherlands Marine Research Foundation (SOZ) and some other
organizations), P.O. Box 93.120, 2509 AC The Hague, the Netherlands.

CONTENTS

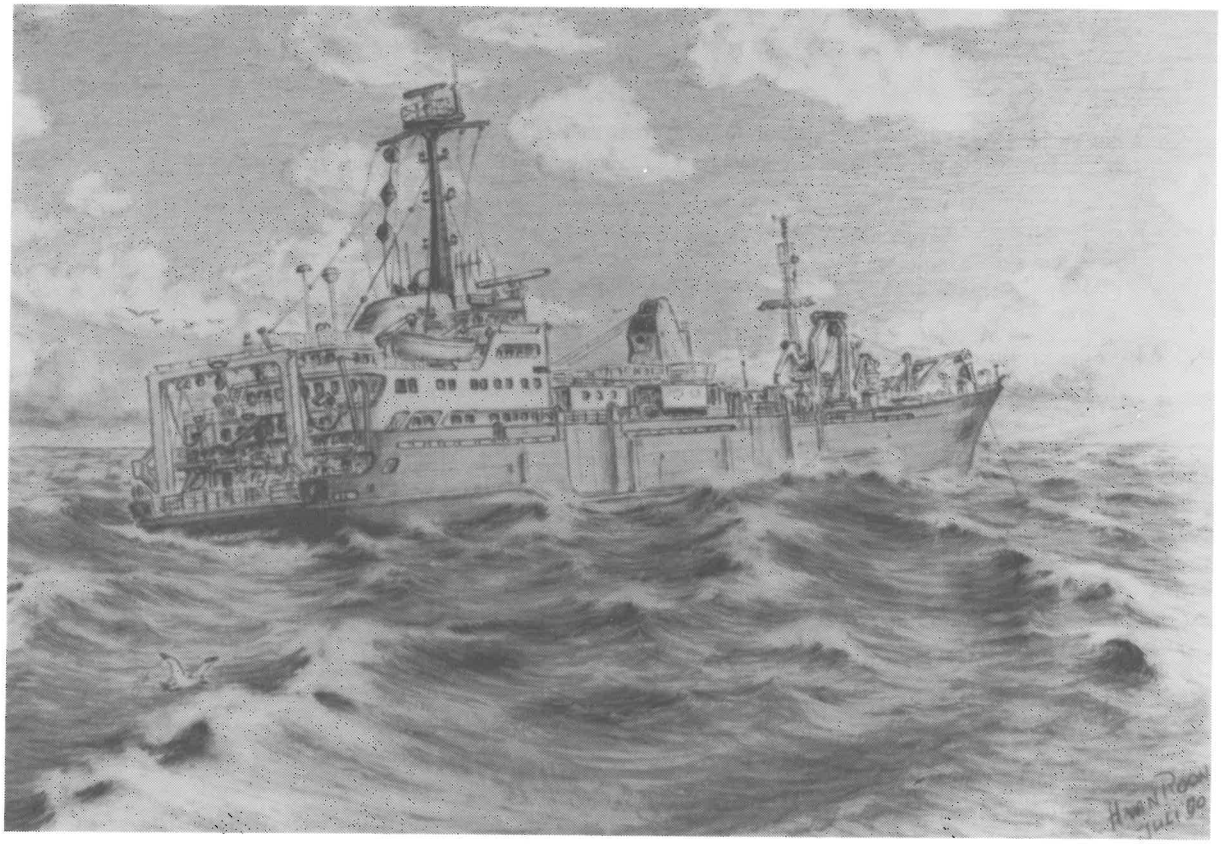

THE NETHERLANDS INDIAN OCEAN PROGRAMME

Jacob van der Land & Jan H. Stel
Chairman & Secretary Indian Ocean-Committee

Since the late seventies marine, but especially blue ocean research was stimulated by the Netherlands government. During the last fifteen years our Government through the Netherlands Geosciences Foundation (GOA) and its predecessors the Netherlands Marine Research Foundation (SOZ) and the Netherlands Council of Oceanic Research (NRZ), allocated some hundred million Dutch guilders to support this development. In a recent policy evaluation it is demonstrated that the objectives set by the Government are met. By this the Netherlands' blue ocean research is brought onto the European scene.
The execution of the Snellius II Programme in the mid eighties and the present Indian Ocean programme (1990-1995) were instrumental in reaching these goals. The fast developments of the last decade are reflected in the wide variety and quantity of equipment on board the Dutch research vessel *Tyro* during the expedition phase of the programmes mentioned above. As a rule these programmes are divided in a planning and an elaboration phase prior to and after the research expedition.
During the planning phase the research proposals of Kenyan, Pakistani and Seychellois scientists were integrated with those of the Dutch and brought back to realistic proportions. The central theme of the Indian Ocean programme is Global Change. This multidisciplinary research theme fits very well in a number of international research activities such as the International Geosphere-Biosphere Programme (IGBP), the Joint Global Ocean Flux Study (JGOFS) and programmes on biodiversity. The overall scientific objective of the programme is the study of the effects, on different spatial and temporal scales, of the monsoon on the marine ecosystem in the area.
The planning phase was followed by the execution phase (May 1992 - April 1993) during which onboard training was given. Transfer of scientific knowledge and assistance in education and infrastructure building are objectives of the programme. Junior scientists and technicians of countries involved also were given an opportunity to study at Dutch research institutes.
Dutch scientists gave guest lectures before, during and after the expedition in several countries. A special regional training course was organized in Mombasa in cooperation with the Kenya Marine and Fisheries Research Institute (KMFRI). A detailed description of the programme is given in the "Scientific Programme Plan of the Netherlands Indian Ocean Programme 1990-1995". An overview of the projects is given in Table 1. The research areas covered are given in Figure 1.
The expeditions were organized by the Netherlands Marine Research Foundation (since January 1, 1994

Table 1. Overview of the Netherlands Indian Ocean Programme: projects and responsible scientists

Project A	Monsoons and coastal ecosystems in Kenya C.H.R. Heip & M.A. Hemminga, Centre for Estuarine and Coastal Ecology, Yerseke. In cooperation with the Kenya Marine and Fisheries Research Institute, Mombasa (E. Okemwa)
Project B	Monsoons and pelagic systems M.A. Baars, Netherlands Institute for Sea Research, Texel & S. van der Spoel, Institute for Taxonomic Zoology, University of Amsterdam
Project C	Tracing a seasonal upwelling J.E. van Hinte, Institute of Earth Sciences, Free University Amsterdam & Tj.C.E. van Weering, Netherlands Institute for Sea Research, Texel
Project D	Geology of the Arabian Sea C.H. van der Weijden & W.J.M. van der Linden, Marine Earth Sciences, University of Utrecht. In cooperation with the National Institute of Oceanography, Karachi. (A. Ali Khan)
Project E	Oceanic reefs of the Seychelles J. van der Land, National Museum of Natural History, Leiden & R.W.M. van Soest, Institute for Taxonomic Zoology, University of Amsterdam In cooperation with Seychellois institutes (Nirmal Jivan Shah & D.P. Boullé)

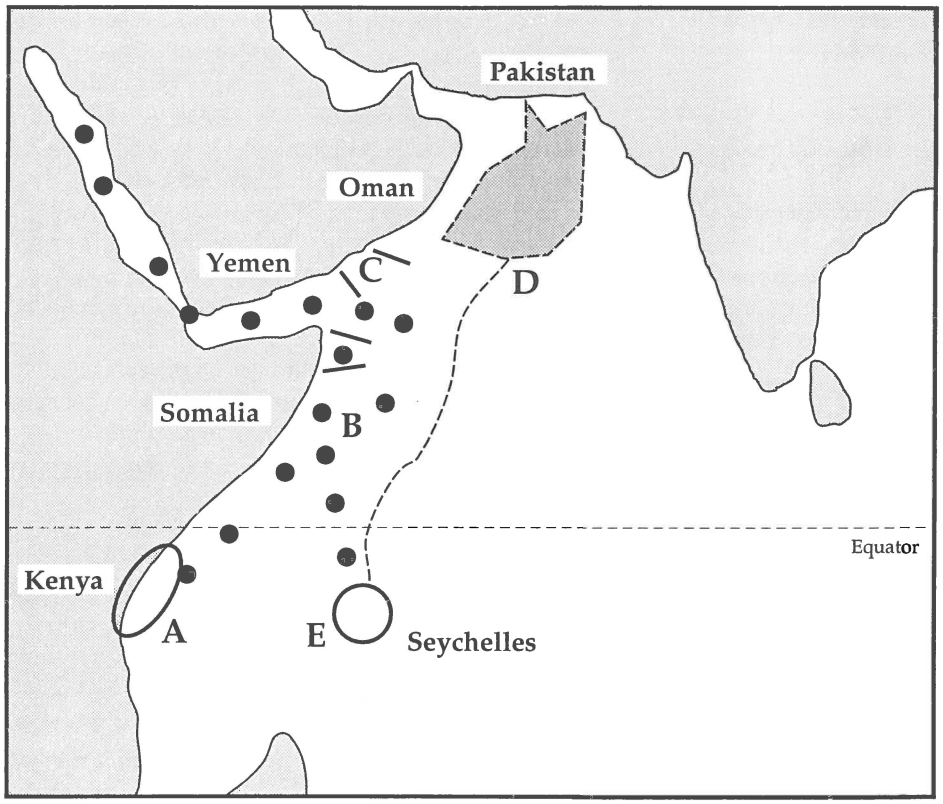

Fig. 1. Research areas covered during the Netherlands Indian Ocean Programme.

Table 2. Cruises of RV *Tyro* in 1992 and 1993

Leg	Ports	Periods	Areas
B0/C0	Port Said - Mombasa	21 May - 12 June 1992	Red Sea, Somali Basin (launch sediment traps)
A 1	Mombasa - Mombasa	18 June - 9 July 1992	Kenyan coast
B 1	Mombasa - Djibouti	12 July - 8 August 1992	Somali Basin, Gulf of Aden
C 1	Djibouti - Victoria	12 August - 4 Sept. 1992	Yemen/Oman, Somali Basin
D 1	Victoria - Karachi	8 Sept. - 26 Sept. 1992	Arabian Sea
D 2	Karachi - Karachi	4 Oct. - 25 Oct. 1992	Northern Arabian Sea
D 3	Karachi - Mombasa	27 Oct. - 16 Nov. 1992	Arabian Sea
A 2	Mombasa - Mombasa	19 Nov. - 8 Dec. 1992	Kenyan coast
E	Mombasa - Victoria	11 Dec. 1992 - 9 Jan. 1993	Seychelles, Amirante Islands
B 2	Victoria - Djibouti	11 Jan. - 6 Feb. 1993	Somali Basin, Gulf of Aden, southern Red Sea
C 2	Djibouti - Djibouti	9 Feb. - 7 March 1993	Somali Basin (retrieval sediment traps) Yemen/Oman

Fig. 2. R.V. *Tyro* of the Netherlands Marine Research Foundation.

the Netherlands Geosciences Foundation). The responsibility for the execution of the expeditions was delegated to a special Indian Ocean Committee. SOZ appointed an operational coordinator at its office in The Hague and took care of the application of research permits, public relations, visa, travel arrangements, custom facilities and other administrative and logistic arrangements.

Research was carried out in the northwest Indian Ocean between May 1992 and April 1993 (Table 2). The operations thus covered two monsoons, being respectively the North-East Monsoon (November-March) and the South-West Monsoon (June-September) for the northern part of the Indian Ocean and the North-East Monsoon and the South-East Monsoon for the area south of the equator. During the SE-SW Monsoon storms are active in July and August.

The main part of the expedition phase was carried out on board the containerized Dutch RV *Tyro*. A land-based project was carried out in June-July 1992 in the coastal area of Kenya, for which a containerized laboratory facility was set up some twenty kilometres south of the Kenyan port Mombasa. During the expedition portcalls were made in Port Said (Egypt), Mombasa (Kenya), Djibouti (Djibouti), Victoria (Seychelles) and Karachi (Pakistan).

Besides the containerized laboratories a variety of oceanographic equipment was available on board the *Tyro*. Maintenance and repair of the equipment as well as the technical assistance on board was sub-contracted to the Netherlands Institute for Sea Research (NIOZ). A few participating research institutes installed their own special instruments aboard ship.

All data and specimens collected during the programme are being shared according to formal agreements between participating countries. Two years after the completion of the project all data will be released to interested third parties, including oceanographic data centres. From then anyone may freely use the information, provided the data is properly acknowledged in publications with reference to the scientist responsible. Any scientist whose data is being used will be offered a co-authorship in case he/she has made a significant contribution.

Shipboard reports were prepared at the end of each cruise, containing pertinent information on the activities, data and specimens obtained during the cruise, reports on lost and damaged equipment and, whenever possible, preliminary results. Of course these reports had a provisional lay-out and were distributed in a limited number only.

The series of Cruise Reports still contain preliminary

results but they are being made available to all interested in the expeditions or the area. We wanted to inform the scientific community about the work done and some of the results as soon as possible. Moreover these reports may serve as works or reference for the publications on special subjects. They contain much background information that has to be omitted from articles in scientific journals.
This particular cruise report gives an outline of one of the five research projects of the Indian Ocean Programme: *Monsoons and Coastal Ecosystems in Kenya.*

publications

Netherlands Indian Ocean Programme 1990/1995: Scientific Programme Plan; 1-118. The Hague, November 1991.

Partners in Science: Kenyan-Dutch Co-operation in Marine Research - I, 1992-1993: 1-74. Mombasa, May 1992.

Partners in Science: Pakistani-Dutch Cooperation in Marine Research - I, 1992-1993: 1-68. Karachi, August 1992.

Partners in Science: Seychelles-Dutch Cooperation in Marine Science, 1992-1993: 1-68. The Hague, December 1992.

Wiese, K., J.H. Stel & F. Hoogervorst, 1994. De Halve Oceaan. Op expeditie tussen Azië en Afrika: 1-105. Uitgeverij Foto, Leusden.

Wiese, K., J.H. Stel & F. Hoogervorst, 1994. The Third Ocean. An expedition between Asia and Africa: 1-105. Foto Publishers, Leusden.

Leendert Blok, captain of r.v. *Tyro* for many years, deceased 6 March 1995.

1. INTRODUCTION

The coastal zone occupies a relatively small part of the oceans but contains a complex set of habitats including low-lying river plains, estuaries and deltas, lagoons and creeks, beaches, salt marshes, rocky shores and coral reefs, the drowned shelves and the shelf-edges and even parts of the continental slope. It is a critical interface between land and ocean because it controls the anthropogenic and terrestrial fluxes and fates of chemicals and biological production to and from the open ocean (Mantoura *et al.*, 1991). It is estimated that coastal zones contribute about 25 % of the global biological production, 80 % of the global carbon burial and 90 % of the global carbon mineralisation (LOICZ Implementation Plan). To better quantify the role of coastal zones in the carbon cycle and the effects of human activities, it is necessary to have far better estimates of production and consumption processes over a large variety of coastal zone types than exist today.

The magnitude of the flux of organic matter from the coastal zone to the open ocean, which may constitute a significant sink of carbon, is uncertain. Terrestrial and littoral ecosystems may be a direct source of organic matter or may increase coastal production by exporting nutrients. Coastal areas where freshwater input is small and where no upwelling exists, are generally considered to be of little importance in the global carbon cycle and most attention in recent years (and during the Netherlands Indian Ocean Programme) has gone to the high productivity areas. However, these areas do not form the largest part of the world's coastline and taken together the 'quiet' coasts of the world may also be of great importance for the carbon fluxes.

The East-African coast south of Somalia is such an area where it seems unlikely that significant amounts of carbon are produced *in situ* or transferred from the land to the oceans. However, it borders the western Indian Ocean over several thousands of kilometers. The shelf is often very narrow and as an export system for the open ocean these coastal waters may be more important than coastal systems with a broad productive shelf where much of the organic material produced will be used and remineralised on the shelf itself. The northwestern Indian Ocean (Somalia and the Arabian Peninsula) is characterized by strong, seasonal fluctuations of biological productivity caused by wind-induced upwelling, but the unique reversal of the currents that is driven by the monsoon also occurs along the Kenyan coast until about 2°S.

The Kenyan coast is of paramount importance for the economy of the country, especially due to the rapidly increasing tourism. The natural values are outstanding: the intertidal areas are wintering grounds for palearctic birds and local populations of several sea turtles, including the leatherback, and the dugong are present. A number of marine parks have been created and are well managed. These parks generate revenue for the local population and the country. Human impact on the coast is rapidly increasing. Overfishing on the coral reefs (parrot fish and especially triggerfish) has lead to extension of sea urchins that predate on the living coral and enhance erosion of the reef. The close proximity of touristic infrastructure leads directly and indirectly to increased human pressure through an increase in fisheries and exploitation of corals and shellfish for ornamental purposes. The mangrove areas are under increasing human pressure as well, as a consequence of wood exploitation. The wood is used for the production of tannins, as fire wood and for the construction of houses: there exists a centuries old trade between Lamu and Jemen for this material. In some cases mangroves have been cut for development of tourism and construction of ponds for aquaculture.

Deforestation and cattle ranching in the interior of Kenya have lead to an important increase of the sediment load of the rivers. The effects of sedimentation of silt on the reefs are especially visible in an extension of the seagrass-beds (Giesen & van der Kerkhof, 1984) and a reduction of the corals (Blom *et al.*, 1985; Van Katwijk *et al.*, 1989) near the mouth of the Sabaki river at Malindi. Effects on the productivity of the coastal waters have not been studied yet. Such effects may be 'positive' as well as 'negative': import of nutrients and oligo-elements may increase productivity but the increased turbidity of the water may decrease it. With the two main river, the Sabaki and the Tana, pollutants from the drainage basins may reach the Indian Ocean. Although the general level of pollution is expected to be low, there may be problems with insecticides and pesticides. Local pollution around Mombasa may threaten the two largest creeks of the country, surrounding the fossil coral island on which Mombasa, the largest harbour of East Africa, is build. Both Kilindili and Tudor creeks are used for the discharge of domestic and industrial waste.

the Indian Ocean and the East-African coastal waters

The Indian ocean has a surface area of approximately 50 million km^2 and an average depth of 3800 m. A characteristic feature of the hydrography of this ocean is the seasonal switch in flow directions caused by the monsoon winds. These winds are influenced by the low pressure Inter-tropical Convergence Zone (ITCZ).

The ITCZ moves to the north during the northern hemisphere summer due to the low pressure belt then existing on the Asian continent. From November until March the NE monsoon (NEM) is blowing, from May until September the wind direction is mainly southeast over the Indian Ocean (SEM) but mainly southwest in Kenya.

The permanently west-flowing South Equatorial Current at 6°S to 20°S is partly diverted along the eastern Madagascar coast becoming the Madagascar current. On approaching the mainland the SEC splits to form two coastal currents: the East African Coastal Current (EACC) to the north and the Mozambique Current to the south. That current later joins the Madagascar Current to form the Agulhas current.

During the SEM, the EACC has a high flow velocity, up to 2 $m.s^{-1}$, particularly in the upper 200 m of the water column; water transport may be up to 65 million m^3/s. This current causes the upwelling along the Somali coast which is among the most extensive ones in the world, and occurs in early summer. Upwelling is not restricted to the Somali coast and Ekman-type upwelling along the Arabian coast is also very extensive. According to CZCS images a maximum in surface chlorophyll is found there in August-September. Another more irregular upwelling occurs near the northern Kenyan coast and CZCS images showed a maximum chlorophyll content there in January, during the NE monsoon, which may be associated with river runoff after the long rains. This also happens during the NE monsoon at the northern ends of the Arabian Sea and Bay of Bengal. In the Somali region the primary productivity during the NEM is roughly equivalent to that of the Sargasso Sea, while during the SEM areas of upwelling have rates of primary production among the highest in the world's ocean. The high productivity of the surface waters during the NEM in Somalia is not reflected in higher organic matter in the sediments. This is because the shelf is narrow and offshore currents are strong. The organic matter is probably not recycled but transported into the interior of the northwestern basin and deposited at depth.

The differences in currents, up and downwelling, water temperatures and nutrients cause a north-south dichotomy between ecosystems along the coast. The southern section (Tanzania-Kenya) is dominated by coral reefs and benthic productivity associated with low-nutrient water. The northern sector (Somalia) has cooler nutrient-rich water and a greater predominance of planktonic productivity.

the Kenyan coast

The coastal ecosystems in Kenya consist of: (1) a shallow shelf area (2) coral reefs (fringing reefs) along the entire coastline, with extensive areas of seagrass beds on the more sheltered parts of the backreefs and in lagoonal areas; (3) mangroves on the shores of the brackish parts of rivers and creeks along the coast; also seagrass beds can be found here. On many places along the Kenyan coast, substantial seepage of freshwater occurs; as a result brackish water is often found in areas of seagrass beds. The system of reefs and seagrass beds is interrupted in a number of places. Two large rivers debouch into the Indian ocean: the river Tana in the north and the river Galana-Sabaki approximately in the middle part; both spring from the volcanic highlands around Mount Kenya and the Aberdare Range. Many smaller rivers from the neighbouring highlands run through the fossil coral beds which are present on many places along the coast, forming creeks with extensive mangrove growth. This is for instance the case near Lamu, Katungu, Kilifi, Mtwapa, Mombasa, Gazi and Shimoni.

Along the Kenyan coast the NEM season lies between November and March, the SEM season between April and October. The SE monsoons are characterized by high cloud, rain, wind energy and decreased temperatures and light. During the NE monsoons the situation is reversed. Due to the currents the major downwelling area and associated low nutrient waters are along the coast of Tanzania and southern Kenya. Downwelling occurs throughout the year but is strongest during SEM when the current speeds are greatest. Upwelling occurs along northern Somalia during SEM but breaks down during NEM as the current direction switches. During NEM currents leave the coast from northern Kenya where upwelling may occur.

The continental shelf is narrow and the ocean becomes very deep close to the Kenyan coast. There was no information on the benthic ecosystems beyond the reefs and also with respect to the pelagic domain only limited information was available prior to the Netherlands Indian Ocean Programme: the classical picture is that these areas combine a low productivity with a high diversity but there is evidence of upwelling and higher productivity in northern Kenya during winter. The interactions between the off-shore and coastal areas and the impact of the monsoon on these interactions were unknown. Along the Kenyan coast the long rains normally occur in April and May whereas the short rains occur in October and November, at times of intermonsoon. During the rainy months terrigenous material enters the Indian ocean, because of the high discharge of the rivers. Especially the rivers Tana and

Galana-Sabaki transport large quantities of silt originating from the interior but exactly how much material is introduced into the ocean and where it goes is unknown; consequently the sedimentology of the Kenyan coastal zone is largely unknown as well.

Because the tidal amplitude is rather large, approximately 4 m near Mombasa, there is an extensive intertidal zone between the reefs and the coast on many places; the substrate in this zone mainly consists of carbonate sands derived from eroding reefs. The productivity of these back-reefs is determined predominantly by the presence of seagrasses and microscopic benthic algae. In the estuaries and in the smaller creeks an extensive brackish water zone is often found; the residence time of the water in these systems is generally short. The mangrove ecosystem, characteristic of these silty brackish transition zones, mainly consists of woody plant species associated with a characteristic fauna and flora. The salinity gradient resulting from the mixing of outflowing river water and the incoming sea water, regulates the presence of the various mangrove plant species. The system is an open one, with input of nutrients from the land and export of organic material to the sea. This organic material originates from a complex detrital food chain and is an important source of energy for numerous brackish and marine organisms (oysters and other bivalves, peneid shrimps and crabs, mullets and other fish species). Mangroves are nursery areas for several commercially exploited species.

projects

The NIOP in the Kenyan coastal waters consisted of two main projects, one based on board *Tyro* to study processes on the shelf and one land-based in Gazi Bay to study the coastal processes.
In the ship-based research programme, the functioning of the pelagic and benthic systems of the open ocean water of the Kenyan shelf as influenced by the monsoon, was the central issue. The coastal project was complementary to this programme and focused on the adjacent mangrove, seagrass and coral reef systems. These marine ecosystems are connected by the tidal water which carries both abiotic and biotic elements to and from the systems. The relation between mangroves, seagrass beds and reefs (in terms of dissolved nutrients- and seston fluxes and shuttle movements of fish) was the central theme of the land-based project. Very little is known concerning the interlinkages between the coastal ecosystems in the East African region; nonetheless, this information is indispensable for a rational management of the coastal ecosystems and their resources.

Within the framework of the coastal programme, attention was also given to the emission of greenhouse gases by the mangrove sediments. Quantitative data on the emission of these gases by tropical wetlands are scarce, and more data are needed to improve the estimates for emission of greenhouse gases by natural wetlands on a global scale.

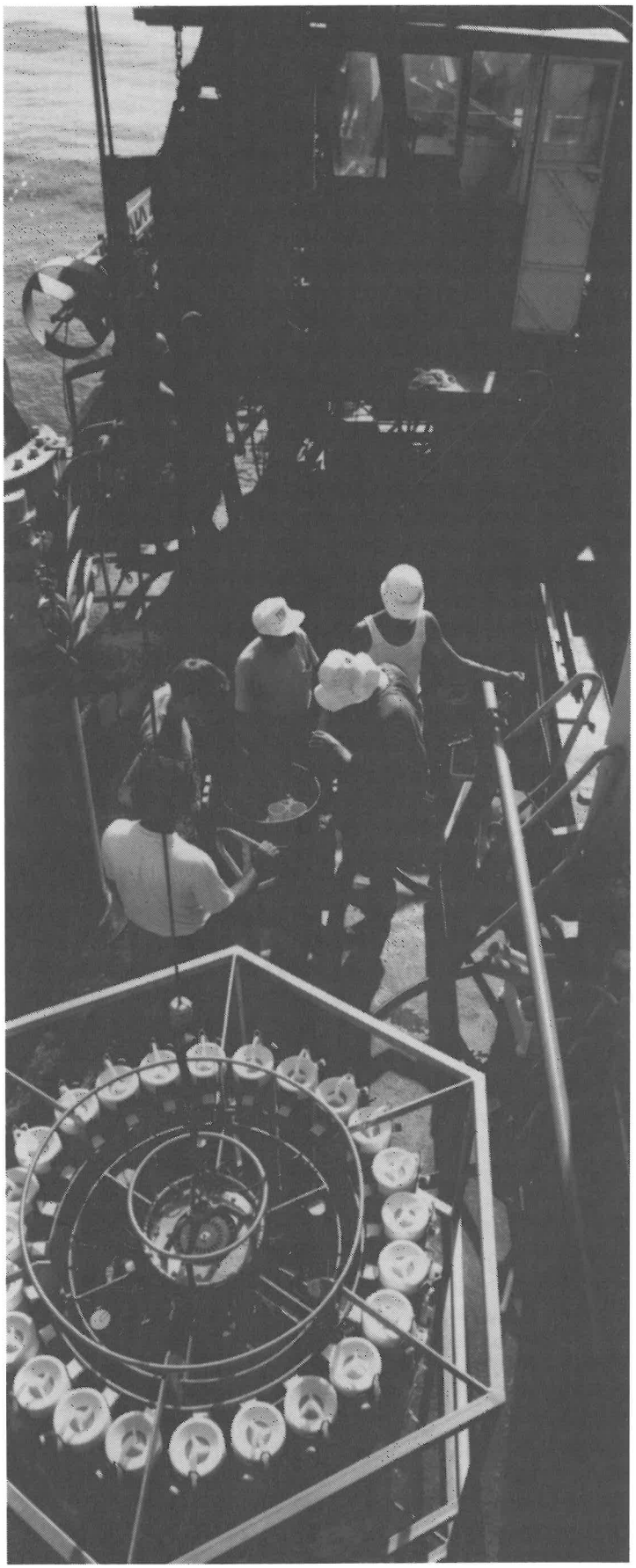

2. REPORT ON THE TWO CRUISES OF R.V. TYRO

2.1. PARTICIPANTS AND INSTITUTES

participating scientists and technicians

Leg A1

Prof.Dr. C.H.R. Heip, chief scientist, NIOO
Dr. M.M. Nguli, co-chief scientist, KMFRI

Dr. N. Goosen, NIOO, bacterial metabolism
J. Peene, NIOO, N_2-fixation
P. van Rijswijk, NIOO, zooplankton
M.J.M. de Bie, NIOO, bacterial metabolism
Dr. J. Kromkamp, NIOO, primary production
J. Sinke, NIOO, nutrients
J. van Ooijen, NIOZ, nutrients
S. Mengesha, VUB, nitrogen

J. Mwaluma, KMFRI, zooplankton
P. Wawiye, KMFRI, phytoplankton

Dr. J.M. Everaarts, NIOZ, heavy metals and organochlorines
G.C.A. Duineveld, NIOZ, benthos
E. Berghuis, NIOZ, benthos
T. Tahey, NIOZ, benthic metabolism
Dr. A. Rowden, PML, benthos

J. Abuodha, Moi University, sedimentology

B. Koster, NIOZ, electronics
M. Laan, NIOZ, electronics

J. Schilling, NIOZ, technics
J.J. Blom, NIOZ, technics
W. Polman, NIOZ, technics
E.J. Nieuwpoort, NIOZ, technics

B. Guillén, NNM, camera

Leg A2

Prof.Dr. C.H.R. Heip, chief scientist, NIOO 1/12 - 8/12
Dr. J. Everaarts. chief scientist, NIOZ 20/11 - 1/12
Dr. M.M. Nguli, co-chief scientist, KMFRI

Dr. N. Goosen, NIOO, bacterial metabolism
J. Peene, NIOO, N_2-fixation
P. van Rijswijk, NIOO, zooplankton
E. van Ham, NIOO, bacterial metabolism
Dr. J. Kromkamp, NIOO, primary production
J. Sinke, NIOO, nutrients
J. van Ooijen, NIOZ, nutrients
S. Mengesha, VUB 1, nitrogen
L. Zhu, VUB 2, zooplankton
J. Mwaluma, KMFRI, zooplankton
P. Gittui, KMFRI, phytoplankton

Prof.Dr. P.A.W.J. de Wilde, NIOZ, benthos
G.C.A. Duineveld, NIOZ, benthos
M.S.S. Lavaleye, NIOZ, benthos
T. Tahey, NIOZ, benthic metabolism

W. Shijeti, Moi University, sedimentology

J. Nieuwenhuis, NIOZ, electronics
M. Laan, NIOZ, electronics

E.B.M. Bos, NIOZ, technics
M. Wijsman, NIOZ, technics
W. Polman, NIOZ, technics
E.J. Nieuwpoort, NIOZ, technics

participating institutes

NIOO = Netherlands Institute of Ecology, Centre for Estuarine and Coastal Ecology, Vierstraat 28, 4401 EA Yerseke, NL.

NIOZ = Netherlands Institute for Sea Research, PO Box 59, 1790 AB Den Burg, NL.

VUB1 = Free University of Brussels, Laboratory of Analytical Chemistry, Pleinlaan 2, B-1050 Brussels, Belgium

VUB2 = Free University of Brussels, Laboratory of Ecology and Systematics, Pleinlaan 2, B-1050 Brussels, Belgium

KMFRI = Kenya Marine and Fisheries Research Institute, P.O. Box 81651, Mombasa, Kenya

Moi University, Nairobi, Kenya

PML = Plymouth Marine Laboratory, Prosect Place, The Hoe, Plymouth, UK

NNM = National Museum of Natural History, PO Box 9517, 2300 RA Leiden, NL

2.2. CRUISE NARRATIVES

leg A1

Thursday 18 June
The vessel left Mombasa at 16.45 h. after a ceremony in which the Kenyan minister of Scientific Policy and the Netherlands' ambassador set it free. There was much 'couleur locale' with singing and dancing, even including a Swahili version of Haendel's Hallelujah. The minister and the ambassador had to wait about 45 minutes, but finally we sailed through Kilindili creek and the passage to Mombasa harbour to reach the Indian Ocean around 18.00 h.. Technicians then prepared the moorings while other participants installed the containers. The first meeting was at 21.00 h., where participants presented themselves and the programme for the next few days was discussed.

Friday 19 June
The current meters were installed at station 101 at a depth of 220 m. Station 101 was chosen slightly south of Mombasa. Everything went smoothly. There was some swell but the vessel remained stable. Since it appeared that there was only one inclinometer on board it was decided to leave it for use on the benthic lander which was going to be used during the next four cruises. The sediment trap was therefore installed at 1500 m instead of at 1000 m as originally planned, to have a little higher chance of an undisturbed series. Interpretation will be difficult if the series does not show some internal consistency, and even then. Setting of the sediment trap went again very smoothly.

Saturday 20 June
In the early morning we made a slow approach to the coast near Gazi Creek. The fringing reef was about two miles east of the vessel when we started working at about 85 m depth. It was decided to spend two days on the shallow station 103 at our southernmost transect. This proved to be a wise decision since many participants were still struggling with their equipment. It turned out that we needed two CTD-casts every time since the amount of water required is about 300 litres and an extra hour was necessary. Before lunch also the first box cores were taken,. Except for the first one they were excellent with mostly fine sand but on one occasion coral rock was hit. At around 17.00 h. the first bell jar was put overboard. Since the current was around three knots it was decided not to launch the benthic lander. After dinner a CTD-station at 300 m depth was sampled (st. 104).

Sunday 21 June
Beginning of the winter in the southern hemisphere. At 7 am the beam trawl was tried for about fifteen minutes but it contained only five coral stones when it was hauled on board, plus a hole in the net. The journalists Herbert Blankesteyn and Cees Wiese were brought ashore near the hotel Jadini Beach where the land programme had its base. We waited for about one hour at the opening in the reef before we were guided through it. After returning, with one of the crew members who came out of Mombasa hospital, the multinet was operated succesfully. It was decided to return to the bell jar since there was no reflection from the pole. After a long search the buoy was miraculously appearing again just 3 m alongside the *Tyro*. It has probably been hit by the very strong current (3-5 knots north). In the evening it appeared that the cooling system of the blue winch needed to be replaced.

Monday 22 June
We first tried to sample at 200 m but again the sediment was very hard. We then decided to skip this station altogether and go to 105 at 500 m. At this station a CTD cast was taken and the big box corer was launched. Jack Schilling and Jan Blom went ashore to replace the cooling of the blue winch. Sediments here are clayey and the first box was too full. The second launch was succesful. The second CTD-cast was till 200 m and arrived on deck near 11.30 h.. In the afternoon two large cores were taken for incubation. At 19.30 h. the benthic lander was launched succesfully, though the transponder was faulty and no signal was registered with this instrument. The second transponder worked well. The vessel steamed during the night to station 106 at 1000 m.

Tuesday 23 June
The programme started with two CTD casts, a deep one till the bottom and a 250 m one for water samples. After that two large box-cores were taken for incubation. Since the blue winch was still under repair it was decided to use the vertical net twice, once till 500 m and once till 100 m depth. At 13.00 h. a second series of water samples was taken and at 14.00 h. the vessel steamed to station 107 at 2000 m. We saw many flying fish in front of the vessel and one booby. The station was reached around 18.30 h. and a deep CTD-cast was taken on JGOFS standard depths. At 2.00 h.0 a large box-core was launched that returned on deck near 21.00 h.. It was divided into four parts, for Jan Everaarts, Joseph Abuodha, Ashley Rowden and Gerard Duineveld.
Jan Blom had finished making a new cooling unit for the blue winch and tests were promising. Problems with electrical tension remained; container 44 with the central computers had no air-conditioning anymore.

Wednesday 24 June
During the night we sailed back to 105 for two box-cores. Around 13.30 h. the benthic lander was approached, localized and peeped to the surface. The apparatus was then brought aboard safely around 16.00 h.. The blue winch was repaired and the multinet was used. The ship then sailed north to Malindi. The weather was cloudy with occasional rain.

Thursday 25 June
The whole day was spent sampling the Bay of Malindi. The CTD cable was cut, so sampling was started with box corers and the multinet. Water samples and CTD casts were only taken after lunch. A transect was made across the whole bay for nutrient analysis and sediments. This took most of the afternoon. In the evening a good spot for the benthic lander and bell jar were sought. The sediment of the bay proved to be very soft red muds in which it was difficult to take box-cores. There are many birds (terns, gulls and several flocs of pelicans) and we were visited by of a group of dolpins three times.

Friday 26 June
Another day of difficulties. The ship had a tank full of sea water that could not be explained and it was thought possible that a leak occurred. The operations with the bell jars and the landers, that had started at 06.00 h., were abruptly interrupted at 09.00 h. when the captain decided to prepare for return to Mombasa. Fortunately it appeared that there was either no hole in the hull or one that could be controlled, so the programme at the 50 m station 111 could be finished.

Saturday 27 June
In the morning the leak was localized and appeared to pose no real problems. Station 114 at 200 m was sampled and the benthic lander was posed down. In the afternoon we sailed to station 117 at 500 m where we remained for twenty hours to permit the plankton people to study a day-night cycle.

Sunday 28 June
The 20 hour cycle on station 117 was continued. In the afternoon we sailed back to 114 to collect the benthic lander. This was achieved without difficulties, although the response was negative for quite a few minutes. In the evening we were without air-conditioning during several hours, but morale remained high and the group was very cooperative and friendly.

Monday 29 June
This was a rather hectic day with two deep stations to sample. At the 1000 m station 118 the first 250 m CTD went right but at the second, deep one, the computer system totally collapsed. The programme was continued with box coring and multinets after which we sailed to the 2000 m station. When we arrived, the electonic engineers had created a new computer system and one CTD and one big box-corer were taken. Due to an error while saving place in the computer's memory the data of the CTD-cast were accidentally erased and we had to sail back in the evening. The 2000 m station was finished after midnight and the 1000 m CTD was taken at 03.00 h.. The technicians, electronic engineers and student Monique de Bie who stayed awake all that time, are to be thanked. The 2000 m cast showed a remarkable fluorescence peak near the thermocline and a deep layer of warm and saline water.

Tuesday 30 June
In the morning we arrived in Ungama Bay. Sediments at St 121 at 50 m was coarse coral sand with red mud and many epibenthic animals (sponges and bryozoans). One big box-core for incubation was taken. The sediment was unfit for the lander so we decided to sail to the North Kenya Banks where the lander was placed at 144 m depth on station 125. Here a big box-core for deck incubation was taken as well. We then sailed back to Ungama Bay where we arrived at 12.30 h.. The coast proved to be too far away with rough sea to attempt an approach to the Tana mouth. Two stations at 20 m and 50 m depth were sampled. A beam trawl tow at 20 m depth gave a rich yield with much seagrasses and red algae and many fish of different species. In the evening an extra CTD on station 126 on the North Kenya Banks was taken.

Wednesday 1 July
The approach to Lamu proved to be very difficult due to heavy swell. Two zodiacs had to return to *Tyro* lying 8 miles offshore. In the afternoon the cameraman Bernardo Guillén was brought ashore at Lamu. The trip back to the vessel proved to be very difficult. It was decided to postpone the investigation of Lamu Archipelago to November.

Thursday 2 July
The northernmost transect, close to 2° South, was started. Station 127 (20 m) was in front of Kiwayuu island, which we could see all day. The station was in a flatter area and had coarse calcium carbonate sediments. While approaching the station the ship went over a very steep trench where the bottom descended quickly from 60 to 260 m and then up again. This feature is not indicated on the map. Station 128 (50 m) was on the slope with no flat surface around. The sediment was very muddy. There was a stiff wind today and the sea was rough.

Friday 3 July
The day was started at the 1000 m station 132 where two CTD's were taken. The sea-floor was very rugged between 100 and 1000 m with numerous faults. No suitable station for the benthic lander was found. It was decided to sample the 2000 m station 133 first and put the lander there. In the evening we returned to 132 to sample the bottom. This proved to be difficult but we finally succeeded after midnight.

Saturday 4 July
In the morning the 500 m station 131 was sampled without great difficulties besides finding a suitably flat surface for the box-corers. The 200 m station 130 appeared impossible to sample. In one of the boxes a large piece of lava was collected showing that the underwater relief is probably volcanic in origin. The stone will be given to Joseph Abuodha for display in the university. The weather was roughening with winds of 7 Beaufort and choppy seas.

Sunday 5 July
The benthic lander was safely brought aboard, although the sea condition and the wind made it a difficult job. Because of heavy wind and currents against the ship, the speed on the ground was only 4 knots. The whole day and night were spent sailing to the Tana river transect, against heavy sea.

Monday 6 July
Two stations at the Tana transect were sampled. The 500 m station proved to be extremely difficult to sample because of extreme relief differences with a rapid succession of trenches and peaks, sometimes several hundred meters of difference within a few minutes sailing. No box-core could be taken. Also at 1000 m there was still rough volcanic bottom, but a box core could be taken here.

Tuesday 7 July
During the night we sailed back to station 118 situated at the oxygen minimum depth at the Sabaki transect. A box core was taken here without problem although the section was oblique. We then sailed to station 137, the last on our programme, at 2000 m depth on the Tana transect. The CTD-cast was taken but the first box core did return empty and the second took a very oblique sample, unfit for incubation. The last action of this cruise was the repeating of the CTD at 2000 m. Very strong currents made it necessary to use more than 4000 m of cable to get it at a depth of 2000 m.

Wednesday 8 July
The day was spent sailing back to Mombasa, cleaning up laboratories and writing the shipboard report.

leg A 2

On Thursday 19 November R.V. *Tyro* sailed again from Mombasa, one night later than planned because of problems with bunkering drinking water. The water pressure in Mombasa became too low and a water boat had to be ordered. This gave Michael Nguli some time to break into KMFRI to obtain a burette for the Winkler titrations at the last moment.

For the following days the weather was excellent, the wind coming from the North East with forth 2-3 Beaufort but the current from the South to South-East. The sea was smooth as a mirror with a blue to green colour. The sampling programme of the cruise was a repetition from the June-July cruise but with one transect less. All stations planned were visited and the programme was run without any difficulty. Only on November 25 the cable of the 'grey' winch became stuck and the winch was damaged. Repair took most of that day.

On Thursday 26 and Friday 27 November two deep stations were sampled, which took nearly the whole day in very hot weather. On Saturday 28 November some repairs of *Tyro* were made. There was more wind and in the evening a strong swell arrived.

On 3 December Jan Everaarts was replaced by Carlo Heip as the chief scientist. This replacement started with the immediate loss of the beam trawl. All trials to locate the beam trawl and recuperate it were in vain. However, the rest of the cruise was uneventful and therefore very succesful. On 3 December we ran into some extensive *Trichodesmium* patches. On 'Sinterklaas'-day (Santa Claus, but the Dutch version) the vessel returned to Mombasa, finishing a cruise in which the spirit on board was excellent.

2.3. STATIONS AND ACTIVITIES

Date	Station	Time	Latitude S	Longitude E	Depth (m)	Instrument
June 19	101	08.36	04°12'03	39°40'84	222	Currentmeters
	102	16.01	04°12'98	39°47'06	190	CTD
		16.35	04°13'59	40°47'39	1482	Sediment trap
June 20	103A	08.20	04°25'87	39°33'76	90	CTD
	103B	09.56	04°25'95	39°33'71	65	CTD
		10.27	04°25'83	39°33'58	62	Box core
	103D	10.47	04°25'89	39°33'56	59	Box core
	103E	11.40	04°25'93	39°33'56	57	Box core
	103F	13.09	04°26'52	39°33'32	65	Box core
	103G	13.23	04°26'44	39°33'34	64	Box core
	103H	13.45	04°26'61	39°33'29	66	Box core
	103I	14.02	04°26'51	39°33'26	63	Box core
	103J	14.25	04°26'87	39°33'22	75	CTD
	103K	15.00	04°26'28	39°33'43	65	Box core
	103L	15.52	04°26'30	39°33'37	62	CTD
	103M	16.03	04°26'31	39°33'39	65	van Veen grab
	103N	16.11	04°2670	39°33'44	71	van Veen grab
	103O	16.14	04°26'54	39°33'52	79	van Veen grab
	103P	16.20	04°26'47	39°33'47	,88	van Veen grab
	103Q	16.35	04°26'54	39°33'22	59	van Veen grab
	103R	16.40	04°26'45	39°33'31	60	van Veen grab
	103S	18.28	04°27'07	39°33'25	79	Bell jar
	103T	19.11	04°26'83	39°36'34	306	CTD
June 21	104	07.12	04°22'55	39°35'58	140	Beam trawl
	103	13.07	04°26'00	39°33'71	80	Multinet
		17.05	04°25'38	39°34'46	127	Box core
		18.48	04°26'28	39°33'50	66	Large box core
		19.52	04°25'87	39°33'66	69	Large box core
		20.32	04°26'05	39°33'40	55	Large box core
June 22	103	07.15	04°24'73	39°35'52	200	Large box core
		09.15	04°25'58	39°44'49	510	CTD
		10.06	04°24'30	39°45'90	528	Box core
		10.36	04°23'57	39°46'43	535	Box core
	105	11.13	04°22'92	39°47'04	544	CTD
		13.18	04°24'06	39°45'99	511	Box core
		13.53	04°23'45	39°46'54	517	Box core
		14.22	04°22;92	39°47'10	526	Box core
		19.39	04°20'78	39°47'31	501	Benthic lander
June 23	106	07.05	04°19'76	40°21'77	1000	CTD
		08.56	04°20'39	40°21'68	1000	CTD
		09.37	04°20'35	40°21'70	1000	Large box core
		10.53	04°20'93	40°21'63	1000	Large box core
		12.00	04°19'33	40°22'04	1000	Vertical net
		12.43	04°18'05	40°22'63	1000	Vertical net

Date	Station	Time	Latitude S	Longitude E	Depth (m)	Instrument
		13.15	04°18'65	40°22'97	1000	CTD
	107	18.07	04°21'38	41°12'33	2012	CTD
		19.20	04°21'83	41°13'16	2053	Large box core
June 24	106	08.11	04°19'77	40°21'56	1000	Box core
		08.51	04°19'07	40°20'91	1000	Box core
	105	15.27	04°17'26	39°48'69	480	Multinet
June 25	108	08.37	03°10'06	40°10'32	18	Box core
		08.58	03°10'27	40°10'21	18	Box core
		09.10	03°10'22	40°10'15	18	Box core
		11.04	03°09'64	40°10'64	21	Box core
	108/1	12.57	03°08'28	40°11'51	27	CTD
		13.10	03°08'01	40°11'57	26	Box core
	108/2	13.45	03°09'02	40°10'71	19	CTD
	108/3	14.10	03°10'00	40°10'53	19	CTD
	108/4	14.55	03°10'38	40°10'24	19	CTD
	108/5	15.27	03°11'20	40°09'94	18	CTD
	108/6	15.52	03°11'80	40°09'71	19	CTD
	108/7	16.18	03°12'48	40°09'40	18	CTD
		16.27	03°12'42	40°09'46	19	Box core
	109	17.15	03°10'09	40°11'34	30	CTD
		17.26	03°09'92	40°11'45	31	Box core
	110	17.48	03°10'08	40°12'21	40	CTD
		18.00	03°09'95	40°12'34	40	Box core
	111	18.55	03°09'78	40°14'41	53	Box core
		19.30	03°09'51	40°14'26	58	Beam trawl
		20.22	03°09'58	40°14'40	61	Box core
	112	20.55	03°09'30	40°14'62	76	Box core
	113	21.26	03°08'92	40°15'53	101	Box core
June 26		06.45	03°09'60	40°14'20	50	Bell jar
		07.07	03°09'67	40°14'04	48	Benthic lander
		07.38	03°09'89	40°14'11	52	Bell jar
	111	09.00	03°09'13	40°13'53	58	CTD
		14.00	03°09'70	40°13'66	50	CTD
		14.30	03°08'70	40°13'49	48	Multinet
		14.50	03°08'62	40°14'13	54	Multinet
		15.10	03°08'77	40°13'82	47	Plankton torpedo
	108/3	16.13	03°09'02	40°10'64	20	Beam trawl
	111	17.23	03°09'12	40°13'56	48	Box core
	112A	17.55	03°09'05	40°14'68	70	Box core
	112B	17.58	03°09'03	40°14'67	70	Box core
	112C	18.12	03°08'93	40°14'82	71	Box core
	112D	18.30	03°08'70	40°14'72	66	Box core
	112E	18.45	03°08'48	40°14'80	64	Box core
	112F	19.01	03°08'35	40°14'92	63	Box core

Date	Station	Time	Latitude S	Longitude E	Depth (m)	Instrument
	112G	19.12	03°08'20	40°15'02	64	Box core
	111	20.44	03°09'52	40°13'96	52	Large box core
June 27	114	08.08	03°10'35	40°17'10	206	CTD
		09.04	03°10'27	40°17'62	213	Box core
		09.22	03°10'19	40°17'79	217	Box core
		10.10	03°10'02	40°16'90	197	Beam trawl
		11.51	03°09'85	40°17'16	202	Bell jar
		12.19	03°09'63	40°17'71	209	Large box core
	115	14.16	03°10'15	40°25'89	300	Box core
	116	15.45	03°09'54	40°34'63	400	Box core
	117	16.45	03°10'04	40°40'48	500	Box core
		17.35	03°0933	40°41'90	500	Box core
		18.05	03°09'08	40°42'23	500	Multinet
		19.36	03°08'36	40°42'93	540	CTD
		22.26	03°08'86	40°41'52	500	Large box core
June 28	117	00.05	03°08'08	40°41'93	480	Multinet
		06.05	03°08'00	40°41'94	500	Multinet
		07.10	03°09'40	40°42'81	500	CTD
		08.34	03°08'42	40°41'55	500	CTD
		10.13	03°08'21	40°41'80	500	Box core
		10.45	03°07'38	40°42'51	500	Box core
		12.25	03°07'52	40°41'95	450	Multinet
		13.11	03°07'41	40°42'00	450	CTD
June 29	118	07.06	03°09'50	40°59'48	1072	CTD
		08.46	03°08'46	41°01'77	1112	Box core
		09.36	03°07'65	41°02'82	1100	Box core
		11.42	03°09'68	40°59'82	1100	Large box core
		12.40	03°08'64	41°00'71	1060	Multinet
	119	17.45	03°10'67	41°14'20	2007	Large box core
		19.03	03°10'11	41°16'32	2157	CTD
		22.18	03°10'00	41°15'90	2134	CTD
June 30	118	02.25	03°09'84	40°58'06	1042	CTD
	124	06.40	02°41'05	40°37'11	53	Box core
		06.50	02°40'38	40°37'36	53	Box core
		07.20	02°39'94	40°38'01	49	Box core
	125	08.47	02°39'80	40°43'96	148	Box core
		09.57	02°40'15	40°43'25	144	Benthic lander
		10.28	02°39'92	40°43'69	150	Large box core
	120/2	13.11	02°41'99	40°31'45	20	CTD
		13.30	02°42'20	40°31'18	21	Box core
		13.45	02°42'30	40°30'99	21	Box core
		14.15	02°42'67	40°30'66	19	Beam trawl
	121	15.55	02°43'20	40°33'69	55	Multinet
		16.28	02°43'37	40°33'29	51	CTD

Date	Station	Time	Latitude S	Longitude E	Depth (m)	Instrument
		16.55	02°43'07	40°33'89	52	Box core
		17.07	02°42'97	40°33'93	53	Box core
		17.22	02°42'84	40°34'04	51	Box core
		17.36	02°42'84	40°34'20	55	Box core
		17.51	02°42'72	40°34'27	53	Box core
		18.04	02°42'65	40°34'41	50	Box core
	122	19.00	02°42'83	40°36'00	100	Box core
		20.25	02°39'74	40°42'32	137	CTD
July 2	127	08.07	02°02'95	41°18'57	28	CTD
		08.39	02°03'61	41°17'80	24	Box core
		08.58	02°03'66	41°17'82	25	Box core
		09.37	02°03'54	41°17'53	23	Large box core
		10.30	02°03'42	41°18'23	26	Beam trawl
		12.15	02°02'66	41°17'57	19	Box core
		12.24	02°02'66	41°17'70	19	Box core
		12.45	02°02'65	41°17'93	20	Box core
	128	13.46	02°03'31	41°18'74	53	CTD
		13.37	02°03'18	41°18'87	50	Beam trawl
		14.45	02°04'65	41°17'72	55	Multinet
		15.30	02°03'16	41°18'48	55	Box core
		15.45	02°02'98	41°18'98	55	Box core
		15.58	02°02'58	41°19'06	46	Box core
		16.16	02°02'44	41°19'34	55	Box core
		16.33	02°02'46	41°19'37	56	Box core
		16.52	02°01'96	41°19'54	51	Box core
		17.21	02°02'84	41°19'04	52	Box core
		17.36	02°02'65	41°19'20	55	Box core
		19.25	02°02'69	41°19'16	53	Large box core
July 3	132	08.40	01°58'80	41°35'17	930	CTD
		10.00	01°57'09	41°35'90	1027	CTD
	133	13.38	02°02'02	41°46'37	1996	CTD
		14.04	02°01'49	41°46'96	2015	Large box core
	134	15.44	02°00'82	41°48'00	2013	Benthic lander
		16.00	02°00'54	41°48'27	2028	Multinet
		18.10	02°00'80	41°47'76	2017	CTD
	132	21.52	01°56'03	41°37'54	1000	Large box core
		23.44	01°56'42	41°36'85	1000	Large box core
July 4	131	08.00	02°00'71	41°26'80	492	CTD
		09.00	02°00'27	41°27'66	500	CTD
		10.32	02°00'27	41°26'62	500	Large box core
		11.14	02°00'76	41°26'92	500	Box core
		11.44	02°00‘59	41°27'48	500	Multinet
		13.55	02°02'84	41°14'84	172	CTD
		14.13	02°02'71	41°20'15	196	Box core

Date	Station	Time	Latitude S	Longitude E	Depth (m)	Instrument
		15.06	02°02'61	41°20'16	180	Box core
	129	17.30	02°02'14	41°20'14	84	Box core
		17.53	02°02'14	41°19'97	75	Box core
	?	20.00	01°56'13	41°37'74	987	Multinet
July 6	135	08.08	02°43'17	41°03'27	630	CTD
		13.53	02°41'01	41°06'21	780	Multinet
	136	15.40	02°40'16	41°10'13	1000	CTD
		17.10	02°40'11	41°10'19	1000	CTD
		18.48	02°40'05	41°10'17	992	Large box core
July 7	118	07.21	03°09'49	40°59'65	1080	Large box core
	137	11.35	02°41'89	41°21'23	1952	CTD
		13.30	02°41'66	41°22'67	2267	Box core
		15.30	02°42'18	41°23'07	2064	Box core
		16.42	02°40'18	41°25'09	2221	CTD
Leg	**A2**					
Nov. 20	531	08.10	02°00'47	41°26'98	520	CTD (bottom)
		09.12	02°00'48	41°27'14	536	Small box core
		10.04	02°00'60	41°26'94	516	Large box core
		10.51	02°00'46	41°26'99	525	CTD (thermocline)
		11.54	02°00'36	41°26'96	521	Large box core
		12.53	02°00'53	41°27'15	520	Small box core
		13.45	02°00'46	41°26'96	495	Multinet
		15.15	02°00'51	41°26'95	508	Vertical net
		16.10	02°00'53	41°26'96	498	Vertical net
	527	18.17	02°02'72	41°18'39	25	CTD (bottom)
		18.40	02°02'71	41°18'67	28	Small box core
		18.55	02°02'71	41°18'50	28	Small box core
		19.15	02°02'65	41°18'34	26	Beam trawl
Nov. 21	533	06.15	02°00'86	41°47'71	2026	Small box core
		07.48	02°01'15	41°47'75	2030	Benthic lander
		08.36	02°00'73	41°47'68	2024	CTD (bottom)
		11.22	02°01'29	41°47'38	2027	Large box core
		12.55	02°01'14	41°47'90	2040	CTD (thermocline)
		13.33	02°01'40	41°47'84	2048	Multinet
		15.00	02°00'85	41°47'75	2030	Large box core
		16.35	02°01'30	41°47'69	2030	Vertical net
Nov. 22	532	09.19	01°56'32	41°37'36	945	CTD (bottom)
		10.19	01°56'02	41°37'56	933	Small box core
		11.24	01°56'67	41°37'30	924	CTD (thermocline)
		12.43	01°55'91	41°37'20	904	Large box core
		13.50	01°54'82	41°38'22	943	Multinet
		16.15	01°55'60	41°37'18	899	Large box core

Date	Station	Time	Latitude S	Longitude E	Depth (m)	Instrument
		17.15	01°56'28	41°36'90	919	Vertical net
		17.30	01°55'94	41°36'98	902	Vertical net
Nov. 23	528	06.15	02°04'76	41°17'40	39	Small box core
		06.54	02°04'84	41°17'40	42	Small box core
		07.30	02°04'82	41°1747	47	Benthic lander
		09.14	02°04'91	41°17'41	48	Bell jar
		10.00	02°04'89	41°17'36	44	CTD (bottom)
		11.04	02°04'76	41°17'35	37	Large box core
		11.44	02°05'16	41°17'62	64	Multinet
		14.15	02°05'01	41°17'19	40	Large box core
		15.00	02°04'94	41°17'24	40	Small box core
	527	19.10	02°02'96	41°18'72	40	Beam trawl
Nov. 24	527	07.05	02°03'07	41°18'75	45	CTD (bottom)
Nov. 25	517	08.11	03°09'43	40°41'25	542	CTD (bottom)
		09.14	03°09'54	40°40'99	509	Small box core
		11.00	03°09'52	40°40'40	508	Large box core
		13.16	03°09'59	40°40'93	507	Vertical net
		13.27	03°08'98	40°41'25	548	Vertical net
		14.35	03°09'27	40°40'77	496	Large box core
		15.22	03°09'58	40°40'90	509	Large box core
		16.13	03°09'53	40°41'14	517	Multinet
		18.30	03°09'61	40°40'98	509	Small box core
Nov. 26	518	06.10	03°07'98	40°59'96	965	Small box core
		07.03	03°08'03	40°59'96	965	Benthic lander
		07.25	03°08'20	41°00'00	974	CTD (bottom)
		09.34	03°08'09	40°59'86	963	Large box core
		10.47	03°08'30	40°59'75	967	CTD (thermocline)
		11.36	03°08'21	40°59'79	965	Large box core
		13.07	03°08'54	40°59'78	988	CTD (thermocline)
		13.28	03°08'34	40°59'91	982	Multinet
		14.35	03°08'49	40°59'84	988	Vertical net
		14.56	03°07'93	41°00'07	971	Vertical net
	519	18.30	03°10'04	41°16'33	2165	CTD (bottom)
Nov. 27	519	08.44	03°09'47	41°16'30	2173	CTD (thermocline)
		09.00	03°09'28	41°16'53	2169	Small box core
		10.31	03°09'66	41°16'59	2176	Multinet
		12.34	03°09'41	41°16'80	2179	Large box core
		14.18	03°09'27	41°16'75	2177	Large box core
		15.53	03°09'99	41°16'44	2188	Vertical net
		16.03	03°09'69	41°16'59	2188	Vertical net
Nov. 28	511	06.10	03°09'59	40°13'94	53	Small box core
		06.40	03°09'66	40°14'03	53	Benthic lander
		07.20	03°09'75	40°13'88	50	Bell jar 1
		08.39	03°09'53	40°14'08	56	Small box core

Date	Station	Time	Latitude S	Longitude E	Depth (m)	Instrument
		08.52	03°09'50	40°13'92	52	CTD (bottom)
		09.27	03°09'65	40°14'21	53	Bell jar 2
		10.33	03°09'81	40°14'14	48	Multinet
		19.33	03°09'53	40°14'12	57	Large box core
		20.15	03°09'58	40°14'02	53	Large box core
Nov. 29	508	08.00	03°09'90	40°10'56	22	CTD (bottom)
		08.46	03°10'17	40°10'30	19	Small box core
		09.06	03°10'03	40°10'54	21	Small box core
		09.21	03°10'26	40°10'54	23	Small box core
		09.50	03°10'28	40°11'05	25	Multinet
	511	10.47	03°09'61	40°14'13	53	CTD (bottom)
	508	14.00	03°10'31	40°10'74	23	Beam trawl
		15.33	03°10'21	40°10'52	22	Beam trawl
	511	16.00	03°09'37	40°13'86	53	Beam trawl
	514	18.40	03°10'27	40°17'34	210	Small box core
		19.00	03°10'21	40°17'63	212	Beam trawl
		20.25	03°09'98	40°17'26	207	Large box core
		21.08	03°10'32	40°17'38	210	Large box core
Nov. 30	503	15.00	04°19'36	39°35'56	41	Small box core
		15.28	04°19'28	39°35'59	45	Large box core
		15.35	04°19'26	39°35'65	47	Large box core
		16.05	04°19'34	39°35'55	44	Large box core
		16.50	04°19'42	39°35'48	56	Bell jar 1
		17.30	04°19'63	39°35'48	64	Bell jar 2
		17.55	04°19'49	39°35'54	48	Benthic lander
Dec. 1	503	10.39	04°19'37	39°35'55	46	CTD (bottom)
		13.14	04°27'00	39°33'26	81	Large box core?
		15.10	04°27'20	39°33'43	110	Multinet
Dec. 2	507	09.07	04°21'31	41°13'64	2130	CTD
		10.57	04°21'22	41°12'88	2088	Large box core
		12.48	04°21'37	41°12'70	2034	CTD (thermocline)
		13.25	04°21'56	41°12'49	1995	Multinet
		15.14	04°21'59	41°12'69	2007	Large box core
		16.45	04°21'66	4112'71	1998	Box core
		17.40	04°20'73	41°12'46	2058	Vertical net
		17.56	04°30'45	41°20'45	2057	Vertical net
Dec. 3	506	06.03	04°19'68	40°21'83	989	Lander down
	505	10.57	04°25'17	39°45'31	522	CTD 250 m
		11.28	04°25'31	39°45'51	540	Box core
		12.40	04°25'32	39°45'25	521	CTD (bottom)
		13.28	04°25'01	39°45'67	547	Multinet
		15.04	04°25'29	39°45'28	524	Vertical net
		15.21	04°24'86	39°45'73	547	Vertical net
		20.09	04°25'33	39°45'21	520	Large box core

Date	Station	Time	Latitude S	Longitude E	Depth (m)	Instrument
		20.46	04°25'31	39°45'19	520	Large box core
Dec. 4	506	06.08	04°19'66	40°21'64	984	Lander up
		08.04	04°19'37	40°22'06	1000	CTD 250 m
		08.42	04°19'92	40°21'98	1012	Multinet
		10.23	04°19'18	40°21'99	1004	CTD (bottom)
		11.23	04°19'45	40°21'80	1020	Large box core
		13.03	04°19'79	40°21'69	991	Vertical net
		13.15	04°19'41	40°21'75	988	Vertical net
		13.46	04°19'00	40°21'90	987	Large box core
Dec. 5	502	09.04	04°11'40	40°47'78		Sediment trap up

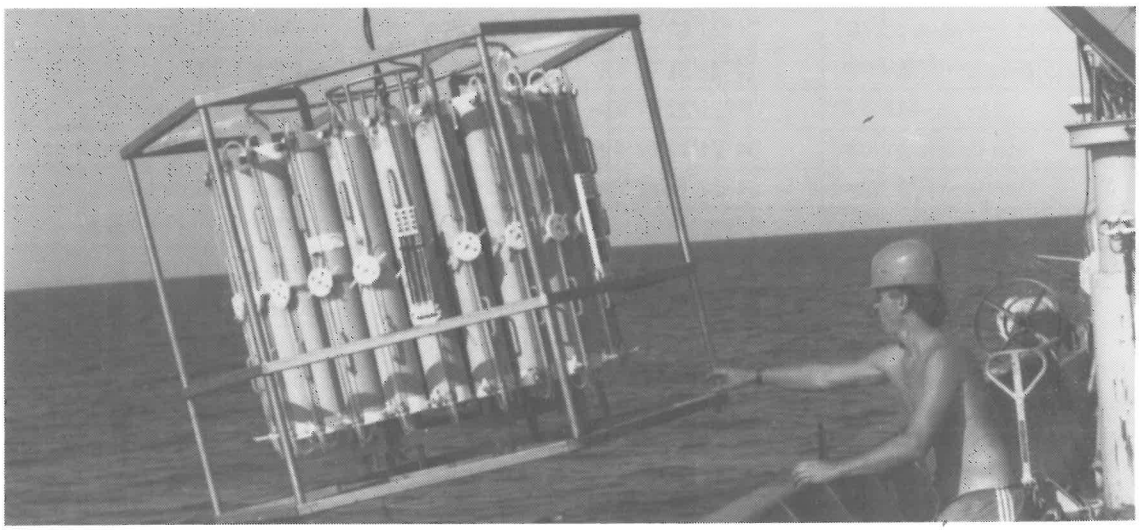

CTD-Rosette sampler.

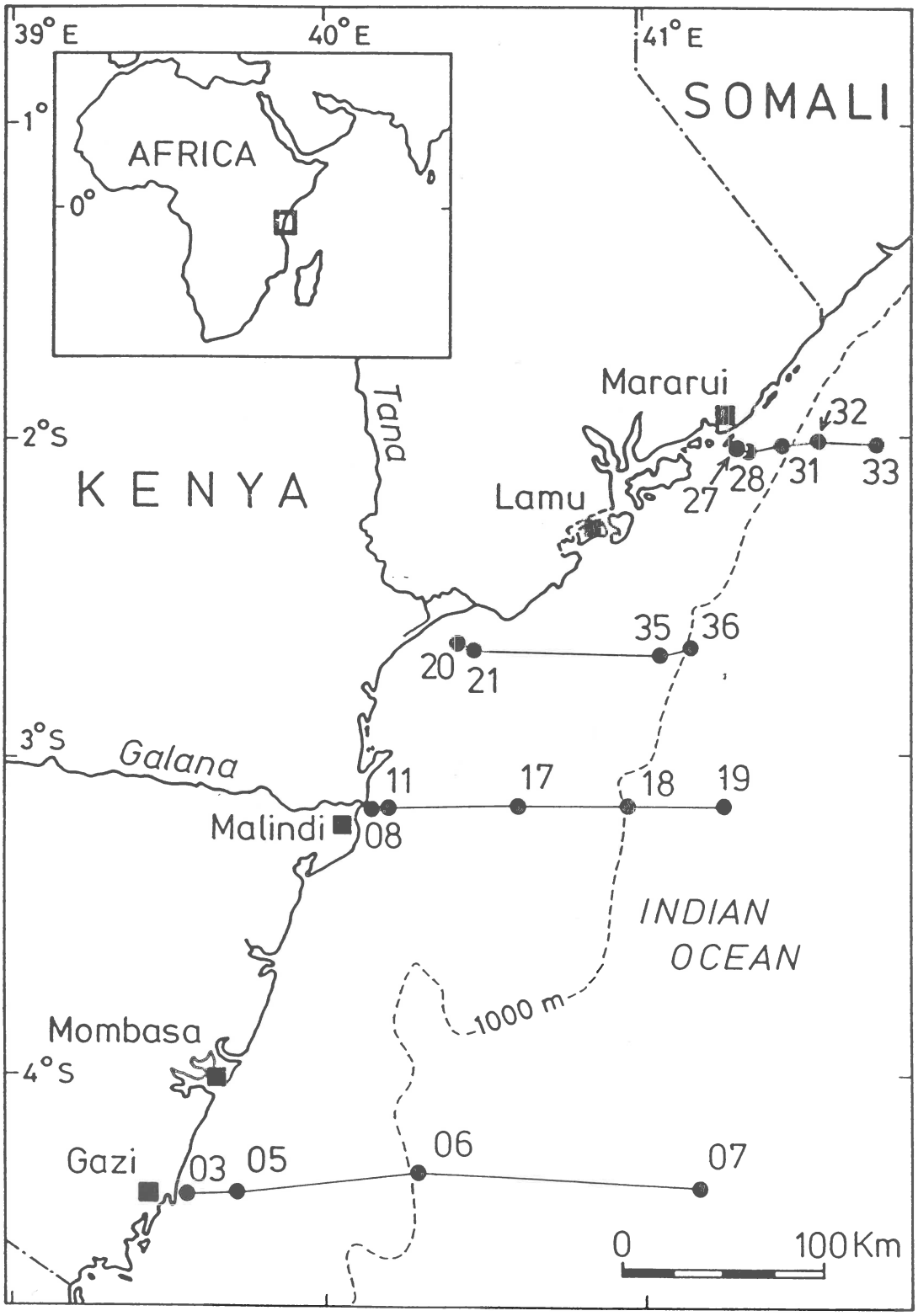

Fig. 2.3.1. Map with location of stations. Station numbers are without reference to either leg A1 (1 added before station number) or leg A2 (5 added before station number). Stations 08-19 were skipped during the A2 leg.

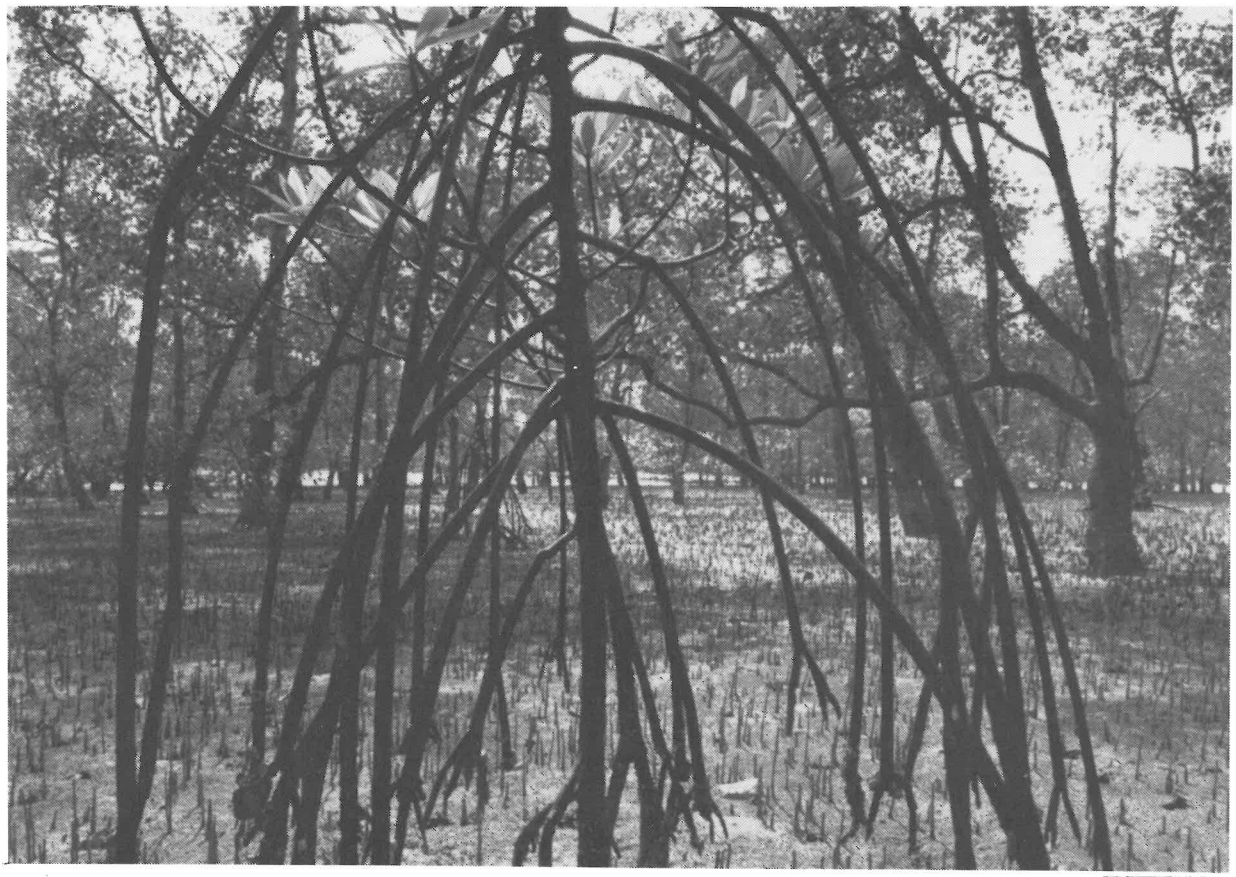

Open mangrove stand of Kenyan coast.

3. KENYAN COASTAL ECOSYSTEMS AND THEIR INTERRELATIONS

3.1. INTRODUCTION

M.A. Hemminga
Centre for Estuarine and Coastal Ecology, Yerseke

Going from the coast in a seaward direction, a number of characteristic ecosystems can be successively found along the Kenyan coast: a zone with mangroves is followed by a zone with seagrass vegetations in backreef lagoons; these lagoons are bordered by a belt of coral reefs; beyond the coral reefs the open ocean begins. In the ship-based research programme described above, the pelagic system of the open ocean water of the Kenyan shelf is the central issue. The coastal project was complementary to this programme: the research focus was on the adjacent mangrove, seagrass and coral reef systems. These marine ecosystems are connected by the tidal water which carries both abiotic and biotic elements to and from the systems. The relation between mangroves, seagrass beds and reefs (in terms of dissolved nutrients- and seston fluxes and shuttle movements of fish) was the central theme of the coastal project. Very little is known concerning the interlinkages between the coastal ecosystems in the East African region; nonetheless, this information is indispensable for a rational management of the coastal ecosystems and their resources. Within the framework of the coastal programme, attention was also given to the emission of greenhouse gases by the mangrove sediments.
The coastal research programme was carried out in Gazi Bay, c. 50 km south of Mombasa. This site has the advantage of the presence of nearby laboratory facilities at the Kenya Marine and Fisheries Research Institute in Mombasa, and facilitated the participation of Kenyan scientists in the project. Furthermore, Gazi Bay is the location where EC-funded research projects focussing on the ecological functioning of mangroves and on the interlinkages between mangroves and adjacent systems were (and still are) in progress. The participants of the EC project were in majority involved in the expedition. These factors implied that an optimal use of existing knowledge was possible, and also that a concerted research effort with input both from the EC-funded programme and from the expedition could be realized.

The coastal programme focussed on several research lines:
in order to understand the influence of the Kenyan coastal ecosystems on each other, the transfer of organic matter from the mangrove to the adjacent systems (seagrass meadows and coral reefs) and *vice versa* was studied. For this part of the work the stable carbon isotope technique proved particularly useful.

Seagrass leaves are capable of capturing nutrients from the ambient water. In addition, the seagrass canopy tends to trap seston particles from the watercolumn. The position of extensive seagrass vegetations between mangroves and coral reefs in Gazi Bay implies that these littoral vegetations may function as a trap which reduces the extent of the fluxes of seston and nutrients between mangrove and ocean. Such a phenomenon would be of considerable ecological interest. In this context three questions were specifically addressed: (1) Do seagrass meadows change the nutrient and seston content of tidal water flowing between mangroves and reefs? (2) What is the relative importance of sedimentation and N_2 fixation for nutrient input into the seagrass meadow of a backreef lagoon? (3) Does the above mentioned nutrient input in the seagrass meadows influence the productivity in these systems?

To investigate the importance of mangroves and seagrass beds for coral reef fishes was another aim of the coastal programme. Mangroves and seagrass beds are known to be nursery grounds or feeding areas of many fish species. Although mangroves, seagrass beds and coral reefs often occur in adjacent zones, their fish fauna is mainly studied separately. The field work in Gazi Bay for this part of the programme implied that fishes were caught in the mangroves and seagrass zone, or were visually censused in reef zones to investigate the species composition, the length distribution of the various species and the densities over the various zones. Furthermore, the data were collected to gain insight in the migratory movements and activity patterns of the various species. A study of stomach contents was underteaken and tissue analyses were performed to gather information on the dependence of the fish fauna on various food sources.

The fluxes of greenhouse gases from the mangrove to the atmosphere were investigated as a separate part of the programme. CO_2, CH_4 and N_2O are released from the sediments of tidal wetlands as the result of decomposition processes. Quantitative data on the emission of these gases by tropical wetlands are scarce, and more data are needed to improve the estimates for emission of greenhouse gases by natural wetlands on a global scale. To that aim, the production of the above-mentioned gases by mangrove sediments was studied, in various vegetation types. Gas-fluxes were estimated using incubation chambers connected to a gas-monitor. In addition, pore water characteristics were determined, to elucidate the soil decomposition processes.

Participants:
From the Netherlands Institute of Ecology, Centre for Estuarine and Coastal Ecology (Yerseke, The Netherlands):

M.A. Hemminga (expedition leader)
J.B.M. Middelburg
F.J. Slim
J. Nieuwenhuize
M.M. Markusse
P. de Koeijer

From the Kenya Marine and Fisheries Research Institute (Mombasa, Kenya):

J.M. Kazungu (co-expedition leader)
B.O. Ohowa
G.K. Mwatha
P.Gwada
M. Osore

From the University of Nairobi (Nairobi, Kenya):

M.J. Ntiba

From the Catholic University Nijmegen (Nijmegen, The Netherlands):

G. van der Velde
P.H. van Avesaath
M.G. Versteeg
M. van der Gaag
I.A. Nagelkerken
P.J.M. Bergers
W.P.M. van der Hoek

From the University of Brussels (Brussels, Belgium):

A.F. Woitchik

3.2. CARBON FLUXES BETWEEN MANGROVES AND SEAGRASS MEADOWS IN GAZI BAY

M.A. Hemminga[1], F.J. Slim[1], J. Kazungu[2], G.M. Ganssen[3], P. Gwada[2] and J. Nieuwenhuize[1]
[1] Netherlands Institute of Ecology, Centre for Estuarine and Coastal Ecology, Yerseke,
[2] Kenya Marine and Fisheries Research Institute, Mombasa, Kenya
[3] Institute of Geological Sciences, Free University Amsterdam

introduction

Mangroves are open systems, coupled to the coastal waters by tidal currents. Several studies indicate that export of particulate organic matter from mangrove forests may be a general feature of these systems (Boto & Bunt 1981; Twilley, 1985; Robertson, 1986; Flores-Verdugo *et al.*, 1987). The factors that determine the magnitude of this transport and the spreading of the material in the adjacent coastal zone are poorly known, but they will include geomorphological and hydrodynamic factors (Twilley, 1985; Woodroffe, 1992; Wolanski *et al.*, 1992). Mangroves occur in a number of different environmental settings. An intriguing situation is the co-occurrence of mangroves, seagrass meadows and coral reefs. These can be found as adjacent systems in tropical coastal zones. It is known that the level of nutrient availability in both seagrass and reef systems may have profound effects on their structure and function (*e.g.* Harlin & Thorne-Miller, 1981; Smith *et al.*, 1981; Brock & Smith, 1983; Birkeland, 1987; Short, 1983, 1987; Hallock, 1988; Fourqurean *et al.*, 1992). Thus, if particulate organic carbon and associated nutrients such as nitrogen and phosphorus are exported from the mangrove forest and enter the adjacent seagrass and reef systems, an influence on the structure and functioning of these systems is not unlikely.
During the coastal programme, we investigated the fluxes of particulate carbon between the mangrove in Gazi Bay and the adjacent seagrass meadows and reef zones. Moreover, we investigated if the productivity and nutrient contents of the seagrass *Thalassodendron ciliatum* was related to these fluxes.

study area

Gazi Bay is situated 50 km south of Mombasa on the Kenyan coast (4°25'S, 39°30'E). On the landward side a mangrove of 6.61 km^2 covers much of the Bay (Fig. 3.2.1). There are two major tidal creeks penetrating the mangrove forest. The western creek is the mouth of the river Kidogoweni, a seasonal river. The eastern creek, called Kinondo creek, is a tidal creek. The present investigation focussed on the outflow of this creek. A total of 8 mangrove species are found in Gazi Bay. Directly adjacent to the mangroves on the seaward side are intertidal flats intersected by some channels, and shallow, subtidal areas. Both the intertidal and subtidal areas are to a large extent covered by various species of seagrasses and, to a lesser extent, by macro-algae. Particularly relevant to this study was the subtidally growing seagrass *Thalassodendron ciliatum*. *Thalassodendron* forms dense beds in Kinondo creek and in the channels between the tidal flats. In subtidal parts of the bay, the species is present in monospecific meadows which spread to the reef zone. *Thalassodendron* is a stem-forming species, giving the plant a total height of up to 80 cm. The reef zone in front of the bay is part of the fringing reef that forms a nearly uninterrupted belt along the Kenyan coast. The distance between the mouth of Kinondo creek and the reef zone is approximately 4 km.

materials and methods

Sampling was carried out from June 19 to July 7, 1992. Various types of samples (see below) were taken on four subtidal transects, positioned in the channel forming the continuation of Kinondo creek and in the shallow bay waters more closely to the reefs. *Thalassodendron ciliatum* was the only or the dominant seagrass species on these transects. On each transect, four sediment cores were taken using a sediment corer with an internal diameter of 7 cm. The distance between sampling sites on a transect was approximately 20 m. The upper 7 cm of each core was immediately transferred to a sample container. At each sampling site, the above-ground biomass of *Thalassodendron* was clipped from three plots of 25 × 25 cm. Sediment and seagrass samples were lyophilized. The lyophilized sediments were sieved over a 2-mm mesh sieve to remove coarse material (mainly seagrass roots and mollusc shells). The three seagrass samples collected at each sampling site were pooled, yielding a total of four samples per transect. To decrease the variability which might arise from analyzing seagrass leaves of different developmental stage, only the third youngest leaves of each *Thalassodendron* shoot in a sample were collected and used for further chemical analyses (stable carbon isotope signature, nutrient contents). These third-youngest leaves are nearly full-grown, but they lack the crust of epiphytes complicating the analysis of older leaves. Analyses were carried out after drying of the leaf material at 70°C.
Sediment traps were used to obtain particulate matter depositing in the seagrass zone. Four traps were were positioned on each transect, in the plots which had been cleared of *Thalassodendron*. They were made of PVC tube with a internal diameter of 7.6 cm and a

length of 33 cm, closed on one side by a PVC disc. A steel pin connected to the disc was used to anchor the tube in an upright position in the sediment. The opening of the traps was positioned at the level of the canopy of the *Thalassodendron* vegetation. After 10-17 days of deployment, the sediment traps were closed underwater with rubber stoppers and returned to the field laboratory. The contents were filtered through a 1-mm sieve, and the coarse matter retained on the filter was discarded. Subsequently, 200-400 ml of the filtrate was filtered over Whatmann GF/C filters. The particulate material retained on the filters was lyophilized prior to further chemical analyses.

To investigate changes in seston characteristics in the tidal water when it passed the seagrass zone, seston samples were collected during one ebb tide (June 24) and two flood tides (June 30 and July 1). Ebb water flowing from the mangrove forest in seaward direction

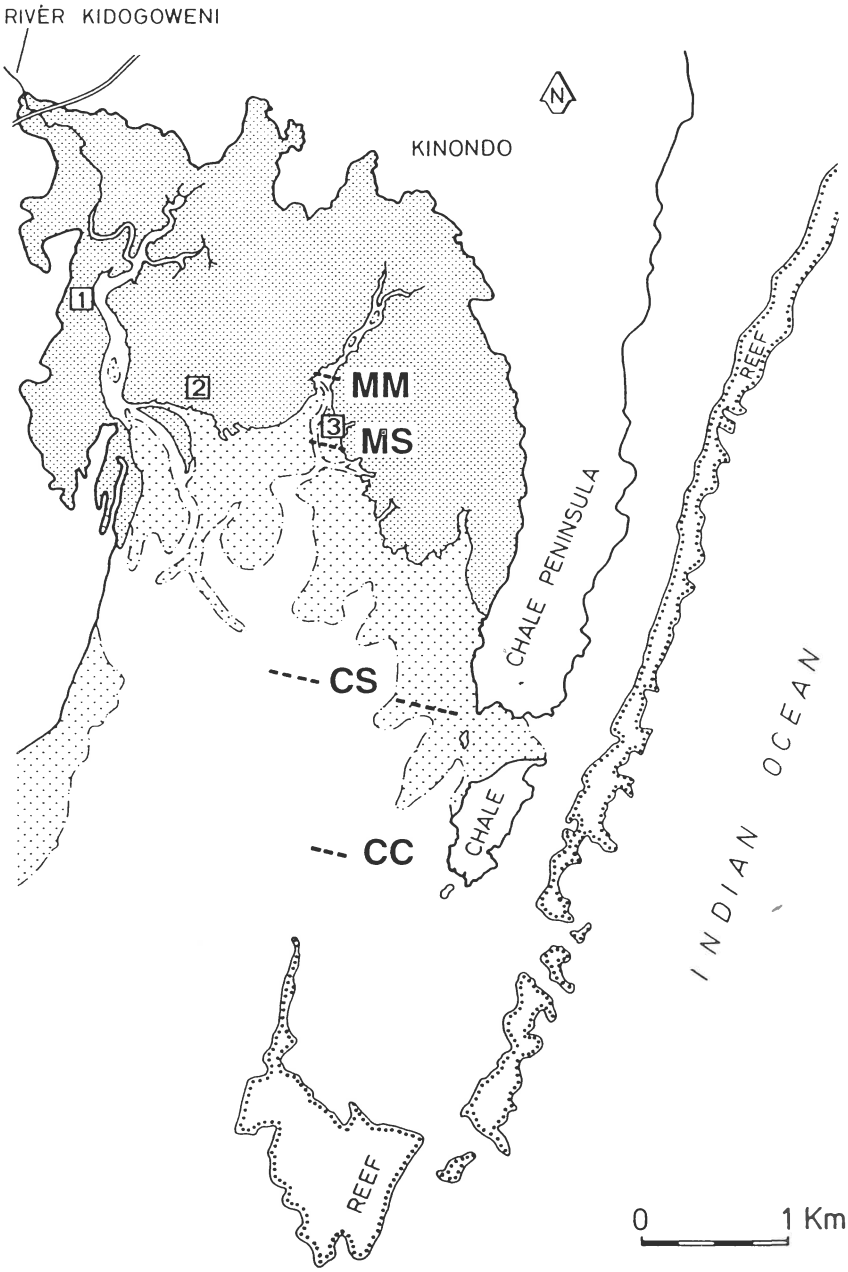

Fig. 3.2.1. Map of Gazi Bay. The mangrove area is indicated in dark grey. The seagrass zone is south of the mangrove; the intertidal part of it is indicated in light grey. Sampling transects in the seagrass zone are indicated with a two-letter code. 1: *Ceriops tagal* sampling site; 2: *Rhizophora mucronata* sampling site; 3: location of work platform.

was collected on the MM and the CS transect. Incoming flood water was collected on the CC and MM transect. Water samples were collected over the full duration of each tide (approximately one sample per hour on each transect). Water samples (25 l each) were collected with a hand diaphragm pump, 1 m above the subtidal sediment surface. The samples were filtered over Whatmann GF/C filters. The filters were dried by lyophilization.

Additional sediment samples (upper 7 cm) were collected from the intertidal flats adjacent to the subtidal MS and CS transects, from stands of *Rhizophora mucronata* and *Ceriops tagal*, and from Chale lagoon, directly east of Gazi Bay (Fig. 3.2.1). This lagoon is separated from Gazi Bay by Chale Peninsula and Chale Island by a broad sill of fossil coral inbetween both formations, restricting direct water exchange between Gazi Bay and the lagoon. *Thalassodendron* is abundant in the lagoon and samples of this seagrass were also collected here. Processing of the sediment and seagrass samples was carried out as described above. Finally, green, fully-grown leaves of all mangrove species present in Gazi Bay were collected and dried (70°C) for chemical analyses.

Primary production measurements of *Thalassodendron ciliatum* were carried out on the MM, MS and CS transects. On each of these subtidal transects, *T. ciliatum* was the only or the dominant seagrass species.

Leaf production of *T. ciliatum* was measured with the plastochrone interval method (Jacobs, 1979). This method has been applied previously by Brouns (1985) for production measurements on *T. ciliatum*. Observations were carried out on four sites per transect. On each site the youngest leaf (length > 10 mm above the leaf sheath) of a number of shoots was marked by punching a small hole through the leaf. These shoots were harvested 14-17 days later. The number of new leaves on the shoots were counted to determine the plastochrone interval of the leaves (PIL), *i.e.*, the time interval between the formation of two successive leaves:

$$PIL = \frac{\text{Number of new leaves since marking}}{\text{Number of days between marking and harvesting}}$$

In addition, 15 shoots of each site were randomly selected for measurements of length and dry weight (DW) of successive leaves.

results

Leaves form the major category of organic material produced by the mangrove trees in Gazi Bay (F.J. Slim, unpublished data). Table 3.2.1 shows the $\partial^{13}C$ values the leaves of the various mangrove species occurring in Gazi Bay, ranging from -28.25‰ in *Rhizophora mucronata* to -24.12‰ in *Ceriops tagal*.

$\partial^{13}C$ values of organic matter in the sediments of *Rhizophora* and *Ceriops* stands (-25.31 and -22.69‰, respectively, see Table 3.2.2), are less depleted than those of the leaves. The $\partial^{13}C$ value of the sediment of the Kinondo creek (MM transect) falls in the range of the mangrove sediments. However, as Table 3.2.2 shows, there is a conspicuous enrichment in ^{13}C in the seagrass zone away from the mangrove. At the CC transect the $\partial^{13}C$ value of the sediment (-15.14‰) is not significantly different from that of the Chale lagoon sediment (-14.75‰), the sample location outside Gazi Bay. The data of the two intertidal locations show a similar trend.

The organic carbon content of sediment at the MM transect is relatively high. However, coinciding with the enrichment in ^{13}C in seaward direction, the organic carbon content of the subtidal sediments decreases significantly. These data suggest outwelling of mangrove-derived POM, but also suggest that this POM is trapped in the seagrass zone, close to the mangrove.

Enrichment in ^{13}C with increasing distance from the mangrove is also very clearly found in the *Thalassodendron* growing on these sites (Table 3.2.3). Seagrass at any of the four subtidal transects, however, is always more enriched in ^{13}C than sediment of the same site.

$\partial^{13}C$ values of seston were determined to investigate if shifts in organic composition of the seston occurred during the flow of the tidal water mass over the seagrass zone. During ebb tide, the seston was less

Table 3.2.1. Carbon isotope signature ($\partial^{13}C$) of mangrove leaves occurring in Gazi Bay. Means of two samples of pooled (10-20) leaves.

Species	$\partial^{13}C$ (‰)
Rhizophora mucronata	-28.25
Ceriops tagal	-24.12
Sonneratia alba	-27.15
Avicennia marina	-26.84
Bruguiera gymnorrhiza	-27.30
Xylocarpus granatum	-24.86
Lumnitzera racemosa	-26.99
Heritiera littoralis	-27.73

Table 3.2.2. Carbon isotope signature ($\partial^{13}C$), and carbon and carbonate content (% weight) of sediment samples in Gazi Bay and Chale lagoon. Means and S.D. Data in a column sharing a common superscript letter are not significantly different (α=0.05).

Location		$\partial^{13}C$ (‰)	% carbon	% carbonate	Nr. of observations
Mangrove (Rhizophora)		-25.31 ± 0.33[a]	15.37 ± 5.02	1.20 ± 0.66	3
Mangrove (Ceriops)		-22.69 ± 0.57[b]	1.71 ± 0.24	0.60 ± 0.26	3
subtidal	MM	-22.94 ± 0.26[b]	3.78 ± 0.95[a]	38.77 ± 4.86[a]	4
subtidal	MS	-20.61 ± 1.46[c]	2.22 ± 0.88[b]	43.30 ± 6.11[a]	4
subtidal	CS	-18.48 ± 0.31[d]	0.68 ± 0.16[c]	27.65 ± 7.85[b]	4
subtidal	CC	-15.14 ± 0.77[e]	0.67 ± 0.45[c]	80.30 ± 2.01[c]	4
Chale lagoon		-14.75 ± 0.52[e]	0.63 ± 0.19[c]	88.03 ± 0.83[c]	3
intertidal	MS	-20.99 ± 1.02[c]	5.13 ± 2.86	55.42 ± 5.87	4
intertidal	CS	-17.13 ± 0.76[f]	0.67 ± 0.53	59.70 ± 33.30	4

depleted in ^{13}C than at the CS transect (at a distance of 2.5 km from the mangroves) than at the MM transect. The difference is statistically significant ($p < 0.01$). No difference was found in salinity of the water between these locations. These results exclude the possibility that mixing of water ebbing from the eastern part of the mangroves with water from the river Kidogoweni caused the shift in carbon isotope signature. The increase in the $\partial^{13}C$ value of the seston is consistent with the above-mentioned process of sedimentation of mangrove-POM in the seagrass zone. However, uptake of particulate material from the seagrass zone could contribute to the shift in $\partial^{13}C$ values: there was a moderate increase in average seston and seston-POC content going from the MM to the CS transect (Table 3.2.4), but the differences were not significant. Clearly, more data are needed before any conclusion can be made regarding this point.

Table 3.2.3. Carbon isotope signature ($\partial^{13}C$) of *Thalassodendron ciliatum* growing at increasing distance from the mouth of Kinondo creek, Gazi Bay, and in Chale lagoon. Means and S.D. of 4 (pooled leaf) samples. Data sharing a common superscript letter are not significantly different (α=0.05).

Location		∂13C (‰)
subtidal	MM	-19.65 ± 0.39[a]
subtidal	MS	-18.30 ± 0.45[b]
subtidal	CS	-15.77 ± 0.47[c]
subtidal	CC	-10.70 ± 0.23[d]
Chale Lagoon		-10.72 ± 0.36[d]

The seston of the ocean water that enters the bay during flood tide (1 July), sampled at the CC transect, has $\partial^{13}C$ values ranging between -17.27 and -19.04‰ (mean value -18.10‰). However, when the water has crossed the seagrass zone and is about to enter the mangroves, the $\partial^{13}C$ values are consistently shifted to more negative values, ranging from -22.04 to -23.70‰ (mean value: -22.88‰). For the flood tide of June 30th (not shown) identical results were obtained (mean $\partial^{13}C$ value at CC transect -18.22‰; at MM transect -23.43‰; means of 5 observations). These highly significant shifts ($p<0.001$) most probably are due to resuspension and uptake of organic material in the seagrass zone, not to sedimentation processes: the ocean water that enters the bay has a relatively low POC content (CC transect, Table 3.2.4), but on reaching the MM transect the POC content has increased significantly. Thus it appears that, besides outwelling of mangrove carbon, there is also a reversed transport of POC from the seagrass zone to the mangroves, achieved by the incoming flood tides.

Most of the sediment traps deployed in the seagrass zone contained some detached leaves or large leaf fragments of *Thalassodendron*. This coarse material was not included in the chemical analyses of the trap contents, as the contents of the traps were filtered over a 1-mm sieve prior to analysis. The remaining material consisted of very fine, dark brown to black coloured, unrecognizable particles. $\partial^{13}C$ values of this material increased from a strongly negative value of -23.30‰ at the MM transect to a value of -13.96‰ at the CC transect (Table 3.2.5). The C:N ratios of the material collected in the sediment traps (Table 3.2.6), show values between 8.5 and 11.2. The C:N ratio of the ses-

Table 3.2.4. Seston and POC levels in tidal water crossing the seagrass zone.
Means and S.D. of samples taken at approximately hourly intervals over the duration of the tide. Differences between transect seston and POC data were statistically analysed for each tide separately. Data sharing a common superscript letter are not significantly different (α=0.05).

Tide	Date	Transect	Seston (mg/l)	POC (mg/l)	Nr. of observations
ebb	24/6	MM	1.99 ± 1.63[a]	0.32 ± 0.06[a]	5
		CS	3.30 ± 1.53[a]	0.46 ± 0.16[a]	5
flood	30/6	CC	3.45 ± 1.71[a]	0.28 ± 0.13[a]	5
		MM	6.23 ± 2.56[a]	1.12 ± 0.39[b]	5
flood	1/7	CC	2.78 ± 0.95[a]	0.35 ± 0.07[a]	6
		MM	8.65 ± 6.61[a]	1.76 ± 1.27[b]	5

ton filtered from the water were on average between 6.5 and 10, and are thus of the same order of magnitude. There is a remarkable contrast between these values and the C:N ratios of mangrove leaves, particularly senescent leaves, which can have C:N ratios of more than 200.

The data showed that leaf weights of shoots from the MM transect were conspicuously lower than leaves of comparable age sampled from the MS and CS transects. On all three transects, the increases of leaf weight from the fourth to the fifth leaf were small. Leaf lengths of fourth and fifth leaves were similar. Thus, full growth of the leaves is attained when they have reached the fourth or the fifth position in the leaf cluster. For calculations of leaf production (see below), we used the data on mean dry weights of the fourth leaves.

Measurement of the PIL reflects the rate of leaf renewal. The values for the plastochrone interval were based on observations of 13-62 marked shoots per site, with an average of 32 shoots. On the MM transect the average leaf rate renewal appeared to be significantly slower (PIL = 10.98 days) than on MS and CS transects (PIL = 8.46 and 8.17 days, respectively; Table 3.2.7). To calculate leaf production per shoot per day, we multiplied the PIL of each site with the mean dry weight of fourth leaves at that site. The results (Table 3.2.7) show that there is a highly significant difference between the groups ($p<0.001$). Post-Hoc contrasts indicate that significant differences exist between the MM transect, which has the lowest production per shoot (3.08 mg DW shoot^{-1} day^{-1}) and the MS and the CS transects, which have higher production rates (7.69 and 9.51 mg DW shoot^{-1} day^{-1}, respectively). The difference between the MS and CS transect is only just significant ($p=0.04$).

Table 3.2.5. Carbon isotope signature ($\partial^{13}C$) of particulate organic material collected with sediment traps in the seagrass zone of Gazi Bay. Means and S.D. Data sharing a common superscript letter a not significantly different (α=0.05).

Location		$\partial^{13}C$ (‰)	No. of obs.
subtidal	MM	-23.30 ± 0.40[a]	4
subtidal	MS	-22.47 ± 0.21[a]	3
subtidal	CS	-19.15 ± 0.85[b]	3
subtidal	CC	-13.96 ± 0.63[c]	4

The phosphorus contents of the third leaves of *T. ciliatum* on the different transects were similar, ranging from 0.17% DW (at the MM transect) to 0.23% DW (at Chale). Analysis of variance showed that the differences between groups were not significant.

The nitrogen contents on the various transects varied between 1.76% DW (at Chale) to 2.46% DW (at the CS transect). Analysis of variance followed by Post-Hoc contrasts shows that the nitrogen contents at the CS and Chale locations were significantly different from the other values determined at the MM, MS and CC transects. The nitrogen contents at these three transect were nearly identical.

The carbon content of the various leaf samples showed little variation, ranging between 37 and 42%. The C:N:P (atomic) ratios that can be calculated from the data are presented in Table 3.2.8.

discussion

The carbon isotope signatures of leaves and sediments

Table 3.2.6. C:N ratios of seston collected at subtidal transects during one ebb and two flood tides (data of the two flood tides were pooled), and of sediment trap contents. Seston data were statistically analysed per row. Data sharing a common superscript letter are not significantly different (α=0.05). For comparison, C:N ratios of the dominant seagrass and mangrove species in the study area are also given. The data of *Thalassodendron* are from the 3 samples of pooled third-youngest leaves collected at the MM transect. Data of mangrove leaves are based on two samples of pooled leaves (10-20 leaves).
Means and S.D. Number of observations given in brackets.

Location	sedim. traps	seston ebb water	seston flood water
subtidal MM	10.0 ± 1.0^{ab} (4)	7.0 ± 1.7^{b} (5)	10.0 ± 1.6^{a} (10)
subtidal MS	11.2 ± 0.5^{b} (3)		
subtidal CS	9.1 ± 1.5^{a} (3)	6.8 ± 1.2^{b} (6)	
subtidal CC	8.5 ± 0.7^{a} (4)		6.5 ± 0.9^{b} (11)

seagrass and mangrove leaves

	fresh leaves		senescent leaves	
Thalassodendron ciliatum	19.3 ± 0.4	(3)		
Rhizophora mucronata	43.0	(2)	193	(*)
Ceriops tagal	59.2	(2)	218	(*)
Bruguiera gymnorrhiza	44.5	(2)	187	(*)
Sonneratia alba	25.1	(2)	72	(*)
Avicennia marina	31.8	(2)	88	(*)

(*) data from Rao *et al.*, (1993)

collected in the mangrove forest show that the organic matter in the mangrove is characterized by strongly negative $\partial^{13}C$ values. Only the $\partial^{13}C$ value of the sediment of the seagrass zone in direct proximity of the mangrove (MM transect) falls in the range of the mangrove sediment values. Further away the mangrove signal fades out rapidly and our data indicate that already at a distance of 2 km from the mouth of Kinondo creek the input of mangrove carbon is of marginal influence in determining the $\partial^{13}C$ value of the sediment. Thus it appears that during ebb flow carbon depleted in ^{13}C is exported from the mangrove but that all or part of this outwelling carbon is trapped in the seagrass zone before it reaches the coral reefs. Remarkably the carbon isotope signature of *Thalassodendron* shows a trend similar to that of the sediment values with increasing distance from the mangrove. It

Table 3.2.7. Production characteristics of *T. ciliatum* meadows on the MM, MS and CS transects in Gazi Bay. Means and S.D. of observations on four plots per transect. Data in columns sharing a common superscript letter are not significantly different.

Transect	PIL (days)	Production/shoot (mg DW shoot^{-1} day^{-1})
MM	10.98 ± 1.24^{a}	3.08 ± 0.64^{a}
MS	8.46 ± 0.59^{b}	7.69 ± 1.02^{b}
CS	8.17 ± 0.39^{b}	9.51 ± 1.35^{c}

Table 3.2.8. Relationship between the carbon, nitrogen and phosphorus contents (C:N:P atomic ratios) of third-youngest leaves of *T. ciliatum*, collected at the four transects in Gazi Bay and in Chale lagoon.

Location	C:N:P atomic ratio
MM	605 : 26 : 1
MS	545 : 24 : 1
CS	524 : 28 : 1
CC	583 : 25 : 1
Chale	454 : 17 : 1

is known that the isotope signature of seagrasses is highly variable (McMillan *et al.*, 1980). Probably, these values are a reflection of the amount of mangrove carbon that is available for assimilation by the seagrasses. CO_2 resulting from the mineralization of mangrove-POM trapped in the seagrass zone will supply *T. ciliatum* with inorganic carbon relatively depleted in ^{13}C; moreover, it cannot be excluded that dissolved respiratory CO_2, directly exported from the mangrove forest, is a source of carbon for the seagrass.

There appears to be not only a simple unidirectional efflux of carbon from the mangroves, but also a reversed flux from the seagrass zone back to the mangroves. During both flood tides which were studied, highly significant decreases in the $\partial^{13}C$ values of the seston from the CC to the MM transects were found (± 5‰), coinciding with significant increases in the POC content of the seston. The $\partial^{13}C$ values of the flood seston at the MM transect (ca. -23‰) are clearly more negative than the $\partial^{13}C$ value of the seagrass vegetation at this transect (-19.65‰). These strongly negative values suggest that at least part of the carbon taken up in the seagrass zone by the flood tides, originally comes from the mangrove forest. Presumably, both autochtonous seagrass particles and allochtonous particles from the mangroves, deposited in the seagrass zone at earlier ebb tides, will be taken up by the incoming water and transported into the forest. Circumstantial evidence for this process, moreover, is found in the carbon isotope signature of the mangrove sediment. The $\partial^{13}C$ sediment value of the *Rhizophora mucronata* sample site, a low-lying site that is inundated each flood tide, is conspicuously less negative (2.9‰) than the $\partial^{13}C$ values of the *R. mucronata* leaves. Such a decrease would not be expected if litter from the tree was the only source of the organic matter in the sediment, the more so as the carbon isotope signature of leaves of *R. mucronata* in Gazi bay shows more pronounced ^{13}C depletion in senescent leaves prior to leaf fall (Rao *et al.*, in press). Sedimentation of particulate material from the seagrass zone in the *R. mucronata* zone would result in less depleted sediment $\partial^{13}C$ values. Using the $\partial^{13}C$ values of the flood seston and of those the *R. mucronata* leaves as end members, a simple calculation indicates that to arrive at the $\partial^{13}C$ sediment value, *R. mucronata* carbon and flood seston carbon would have to be mixed in a proportion of 1: 1.33. At the *Ceriops tagal* site the difference between carbon isotope signature of sediment and leaf material is small (1.4‰ lower in the sediment). This site is only inundated at spring tides, and the external input of tidally born particulate matter probably is more restricted.

The material captured by the sediment traps in the seagrass zone will be a mixture of locally derived resuspended particles and allochtonous material. It is remarkable that the C:N ratio of the seston collected in the sediment traps is low, varying between 8.5 and 11.2. Neither these values, nor the C:N ratios of the seston obtained by filtering the tidal water above the seagrass zone (C:N ratios 6.5 to 10), are close to the C:N ratios of either mangroves or seagrasses (Table 3.2.4). Possibly, the seston contains an important fraction of organic particles derived from the mangroves and seagrass vegetation that has already gone through a phase of intensive processing; this has resulted in shifts in the chemical characteristics of these particles. We have suggested above that the organic particles from the mangroves (together with seagrass particles) may go through repeated efflux-reflux cycles. These transport cycles enhance the proportion of older, more processed organic material in the seston and may therefore be a crucial element in explaining the low C:N ratios of seston and seston trap material.

A progressive change in C:N ratios may be caused by several processes. Increases in nitrogen levels during decomposition have been observed in many types of vascular plant detritus (Swift *et al.*, 1979). Robertson (1988) observed this phenomenon also during decomposition in mangrove leaves. The C:N ratio in decomposing leaves of *Rhizophora stylosa*, *Avicennia marina* and *Ceriops tagal* was approximately halved after 160 days of decomposition. Secondly, nitrogen fixation may enrich the litter. Nitrogen fixation activity is widespread in the mangrove forest (Alongi *et al.*, 1992), and is also found in association with decaying leaf litter (Goto & Taylor, 1976; van der Valk & Attiwill, 1984). Nitrogen fixation was found both in the mangroves and in *Thalassodendron* meadows in Gazi bay (A.F. Woitchik, this cruise report). Thirdly, several studies have shown that planktonic bacteria have a low carbon conversion efficiency on detrital substrates (Newell *et al.*, 1981; Linley & Newell, 1984; Bauerfeind, 1985; Bjornsen, 1986). We may speculate that a decrease in C:N ratio of detritus-bacteria aggregates is furthered by such a low conversion efficiency of the heterotrophic bacteria associated with the particles.

We may summarize the key features of POM fluxes in Gazi Bay which emerge from this study as follows: (1) spatially restricted outwelling of mangrove carbon; (2) reversed fluxes of POM from the seagrass zone to the mangroves; (3) transported POM characterized by low C:N ratios.

In Gazi Bay, the seagrass zone appears to function as a buffer in between the mangroves and the coral reefs, trapping outwelling POM at close distance from the mangroves. This spatially restricted outwelling of mangrove-POM implies that effects of the exported

mangrove-POM primarily must be sought in the adjacent seagrass zone. The data on the stable carbon isotope analyses indicate that the MM transect is most prominent under the influence of carbon fluxes outwelling from the mangrove. We found that the rate of leaf renewal and leaf production were significantly lower at the MM transect than at the MS and CS transects (Table 3.2.7). This result does not support the assumption of an increased nutrient availability in the transect nearest to the mangrove. Moreover, the data also show that the differences between the MS and CS transects as far as PIL or leaf production are concerned, are small or absent, although there is a conspicuous difference between these transects with respect to the input of mangrove-carbon. The combined data thus do not point to a consistent relation between the trapping of carbon from the mangrove on the one hand and the rate of leaf renewal and leaf production on the other hand.

The phoshorus and nitrogen contents of third-youngest leaves of *T. ciliatum* ranged between 0.17-0.23% DW and 1.76-2.46% DW, respectively. These values are typical for the nutrient content of seagrass leaves in general (Duarte, 1990). Our data show that there is no significant difference between the leaf phosphorus contents at the various locations. The leaf nitrogen contents at the four transects are similar except for the leaves originating from the CS transect, which have a relatively high content. These data on nutrient content thus indicate that the outwelling material flux from the mangrove does not enhance the nutrient contents of adjacent *T. ciliatum* vegetation.

What can be the reason that neither leaf production nor leaf nutrient contents are increased in *T. ciliatum* meadows that are the evident recipients of outwelling mangrove carbon? A first possibility would be that nutrients are not limiting to the *T. ciliatum* meadows in Gazi bay. In that case, trapping of nitrogen and phosphorus associated with outwelling mangrove carbon would not be expected to enhance growth or leaf nutrient contents. With the data on growth only, this possibility can neither be rejected nor supported, as these data do not tell us if there would be further scope for growth with an increased nutrient supply. The nutrient content of the leaves probably allows a better assessment of the nutrient availability in the *T. ciliatum* meadows. The third-youngest leaves of *T. ciliatum* had phosphorus and nitrogen contents (c. 0.2% DW phosphorus and 2.3% DW nitrogen) which are much lower than the maximum phosphorus (> 0.7%) and nitrogen (> 5%) values reported in a literature survey (Duarte, 1990). The last-mentioned author also made a comparison of nutrient enrichment studies which led him to the conclusion that seagrasses with phosphorus contents below 0.2% DW and nitrogen levels below 1.8% DW were probably nutrient limited. In view of these findings we consider it unlikely that in Gazi bay phosphorus and nitrogen were available at saturation levels for *T. ciliatum*. We thus reject the possibility that the absence of nutrient limitation caused the lack of effect of mangrove outwelling on seagrass growth and nutrient content.

A second possibility that must be considered is that outwelling and trapping of mangrove carbon is a phenomenon on itself, *i.e.*, that this process does not coincide with a simultaneous outwelling and uptake of nutrients (phosphorus and nitrogen). This could be the case if the outwelling mangrove carbon only consisted of inorganic carbon (dissolved CO_2, bicarbonate and carbonate) depleted in ^{13}C. The $\partial^{13}C$ of oceanic dissolved inorganic carbon normally is c. 0‰ (Boutton, 1991). Mangrove leaves, the major category of organic litter produced by the mangrove trees in Gazi Bay, have $\partial^{13}C$ values ranging from c. -25 to -28‰ (Table 3.2.1). Uptake of ^{13}C-depleted CO_2 resulting from leaf decomposition in the tidal water inundating the mangrove, thus would reduce the $\partial^{13}C$ value of the inorganic carbon pool. This ^{13}C depleted inorganic carbon subsequently would become available to *T. ciliatum* when the ebb water crossed the seagrass zone.

Although this process may explain the ^{13}C depletion of *T. ciliatum* in the proximity of the mangrove, the exclusive outwelling of inorganic mangrove carbon is difficult to reconcile with the observations presented in the foregoing which clearly indicate that particulate organic matter is exported from the mangrove. We therefore assume that the most likely explanation for our findings is that carbon outwelling from the mangrove includes both dissolved inorganic and particulate organic compounds, but that the nutrient input associated with trapping of the latter category is insufficient to have a measurable influence on seagrass functioning.

references

Alongi, D.M., K.G. Boto & A.I. Robertson, 1992. Nitrogen and phosphorus cycles, p. 251-292. In: Robertson, A.I., Alongi, D.M. (eds), Tropical mangrove ecosystems. American Geophysical Union.

Bauerfeind, S., 1985. Degradation of phytoplankton detritus by bacteria: estimation of bacterial consumption and respiration in an oxygen chamber. Mar. Ecol. Prog. Ser. 21: 27-36.

Birkeland, C., 1987. Nutrient availability as a major determinant of differences among hard-substratum communities in different regions of the tropics. In: Birkeland, C. (ed.), Differences between Atlantic and Pacific tropical marine coastal ecosystems: community structure, ecological processes, and productivity: 45-90. UNESCO, Paris.

Bjornsen, P.K., 1986. Bacterioplankton growth yield in continuous seawater cultures. Mar. Ecol. Prog. Ser. 30: 191-196.

Boto, K.G. & J.S. Bunt, 1981. Tidal export of particulate organic matter from a Northern Australian mangrove system. Est. Coast. Shelf Sci. 13: 247-255.

Boutton, T.W., 1991. Stable carbon isotope ratios of natural materials: II. Atmospheric, terrestrial, marine, and freshwater environments. In: D.C. Coleman & B. Fry (Eds), Carbon isotope techniques: 173-187. Academic Press, New York.

Brock, R.E. & S.V. Smith, 1983. Response of coral reef cryptofaunal communities to food and space. Coral Reefs 1: 179-193.

Brouns, J.J.W.M., 1985. A preliminary study of the seagrass *Thalassodendron ciliatum* (Forssk.) den Hartog from Eastern Indonesia. Aquat. Bot., 23: 249-260.

Duarte, C.M., 1990. Seagrass nutrient content. Mar. Ecol. Prog. Ser.,67: 201-207.

Flores-Verdugo, F.J., J.W. Day & R. Briseno-Duenas, 1987. Structure, litter fall, decomposition, and detritus dynamics of mangroves in a Mexican coastal lagoon with an ephemeral inlet. Mar. Ecol. Prog. Ser. 35: 83-90.

Fourqurean, J.W., J.C. Zieman & G.V.N. Powell, 1992. Relationships between porewater nutrients and seagrasses in a subtropical carbonate environment. Mar. Biol. 114: 57-65.

Goto, J.W. & B.F. Taylor, 1976. N_2 fixation associated with decaying leaves of the red mangrove (*Rhizophora mangle*). Appl. Env. Microbiol. 31: 781-783.

Hallock, P., 1988. The role of nutrient availability in bioerosion: consequences to carbonate buildups. Palaeogeogr., Palaeoclimat., Palaeooecol. 63: 275-291.

Harlin, M.M. & B. Thorne-Miller, 1981. Nutrient enrichment of seagrass beds in a Rhode Island coastal lagoon. Mar. Biol. 65: 221-229.

Jacobs, R.P.W.M., 1979. Distribution and aspects of the production and biomass of eelgrass, *Zostera marina* L., at Roscoff, France. Aquat. Bot., 7: 151-172.

Linley, E.A.S. & R.C. Newell, 1984. Estimates of bacterial growth yields based on plant detritus. Bull. Mar. Sci. 35: 409-425.

McMillan, C., P.L. Parker & B. Fry, 1980. $^{13}C/^{12}C$ ratios in seagrasses. Aquat. Bot. 9: 237-249.

Newell, R.C., Lucas, M.I., Linley, E.A.S. (1981). Rate of degradation and efficiency of conversion of phytoplankton debris by marine micro-organisms. Mar. Ecol. Prog. Ser. 6: 123-136.

Rao, R.G., A.F. Woitchik, L. Goeyens, A. van Riet, J. Kazungu & F. Dehairs. Carbon, nitrogen contents and stable carbon isotope abundance in mangrove leaves from an East African coastal lagoon (Kenya). Aquat. Bot. (in press)

Robertson, A.I., 1986. Leaf-burying crabs: their influence on energy flow and export from mixed mangrove forests (*Rhizophora* spp.) in north east Australia. J. Exp. Mar. Biol. Ecol. 102: 237-248.

Robertson, A.I., 1988. Decomposition of mangrove leaf litter in tropical Australia. J. Exp. Mar. Biol. Ecol. 116: 235-247.

Short, F.T., 1983. The seagrass, *Zostera marina* L.: plant morphology and bed structure in relation to sediment ammonium in Izembek Lagoon, Alaska. Aquat. Bot. 16: 149-161.

Short, F.T., 1987. Effects of sediment nutrients on seagrasses: literature review and mesocosmos experiment. Aquat. Bot. 27: 41-57.

Smith, S.V., W.J. Kimmerer, E.A. Laws, R.E. Brock & T.W. Walsh, 1981. Kaneohe Bay sewage diversion experiment: perspectives on ecosystem responses to nutritional perturbation. Pac. Sci. 35: 279-395.

Swift, M.J., O.W. Heal & J.M. Anderson, 1979. Decomposition in terrestrial ecosystems. Blackwell.

Twilley, R.R., 1985. The exchange of organic carbon in basin mangrove forests in a southwest Florida estuary. Est. Coast. Shelf Sci. 20: 543-557.

Van der Valk, A. & P.M. Attiwill, 1984. Acetylene reduction in an *Avicennia marina* community in southern Australia. Austr. J. Bot. 32: 157-164.

Wolanski, E., Y. Mazda & P. Ridd, 1992. Mangrove hydrodynamics. In: Robertson, A.I., Alongi, D.M. (eds), Tropical mangrove ecosystems: 43-62. American Geophysical Union.

Woodroffe, C., 1992. Mangrove sediments and geomorphology. In: Robertson, A.I., Alongi, D.M. (eds), Tropical mangrove ecosystems: 7-42. American Geophysical Union.

Identifying fish samples.

3.3. FISH FAUNA OF MANGROVE CREEKS, SEAGRASS MEADOWS AND SAND FLATS IN GAZI BAY: A STUDY WITH NETS AND STABLE ISOTOPES

G. van der Velde[1], P.H. van Avesaath[1], M.J. Ntiba[2], G.K. Mwatha[3], S. Marguillíer[4], A.F. Woitchik[4]

[1] Catholic University, Department of Aquatic Ecology, Nijmegen

[2] University of Nairobi, Nairobi, Kenya

[3] Kenya Marine and Fisheries Research Institute, Mombasa, Kenya

[4] Free University, Brussels, Belgium

introduction

Shallow bays with mangroves and seagrass meadows are known to be nursery grounds or feeding areas for many fish species. Some species occur both as juveniles and as adults in these biotopes, but others move to other biotopes as adults such as depth zones on the coral reef and *vice versa.*

Although seagrass meadows and mangroves often coexist in close proximity, their fish faunas have usually been studied separately. Very few studies included fishes of coral reefs, seagrass beds and mangroves together. This has been partly due to methodological problems. In this progress report the study of the relation between the fish assemblages of the biotopes in Gazi Bay (Fig. 3.3.1) is described. The combined measurement of $\partial^{13}C$ and $\partial^{15}N$ of the tissue of fish and the natural abundance of these isotopes provides a tool to determine the sources of nutrition for the fish and indicates trophic relationship among the fish and other organisms. Isotope enrichment occurs between animals and their foods. ^{13}C enrichment is estimated at about 1‰ per trophic level for carbon ^{15}N enrichment at 3-4‰ for nitrogen (Fry & Sherr, 1984, Minagawa & Wada, 1984). This information may provide insight into the role in the food web of the fish species selected.

materials and methods

Several locations in Gazi Bay were sampled (Fig. 3.3.2). Various fishing techniques were used to describe the community structure of the fish assemblages of the different sites. Of the passive fishing gear, the fike nets (stretched mesh size 20 mm, length 1.6 m) were the most successful. They were used to catch fish at several sites in the eastern creek of the mangrove area. Due to the relatively poor visibility in the water, the visual census count technique could only be used in or near the mangrove area and the inner slope of the coral reef. Of the active fishing gear, the beam trawl (stretched mesh size 20 mm, width 1.5 m) appeared to be the most successful. Using this technique, several habitats were sampled, creating a transect from the mangroves towards the coral reef. The hauls of the beam trawl were standardized to allow a comparison of the relative abundance of the fish caught at the various locations. At each site 3 hauls of about 500 m length were made during daytime. These hauls were regarded as replicate samples. The trawl was towed by two inflatables with 25 Hp outboard engines at low speed. The fish caught during a haul were put in marked plastic bags which were subsequently stored in styrofoam boxes filled with ice for transport. The fishes were stored in a freezer the same day and identified, measured (total length) and weighed the next day. After formaline (4%) had been injected into the intestines via the anus, the fishes of each sample were put together in plastic bags with pores in which a waterproof label was introduced. The fish were kept in formaline (4%) for one day. The next day, the formaline was replaced by ethanol (70%). To allow optimum preservation, the bags with the samples were put in plastic barrels containing 70% alcohol after 2-3 days and stored in a deep freezer for transport to the Netherlands on board the RV *Tyro*. The intention was to use the preserved fish for a study of the stomach content. Part of the collection was transported to the University of Nairobi.

Tissue samples were taken from a selection of fish species for a combined $\partial^{13}C$ and $\partial^{15}N$ analysis. The samples were stored in a freezer. The Laboratory for Analytical Chemistry of the Free University of Brussels carried out this analysis. Dry muscle tissue was lyophilized and ground to a fine powder. This powder was directly used for nitrogen and carbon analyses. The analyses were performed using mass spectrometric measurements (Delta E, Finnigan Mat Isotope ratio mass spectrometer). Stable carbon isotope abundances are expressed relative to the PDB (Pee Dee Belemnite) standard:

$$\partial^{13}C = \left[\left(\frac{^{13}C/^{12}C_{sample}}{^{13}C/^{12}C_{PDBstandard}}\right) - 1\right] \times 1000$$

$\partial^{15}N$ values are reported relative to nitrogen in air. High-purity tank nitrogen gas was used as working standard during sample analysis. This working standard was calibrated against N1 and N2 ammonium sulphate (IAEA, ref. 100 and 106) for $\partial^{15}N$ (Minagawa *et al.*, 1984; Nevins *et al.*, 1985).

$\partial^{15}N$ was calculated as:

$$\partial^{15}N = \left[\left(\frac{^{15}N/^{14}N_{sample}}{^{15}N/^{14}N_{standard}}\right) - 1)\right] \times 1000$$

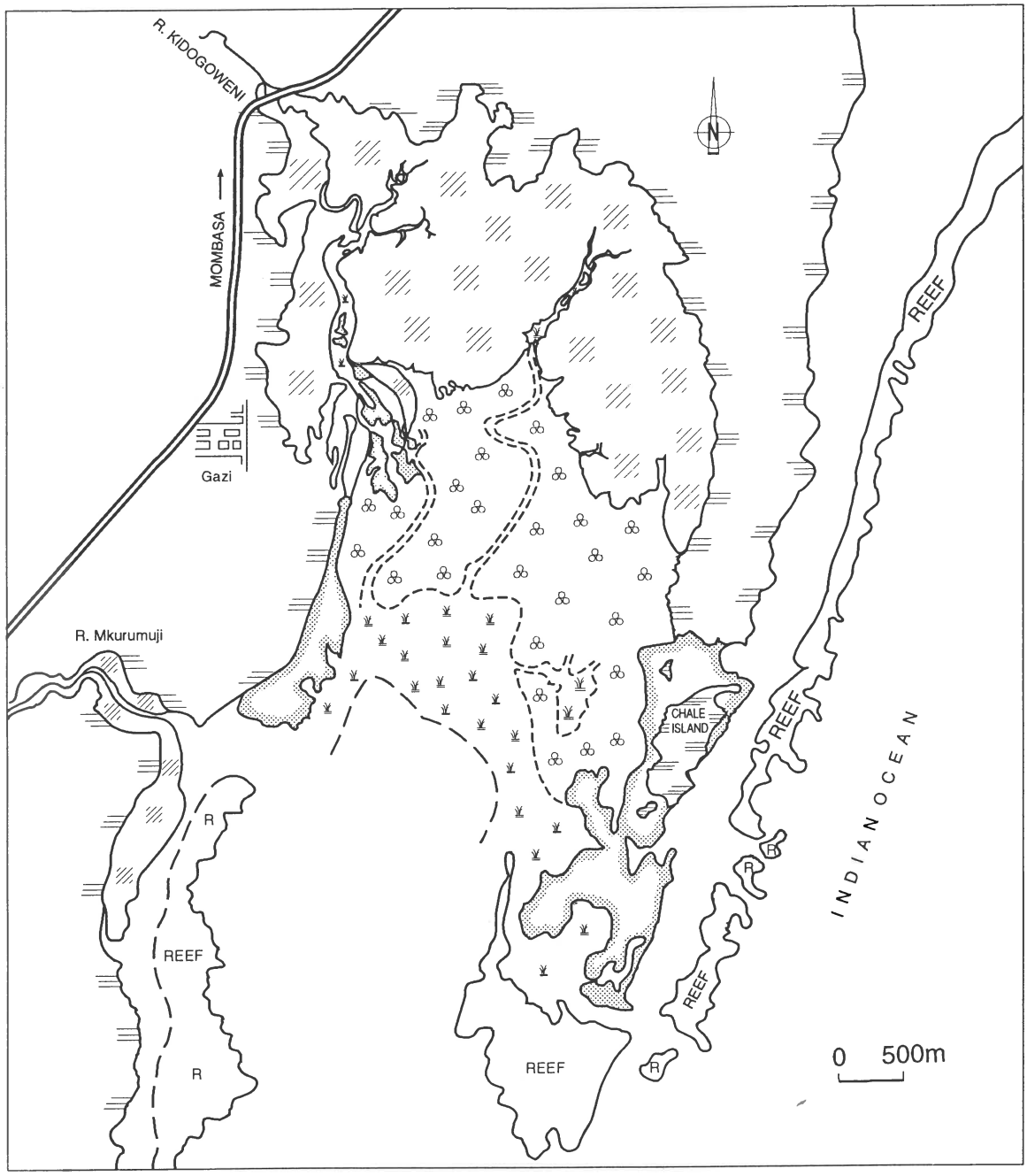

Fig. 3.3.1. Gazi Bay with the main biotopes.

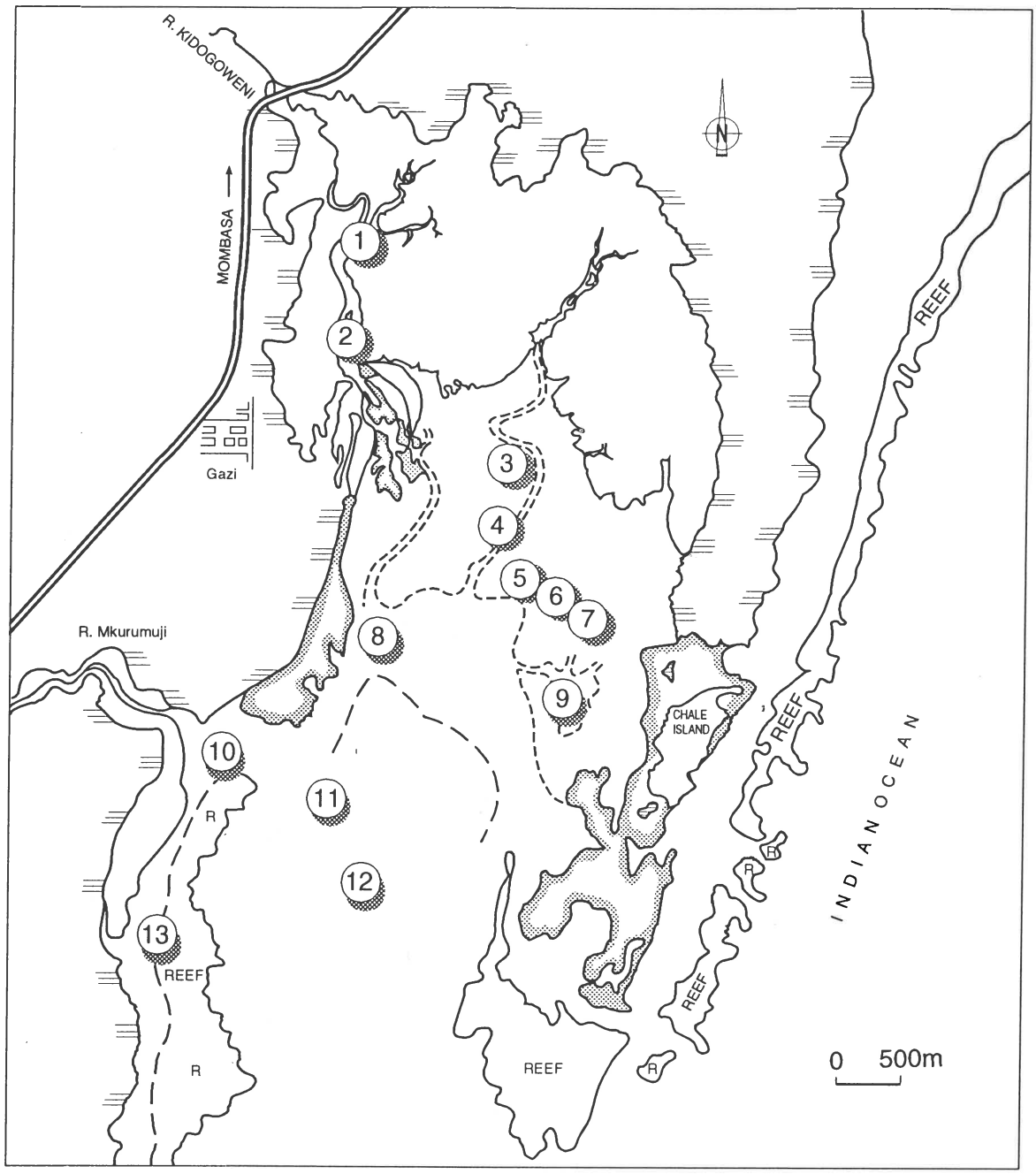

Fig. 3.3.2. Location of beam trawl sampling sites

The data of the fish catches were processed using (SAS (Statistical Analyzing System). Computer programs (TWINSPAN, FLEXCLUS) were used for the clustering of the data.

preliminary results

The various fishing techniques yielded a total of about 2000 specimens of fish, belonging to 95 fish species (Table 3.3.1). A spectacular fish caught was that of a specimen of the Slender guitarfish (*Rhinobatos holcorhynchus*) in shallow water in the mouth of the bay. This rare fish species is normally caught at depths of 75-183 m and considered to be endemic for the coast from Port Shepstone to kwaZulu (Smith & Heemstra, 1986; Compagno *et al.*, 1989). Its occurrence can the result of upwelling during the monsoon period. Another species indicating this is the Blackspotted electric ray (*Torpedo fuscomaculata*) of which a decaying specimen was found. It was not collected because of the bad state of the specimen. This species

Table 3.3.1. Preliminary list of fish species with numbers of caught specimens from Gazi Bay. Nomenclature according to Smith & Heemstra (1986).

Fowleria aurita	234	Cheilinus trilobatus	6
Siganus sutor	214	Epibulus insidiator	6
Leptoscarus vaigiensis	185	Calotomus spinidens	6
Apogon thermalis	166	Canthigaster solandri	6
Plotosus lineatus	93	Gerres oyena	5
Archamia fucata	83	Cheilinus chlorourus	5
Scarus ghobban	80	Dascyllus aruanus	4
Lethrinus ramak	76	Synodus binotatus	3
Gazza minuta	75	Histrio histrio	3
Parascorpaena mossambica	70	Aeoliscus punctulatus	3
Paramonacanthus barnardi	65	Pterois miles	3
Archamia mozambiquensis	45	Apogon fraenatus	3
Lethrinus harak	43	Cheilodipterus quinquelineatus	3
Foa brachygramma	38	Abudefduf vaigiensis	3
Sphaeramia orbicularis	35	Valamugil seheli	3
Petroscirtes mitratus	31	Sphyraena barracuda	3
Apogon cookii	28	Lactoria cornuta	3
Plotosus nkunga	24	Arothron immaculatus	3
Syngnathoides biaculeatus	20	Taeniura lymma	2
Plectorhinchus gaterinus	20	Hippocampus histrix	2
Stethojulis strigiventer	20	Epinephelus sp.	2
Bothus pantherinus	20	Terapon jarbua	2
Apogon savayensis	19	Parupeneus indicus	2
Arothron hispidus	19	Amblygobius albimaculatus	2
Apogon guamensis	17	Torpedo fuscomaculata[1]	1
Pelates quadrilineatus	16	Rhinobatos holcorhynchus	1
Plectroglyphidodon lacrymatus	15	Anguilla bicolor bicolor	1
Apogon nigripes	13	Myrichthys maculosus	1
Lutjanus cf. fulviflamma	13	Myrichthys colubrinus	1
Siganus stellatus	13	Pisodonophis cancrivorus	1
Canthigaster valentini	13	Chirocentrus dorab	1
Papilloculiceps longiceps	12	Synodus variegatus	1
Siphamia mossambica	12	Antennarius pictus	1
Pardachirus marmoratus	11	Sargocentron diadema	1
Diodon holocanthus	11	Myripristis kuntee	1
Chrysiptera annulata	10	Fistularia commersonii	1
Petroscirtes breviceps	10	Neoniphon sammara	1
Lactoria fornasini	10	Hippichthys spicifer	1
Lethrinus variegatus	9	Solenostomus cyanopterus	1
Priolepis inhaca	9	Dactyloptena sp.	1
Gymnothorax sp.	8	Upeneus tragula	1
Pomacentrus trilineatus	8	Cheilio inermis	1
Cyclichthys spilostylus	8	Pseudojuloides argyreogaster	1
Novaculichthys macrolepidotus	7	Synchiropus marmoratus	1
Pteragogus flagellifer	7	Amblygobius sphynx	1
Conger cinereus cinereus	6	Acanthurus sp.	1
Saurida gracilis	6	Naso brevirostris	1
Cheilinus bimaculatus	6	Cynoglossus sp.	1

[1] Not collected

13 fishes were identified to the family level only and are not included in this list.

is recorded from deep water but also from estuaries. It was not known from Kenya (Smith & Heemstra, 1986; Compagno *et al.*, 1989). *Fowleria aurita*, *Siganus sutor*, *Leptoscarus vaigiensis* and *Apogon thermalis* were caught in the highest numbers. *Siganus sutor* and *Leptoscarus vaigiensis* were caught most frequently, being present in 70 % of the beam trawl catches. *A. thermalis* and *F. aurita* were caught in high numbers locally. Of the fish species that were caught in lower numbers, *Parascorpaena mossambica* was caught most frequently: like *S. sutor* and *L. vaigiensis*, it was found in 70 % of the beam trawl catches. Demersal fish species such as *Fistularia commersonii* and *Sphyraena barracuda* were caught in small numbers.

As the beam trawl appeared to be the most successful fishing gear, most fish were caught using this technique. A total of 13 sites were sampled (Fig. 3.3.2) with the beam trawl by which a transect was made from the mangrove area (western creek) towards the coral reef. The substrates of the sites consisted mainly of sand, with or without a vegetation of seagrass. The substrate of sites 10 and 12 did not have any vegetation. The vegetation of site 1 and 11 was sparse, consisting mainly of *Thalassia hemprichii*. The vegetation of the other sites consisted mainly of dense *Thalassodendron ciliatum* beds at depths ranging from 1 to 2 m at low tide. *Enhalus acoroides* was found locally only at site 3.
The highest numbers of fish were caught in the *Thalassodendron ciliatum* beds near the eastern mangrove creek (sites 3 and 5, Fig. 3.3.3). Due to the presence of coral blocks in the eastern creek, it was not possible to trawl in or near the eastern part of the mangrove area. In general, the eastern part of the bay yielded more fish belonging to more species. The trawls in or near the western creek were not very successful. The substrate of these sites (nos. 1, 2 and 8) consisted mainly of bare sand with little or no vegetation. The water current at sampling time at sites 1 and 2 was relatively strong. At site 12 no fish were caught at all. The site was in the middle of a bare sand flat at a depth of approximately 8 m at low tide.

As the distribution patterns of the more frequently caught fish species did not provide a clear insight into the use of the different areas of Gazi bay by the fish, statistical analysis programmes as TWINSPAN and FLEXCLUS were used to group the data (Tables 3.3.2, 3.3.3, 3.3.4 and 3.3.5). Only the beam trawl data were used in the analysis.

Clustering the compositions of the fish catches at the family level yielded three distinguishable groups. Two samples (fish catches at sites 1 and 11, Tables 3.3.3, 3.3.4) showed no similarity with other samples. The sample at site 11 was separated at the first level, while the sample at site 1 was separated at the third level. The first group of samples (cluster A, Table 3.3.2) represents fish catches near the mangrove area. The second group of samples (cluster B, Table 3.3.2) consists of samples from sites in seagrass meadows in the bay. The third group (cluster C, Table 3.3.2) consists of two samples taken at sites with little or no vegetation. The sample of site 12 was not taken into account in the

Table 3.3.2. Dendrogram of the hierarchic clustering of the composition of the fish catches of the several locations at the family-level (TWINSPAN).

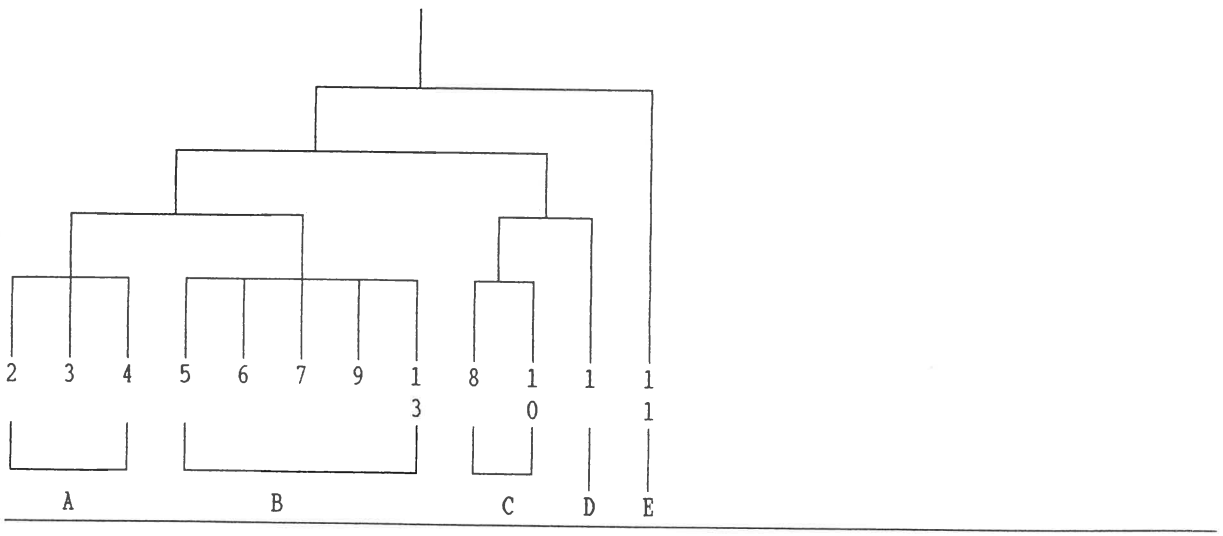

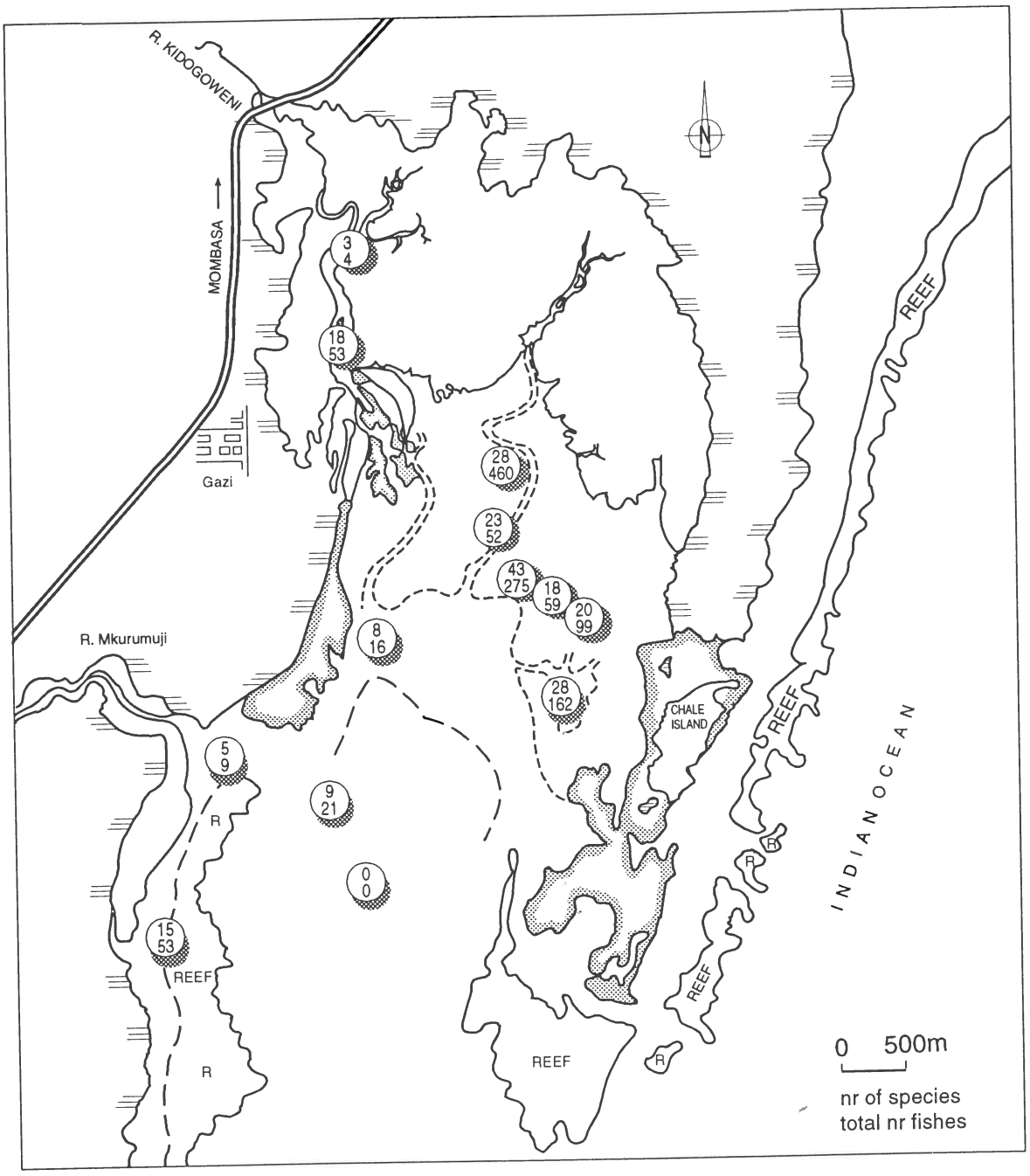

Fig. 3.3.3. Distribution of species numbers and total numbers of caught fishes.

analysis, because no fish were caught at this site. The average similarity between the groups created with TWINSPAN is relatively low (Table 3.3.3). The isolation (the average similarity of the samples within the groups divided by the average similarity between the groups, Table 3.3.3) of clusters A and B is low, implying a high similarity between the clusters. Despite this fact, the distinction between the clusters was maintained because of the occurrence of specific families in the clusters. Muraenidae, Teraponidae, Haemulidae, Blenniidae and Gobiidae were specific for cluster A, while Synodontidae and Lutjanidae were only present in cluster B. Monacanthidae and Ostraciidae were only found at the sites of cluster C, while Labridae and Diodontidae were found here with high frequencies. Syngnathidae and Platycephalidae only showed up with high frequencies in the samples of clusters B and C. Plotosidae were only frequent in cluster D.

The clustering of the data at the species level showed

Table 3.3.3. Resemblance of the samples of the clusters of the composition of the fish catches of the several locations at family level (FLEXCLUS).

CLUSTER	SIZE	AVERAGE RESEMBLANCE	MOST SIMILAR TO	RESEMBLANCE	ISOLATION
E	1	1.0000	F	0.0345	29.0000
A	3	0.1065	B	0.6496	0.1639
B	5	0.5052	A	0.6496	0.7776
C	2	0.2169	B	0.1554	1.3956
F	1	1.0000	B	0.0397	25.1761

a similar pattern. At the third level of the hierarchic clustering programme TWINSPAN two groups were distinguished (Table 3.3.4). Sites 1 and 11 were separated just as in the clustering at family level. In contrast with the clustering at family level, the samples taken at sites 8 and 10 did not constitute a separate group. Furthermore, the sample of site 5 was joined with the samples of sites 2, 3 and 4 (cluster A of the clustering at family level). These samples were grouped together because *Apogon thermalis*, *Foa brachygramma*, *Plectorhinchus gaterinus*, *Lethrinus harak*, *Petroscirtus mitratus*, *Siganus stellatus*, *Bothus pantherinus* and *Arothron immaculatus* were only present in this cluster. *Apogon nigripes* was found only in cluster A of the clustering at species level. In general, the distinction between the samples from sites in seagrass meadows near the mangrove area and those from sites in seagrass beds in the bay remained intact.

In order to describe the use of the seagrass beds by the fish assemblage, the stable isotope content of muscle tissue of a selection of fish species were determined. The fish were caught near the mangroves. The $\partial^{13}C$ values ranged from -13.3 to -21.2‰ and $\partial^{15}N$ values ranged from +3.5 to +12.2‰ (Fig. 3.3.4). A first distinction in the data was made using cluster analysis (FLEXCLUS) (Fig. 3.3.4). Two groups were distinguishable. The programme clustered a group of fish species with relatively high $\partial^{15}N$ and low $\partial^{13}C$ ratios of the muscle tissue. These are fish species that use the seagrass meadows as a life time habitat. A second group was formed of fish species with lower $\partial^{15}N$ and higher $\partial^{13}C$ ratios of the muscle tissue. Based on literature data, these can be considered migrating fish species. The smaller specimens of *Siganus sutor* did not show a similarity with the two distinct groups. An explanation for this effect could not be found. Within a species bigger fish show a higher $\partial^{15}N$ and $\partial^{13}C$ ratio of the muscle tissue. This indicates that the age or volume or the fish influences either feeding characteristics of the fish or the allocation of the stable isotopes (or both). More research is needed to study this

Table 3.3.4. Dendrogram of the hierarchic clustering of the composition of the fish catches of the several locations at the species-level (TWINSPAN).

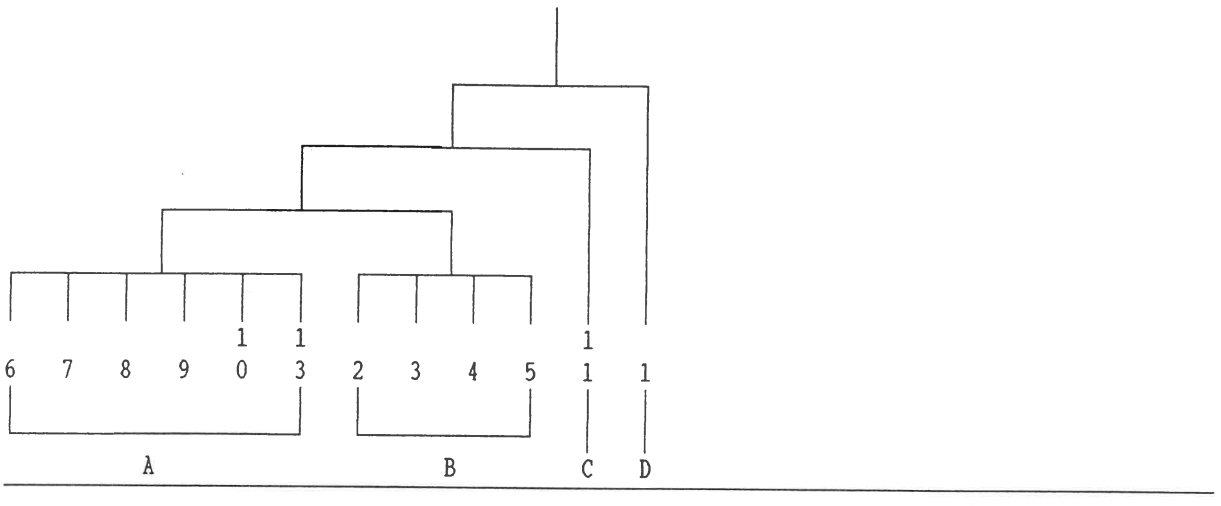

Table 3.3.5. Resemblance of the samples of the clusters of the composition of the fish catches of the several locations at species level (FLEXCLUS).

CLUSTER	SIZE	AVERAGE RESEMBLANCE	MOST SIMILAR TO	RESEMBLANCE	ISOLATION
D	1	1.0000	C	0.0123	81.0000
B	4	0.3000	A	0.2173	1.3808
A	6	0.3191	B	0.2173	1.4686
C	1	1.0000	A	0.0193	51.6878

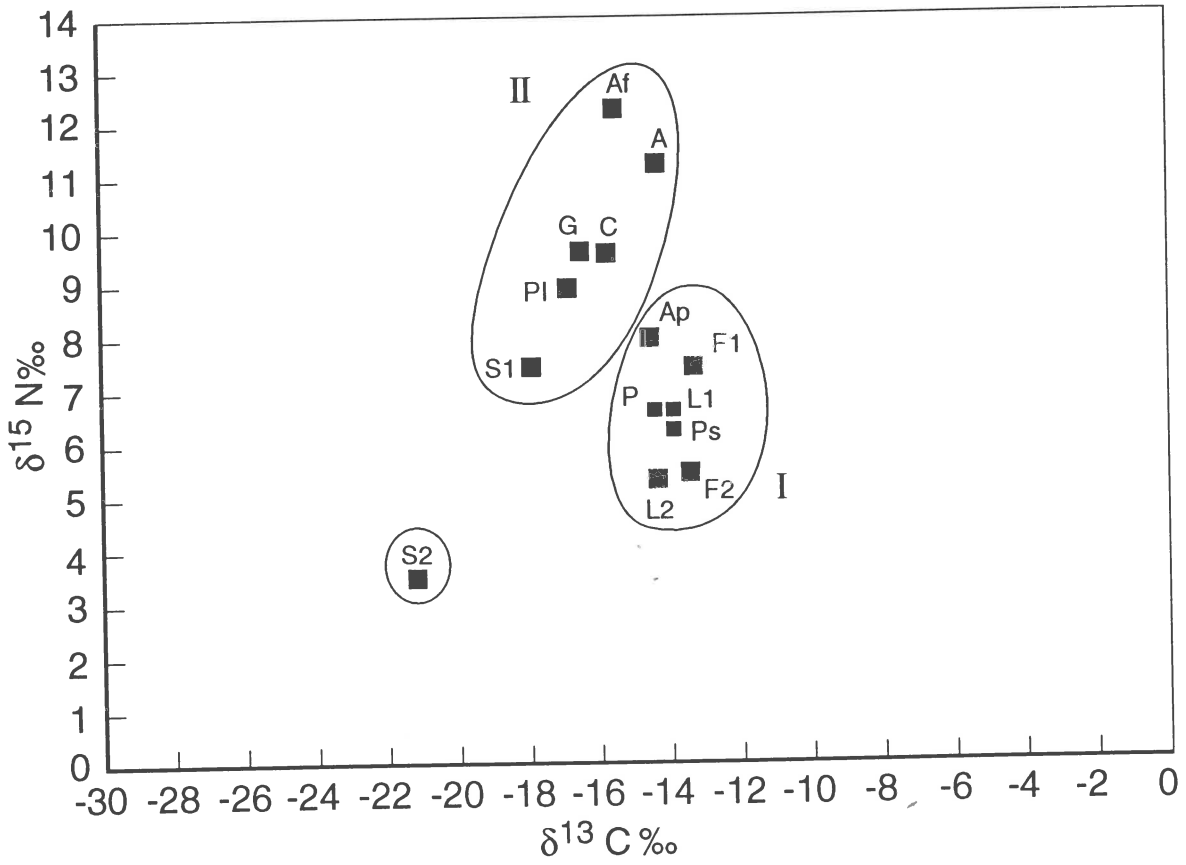

Fig. 3.3.4. Stable isotope ratios ($\partial^{13}C/\partial^{15}N$) of fish muscle tissue. Results of cluster analysis (FLEXCLUS). I. Fish species using the seagrass beds as a life time habitat. II. Migrating fish species.
Fish species (total length in cm): A = *Archamia mozambiquensis* (7-8 cm), Af = *Archamia fucata* (7-8), Ap = *Apogon guamensis* (7-9), C = *Conger cinereus cinereus* (55-80), F_1 = *Fowleria aurita* (7-8), F_2 = *Fowleria aurita* (8-9), G = *Gazza minuta* (6-6.5), L_1 = *Leptoscarus vaigiensis* (15-18), L_2 = *Leptoscarus vaigiensis* (12-15), P = *Paramonacanthus barnardi* (8-10), Pl = *Plotosus lineatus* (8-10), Ps = *Parascorpaena mossambica* (7-11),S_1 = *Siganus sutor* (10-15), S_2 = *Siganus sutor* (6-8).

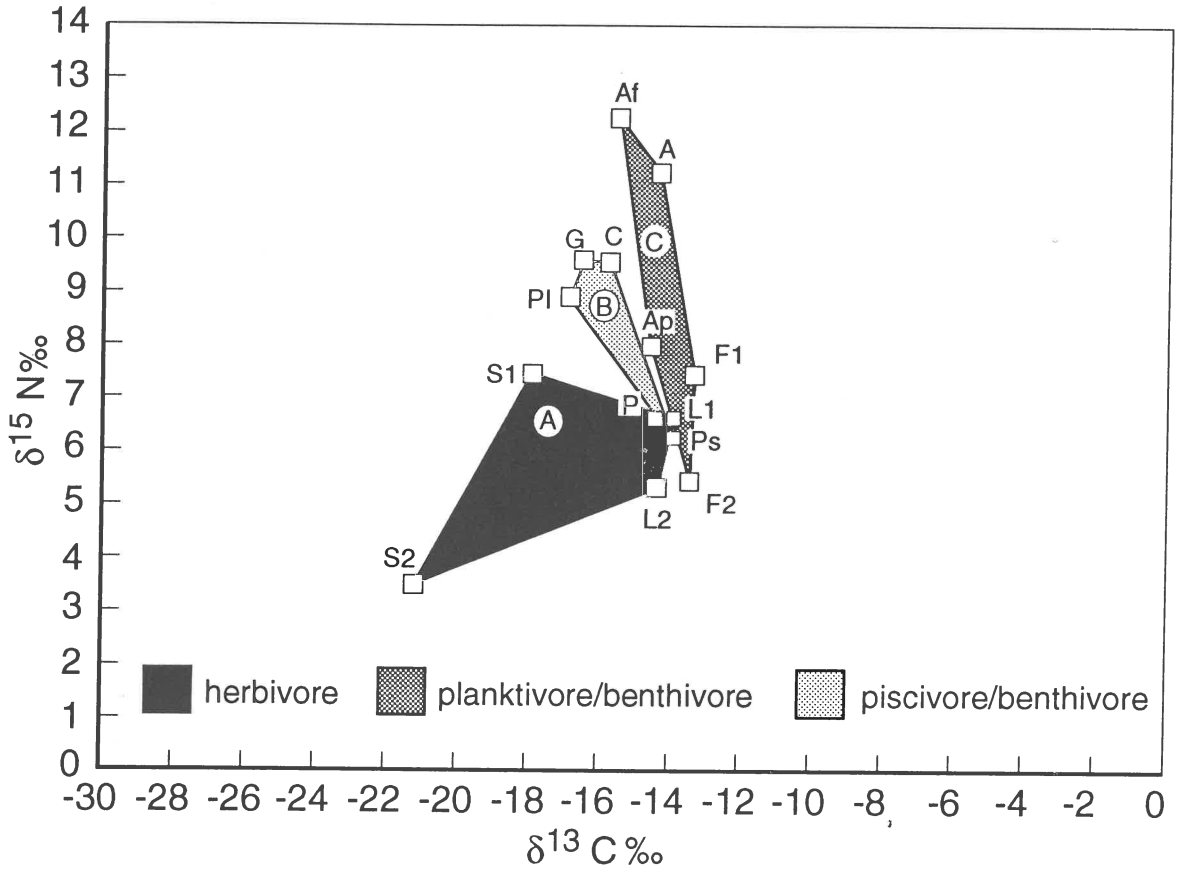

Fig. 3.3.5. Stable isotope ratios ($\partial^{13}C/\partial^{15}N$) of fish muscle tissue. Combination of the isotope ratio and feeding characteristics of the fish species (literature data). Fish species (total length in cm): A = *Archamia mozambiquensis* (7-8 cm), Af = *Archamia fucata* (7-8), Ap = *Apogon guamensis* (7-9), C = *Conger cinereus cinereus* (55-80), F_1 = *Fowleria aurita* (7-8), F_2 = *Fowleria aurita* (8-9), G = *Gazza minuta* (6-6.5), L_1 = *Leptoscarus vaigiensis* (15-18), L_2 = *Leptoscarus vaigiensis* (12-15), P = *Paramonacanthus barnardi* (8-10), Pl = *Plotosus lineatus* (8-10), Ps = *Parascorpaena mossambica* (7-11),S_1 = *Siganus sutor* (10-15), S_2 = *Siganus sutor* (6-8).

effect. At this moment publication of data of the stable isotopes ratios of fish require specification of length for proper evaluation of the data.

In order to describe the use of the seagrass beds by the different fish assemblages, a rough distinction in the feeding patterns of the fish species was made. Based on literature data (Smith & Heemstra, 1986; Sale, 1991; Randall *et al.*, 1990; Randall, 1992) three groups of feeding categories were distinguished :
-fish species feeding besides on other food items on seagrasses and/or macro-algae in addition to other food items: herbivores
-fish species mainly feeding on zooplankton and benthic animals: planktivores/benthivores.
-fish species feeding mainly on other fish and/or macro-crustacea: piscivores/benthivores.

The data could also be clustered combining the stable radio isotope data with feeding characteristics of the fish species based on literature data (Fig. 3.3.5). A group of fish species showing relatively low $\partial^{15}N$ and $\partial^{13}C$ ratios of the muscle tissue feed on plant material (Group A in Fig. 3.3.5).
A group of fish species feeding mainly on zooplankton (Group C), but also feeding on benthic animals, show a higher $\partial^{15}N$ and $\partial^{13}C$ ratio than the herbivorous fish species (Group B). The third group, piscivorous fish species also feeding on benthic animals like macro-crustacea, shows intermediate values in between the group of herbivorous and zooplanktivorous/benthivorous fish species.

An overlap in $\partial^{15}N$ and $\partial^{13}C$ ratios of the various groups exists, indicating that a number of fish species can show different feeding characteristics. It is questionable whether this fact is caused by omnivorous feeding characteristics of the fish species that are not

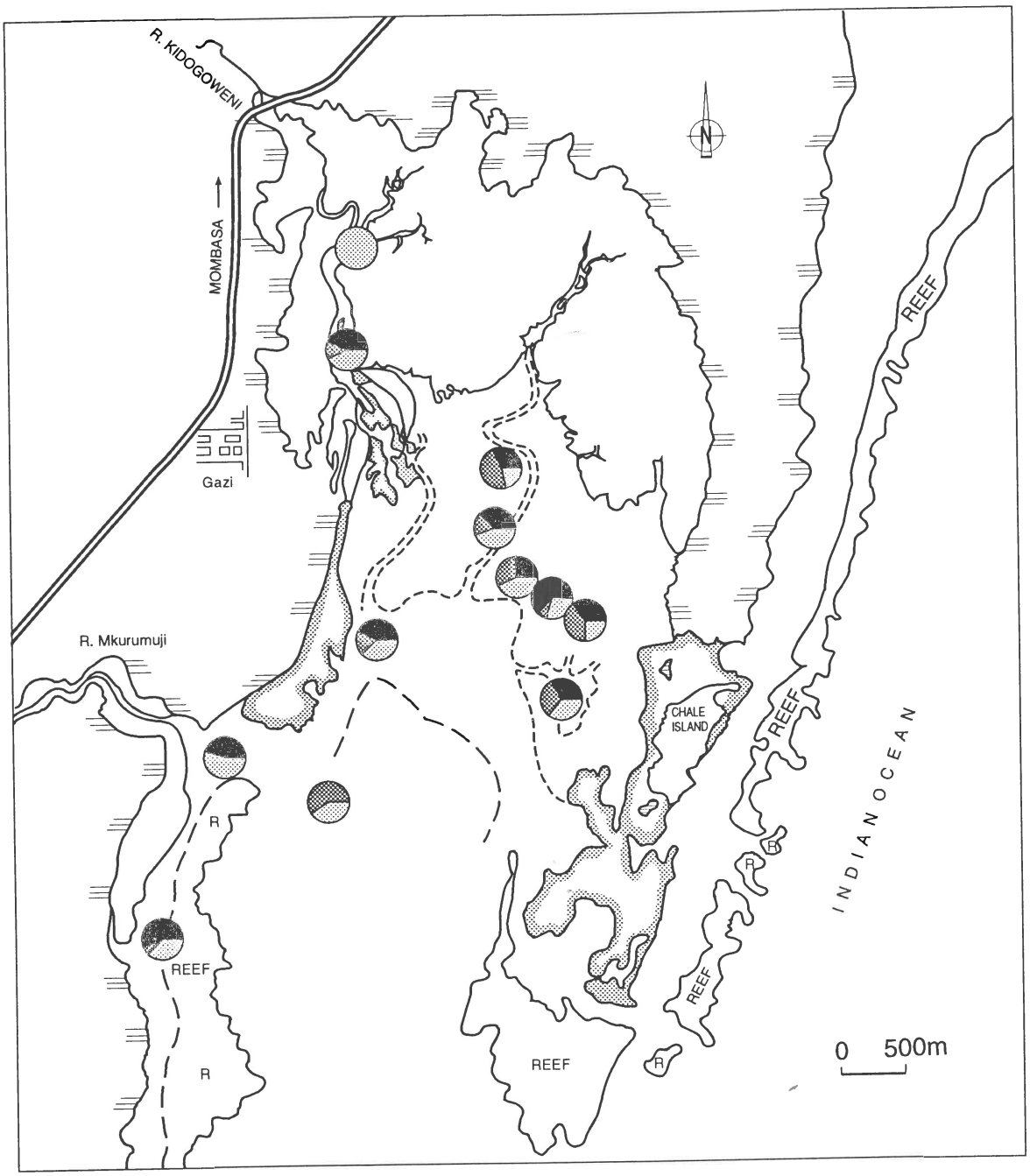

Fig. 3.3.6. Shares of fish feeding categories at the sampling sites.

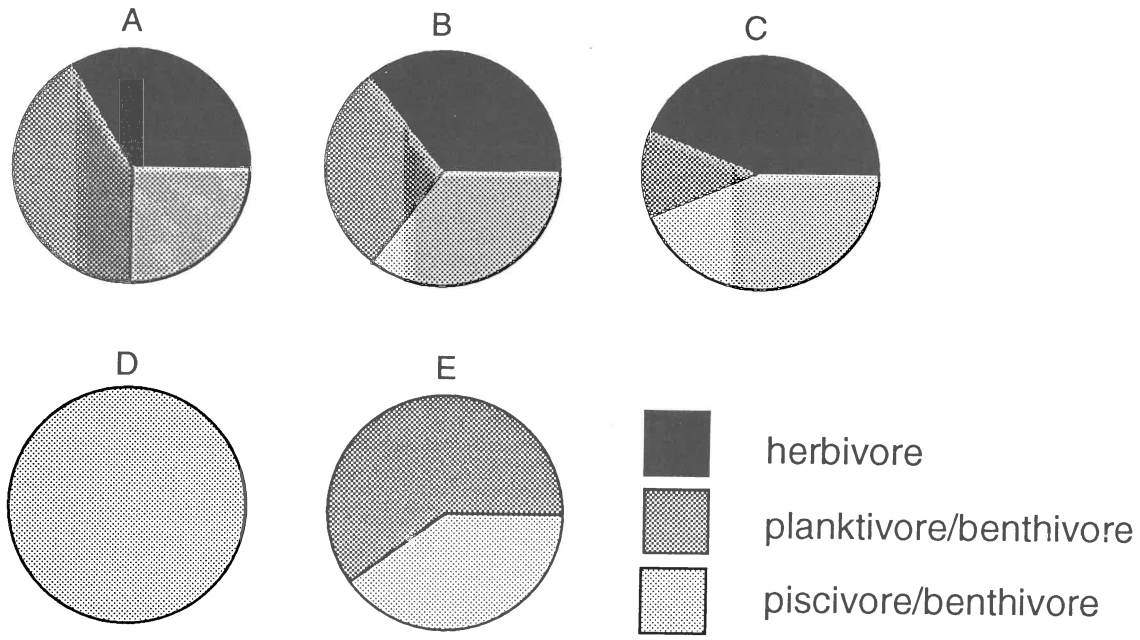

Fig. 3.3.7. Share of three feeding categories of fish based on caught numbers arranged according the clusters distinguished at the family level (see table 3.3.2).

mentioned in literature, changes in $\partial^{15}N$ and $\partial^{13}C$ ratios caused by migrating fish species (Fig. 3.3.5), changes in $\partial^{15}N$ and $\partial^{13}C$ ratios caused by differences in length or the number of data is not sufficient for a proper distinction between the groups. The present data do not allow a further examination of these probable causes at this moment. The valid clustering of the stable radio isotope ratios of the muscle tissue of the fish on bases of feeding characteristics allows the description of the use of the seagrass beds by the fish assemblages on basis of their feeding characteristics.

With regards to the use of the sites as foraging grounds for the fish, it should be stressed that a higher proportion of piscivore/benthivore fish were present in or near channels and creeks. Sites at a greater distance from a channel showed a somewhat lower relative occurrence of fish predators. It can be assumed that these fish species did not use the sites as a permanent habitat but only as foraging grounds. In general about 40 % of the fishes caught were piscivore/benthivore (Fig. 3.3.6). A high share of herbivorous fish was demonstrated in the seagrass meadows near the mangroves. There was a gradual change in the shares of the various feeding groups going from the mangroves, via the seagrass beds within the bay, towards the coral reef (Fig. 3.3.7).

preliminary conclusions

- Fish assemblages of seagrass beds are dense and rich compared with unvegetated areas.
- Cluster analysis at species level as well as family level demonstrated that the fish data can be grouped in four to five clusters.
- The results indicate that the distance from the mangrove area influences the fish community of seagrass beds.
- Fish which are totally or partially herbivorous constitute an important component of the fish community within the seagrass beds.
- Stable isotope analysis showed that $\partial^{15}N$ and $\partial^{13}C$ ratio values of muscle tissue of the fishes are consistent with feeding categories as well as habitat use.
- In the vicinity of the mangroves the share of zooplanktivorous fish is relatively high. This share decreases towards the middle of the bay and concurs with an increase in the share of piscivorous fish.
- The share of piscivorous fish is high in the vicinity of the main channels and lower at some distance from the channels.

references

Compagno, L.J.V., D.A. Ebert & M.J. Smale, 1989. Guide to the Sharks and Rays of southern Africa: 1-160. Struik Publishers, Cape Town.

Fiedler, R. & G. Proksch, 1975. The determination of nitrogen-15 by emission and mass spectrometry in

biochemical analysis: a review, Analytica Chimica Acta 78: 1-62.
Fry, B. & E. Sherr, 1984. $\partial^{13}C$ measurements as indicators of carbon flow in marine and fresh water ecosystems. Contrib. Mar. Sci. 27: 13-47.
Minagawa, M. & E. Wada, 1984. Stepwise enrichment of ^{15}N along food chains. Further evidence and the relation between $\partial\ ^{15}N$ and animal age. Geochim. Cosmochem. Acta 48: 1135-1140.
Minagawa, M., D.A. Winter & I.R. Kaplan, 1984. Comparison of Kjeldahl and combustion methods for measurements of nitrogen isotope ratios in organic matter. Anal. Chem. 56: 1859-1861.
Nevins, J., M.A. Altabet & J.J. McCarthy, 1985. Nitrogen isotope ratio analysis of small samples: sample preparation and calibration. Anal. Chem. 57: 2143-2145.
Randall, J.E., 1992. Red Sea Reef Fishes: 1-192. Immel Publishing Limited, London.
Randall, J.E., G.R. Allen & R.C. Steene, 1990. Fishes of the Great Barrier Reef and Coral Sea: i-xx, 1-507. University of Hawaii Press, Honolulu.
Sale, P.F., 1991. The Ecology of Fishes on Coral Reefs: i-xiv, 1-754. Academic Press, Inc., San Diego.
Smith, M. & P.C. Heemstra (eds), 1986. Smiths' Sea Fishes: i-xx, 1-1047. Springer-Verlag, Berlin.

3.4. SOME PRELIMINARY RESULTS ON THE BIOGEOCHEMISTRY OF MANGROVE SEDIMENTS FROM GAZI BAY

Jack J. Middelburg[1], Joop Nieuwenhuize[1], Rinus Markusse[1] and Boaz Ohowa[2]
[1] Netherlands Institute of Ecology, Centre for Estuarine and Coastal Ecology, Yerseke.
[2] Kenya Marine and Fisheries Research Institute, Mombasa, Kenya

introduction

Mangrove forests are dominant ecosystems along tropical and subtropical coastlines. Their importance to biological, chemical, physical and geological processes occurring in the coastal zone is evident (*e.g.*, Lugo & Snedaker, 1974; Kristensen *et al.*, 1988; 1991; 1992; Alongi, 1989; Alongi *et al.*, 1992; 1993; Woodroffe, 1992; Robertson *et al.*, 1992; Boto & Wellington, 1984; Twiley *et al.*, 1986; Dye, 1983; Hemminga *et al.*, 1994). They provide nursery grounds for many fish and crustacean species, including several of economic importance. Their presence results in a reduction of water movement and consequently enhanced trapping of sediment. Furthermore, they stabilize the sediments, limit coastal erosion, reduce the effect of tropical storms, and support the formation of new islands and the extension of shores. Moreover, mangroves are among the most productive ecosystems and play a key role in the coastal food chain and nutrient cycles (*e.g.* Robertson & Alongi, 1992).

Organic detritus produced by mangroves may either be exported to adjacent ecosystems such as seagrass meadows or coastal waters, or be buried or degraded and recycled in the sediments. Although major attention has been given to the export of mangrove carbon to adjacent systems (*e.g.*, Lugo & Snedaker, 1974; Twiley *et al.*, 1986; Robertson *et al.*, 1992), there are comparatively few data on carbon and nutrient pools, transformations and fluxes within mangrove forests (*e.g.* see reviews by Robertson *et al.*, 1992; Alongi *et al.*, 1992, 1993). This is somewhat surprising since the high productivity of mangroves implies a high nutrient demand. Moreover, several studies have indicated that mangroves may be nutrient limited at the whole-forest scale (Boto & Wellington, 1984; Alongi *et al.*, 1992; Clough, 1992). The carbon and nutrient cycles in mangroves are temporarily and spatially highly variable since they are regulated by a variety of factors such as soil type and texture, tidal range and elevation, redox state, bioturbation intensity, forest type, temperature and rainfall (Lugo & Snedaker, 1974; Kristensen *et al.*, 1988; 1991; 1992; Alongi, 1989; Alongi *et al.*, 1992; 1993; Woodroffe, 1992; Robertson *et al.*, 1992).

Due to the limited data available on carbon and nutrient cycling and the great variability within and between mangroves, there is still confusion about whether mangroves represent a net carbon source (export) or sink (import). On the one hand, biologist view mangroves as highly productive systems that export organic matter, whereas on the other hand geologist consider mangroves as traps for sediment and its associated organic matter (Woodroffe, 1992).

Our current knowledge on elemental cycling in mangroves is mainly based on studies from North America, Australia and Southeast Asia. In this study we will report our initial results on the sediment characteristics and pore-water chemistry of mangrove sediments in Gazi Bay, a coastal lagoon in Kenya, Africa. We have also determined the carbon dioxide, methane and nitrous oxide fluxes from the sediment to the atmosphere. The objectives of this study are: (1) to establish the magnitude and variability of carbon dioxide, methane and nitrous oxide fluxes from mangrove sediments, (2) to test the hypothesis that the forest type regulates nutrient status in mangrove sediments, and (3) to trace the processes involved in cycling of carbon and nitrogen within mangrove forests.

materials and methods

This study is limited to five of the eight mangroves species occurring in Gazi Bay, namely *Sonneratia alba*, *Rhizophora mucronata*, *Bruguiera gymnorrhiza*, *Ceriops tagal* and *Avicennia marina*. Criteria for site selection included the monospecificity of the stands, the position along the river Kidogweni (*i.e.* expected salinity), the tidal elevation, the accessibility and the feasability of flux measurements. The mangrove species occur in clear zonation patterns, which can be easily recognized in the field. In general, *Sonneratia alba* forms the outermost zone towards the open water, followed by pure stands of *Rhizophora mucronata*, or mixed stands of *Rhizophora mucronata* and *Bruguiera gymnorrhiza*. These are followed by pure or mixed stands of *Ceriops tagal* and *Avicennia marina*. Along the River Kidogweni and other creeks *Avicennia marina* usually replaces *Sonneratia alba*. Creek and river fringing *Avicennia marina* stands are much higher (12-18 m) than those on higher areas (about 2-3 m; scrub-type).

During June/July 1992 replicate measurements of carbon dioxide, methane and nitrous oxide fluxes were made at twelve stations (Fig. 3.4.1). At low tide the release of these gases was measured by monitoring accumulation of the gas beneath chambers placed over the sediment surface. The chambers have a 0.11 m^2 base, a volume of 45 l and are made of non-transpar-

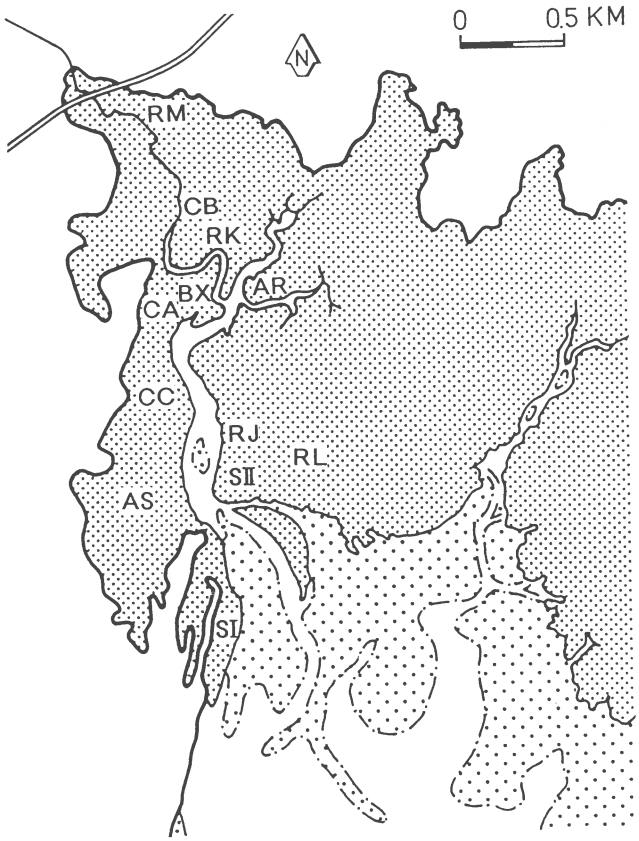

Figure 3.4.1. Map of the Gazi Bay and mangroves along the river Kidogoweni. Stations are indicated: AS = *Avicennia* saline basin-type; AR = *Avicennia* river-fringing; BX = *Bruguiera*, station X, CA = *Ceriops* station A; CB = *Ceriops* station B; CC = *Ceriops* station C; RJ = *Rhizophora* station J; RK = *Rhizophora* station K; RL = *Rhizophora* station L; RM = *Rhizophora* station M; SI = *Sonneratia* station I; SII = *Sonneratia* station II.

ent polypropylene to exclude any phototrophic activity. When necessary a sun shield was placed over the chamber to maintain the chamber temperature and relative humidity within 25 % of their ambient values. Carbon dioxide, methane and nitrous oxide concentrations were measured by circulating chamber air through Teflon tubes between chamber and the gas monitor. The measurement principle of the multi-gas monitor used, a Brüel & Kjaer type 1302, is based on the photoacoustic infra-red detection method. After thorough flushing of the Teflon tubes and analysis cell the air sample is hermetically sealed in the analysis cell. The light emitted by a pulsating infra-red light source and purified by a narrow-band optical filter is selectively adsorbed. The temperature of the gas increases and decreases in response to the pulsating light transmitter and this causes an equivalent increase and decrease of the pressure of the gas in the closed cell. Two ultrasensitive microphones mounted in the cell are used to measure this pressure wave, which is directly proportional to the concentration of the gas.

Various gases can be measured in the same sample using different filters. The response time for a sequential measurement of carbon dioxide, methane and nitrous oxide is about 90 sec. Detection limits for carbon dioxide, methane and nitrous oxide are 3, 0.1 and 0.05 ppmv, respectively, and their response is linear upto several thousands of ppmv for carbon dioxide and methane and 5 ppmv for nitrous oxide. The reproducibilities at ambient levels are about 1, 10 and 15 %, respectively. Fluxes are calculated by regression analysis from the recorded change in concentration over time. Fluxes significant at $p < 0.01$ are normally obtained as low as 0.1 mol CH_4, 1.5 mol CO_2 m^{-2} yr^{-1} and 5 mmol N_2O m^{-2} yr^{-1}, within 30 minutes.

At each station, pore-water samples from intertidal muds were obtained by pressure filtration of sediments following the collection of cores by hand at low tide. Coinciding sections of three replicate cores were combined to reduce spatial heterogeneity and treated as one sample. No special precautions were taken to con-

trol temperature and oxygen levels during squeezing. The recovered pore-water samples were first used for the analyses of ammonium according to the phenol-hypochlorite method and subsequently stored at -20°C for transport to our home laboratory. The stored pore-water samples were analyzed for ammonium, nitrate, phosphate and sulfate concentrations using standard colorimetric methods on a Skalar autoanalyzer. The agreement between ammonium measurements made directly in Kenya and those made after one year of storage is fair (r=0.9). The chlorinity was determined by potentiometric titrations.

Sediment samples were taken at depth intervals of 0-5, 5-20 and 20-40 cm and were analyzed for grain size distribution, particulate organic carbon, total nitrogen and phosphorus, $CaCO_3$, salinity and pH. Grain-size distribution was assessed with a laser diffraction technique (Malvern Particle Sizer type 3600 Ec). The organic carbon and nitrogen contents of the sediments were determined using a Carlo-Erba CN-analyzer following a recently developed in situ HCl acidification prodecure (Nieuwenhuize *et al.* 1994). Total phosphorus was analysed using a standard colorimetric determination of phosphate following digestion by strong oxidizing acid reagents (hydrochloric acid + nitric acid + perchloric acid). The inorganic carbon content was determined by gas-volumetry (Scheibler-method), the salinity was estimated from measured chlorinities and the pH was determined in a KCl suspension.

In order to reveal the depth distribution of POC and TN, two stations (*Rhizophora* L and *Ceriops* C) were selected for detailed investigation. Sediment samples were taken with a depth resolution of 1 cm and also an attempt was made to separate of living (root) from non-living organic matter.

Analysis of variance with a nested design was used to evaluate differences between different mangrove types and stations within a certain mangrove type. Six mangrove types are distinguished namely, large creek-fringing *Avicennia marina*, small basin *Avicennia marina* and the four other species. Data were log-transformed if appropriate. SYSTAT (Wilkinson, 1990) was used for statistical calculations.

results

Carbon dioxide, methane and nitrous oxide fluxes were determined at 12 stations covering 65 locations in total. Methane and nitrous oxide emission rates were below the detection limit of our system, *i.e.* 0.1 mol CH_4 and 5 mmol N_2O m^{-2} yr^{-1}. Bartlett *et al.* (1989) reported methane fluxes of 0.085 and 1.66 mol C m^{-2} yr^{-1} for fringing and scrub-type *Rhizophora mangle* in the Florida Everglades. To the best of our knowledge, there are no data on nitrous oxide fluxes from mangroves. Carbon dioxide fluxes range from about 4 to 165 mol C m^{-2} yr^{-1} (Table 3.4.1). Statistical analysis through one-way nested ANOVA indicates that carbon dioxide fluxes differ significantly between the mangrove species and between stations for a certain type of mangrove (Table 3.4.2).

Sediment characteristics, such as the median grain size, pH, soil salinity, and the calcium carbonate, organic carbon, nitrogen and phosphorus contents were measured at three depth levels (Table 3.4.3). The median grain size, as determined by a Malvern particle analyzer, ranges from 20 µm at the creek-fringing *Avicennia marina* to 320 µm at bay fringing *Sonneratia alba*. The pH and inorganic carbonate content range from 3.5 to 8.3 and 0.0 to 1.4 wt %, respectively. At calcium carbonate concentrations above 0.2 wt%, the pH is effectively buffered at values around 8 (Figure 3.4.2). The salinity of the mangrove sediments ranges from 16 to 68 psu, though the majority of the data cluster between 30 and 35 psu. The organic carbon and nitrogen contents exhibit a wide range, namely from 0.3 to 18 wt% and 0.01 to 3.5 wt% C and N, respectively. The organic carbon and nitrogen contents are closely correlated (r^2=0.89) with a slope corresponding to a molar C/N ratio of 24.3 (Fig. 3.4.3). Sedimentary phosphorus concentrations range from 35 to 740 ppm and show a weak correlation with organic carbon (not shown). One-way nested ANOVA analyses indicates that the median grain size and the organic carbon, nitrogen and phosphorus contents differ significantly between the mangrove species (Table 3.4.4). There are no significant differences between sites for a certain type of mangrove or between depth different depth levels.

The pore-water composition of Gazi Bay sediments was analyzed for ammonium, nitrate, nitrite, phosphate, sulfate and chloride (Table 3.4.5). In general, nutrient concentrations are very low for coastal sediments; ammonium ranges from 3 to 390 µM, nitrate from 1 to 50 µM, nitrite from < 0.1 to 2.3 µM, and phosphate from < 0.05 to 1 µM. The major components sulfate and chloride show considerable variability related to salinity fluctuations; they range from 12 to 68 mM and 210 to 1125 mM. All pore-water constituents show significant differences between mangrove-types, ammonium, phosphate and sulfate with location as well, and chloride exhibit significant variability with mangrove-type, location and depth (Table 3.4.6).
At two locations, *Ceriops* C and *Rhizophora* C, we have also examined in rather detail the depth distribu-

Table 3.4.1. Carbon dioxide fluxes from mangroves in Gazi Bay.
R^2 = coefficient of determination; N = number of observations

Type	Station	CO_2 (mol $m^{-2}yr^{-1}$)	R^2	N
Avic	R	141.24 ± 3.46	0.99	14
		151.56 ± 4.49	0.99	13
		129.34 ± 3.73	0.99	15
		145.44 ± 7.30	0.98	12
Avic	S	125.08 ± 0.74	0.99	34
		91.52 ± 0.58	0.99	27
		99.80 ± 4.33	0.98	11
		140.52 ± 3.17	0.99	13
		131.99 ± 2.51	0.99	13
		114.41 ± 6.01	0.98	8
		120.61 ± 7.60	0.98	8
Brug	X	22.10 ± 1.82	0.92	15
		3.52 ± 1.99	0.21	14
		38.51 ± 1.00	0.99	16
		55.64 ± 1.19	0.99	12
Ceriops	A	133.38 ± 2.17	0.99	16
		113.85 ± 1.28	0.99	17
		26.36 ± 0.62	0.99	15
		60.61 ± 0.88	0.99	18
		137.81 ± 2.68	0.99	14
		165.01 ± 2.32	0.99	15
Ceriops	B	7.39 ± 4.63	0.3	8
		48.76 ± 6.45	0.86	11
		25.83 ± 3.30	0.87	11
		26.09 ± 2.55	0.92	11
		38.86 ± 12.56	0.66	7
Ceriops	C	77.02 ± 1.40	0.99	24
		11.09 ± 2.20	0.55	23
		15.16 ± 2.55	0.7	17
		123.19 ± 4.33	0.99	4
		39.40 ± 1.47	0.98	14
		21.40 ± 1.01	0.97	15
Rhiz	J	19.08 ± 4.43	0.61	14
		4.74 ± 0.74	0.79	13
		22.89 ± 0.93	0.98	16
		28.52 ± 0.92	0.99	15
		23.40 ± 3.15	0.85	12
Rhiz	K	61.19 ± 1.90	0.98	18
		65.20 ± 2.94	0.98	14
		29.08 ± 1.75	0.95	16
		114.98 ± 1.91	0.99	15
		44.13 ± 0.44	0.99	17
		41.51 ± 1.77	0.97	19
Rhiz	L	30.73 ± 2.83	0.88	18
		11.26 ± 0.74	0.95	15
		10.64 ± 0.65	0.95	16
		24.18 ± 2.14	0.92	13
		14.74 ± 0.79	0.95	19
		41.39 ± 0.62	0.99	19
		21.72 ± 0.97	0.97	17
Rhiz	M	42.12 ± 2.75	0.94	18
		47.26 ± 1.42	0.99	15
		25.37 ± 0.49	0.99	22
		30.90 ± 0.99	0.98	17
		26.50 ± 0.63	0.99	19
		30.87 ± 0.56	0.99	16
		22.28 ± 1.87	0.92	15
		46.10 ± 1.81	0.98	11
Son	I	95.93 ± 2.32	0.99	11
		59.72 ± 1.73	0.99	10
		60.70 ± 1.57	0.99	12
		69.45 ± 1.14	0.99	11
		77.28 ± 2.48	0.99	10
Son	II	40.25 ± 3.44	0.9	17
		64.18 ± 7.00	0.87	14
		128.86 ± 3.06	0.99	13

tion of organic carbon and nitrogen (Fig. 3.4.4). At station *Ceriops* C, organic carbon and nitrogen concentrations in the top 16 cm are about 2 and 0.1 wt % respectively, they subsequently increase upto about 5 wt% C and 0.24 wt% N. At station *Rhizophora* C organic carbon concentrations range from 3 to 8 wt% without any trend with depth, whereas nitrogen contents show a drastic decrease at depths more than 40 cm.

discussion

One-way nested ANOVA analyses has shown that mangrove forest type regulates carbon dioxide fluxes, sediment grain sizes, sedimentary organic carbon, nitrogen and phosphorus contents, and pore-water characteristics. Differences between stations are primarily due to differences in forest type. Site variability, not related to forest type, is only significant for pore-water ammonium, phosphate, sulfate and chloride.

These differences in mangrove sediment biogeochemistry could be due to either species-specific processes or to differences in elevation at which these mangrove types occur. Differences in elevation relate directly to differences in tidal inundation frequencies, litter input and aerial exposure. In Gazi Bay, differences in elevation between various mangroves are only small (Van Speybroeck, 1992). Median elevation values (in cm) for the mangroves are: *Sonneratia alba* (160), *Rhizophora mucronata* (212), *Bruguiera gymnorrhiza* (212), *Ceriops tagal* (245) and basin scrub-type *Avicennia marina* (258). Van Speybroeck (1992) did not report a median elevation value for creek-fringing *Avi-*

Table 3.4.2. Analysis of variance (ANOVA) of the influence of mangrove species and station on the carbon dioxide fluxes

Source of variation	Sum-of-Squares	DF	Mean-Square	F-ratio	P
Species	4.077	5	0.815	11.737	0.000
Station{Species}	1.908	6	0.318	4.5711	0.001
Error	3.752	54	0.069		

cennia marina, but this type of mangroves can probably be found between 160 and 212 cm. Accordingly, the relative altitude sequence at which the mangrove types occur is: *Sonneratia* ≈ creek-type *Avicennia* < *Rhizophora* ≈ *Bruguiera* < *Ceriops* ≤ basin scrub-type *Avicennia*. This sequence does not concur with sequences in sediment characteristics. Hence, mangrove forests regulate the nutrient status of mangrove sediments.

Mangroves may also affect the acid-base balance of mangrove sediments. The data in Fig. 3.4.3 indicate that there are strong acidifying processes related to mangrove activity. Mangrove can acidify the sediments in a variety of ways. Firstly, through oxygen translocation from their leaves to their roots and subsequent release or leakage of this oxygen to the sediments, they may alter the redox conditions in the sediments. The net effect of oxygen release will be an enhancement of aerobic degradation of organic matter according to:

$CH_2O + O_2 \longrightarrow H_2CO_3$ (1),

and oxidation of reduced components such as:

ammonia:

$NH_3 + 2O_2 \longrightarrow HNO_3 + H_2O$ (2a; nitrification)

sulfide:

$H_2S + 2O_2 \longrightarrow H_2SO_4$ (2b; sulfide-oxidation)

ironsulfide:

$FeS_2 + 3.75O_2 + 2.5\,H_2O \longrightarrow FeOOH + H_2SO_4$ (2c: sulfide-oxidation).

The acids generated (H_2CO_3, H_2SO_4, HNO_3) will first lower the pH, the alkalinity and the saturation state, and then cause dissolution of solid-phase calcium carbonate:

$CaCO_3 + H_2CO_3 \longrightarrow Ca^{2+} + 2\,HCO_3^-$ (3).

Secondly, the carbon dioxide respired by mangrove roots will also support reaction (3). Thirdly, ammonium uptake by mangrove roots will lead to a release of H^+. If carbonate dissolution in mangrove sediments prooves to be a general and important process it may have implications for the global carbon cycle.

The molar carbon/nitrogen ratio of fresh mangrove leaves in Gazi Bay are about 27 to 32 for basin scrub-type *Avicennia marina*, 28 for creek-fringing *Avicennia marina*, 25 to 34 for *Sonneratia alba*, 59 to 69 for *Ceriops tagal*, 45 to 70 for *Bruguiera gymnorrhiza*, and 43 to 78 for *Rhizophora mucronata* (Rao *et al.*, 1994; Hemminga *et al.*, 1994). Part of the variability in reported C/N ratios may be related to the physiological conditions of the leaves sampled and analysed. During senescence of the leaves, *i.e.* before litterfall, about 64 % of the nitrogen is resorbed by the mangroves (Rao *et al.*, 1994). Consequently, the sediment receives mangrove material that is strongly depleted in nitrogen with respect to fresh mangroves leaves. In contrast, our data indicate that sedimentary carbon/nitrogen ratios are rather low compared to mangrove material and rather independent of mangrove type (Fig. 3.4.3). In other words, there is a benthic nitrogen excess relative to mangrove material. This might indicate that there are either strong losses of carbon relative to nitrogen,or *vice versa* that there are benthic nitrogen inputs. In order to put some limits on these possibilities we have performed some simple conservative mass-balance calculations. The calculations are based on the following assumptions: (1) average carbon dioxide fluxes (based on data presented in Table 3.4.2) can be used to constrain mineralization rates in mangrove sediments. Since an unknown part of the carbon dioxide flux from mangrove sediments is related to root respiration rather than due to organic carbon mineralization, we will overestimate carbon mineralization rates; (2) nitrogen mineralization rates can be calculated by dividing the carbon mineralization rates with the C/N ratio of the material being decomposed; (3) the active sediment layers are about 16 and 40 cm thick for the *Ceriops* and *Rhizophora* station respectively (Fig. 3.4.4).

The results of these calculations are presented in Table 3.4.7. N-mineralization rates at the *Ceriops* station vary from 2.0 mmol m^{-2} d^{-1} to 0.3 mmol m^{-2} d^{-1}, depending on C/N ratio of decomposing organic matter (*e.g.* sedimentary organic matter, fresh leaves or senescent leaves). The inventory of excess nitrogen relative to fresh-leaf input amounts to about 12 mol m^{-2}. Based on these very conservative calculations we estimate

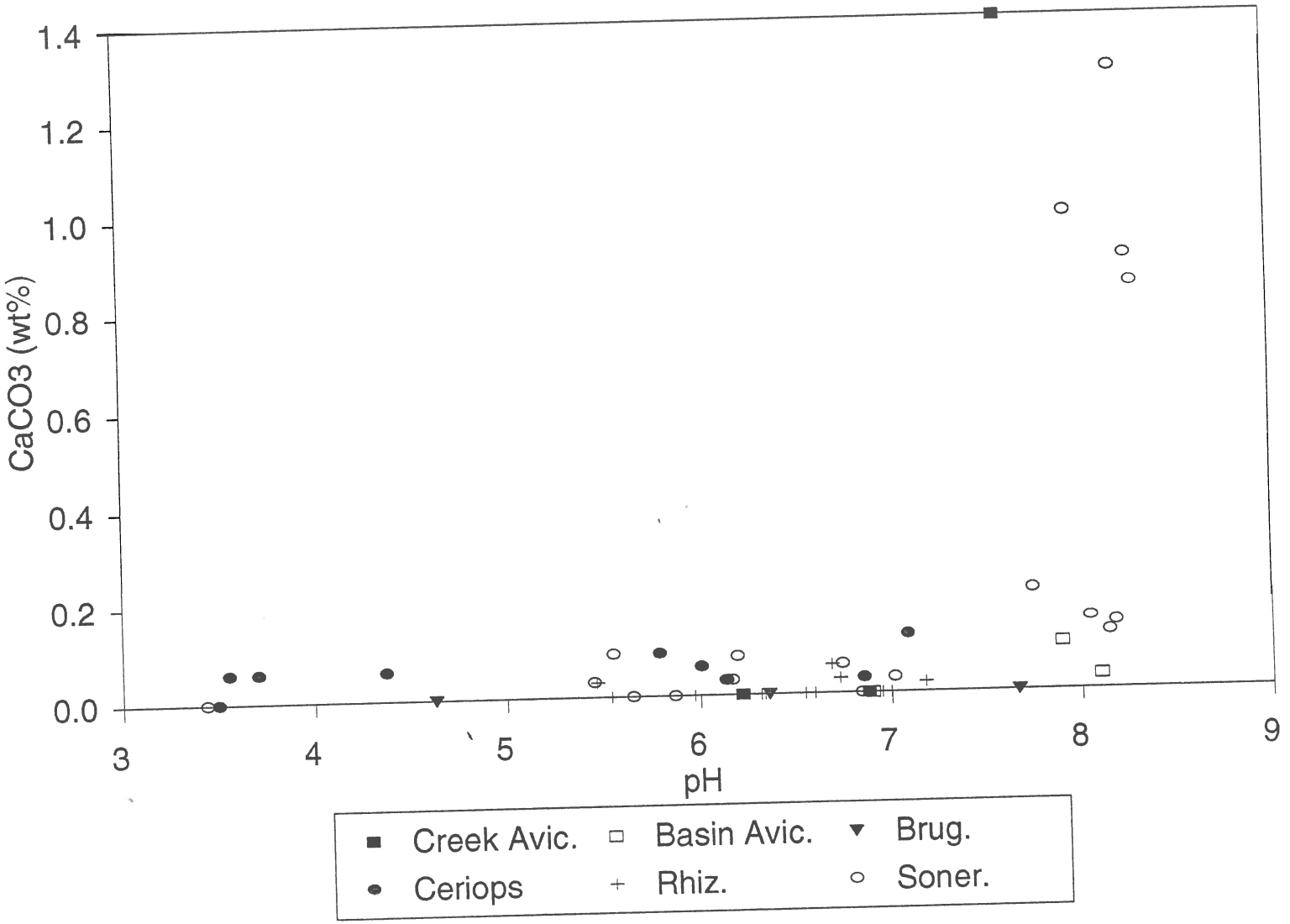

Figure 3.4.2. The relation between soil pH and the calcium carbonate content.

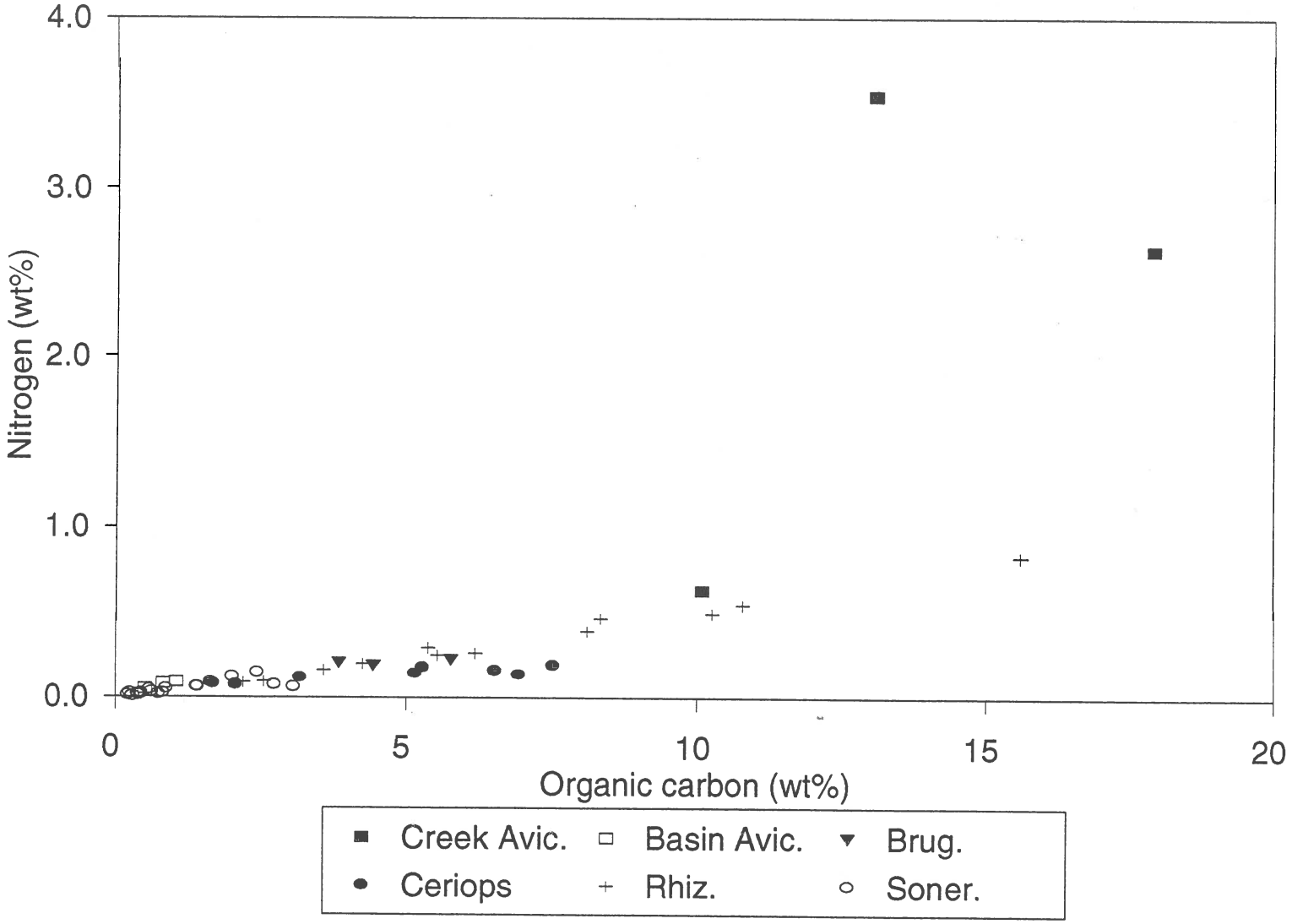

Figure 3.4.3. Relation between the organic carbon and nitrogen contents of Gazi Bay sediments.

Table 3.4.3. Sediment characteristics in Gazi Bay

Type	Site	Depth cm	pH	$CaCO_3$ wt%	Salin psu	Median µm	Corg wt%	Ntot wt%	P ppm
Avic	R	0-5	7.61	1.40	34.91	28.90	10.10	0.63	711.69
Avic	R	5-20	6.88	0.00	33.34	20.40	17.91	2.64	589.44
Avic	R	20-40	6.22	0.00	31.43	25.60	13.11	3.55	458.45
Avic	S	0-5	6.90	0.00	44.76	215.70	1.04	0.09	91.25
Avic	S	5-20	7.90	0.10	52.15	148.40	0.82	0.08	124.44
Avic	S	20-40	8.10	0.03	68.57	118.80	0.51	0.05	148.45
Brug	X	0-5	7.67	0.00	35.81	178.50	3.85	0.21	235.77
Brug	X	5-20	6.36	0.00	30.20	226.70	4.45	0.19	174.65
Brug	X	20-40	4.63	0.00	30.20	205.00	5.77	0.22	148.45
Cer	A	0-5	6.14	0.03	35.14	259.40	3.17	0.12	82.96
Cer	A	5-20	6.01	0.06	30.87	189.00	5.28	0.18	117.89
Cer	A	20-40	3.56	0.06	38.06	138.10	7.52	0.19	69.86
Cer	B	0-5	7.09	0.12	16.62	273.90	1.68	0.08	187.75
Cer	B	5-20	5.79	0.09	31.88	291.80	2.06	0.07	87.32
Cer	B	20-40	3.71	0.06	33.01	189.60	6.51	0.16	126.62
Cer	C	0-5	6.86	0.03	37.95	256.30	1.64	0.09	61.13
Cer	C	5-20	4.37	0.06	37.38	233.70	5.14	0.14	74.23
Cer	C	20-40	3.50	0.00	60.17	204.50	6.93	0.14	52.39
Rhiz	J	0-5	6.69	0.06	30.65	101.40	2.19	0.09	318.73
Rhiz	J	5-20	6.73	0.03	29.86	172.50	2.55	0.10	253.24
Rhiz	J	20-40	6.55	0.00	31.32	139.40	5.38	0.29	218.31
Rhiz	K	0-5	7.18	0.02	32.00	37.50	4.26	0.20	641.83
Rhiz	K	5-20	6.32	0.00	29.64	33.40	6.18	0.26	580.70
Rhiz	K	20-40	5.46	0.03	31.21	56.40	10.79	0.55	340.56
Rhiz	L	0-5	7.00	0.00	33.12	50.90	15.61	0.83	742.25
Rhiz	L	5-20	6.60	0.00	32.56	111.70	10.27	0.50	375.49
Rhiz	L	20-40	6.34	0.00	26.72	216.00	8.10	0.39	340.56
Rhiz	M	0-5	6.95	0.00	32.44	61.70	8.34	0.47	537.04
Rhiz	M	5-20	5.97	0.00	31.66	195.20	3.60	0.16	157.18
Rhiz	M	20-40	5.54	0.00	30.09	220.90	5.54	0.25	218.31
Sonn	I	0-5	7.02	0.03	37.61	281.40	0.25	0.02	43.66
Sonn	I	5-20	6.85	0.00	28.29	327.20	0.21	0.02	39.30
Sonn	I	20-40	5.45	0.03	32.56	256.60	0.58	0.04	56.76
Sonn	I	0-5	6.75	0.06	34.69	285.10	0.45	0.02	34.93
Sonn	I	5-20	6.17	0.03	32.11	291.60	0.62	0.03	43.66
Sonn	I	20-40	5.65	0.00	32.00	264.10	0.86	0.05	48.03
Sonn	I	0-5	8.15	0.12	37.72	248.20	0.43	0.02	61.13
Sonn	I	5-20	6.20	0.08	26.94	280.80	0.30	0.01	34.93
Sonn	I	20-40	8.18	0.14	39.07	252.00	0.40	0.02	82.96
Sonn	I	0-5	8.20	1.29	30.65	233.60	2.01	0.12	96.06
Sonn	I	5-20	8.05	0.15	36.82	263.40	0.39	0.02	52.39
Sonn	I	20-40	8.29	0.84	16.28	286.40	0.74	0.02	82.96
Sonn	I	0-5	7.95	0.99	35.03	226.90	2.44	0.15	257.61
Sonn	I	5-20	7.75	0.21	29.97	261.90	1.41	0.07	126.62
Sonn	I	20-40	8.26	0.90	35.48	266.70	1.38	0.06	144.08
Sonn	II	0-5	3.44	0.00	25.26	285.90	2.74	0.07	69.86
Sonn	II	5-20	5.55	0.09	30.76	258.70	0.81	0.02	96.06
Sonn	II	20-40	5.87	0.00	26.61	237.60	3.06	0.06	117.89

Table 3.4.4. Analysis of variance (ANOVA) of the influence of mangrove species and station on the sediments characteristics

Source of var.	Sum-of-Squares	DF	Mean-Square	F-ratio	P
pH					
Species	16.994	5	3.399	3.291	0.016
Station{Species}	14.453	6	2.409	2.333	0.054
Depth	8.293	2	4.146	4.015	0.027
Error	35.110	34	1.033		
Median					
Species	214060	5	42812	24.511	0.000
Station{Species}	28603	6	4767	2.729	0.028
Depth	2793	2	1397	0.800	0.458
Error	59385	34	1747		
Organic Carbon					
Species	5.473	5	1.095	16.155	0.000
Station{Species}	1.112	6	0.185	2.736	0.028
Depth	0.247	2	0.123	1.822	0.177
Error	2.304	34	0.068		
Nitrogen					
Species	8.206	5	1.641	20.885	0.000
Station{Species}	0.688	6	0.115	1.459	0.222
Depth	0.246	2	0.123	1.565	0.224
Error	2.672	34	0.079		
Phosphorus					
Species	3.961	5	0.792	21.634	0.000
Station{Species}	0.404	6	0.067	1.841	0.120
Depth	0.108	2	0.054	1.470	0.244
Error	1.245	34	0.037		

that at least 16 years are required to cause the excess nitrogen by mineralizing carbon, while retaining all the nitrogen. This is similar to the residence time due to burial if the sediments accumulate at 1 cm yr^{-1}. Similarly, at the *Rhizophora* station, we estimate that more than 70 years are required to account for the observed excess nitrogen. The residence time due to burial is about 40 year at this station. Thus, even our unrealistically high nitrogen mineralization rates, together with a 100 % retention of the mineralized nitrogen in the sediments, yields nitrogen-enrichment times that are too long relative to the burial rate of the sediments. Hence, there must be addition of nitrogen to mangrove sediments. There are a few possibilities. Firstly, there could be belowground input of nitrogen-rich mangrove material. In order to test this hypothesis we have analysed some living root material. The carbon/nitrogen molar ratio of living root material ranges from 64 to 113 at the *Ceriops* station and 50 to 66 at the *Rhizophora* station. Although we do not know the annual belowground input of carbon and nitrogen, this nitrogen input pathway can not explain the nitrogen excess because of mass-balance constraints discussed before. Secondly, the C/N ratio of material being mineralized is much lower than the sedimentary C/N ratio. One possibility could be degradation of imported algal (C/N ≈ 7) or seagrass material (C/N ≈ 19). The $\partial^{13}C$ values of *Ceriops tagal* (-24.12) and *Rhizophora mucronata* (-28.25) leaves are close to, but depleted, with respect to values of sedimentary organic material (-22.69 and -25.31, respectively; Hemminga *et al.*, 1994). This enrichment in $\partial^{13}C$ values of sedimentary material relative to mangrove material could be related to the import of seagrass or algal material. For instance, for an import end-member with a $\partial^{13}C$ value of -21, it is easily calculated that sedimentary organic matter at the *Ceriops* station comprises about 55 % mangrove derived material and 45 % external materi-

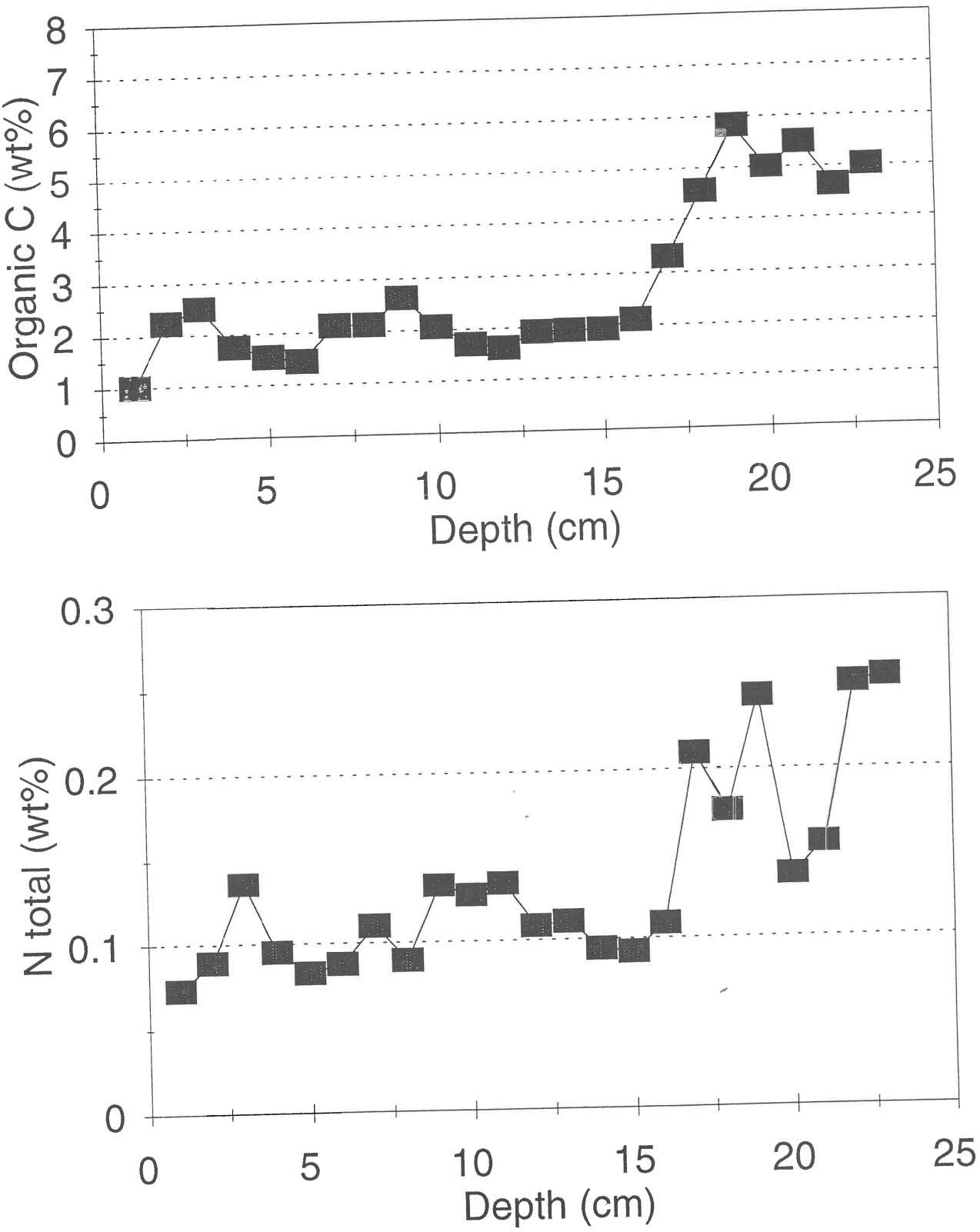

Figure 3.4.4. Concentration versus depth profiles; a) Organic carbon at station *Ceriops* C; b) Nitrogen at station *Ceriops* C; c) and d) idem at station *Rhizophora* L.

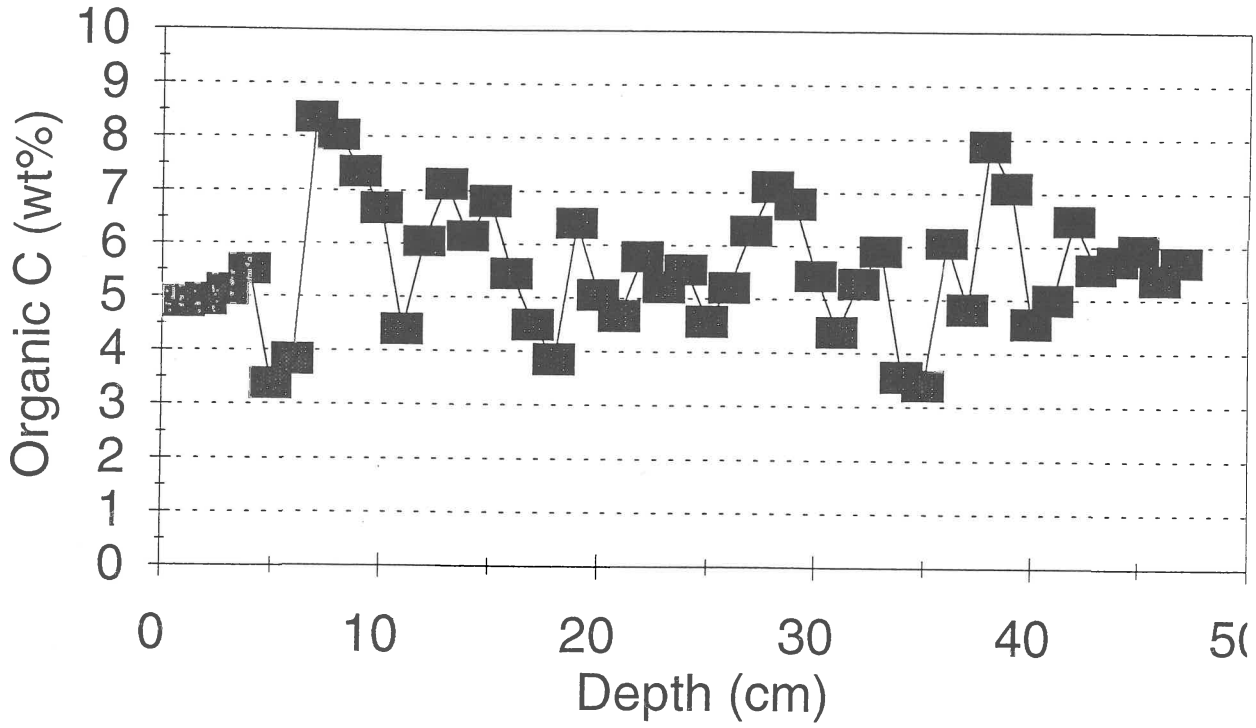
Organic C (wt%)
10
9
8
7
6
5
4
3
2
1
0
0
10
20
30
40
5(
Depth (cm)

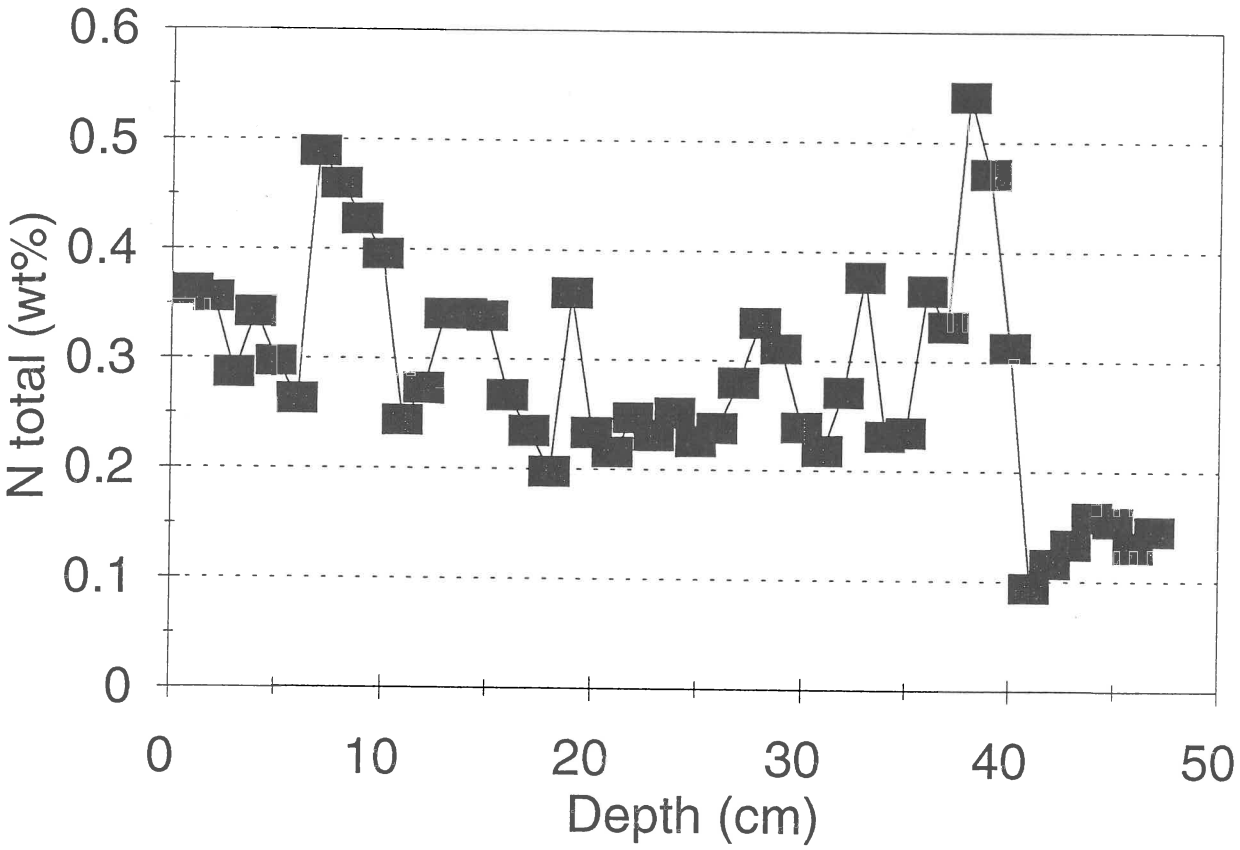
N total (wt%)
0.6
0.5
0.4
0.3
0.2
0.1
0
0
10
20
30
40
50
Depth (cm)

Table 3.4.5. Pore-water chemistry of Gazi Bay sediments

Type	Site	Depth cm	NH_4 µM	NO_3 µM	NO_2 µM	PO_4 µM	SO_4 mM	Cl mM
Avic	R	1	92.4	5.0	0.2		27.6	504
Avic	R	3	111.8	7.9	0.2	0.0	26.8	510
Avic	R	5	83.4	8.8	0.3	0.1	26.8	509
Avec	R	7	62.7	6.9	0.3	0.1	26.7	511
Avic	R	9	69.5	11.8	0.3	0.0	27.1	513
Avec	R	11	51.9	8.2	0.3	0.2	27.4	517
Avic	R	13	52.7	13.2	0.3	0.1	26.8	521
Avic	R	15	44.6	10.8	0.3	0.1	25.0	526
Avic	R	17	55.0	10.8	0.3	0.0	26.7	521
Avic	R	19	42.2	7.0	0.3	0.0	27.2	513
Avic	S	1	40.0	11.9	0.9	0.2	36.8	634
Avic	S	3	59.4	49.1	1.4	0.0	43.6	718
Avic	S	5	67.4	45.1	1.6	0.2	43.3	742
Avic	S	7	55.6	36.0	1.6	0.3	42.2	728
Avic	S	9	45.2	22.0	1.8	0.5	39.9	735
Avic	S	11	96.4	24.6	2.3	0.4	47.1	805
Avic	S	13	68.6	22.6	2.0	0.2	45.8	810
Avic	S	15	75.4	18.5	2.3	0.2	46.9	843
Avic	S	17	83.7	23.4	2.4	0.2	49.2	862
Avic	S	19	51.5	10.5	2.6	0.2	50.6	909
Avic	S	21.5	48.1	8.1	2.9	0.1	60.7	984
Avic	S	24.5	57.2	11.4		0.2	61.9	1047
Avic	S	27.5	52.0	10.3		0.3	60.3	1122
Avic	S	31	39.5	7.4		0.6	68.3	1125
Brug	X	1	212.8	6.6	0.3	0.1	28.2	535
Brug	X	3	361.0	7.3	0.3	0.1	28.0	525
Brug	X	5	269.8	5.6	0.3	0.2	27.5	515
Brug	X	7	245.5	5.9	0.3	0.1	27.9	520
Brug	X	9	302.5	8.3	0.3	0.3	27.8	505
Brug	X	11	359.0	13.8	0.3	0.2	26.2	504
Brug	X	13	387.3	11.3	0.2	0.1	24.5	493
Brug	X	15	315.3	8.6	0.2	0.2	25.4	486
Brug	X	17	340.5	11.0	0.2	0.0	25.3	488
Brug	X	19	170.3	10.7	0.1		24.9	481
Ceriops	A	1	153.6	29.4	1.1		29.8	
Ceriops	A	3	292.1	37.7	0.9	0.0	27.5	
Ceriops	A	5.5	302.9	33.0	0.9	0.1	21.4	494
Ceriops	A	8.5	185.7	21.1	0.6	0.1	24.1	456
Ceriops	A	13.5	194.3	20.6	0.6		30.3	
Ceriops	A	16.5	97.1	13.0	0.5		28.1	
Ceriops	A	19.5	99.3	10.1	0.5	0.0	22.5	
Ceriops	A	22.5	149.3	10.4	0.4	0.0	23.0	436
Ceriops	A	25.5	214.3	11.1	0.4	0.1	23.6	428
Ceriops	A	28.5	192.1	13.3	0.4	0.0	22.2	417
Ceriops	B	1	88.6	6.1	1.7	0.8	12.6	247
Ceriops	B	3	92.6	10.7	0.7	0.7	18.6	375
Ceriops	B	5	74.6	9.9	0.5	0.7	25.1	467
Ceriops	B	7	91.4	14.9	0.4	0.5	26.2	498
Ceriops	B	9	82.9	8.6	0.5	1.0	25.5	511
Ceriops	B	11	144.3	11.4	0.4		26.6	505

Table 3.4.5. Pore-water chemistry of Gazi Bay sediments (continued)

Type	Site	Depth cm	NH_4 µM	NO_3 µM	NO_2 µM	PO_4 µM	SO_4 mM	Cl mM
Ceriops	B	13	80.1	8.0	0.3	0.6	25.4	490
Ceriops	B	15	88.8	9.0	0.4	0.8	25.3	491
Ceriops	B	17	80.9	8.4	0.4	0.5	24.2	504
Ceriops	C	2	216.4	6.7	0.7	0.5	29.7	575
Ceriops	C	6	362.1	18.8	1.3		33.8	608
Ceriops	C	10	294.3	11.9	1.3	0.3	35.1	675
Ceriops	C	14	240.7	9.4	1.6	0.1	40.3	747
Ceriops	C	18	194.3	7.1	2.2	0.2	48.3	867
Rhiz	J	1	56.1	3.0	0.2	0.1	27.1	515
Rhiz	J	3	60.1	2.5	0.2	0.3	24.3	502
Rhiz	J	5	46.2	4.9	0.2	0.1	26.5	506
Rhiz	J	7	18.7	4.8	0.2	0.3	25.7	509
Rhiz	J	9	14.2	6.0	0.2	0.5	26.3	513
Rhiz	J	11	35.6	6.0		0.2	26.9	522
Rhiz	J	13	17.2	4.6	0.2	0.2	26.0	509
Rhiz	J	15	33.1	7.6	0.2	0.1	26.1	511
Rhiz	J	17	56.7	8.0	0.1	0.1	25.8	506
Rhiz	J	19	3.4	5.0	0.1	0.3	24.8	505
Rhiz	J	21.5	60.1	8.7	0.1	0.1	25.7	509
Rhiz	J	24.5	41.7	6.0	0.1	0.2	24.4	505
Rhiz	J	27.5	26.6	4.1	0.3	0.2	25.5	504
Rhiz	J	30.5	23.6	3.2	0.2	0.1	25.6	506
Rhiz	J	33.5	16.1	3.1	0.2	0.0	25.1	500
Rhiz	K	1	40.4	8.1	0.5	0.0	29.1	553
Rhiz	K	3	25.3	5.9	0.2	0.1	26.1	503
Rhiz	K	5	21.4	6.0	0.1	0.1	24.3	488
Rhiz	K	7	24.2	5.8	0.1	0.1	24.5	487
Rhiz	K	9	9.4	0.5	0.1	0.7	24.8	469
Rhiz	K	11	68.4	7.3		0.3	24.7	504
Rhiz	K	13	33.1	9.7		0.3	22.7	517
Rhiz	K	15	61.9	8.6		0.2	23.1	490
Rhiz	K	17	55.2	6.4	0.2	0.5	22.7	461
Rhiz	K	19	58.9	10.0	0.3	0.4	23.2	440
Rhiz	L	1	45.7	3.9	0.4	0.1	29.1	497
Rhiz	L	3	46.3	4.2	0.2	0.3	24.7	485
Rhiz	L	5	36.6	4.3	0.1	0.2	23.2	462
Rhiz	L	7	45.7	5.3	0.1	0.2	23.8	468
Rhiz	L	9	41.0	5.8	0.1	0.2	25.8	496
Rhiz	L	11	62.4	4.9	0.1	0.5	26.0	504
Rhiz	L	13	30.7	4.6		0.3	27.1	503
Rhiz	L	15	30.2	2.5	0.8	0.1	27.3	351
Rhiz	L	17	34.2	4.8		0.2	29.2	477
Rhiz	L	19	48.9	6.5		0.3	33.8	497
Rhiz	M	1	147.1	6.7	0.1	0.1	26.6	440
Rhiz	M	3	109.0	4.5	0.1	0.1	25.3	439
Rhiz	M	5	78.4	5.1	0.2	0.4	25.4	439
Rhiz	M	7	55.6	6.3	0.2	0.2	26.0	496
Rhiz	M	9	60.7	3.9	0.3	0.3	26.1	490
Rhiz	M	11	176.3	7.2	0.1	0.3	25.7	492
Rhiz	M	13	146.8	7.5	0.1	0.5	25.4	549

Table 3.4.5. Pore-water chemistry of Gazi Bay sediments (continued)

Type	Site	Depth cm	NH_4 µM	NO_3 µM	NO_2 µM	PO_4 µM	SO_4 mM	Cl mM
Rhiz	M	15	212.0	9.0	0.7	0.5	25.1	485
Rhiz	M	17	222.3	7.0	0.3	0.4	24.4	485
Rhiz	M	19	155.2	6.9	0.3	0.5	24.6	478
Sonn	II	1	64.1	5.1	0.1	0.1	12.1	212
Sonn	II	3	42.9	4.8	0.2	0.2	24.1	450
Sonn	II	5	41.9	5.8	0.2	0.3	27.1	511
Sonn	II	7	38.4	5.4	0.3	0.3	28.1	515
Sonn	II	9	6.1	5.2	0.3	0.6	28.5	526
Sonn	II	11	9.9	5.8	0.2	0.2	28.6	523
Sonn	II	13	41.4	6.0	0.2	0.2	27.9	506
Sonn	II	15	25.0	2.9	0.2	0.4	28.7	507
Sonn	II	17	33.7	5.0	0.2	0.3	26.2	501
Sonn	II	19	28.6	5.3	0.2	0.3	25.7	496
Sonn	II	21.5	28.1	5.0	0.1	0.1	27.0	505
Sonn	II	24.5	40.2	6.9	0.1	0.1	27.3	505
Sonn	II	27.5	17.4	4.2	0.1	0.2	26.2	503

al; this relates to C/N mixing ratios of 34 and 39.6 for algal and seagrass material. Similar calculations at the *Rhizophora* station yield a 60 to 40 % contribution, and C/N mixing ratios of 36.5 and 41.5 respectively. Thirdly, nitrogen fixing bacteria may enrich the sedimentary material. Nitrogen-fixation activities have been reported in mangrove sediments (Alongi *et al.*, 1992) and are likely to account for part of the nitrogen excess found in mangrove sediments of Gazi Bay (Woitchik *et al.*, 1994). To conclude, mangrove sediments are nitrogen rich with respect to mangrove litter due to nitrogen rentention (by microbial biomass), import of nitrogen-rich particles or nitrogen fixation. The relative importance of these nitrogen enrichment pathways requires further study.

Table 3.4.7. Mass balance constraints on nitrogen excess.

	Ceriops	Rhizophora	
Organic C	1.9	5.6	wt %
N	0.1	0.3	wt %
C/N	21.6	21.4	
Depth	16	40	cm
$C/N_{leavesNew}$	60.5	57.1	
$C/N_{leavesOld}$	152.5	165.7	
Miner.C	43.5	60.5	mmol $m^{-2}d^{-1}$
Miner. N sed.	2.0	2.8	mmol $m^{-2}d^{-1}$
Miner. N leav.New	0.72	1.1	mmol $m^{-2}d^{-1}$
Miner. N leav.Old	0.29	0.37	mmol $m^{-2}d^{-1}$
$N_{excessFreshLeaves}$	11.9	73.1	mol m^{-2}
$N_{excessOldLeaves}$	15.8	100.9	mol m^{-2}
$Time_{FreshLeaves}$	16-114	71-548	year
$Time_{OldLeaves}$	21-152	98-757	year

references

Alongi, D.M., 1989. The role of soft-bottom benthic communities in tropical mangrove and coral reef ecosystems. Rev. Aq. Sci. 1: 243-280.

Alongi, D.M., K.G. Boto & A.I. Robertson, 1992. Nitrogen and phosphorus cycles. In: Robertson A.I. & D.M. Alongi (eds), Tropical mangrove ecosystems: 251-292. AGU, Washington, DC.

Alongi, D.M., P. Christoffersen & F. Tirendi, 1993. The influence of forest type on microbial-nutrient relationships in tropical mangrove sediments. J.Exp. Mar. Biol. Ecol., 171: 201-223.

Bartlett, D.S., K.B. Bartlett, J.M. Hartman, R.C. Harriss, D.I. Sebacher, R. Pelletier-Travis, D.D. Dow & D.P. Brannon, 1989. Methane emissions from the Florida Everglades: patterns of variability in a regional wetland ecosystem. Glob. Biog. Cycles. 3: 363-374.

Boto, K.G. & J.T. Wellington, 1984. Soil characteristics and nutrient status in a northern Australian mangrove forest. Estuaries, 7: 61-69.

Clough, B.F., 1992. Primary productivity and growth of mangrove forests. In: Robertson A.I. & D.M. Alongi (eds), Tropical Mangrove ecosystems: 225-249. AGU, Washington, DC.

Dye, A.H., 1983. Oxygen consumption by sediments in a Southern Africa mangrove swamp. Est. Coast. Shelf Sci. 17: 473-478.

Table 3.4.6 Analysis of variance (ANOVA) of the influence of mangrove species and station on the pore-water composition. (Three depth levels are considered, namely 0-5, 5-20 and 20-40).

Source of variation	Sum-of-Squares	DF	Mean-Square	F-ratio	P
NH_4					
Species	10.027	5	2. 005	7.17	0.000
Station{Species}	3.431	5	0.686	16.139	0.000
Depth	0.135	2	0.068	1.592	0.209
Error	4.379	103	0.043		
NO_3					
Species	4.507	5	0.901	25.369	0.000
Station{Species}	0.673	5	0.135	3.786	0.003
Depth	0.340	2	0.170	4.785	0.010
Error	3.660	103	0.036		
NO_2					
Species	10.587	5	2.117	59.252	0.000
Station{Species}	0.634	5	0.127	3.548	0.006
Depth	0.165	2	0.083	2.315	0.104
Error	3.323	93	0.036		
PO_4					
Species	4.123	5	0.825	8.701	0.000
Station{Species}	4.872	5	0.974	10.282	0.000
Depth	1.130	2	0.565	5.964	0.004
Error	9.098	96	0.095		
SO_4					
Species	0.850	5	0.170	48.840	0.000
Station{Species}	0.159	5	0.032	9.121	0.000
Depth	0.030	2	0.015	4.353	0.015
Error	0.359	103	0.003		
Cl					
Species	0.633	5	0.127	41.271	0.000
Station{Species}	0.147	5	0.029	9.559	0.000
Depth	0.058	2	0.029	9.443	0.000
Error	0.301	98	0.003		

Hemminga M.A. *et al.*, 1994, this report

Kristensen, E., F. Andersen & L.H. Kofoed, 1988. Preliminary assessment of benthic community metabolism in a south-east Asian mangrove swamp. Mar. Ecol. Prog. Ser. 48: 137-145.

Kristensen, E., M. Holmer & N. Bussarawit 1991. Benthic metabolism and sulfate reduction in a south-east Asian mangrove swamp. Mar. Ecol. Prog. Ser. 73: 93-103.

Kristensen, E., A.H. Devol, S.I. Ahmed & M. Saleem, 1992. Preliminary study of benthic metabolism and sulfate reduction in a mangrove swamp of the Indus Delta, Pakistan. Mar. Ecol. Prog. Ser. 90: 287-297.

Lugo, A.E. & S.C. Snedaker, 1974. The ecology of mangroves. Ann. Rev. Ecol. Syst. 5: 39-64.

Nieuwenhuize, J, Y.E.M. Maas & J.J. Middelburg, 1994. Rapid analysis of organic carbon and nitrogen in particulate materials. Mar. Chem. 45: 217-224.

Rao R.G., A.F. Woitchik, L. Goeyens, A. van Riet, J. Kazungu & F. Dehairs, 1994. Carbon, nitrogen contents and stable carbon isotope abundance in mangrove leaves from an east African coastal lagoon (Kenya). Aquat. Bot. 47: 175-183..

Robertson, A.I., D.M. Alongi & K.G. Boto, 1992.

Food chains and carbon fluxes In: Robertson A.I. & D.M. Alongi (eds), Tropical Mangrove ecosystems: 293-326 AGU, Washington, DC.
Robertson, A.I. & D.M. Alongi, 1992 (eds). Tropical Mangrove ecosystems. AGU, Washington, DC.
Twilley, R.R., A.E. Lugo & C. Patterson-Zuccc, 1986. Litter production and turnover in basin mangrove forests in southwest Florida. Ecology, 67: 670-683.
Van Speybroeck, D., 1992. Regeneration strategy of mangroves along the Kenya coast: a first approach. Hydrob. 247: 243-251.
Wilkinson, L., 1990. SYSTAT: The system for statistics. Evanston, IL, Systat Inc.
Woodroffe, C., 1992. Mangrove sediments and geomorphology. In: Robertson A.I. & D.M. Alongi (eds), Tropical Mangrove ecosystems: 7-41. AGU, Washington, DC.
Woitchik, A.F. & F. Dehairs, 1995, this report.

Field-laboratory at Gazi Bay.

3.5. IMPORTANCE OF BIOLOGICAL NITROGEN FIXATION FOR NUTRIENT INPUT INTO THE SEAGRASS MEADOWS OF GAZI BAY

A.F. Woitchik & F. Dehairs
Laboratory for Analytical Chemistry, Vrije Universiteit, Brussels, Belgium.

introduction

Within the framework of the Coastal Research Programme of the Netherlands Indian Ocean Programme 1990-1995, research was carried out at Gazi bay to measure rates of biological nitrogen fixation associated with leaves of *Thalassodendron ciliatum*, from June 16th to July 8th, 1993. The N_2 fixation activity is mainly due to heterocystous cynanobacterial epiphytes (Smith & Hayasaka, 1982; Capone, 1983). This study was undertaken to determine whether nitrogen fixation is an important process contributing to the nitrogen requirement of the seagrass meadows of Gazi Bay.

materials and methods

Intact specimens of *T. ciliatum* were collected by scuba-divers, along a transect going from the mangrove swamps towards the coral reef (locations MM: mangrove-mangrove; MS: mangrove-seagrass; CS: coral-seagrass; CC: coral-coral). In the laboratory, they were sorted in roots and leaves, rinsed gently under tap water and immediately assayed for nitrogen fixation using the acetylene reduction technique (Hardy *et al.* 1968). Leaves were incubated in gas-tight perspex-plexiglas enclosures (diameter: 20 cm, height: 25 cm) fitted with a gas sampling device. Acetylene was injected into the enclosures to a final concentration of 10% in volume. 100 µl ethane was injected in the enclosure as internal standard. Reduction of acetylene into ethylene was followed by hourly analyses of 100 µl gas samples during 6 to 8 hours, with a Varian model 3300 gas chromatograph. Gas samples were separated on a 2 m Porapak N packed column at 50°C. Injector temperature was 200°C; N_2 was used as carrier gas at a flow rate of 25 ml/min. Peak heights were measured with a Varian integrator, model 4400. Gases were calibrated against pure standard gases. An additional experiment was conducted where leaves, stems and roots of *T. ciliatum* were incubated separately for comparison of nitrogen fixation rates. In the absence of acetylene, no natural production of ethylene was detected.

results and discussion

The rates of C_2H_2 reduction associated with *T. ciliatum* stems, roots and leaves are presented in Fig. 3.5.1. Comparison of activities of nitrogen fixers associated with different parts of the *T. ciliatum* show a seven-fold larger activity associated with leaves (17 nmoles C_2H_4 gDW^{-1} h^{-1} than with roots (2.5 nmoles C_2H_4 gDW^{-1} h^{-1}) and stems (2 nmoles C_2H_4 gDW^{-1} h^{-1}).

The rates of C_2H_4 reduction associated with *T. ciliatum* leaves along the MM, MS, CS and CC locations are illustrated in Fig. 3.5.2. The results show a decrease in nitrogen fixation rates from the mangrove area to the coral reef with maximum values of 91 ± 8 nmoles C_2H_4 gDW^{-1} h^{-1} at the MM location and minimal values of 9 to 14 ± 5 nmoles C_2H_4 gDW^{-1} h^{-1} at the CS and CC locations. These results are similar to the ones reported by Capone (1983): values of 0 - 100 nmoles C_2H_4 gDW^{-1} h^{-1} were observed for leaf epiphytes of *Zostera marina* in North Carolina (Smith & Hayasaka, 1982 cited in Capone, 1983). Highest values of 80 - 900 nmoles C_2H_4 gDW^{-1} h^{-1} were obtained for *Thalassa testudinum* leaf epiphytes, in Florida by Capone & Taylor (1977) and of 2000 - 13000 nmoles C_2H_4 gDW^{-1} h^{-1} in Texas by Goering & Parker (1972).

N_2 fixed in the seagrass environment may be of either direct or indirect relevance to plant demand. This nitrogen can ultimately became available to the plant after excretion or exudation by or degradation of the nitrogen fixing organisms (Capone, 1983). To estimate which fraction of the nitrogen demand is supplied by N_2 fixation, we must know the total nitrogen demand of seagrasses and their standing biomass. The standing biomass of *T. ciliatum* in Gazi bay is 647 g DW m^2 (van Avesaath *et al.* 1993). Using the theoretical factor of three acetylene molecules equivalent to one nitrogen molecule (Turner & Gibson, 1980) to convert the acetylene reduction to nitrogen fixation rates and an activity of 12 hours per day, we obtained nitrogen fixation values ranging from 0.652 to 6.522 mg N m^{-2} day^{-1}.

references

Avesaath, P.H. van, G. van der Velde & E. Coppejans, 1993. Seagrasses and macro-algae of eastern and western creeks. in: A.F. Woitchik, ed., Dynamics and Assessment of Kenyan Mangrove Ecosystems. nr. TS2-0240-C. CEC, STD-2 Final report: 35-55.

Capone, D.G. 1983. N2 fixation in seagrass communities. Mar. Tech.Soc. J. 17: 32-37.

Capone, D.G & B.F. Taylor, 1977. Nitrogen fixation (acetylene reduction) in the phyllosphere of *Thalassia testudinum*. Mar. Biol. 40: 19-28.

Goering, J.J. & P.L. Parker, 1972. Nitrogen fixation by epiphytes on seagrasses. Limnol. Oceanogr. 17: 320-323.

Hardy, R.W., R.D. Holsten, E.K. Jackson & R.C.

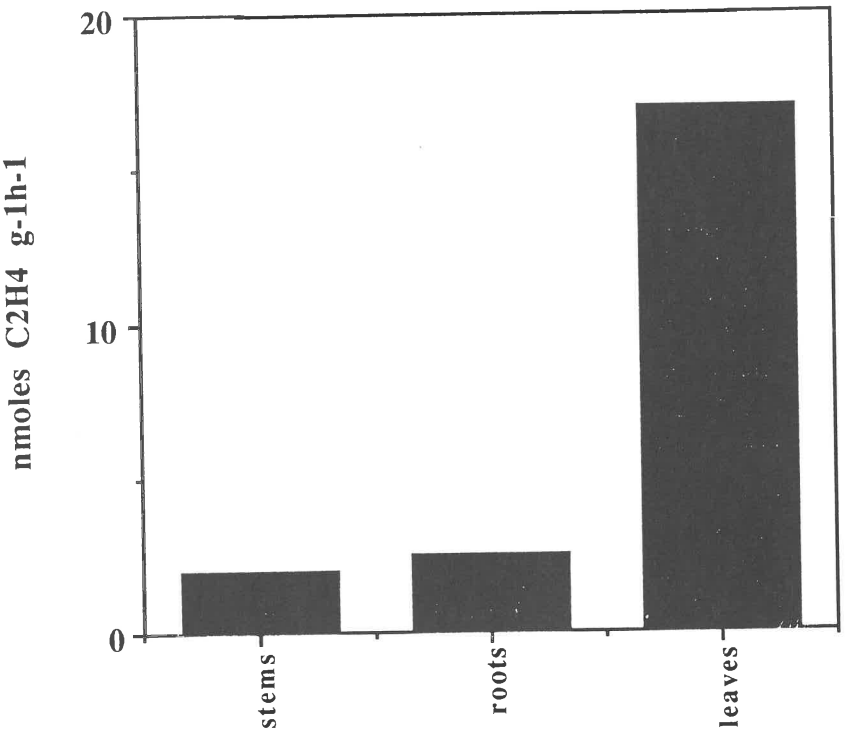

Figure 3.5.1. N_2-fixation associated with different parts of *T. ciliatum*.

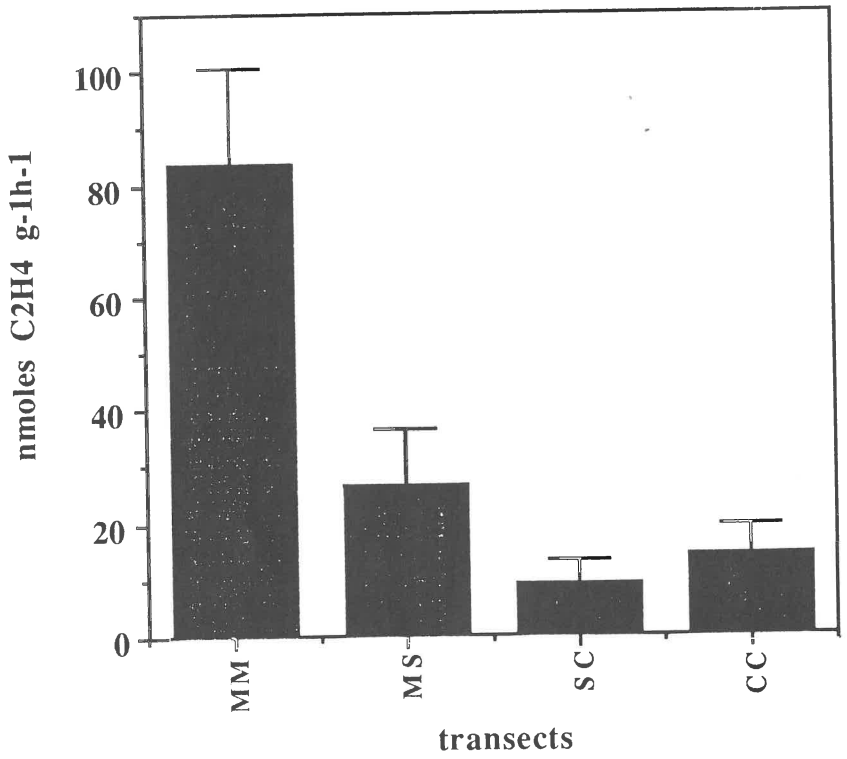

Figure 3.5.2. N_2-fixation associated with leaves of *T. ciliatum*.

Burns, 1968. The acetylene - ethylene assay for N2-fixation: laboratory and field evaluation. Plant Physiol. 43: 1158-1207.
Smith, G.W. & S.S. Hayasaka, 1982. Nitrogenase activity associated with *Zostera marina* from a North Carolina estuary. Can. J. Microbiol. 28: 448-451.
Turner, G.L. & A.H. Gibson, 1980. Measurement if nitrogen fixation by indirect means. In: F.J. Bergersen ed. Methods for evaluating biological nitrogen fixation: 111-138. Wiley & Sons Ltd.

Three container laboratories were placed near Jadini Beach Hotel in the vicinity of Gazi Bay. For protection against the sun they were covered with locally prepared roofs.

4. PRELIMINARY RESULTS OF THE SHIP-BASED PROGRAMME

4.1. TEMPERATURE, SALINITY AND WATER MASS STRUCTURE ALONG THE KENYAN COAST DURING THE 1992 CRUISES A1 AND A2 OF R.V. *TYRO*

Michael Mutua Nguli
Kenya Marine and Fisheries Research Institute, P.O. Box 81651, Mombasa, Kenya

abstract
Three hydrographic transects were studied in the later half of June-July and November -December 1992 at latitude 1.5-4.5°S during cruises A1 and A2 of R.V. *Tyro* in the Western Indian Ocean. Water structure characteristics for the Kenyan coast under the influence of the Southeast monsoon and the Northeast monsoon were studied. The surface layer responds to the Southeast monsoon (June) by formation of a deep homogeneous layer with upper and lower main thermocline at 70-120 m, whereas during the Northeast monsoon (November) the thermocline was uplifted by 30 m above the June position. Nutrients and salinity near the coast are relatively low due to river influence, however, nutrient levels increase ocean-ward suggesting an oceanic origin and are relatively high in November. The water at intermediate depth has an elaborate structure with several high salinity and low salinity layers mingling at various levels. The mingling is attributed to mixing of various water masses of Indian and Pacific Oceans origin.

introduction
The Netherlands research vessel R.V. *Tyro* made two cruises in the Kenyan coastal waters in 1992, aimed at studying the monsoonal effect on Kenyan coastal ecosystems. During the cruises CTD, plankton, nutrients and sediment measurements were made at various stations along three main transects: Gazi, Sabaki and Kiwayu, laying perpendicular to the coast. The Gazi transect lays to the south of Mombasa within the non-reversing part of the East African coastal current (EACC) whereas the Sabaki and Kiwayu transects were located in the northern part of the coast where currents reverse seasonally. Current measurements were also made with three self recording current meters placed at 30 m, 105 m and 160 m water depth, ten kilometers to the south of Mombasa. In this paper, we present the analysis of salinity, temperature, nutrients and water mass structure on the shelf during the two cruises.

background
The Kenya coast can be described as an exceptionally narrow (0-3 km) continental shelf except for the northern part between Malindi and Lamu where the shelf width is 15-60 km due to the presence of the Malindi and the North Kenya Banks. The entire coast lies within the Indian Ocean monsoon region with its northern part influenced by the reversing Somali Current.

Earlier hydrographic work in the area was carried out by Newell (1957, 1959), who described the general behaviour and some properties of the water. Later work focused on the reversal and the switching mechanism of the coastal current (Leetmaa, 1972, 1973; Duing & Schott, 1977; Johnson *et al.*, 1982). Inversen & Myklevol (1984) also made some hydrographic observations in the same area. The latest report by Swallow *et al.* (1992) discusses the structure and the transport of the East African Coastal Current (EACC). Observations emerging from these previous studies are that the area north of Malindi is evidently influenced by the EACC, which flows northward during the Southeast monsoon (April to September), the Somali Current (SC) and the eastward moving Equatorial Counter Current (ECC). The latter current is formed during the Northeast monsoon (November to April) when the SC and the EACC meet near Malindi. There is evidence to show that between November and January a clockwise gyre exists within the permanently northward flowing EACC to the south of Malindi that breaks up after January (Newell, 1959). The EACC flows at greater speed during the Southeast monsoon than during the Northeast monsoon as indicated in fig. 4.1.1 where the current patterns represent the flow condition, off Kenya, at a period closely corresponding to the time of the cruises. The intermonsoon periods occur in May and November and are characterized by an eastward jet (Wyrtki, 1973; O'Brien & Hurburt, 1974; Findlater, 1971). The water masses are generally those found in the Indian Ocean and discussed by Tomczac and Godfrey (1994) but their precise identity and position off Kenya are not clearly defined.

material and methods
R.V. *Tyro* made two cruises for a total of 36 days. Cruise A1 was from 18 June to 7 July during the Southeast monsoon whereas cruise A2 took place during the Northeast monsoon from 20 November to 8 December 1992. Four transects laying perpendicular to the coast were sampled (Fig. 4.1.2). Gazi transect was located in the south, whereas the Sabaki transect was near Malindi and Kiwayu was the northernmost transect. An additional transect, the Tana transect and seven inner shelf stations were occupied along the

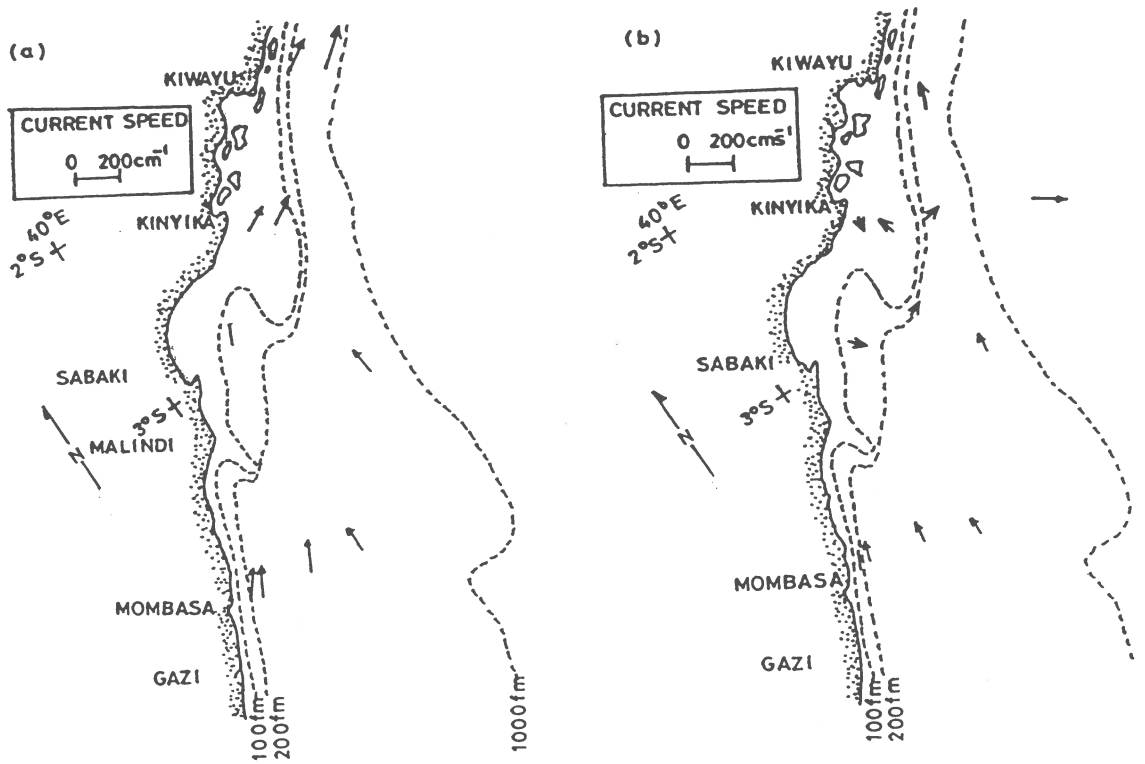

Fig. 4.1.1. Currents along the Kenyan coast during (a) July and (b) December (after Johnson *et al.*, 1982)

coast during the cruise A1 in order to identify the Sabaki and Tana river plumes. Four stations were occupied in each transect with depths approximately 50, 500, 1000 and 2000 m. At most transects shallower stations (20 m) were sampled as well. CTD measurements were made using standard ship equipment and salinity calibration was done by titration method aboard the ship using a Salinometer model 800. Samples were also collected for plankton, nutrients and sediment analysis and current observations made at three depths 30 m, 105 m and 160 m at a single mooring site at Tiwi, ten kilometers south of Mombasa.

results and discussion

Temperature profile

Figures 4.1.3 a-f show some examples of the vertical variation of temperature with depth for cruise A1 and A2. Fig. 4.1.3 a,c,e reveal the initial effects of the monsoon on the surface waters (0-200 m) of the Kenyan coastal waters. In June the water appears to respond by formation of a homogeneous surface layer overlying a main thermocline at 70-120 m. In November (fig.4.1.3.b,d,f) the homogeneous layer is much shallower and restricted to 50 m and the thermocline is uplifted by 30 m from the June position. Lower temperatures occurred in the landward stations, particularly near Malindi, than offshore ones in both June and November, and slightly higher temperatures were evident in November than in June. The lower temperature near the shore are associated with fresh water input from rivers. The high temperature in November indicates the coastal waters hand gained heat between June and November. Fig 4.1.4 a-f compares profiles for June and November. On the surface a homogeneous layer with temperature 27°C is observable. Within the thermocline zone the temperature ranges from 24°C to 18°C and 18°C to 4°C in the intermediate depth. Several temperature maxima and minima appear at various depth levels. These observations can be explained by a combination of factors mainly related to flow. In June the monsoon effects are greater than in November as a result of strong winds and swift surface flow (Newell, 1957, 1959, Swallow *et al.*, 1992). These conditions cause mixing in the surface layer, produce the observed homogeneous layer and deepen the thermocline. The observed uplift, which has also been mentioned by Kabanova (1968) may be as high as 50 m at the peak of the Northeast monsoon and is initiated in October by an eastward Equatorial jet caused by westerly winds (Finlater, 1972; Wyrtki, 1973; Duing & Schott, 1977; O'Brien & Hurburt, 1974) which occurs during the intermonsoon months. We believe that the position of this thermocline is more or less maintained throughout the Northeast monsoon

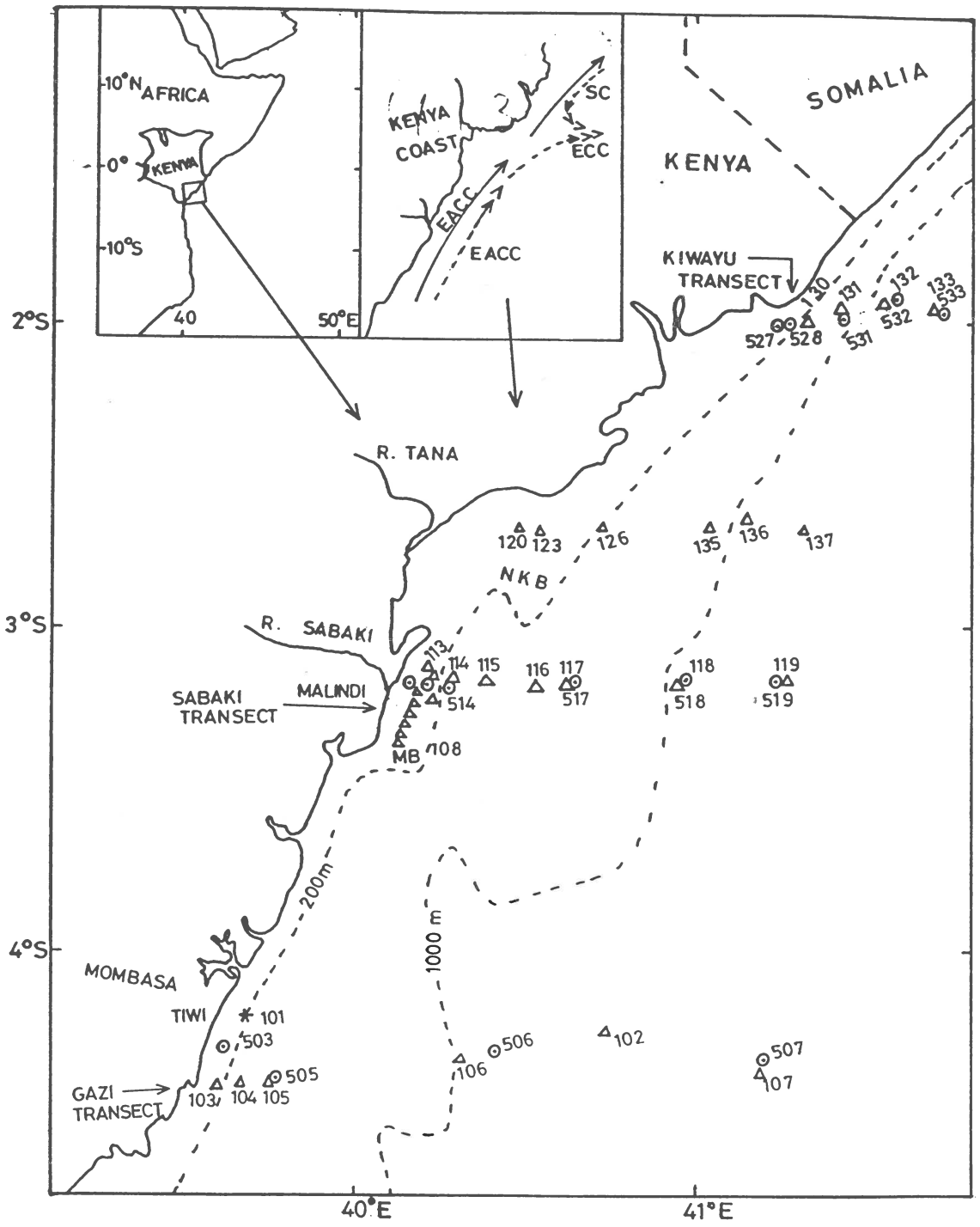

Fig. 4.1.2. Map of stations. Circles correspond to A1, triangles to A2. NKB = North Kenya Banks, MB = Malindi Banks, EACC = East African Coastal Current, SC = Somali Current, ECC = Equatorial Counter Current.

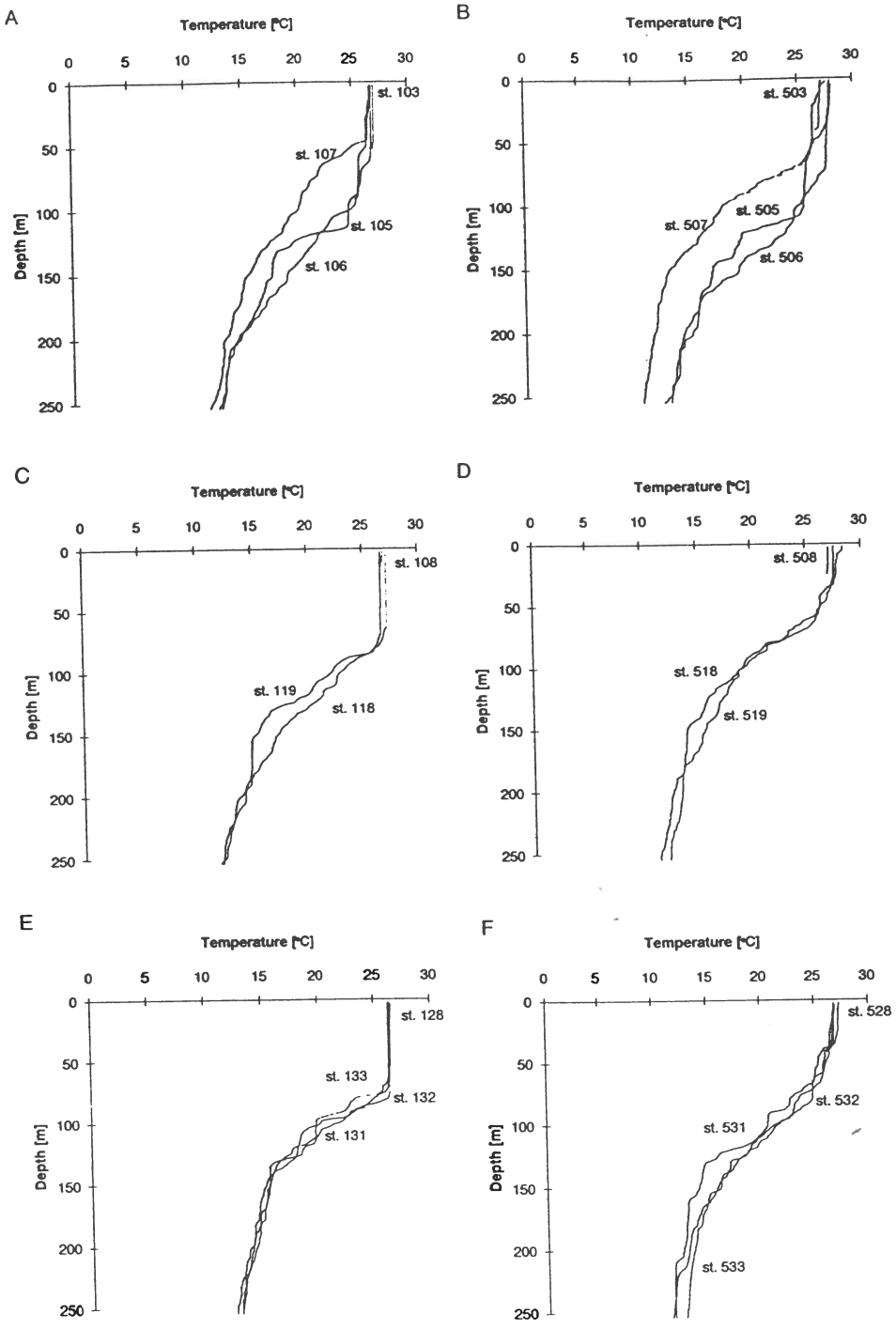

Fig. 4.1.3. Temperature-depth profiles in the upper 250 m. Leg A1 on the left side, leg A2 on the right side of the figure, Gazi upper, Sabaki middle and Kiwayuu lower side of the figure.

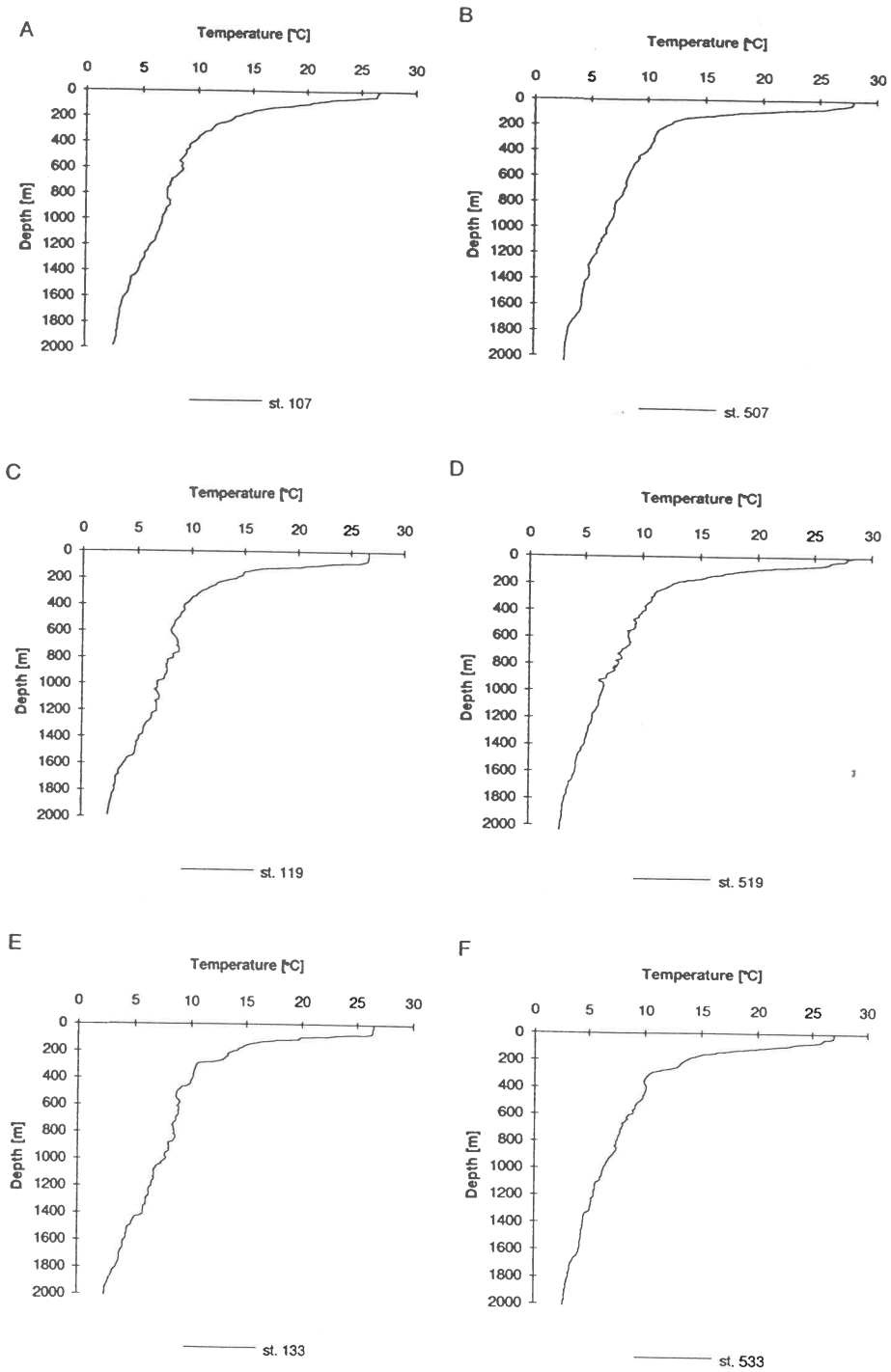

Fig. 4.1.4. Deep Temperature-depth profiles. As in fig. 4.1.3.

season by the Ekman flow or the Equatorial Counter Current, but deepens at the onset of the Southeast monsoon.

Salinity profiles

Fig. 4.1.5 a-f show some examples of the salinity profiles in June for several stations along the coast. Near the surface salinity ranges from 34.8-35.0 psu. The lowest values of salinity, much like the temperature, occur in the landward stations due to river influence. The salinity increases in the subsurface layer to a maximum value of 35.48 psu just below the thermocline. Between 300-550 m the salinity has a mean value of 34.7 psu. Another maximum of 35.3 psu occurs at 630 m followed by a minimum at 1025 m. At depths greater than 1500 m the salinity value falls to 34.6 psu. Slightly higher salinity occurs in the northern transects than in the southern ones for depths between 0-630 m during the same cruise. The along shelf difference in salinity indicates that the EACC gradually gains salinity as it moves northward.

Nutrients and oxygen concentrations

Nutrients were low in the surface water during the two cruises, although they were slightly higher in December particularly in the northern transects. There was a general increase in nutrient with depth and away from the shallow stations suggesting that the nutrients were largely of oceanic origin. Above the thermocline silicate, phosphate and nitrate were less than 3µm, 0.6µm and 2µm respectively. Nitrite was almost zero during cruise A1 and higher in cruise A2 with an apparent maximum at about 70 - 100 m and a minimum at 20 m. In the intermediate water silicate, phosphate and nitrate showed highest concentration of 114µm, 2.54µm and 36µm respectively with very low nitrite concentration. Oxygen concentrations were higherin the upper layers of the surface layer with values between 240 - 200µm. The concentrations fell to half this value between 150 -300 m but dropped to a minimum of about 60µm in the intermediatewaters. The position of this minimum occurred at about 400 - 800 m. The concentration increased slightly in deeper waters below 1500 m.The higher nutrients especially in the deep waters off Kiwayu can be explained by the arrival of higher salinity water from the north and complicated currents there. The fluctuation in properties was attributed largely to various water masses.

Water masses

In an effort to understand the water mass structure during the two cruises, the analysis of T - S characteristics and in some cases, of dissolved oxygen are of value. However, since oxygen is somewhat an ambiguous water mass property, we shall concern ourselves principally with salinity structure. The water off the Kenyan coast can be envisaged as an elaborate interplay of the South and North Indian Ocean water. We have chosen to identify the watermasses on the basis of the classification given mainly Tomczac & Godfrey (1994)

Surface water and thermocline layer

Since the surface (0 - 200 m) is in direct contact with the atmosphere its temperature and salinity are not sufficiently conservative to permit adequate definition of water type. Fig. 4.1.6 reveals a top layer (0 - 20 m) with warm fresher water than the underlying subsurface water with a maximum salinity of 35.45 psu at about 50 m. The second salinity maximum, at about 100 m, overrides a much cooler and fresher layer which extends from 200 m to 600 m and which will be considered later. The top layer of water is a mixture of the Bay of Bengal Water(BBW) from the Indian and Indochinese Subcontinent (Tomczac & Godfrey, 1994), river discharge, whereas we believe the subsurface maximum is caused by the high salinity end of Indian central water. Since the salinity maximum occurs within the thermocline layer (50-120 m) we have referred to it as the BBW-ICW thermocline. The actual position of this maximum and structural complexity is influenced by topography and seasonal reversals of the Somali Current. The tongue of Arabian Sea water which William (1970) suggested as penetrating along the Kenyan Coast upto 3°20'S and referred to as the 'Somali water' is according to this classification, the high salinity end of the Indian Central Water, however, the extent of the subsurface maximum as far South as Gazi is in agreement with Leetmaa & Truesdale (1972) who suggested Zanzibar (7°S) as the limit of the Somali current.

Intermediate and deep water

The T-S diagram (Fig. 4.1.6) shows the complicated mingling of watermasses at various levels. At the intermediate depth below the thermocline (200 - 2000 m) at least three water masses are capable of producing the complicated intermingling. The fresher layer below the maximum within the thermocline layer is due to the Australasian Mediterranean Water (AAMW) which is a tropical watermass derived from Pacific Ocean Central Water and formed during transit through the Australasian Mediterranean sea (Tomczac & Godfrey, 1994). This is the water mass which Warren *et al.* (1966) and Invenkov & Gubin (1960) probably referred to as the upper branch of subtropical surface water of salinity 34.7 - 35.5 psu and temperature 7 - 15°C. The salinity maximum that occurs in the layer 600 - 800 m and coincides with the oxygen minimum is very likely caused by the Red Sea water which

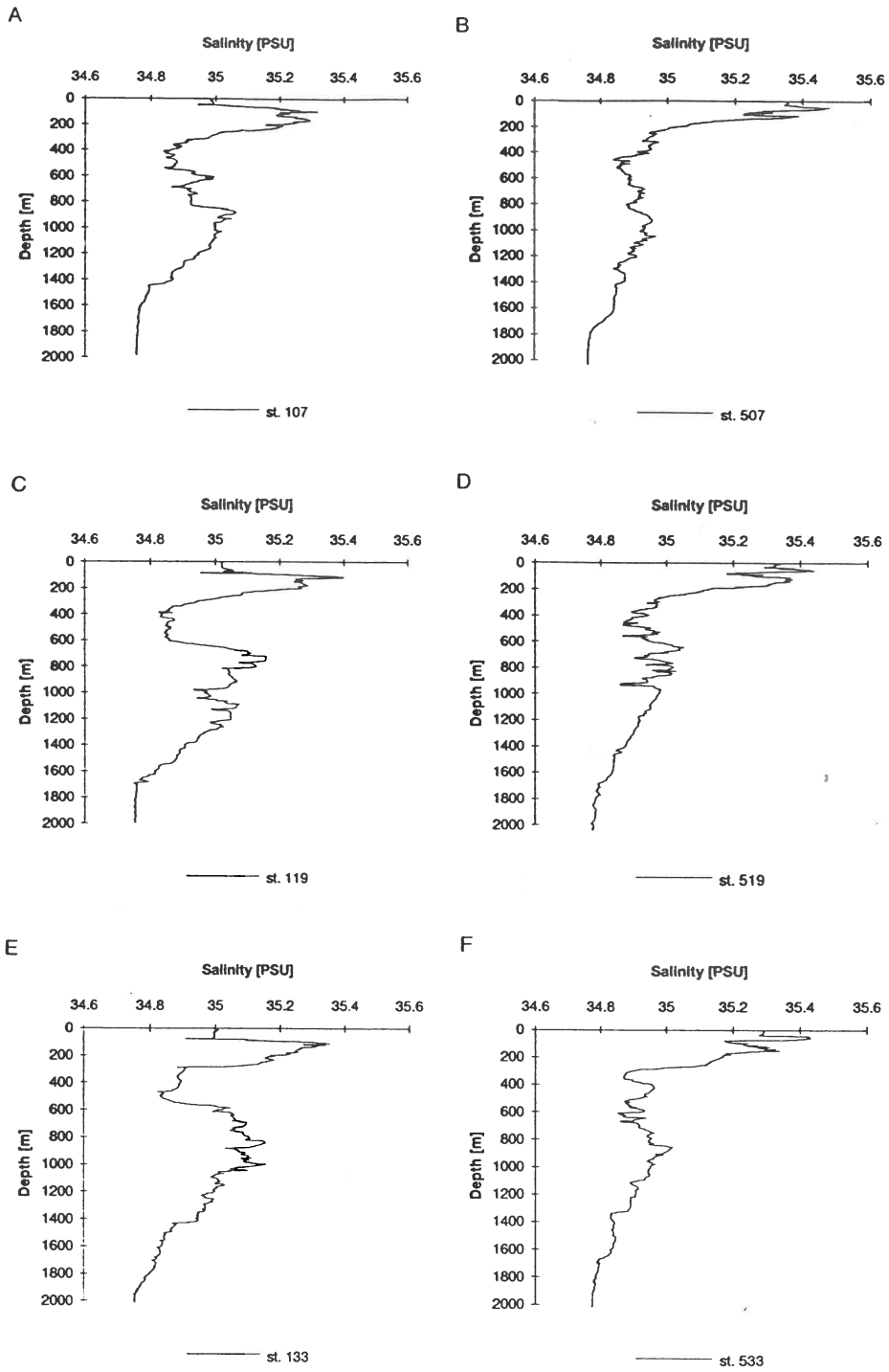

Fig. 4.1.5. Deep salinity-depth profiles. As in fig. 4.1.3.

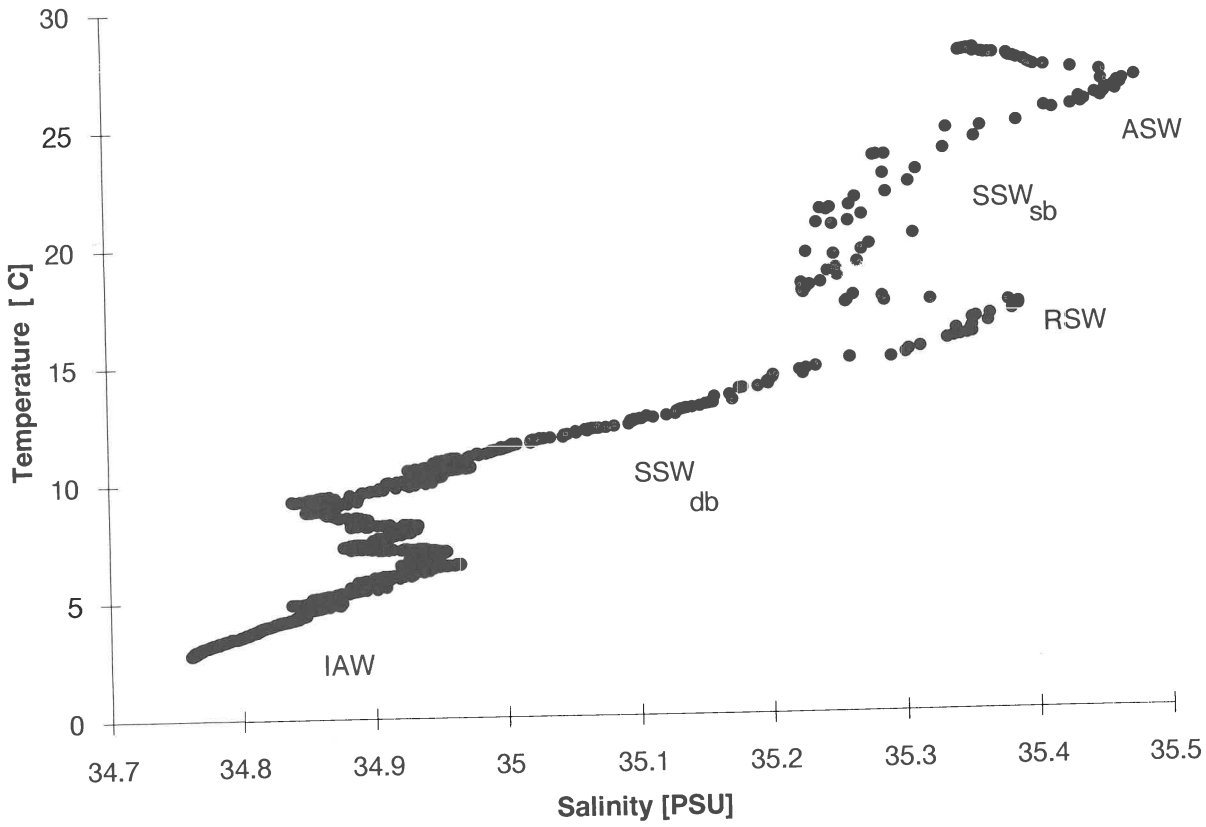

Fig. 4.1.6. T-S diagrams. ASW = Arabian Sea Water, SSW-sb = Subtropical Subsurface Water (shallow branch), SSW-db = Subtropical Subsurface Water (deep branch), RSW = Red Sea Water, IAW = Intermediate Antarctic Water.

originates from the North Indian Ocean and moves southward, sinking to deeper levels on account of its high density. The water below 1000 m, where oxygen concentration increases slightly, can be associated with the Antarctic Intermediate Water (AIW) with salinity less than 34.65 psu and temperature 3.5 - 7°C. This water mass has its origin at the sea surface in the vicinity of the subtropical convergency near 40°S (Warren et.al., 1966).

conclusion

In this paper we have attempted to describe temperature and salinity characteristics and the water masses represented by the elaborate structure seen off the Kenya coast during the 1992 cruises Al and A2 of R.V. *Tyro*. A homogeneous surface layer is observed in June overlying a thermocline at 70 to 120 m depth. In November the layer is much shallower and the thermocline is lifted by 30 m from its June position. The Bay of Bengal Water (BBW) is observed in the surface layer where it overrides Indian Central Water with maximum salinity within the thermocline layer. The Red Sea Water forms a core of high salinity at 800 m overlying cold, fresh Antarctic Intermediate Water. High biological productivity observed during the Northeast monsoon is probably due to the arrival of the ICW ('Somali water') on the shelf, the uplift and complicated currents in the vicinity of the north Kenya Banks.

acknowledgments

The author is grateful to the officers, crew and scientific parties of the R.V. *Tyro* for executing the hydrographic stations and to Dr E. Okemwa, the Director of Kenya Marine and Fisheries Research Institute (KMFRI) and Dr Jan H. Stel, the director of the Netherlands Geosciences Foundation for assisting in numerous ways. The work of *Tyro* in the Kenya coastal waters formed part of the Netherlands Indian Ocean expedition. The cruise was supported by the Netherlands Marine Research Foundation.

references

Duing, W. & F. Schott, 1977. Measurements in the source region of the Somali current. J. Phys. Oceanogr. 8: 278-289.

Findlater, J., 1971. Mean monthly airflow at levels over the western Indian Ocean. Geophys. Mem. 115: 53.

Invankov V.N. & F.A. Gubin, 1960. Water masses and hydrochemistry of the western and southern parts of the Indian Ocean. English translation of: Trans. Mar. Hydrophys. Inst., Acad. Sci. U.S.S.R. 22: 27-99.

Inversen, S.A. & S.Myklevol, 1984. Kenya Marlin fish resources in waters deeper than 10 m investigated by R.V "Dr. Fridjof Nansen" in: S.A. Iversen & S. Myklevoll (eds.), The proceedings of Norad fish stocks and fisheries in Kenya. 210pp.

Johnson D.R., M.M. Nguli & E.J. Kimani, 1982. Response to annually reversing monsoon winds at the southern boundary of the Somali current. Deep-Sea Res. 29: 1217-1227.

Kabanova, Yu.G., 1968. Primary production in the northern part of the Indian Ocean. Oceanology 8: 214-275.

Kromkamp, J., E. Ham & J.Peene, 1992. Primary production along the Kenyan coast during the rain period at the end of the South-east monsoon. R.V. *Tyro* Shipboard Report.

Leetmaa, A., 1972. The response of the Somali current to the South East monsoon of 1970. Deep-Sea Res. 19: 319-325.

Leetmaa, A., 1973. The response of the Somali Current at 2 deg S to the South West monsoon of 1971. Deep-Sea Res. 20: 397-400.

Leetmaa, A. & V. Truesdale, 1972. Changes in the Somali current in 1970 off the east Africa coast with the onset of the South East monsoon. J.Geophys. Res. 77: 3281-3283.

Morgans, J.F.C., 1979. The sea we fish in E. Africa. Agric. J. 25: 91-96.

Morgans, J.F.C., 1959. The north Kenya Banks. Nature 184: 2259-2260.

Newell, B.S., 1957. A preliminary survey of the hydrography of British East African Coastal waters. Fish Publ. London 9: 1-20.

Newell,B.S., 1959. The hydrography of the East African coastal waters. Part II. Fish Publ. London 12: 1-18.

O'Brien, J.J. & J.E. Hurburt, 1974. Equatorial jet in the Indian Ocean. Theory. Science 184: 1075-1077.

Swallow, J., C.F. Schott & M. Fieux, 1992. Structure and transport of the East African Coastal Current. J. Geophy. Res. 93: 22, 245-22,570.

Tchernia, P., H. Lacombe & P. Guilbout, 1958. Sur quelques nouvelles observations hydrologiques relative à la région equatoriale de l'Ocean Indien. Bull. Inf. Com. Cont. Oceanogr. Étude Cotes 10: 115-143.

Tomczac, M. & J.S.Godfrey, 1994. Regional oceanography, An introduction: 221-236. Pergamon Press.

Warren, B., H. Stomnel & J.C. Swallow, 1966. Water masses and patterns of flow in the Somali basin during the Southwest Monsoon of 1964. Deep-Sea Res. 13: 825-860.

William, F., 1970. The sport fishery for sail fish at Malindi, Kenya 1958-1968, with some biological notes. Bull. Marine Sci. 20 : 831-852.

Wyrtki, K., 1973. An equatorial jet in the Indian Ocean. Science 181: 262-264.

CTD-Rosette sampler.

4.2. NUTRIENTS

Carlo Heip & Monique de Bie
Centre for Estuarine and Coastal Ecology, Netherlands Institute of Ecology, Yerseke, The Netherlands

introduction

The changes in nutrient concentrations occurring between the onset of the SE monsoon in June-July and the start of the NE monsoon in November-December are shown in figs 4.2.1-9. All figures are arranged so that data are shown from south (Gazi transect) (upper part of the figures) to north (Kiwayuu transect) (lower part of the figures) and from the first leg A1 (left part of the figures) and the second leg A2 (right part of the figures). For all variables profiles of the entire water column (2000 m) and of the upper 250 m are shown.

results

Nitrate

The nitrate profiles (fig. 4.2.1 and 4.2.2) are similar both between stations and between cruises. In surface waters nitrate is nearly or completely absent and the concentrations increase from below the mixed layer till a maximum around 39 µM at about 1200-1400 m. At all deep stations concentrations decrease again slightly and reach about 36 µM near the bottom.
A comparison of nitrate concentrations in the upper 250 m is more interesting. During leg A1 nitrate is below detection limit in the surface mixed layer until a depth of about 70 m at all stations. Concentrations then increase till values of about 15 µM at about 150 m depth and then remain more or less constant until 250 m. During A2 there was a slight uplift of the near-zero concentration limit to about 50 m depth coinciding with the uplift of the thermocline.

Ammonium

The extremely low ammonium levels during A1 and the analytical problems caused by them at the start of the cruise resulted in a wide scatter of results in the Gazi transect stations (fig. 4.2.3). At the other transects the values are more constant and hardly vary over depth, being around 0.5 muM. During A2 the same profile persists but values are lower, around 0.2 µM. The surface values (fig. 4.2.4) show more scatter but appear to show similarly that concentrations remain unchanged over the entire water column. The persistent lower valuues of ammonium are one of the more striking results of the cruise.

Phosphate

As is the case for nitrate, the deep profiles of phosphate are similar at all transects with surface values slightly above 0 increasing till about 800 m to about 3 µM and sligthly decreasing again to about 2.5 µM near the bottom (fig. 4.2.5). The surfac profiles show low values of about 0.2 µM until depths of about 70 m during A1 and 50 m or less during A2 (fig.4.2.6)

N:P ratios

In the deeper water layers the molar N:P ratio is about 14-15 in all stations and does not change from A1 to A2. In the upper layers the ratio strongly decreases towards the surface. During A1 the minimum is about 3 whereas during A2 the minimum approaches zero (fig. 4.2.7).

Oxygen

The deep oxygen profiles (fig. 4.2.8) show marked differences between A1 and A2. During A1 at the Sabaki and Kiwayuu transect there is a low surface value of around 150 µM and concentrations increase till a maximum of about 190 µM at around 200 m depth, then decrease again till the oxygen minimum of about 50 µM that exists at all transects and during both cruises at about 1000 m depth. At the Gazi transect during A1 there is a maximum in the surface waters and a pronounced decrease starting at the base of the mixed layer. This profile is similar to all profiles from A2. The profiles from the upper water layers (fig. 4.2.9) are complex with very small variations that probably reflect daily changes in photosynthesis and respiration.

conclusions

The characteristics of the deep water layers are very similar between the two cruises and have been discussed by Nguli (this volume). In the surface layers, where biological production takes place, the most striking differences between the two legs in the surface waters are
1) a much deeper mixed layer during the first cruise with nitrate levels below detection limit in the upper 70 m at most stations.
2) no evidence of uptake or production of ammonium during both cruises but much lower concentrations during A2.
3) the molar N:P ratio going close to zero during A2

During A1 nitrate was near or below detection limit in the upper 70 m of the water column and primary production is limited by nitrate availability (see reports of Kromkamp *et al.* and Mengesha *et al.* in this volume). Although the winds were much weaker and had already turned during A2, the waters were still flowing northward at the Kiwayuu transect and the transition between the two monsoon periods still had to occur. The mixed layer was therefore less well developed during A2.

The oxygen profiles also support the notion that primary production was much lower during A1. At the Sabaki and Kiwayuu transects there is no oxygen maximum in the surface layers and the clear oxygen minimum that occurs just below the mixed layer at Gazi during A1 and at all transects during A2, is missing. This 100-200 m deep oxygen minimum can be attributed to heterotrophic processes depending on primary production in the mixed layer and especially by the deep chlorophyll maximum occurring at its base. Oxygen in the photic zone during A1 appears to be mainly consumed and the system may have been net heterotrophic. During A2 there is a clear oxygen maximum in the surface layers at all transects, and the system may have been net autotrophic.

The deep oxygen minimum of around 50 µM is present at all stations and during both legs at a depth between 600-1000 m, most often around 900 m during A2 but more variable during A1 with an apparent uplift (or two mixing water masses) present in the Sabaki and Kiwayuu transects. The consequences of this deep oxygen minimum for benthic respiration have been discussed by Duineveld *et al.* (this volume).

references

Duineveld, G.C.A., E.M. Berghuis, T. Tahey & P.A.W.J. de Wilde, 1995. Distribution and activity of the benthic infauna along the Kenyan shelf (this volume: 117-122.)

Kromkamp, J,, J. Peene, P. van Rijswijk, J. Sinke & N. Goosen, 1995. Primary production of phytoplankton in the coastal ecosystem of Kenya (this volume: 93-99).

Nguli, M.M., 1995. Temperature, salinity and water mass structure along the Kenyan coast during the 1992 cruises A1 and A2 of R.V. *Tyro*. (This volume: 71-79).

Semeneh, M., F. Dehairs & L. Goeyens. Uptake of nitrogenous nutrients by phytoplankton in the tropical western Indian Ocean (Kenyan coast): monsoonal and spatial variability (this volume: 101-104).

Filmer Bernardo Guillén.

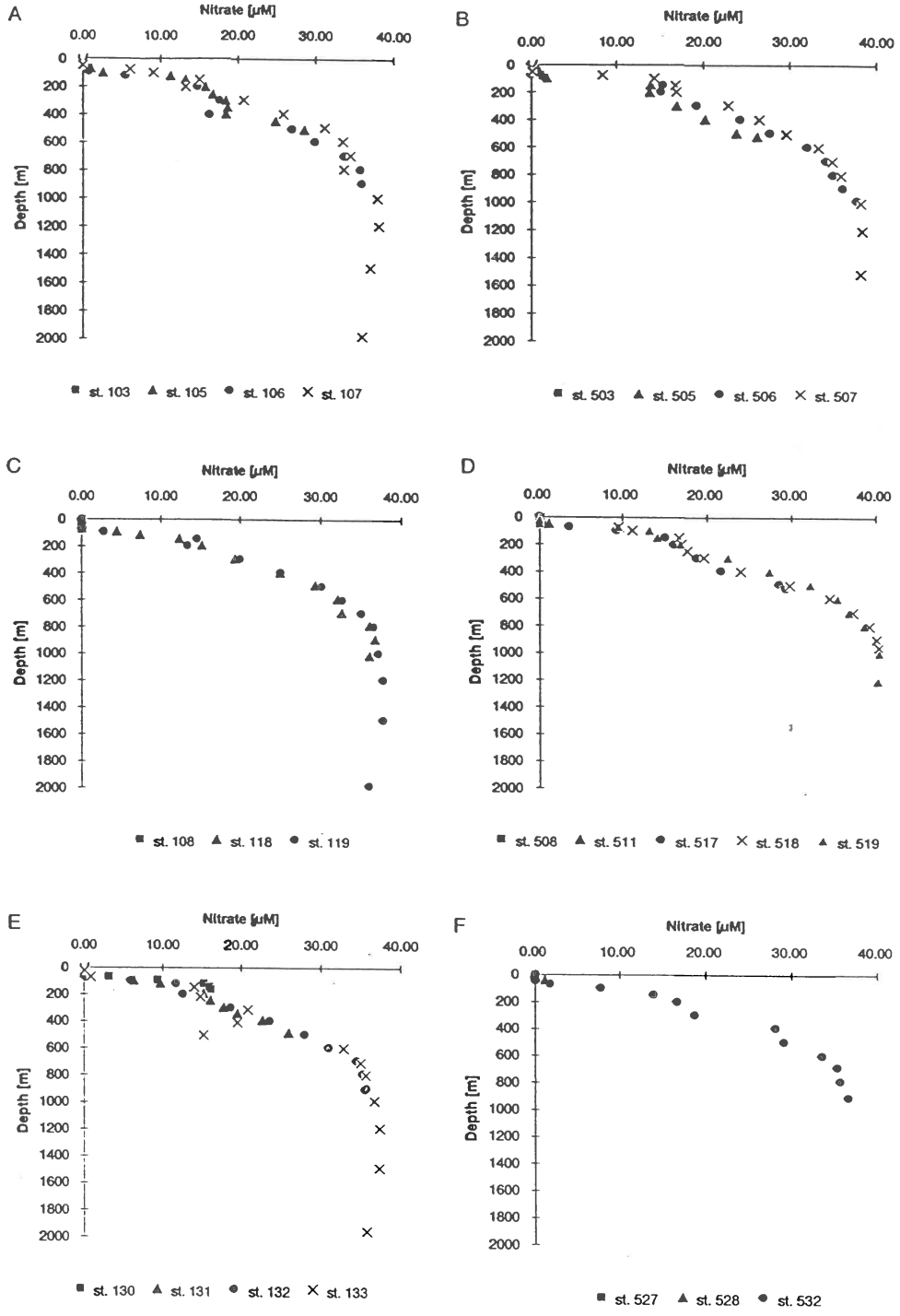

Fig. 4.2.1. Deep nitrate-depth profiles. As in fig. 4.1.3.

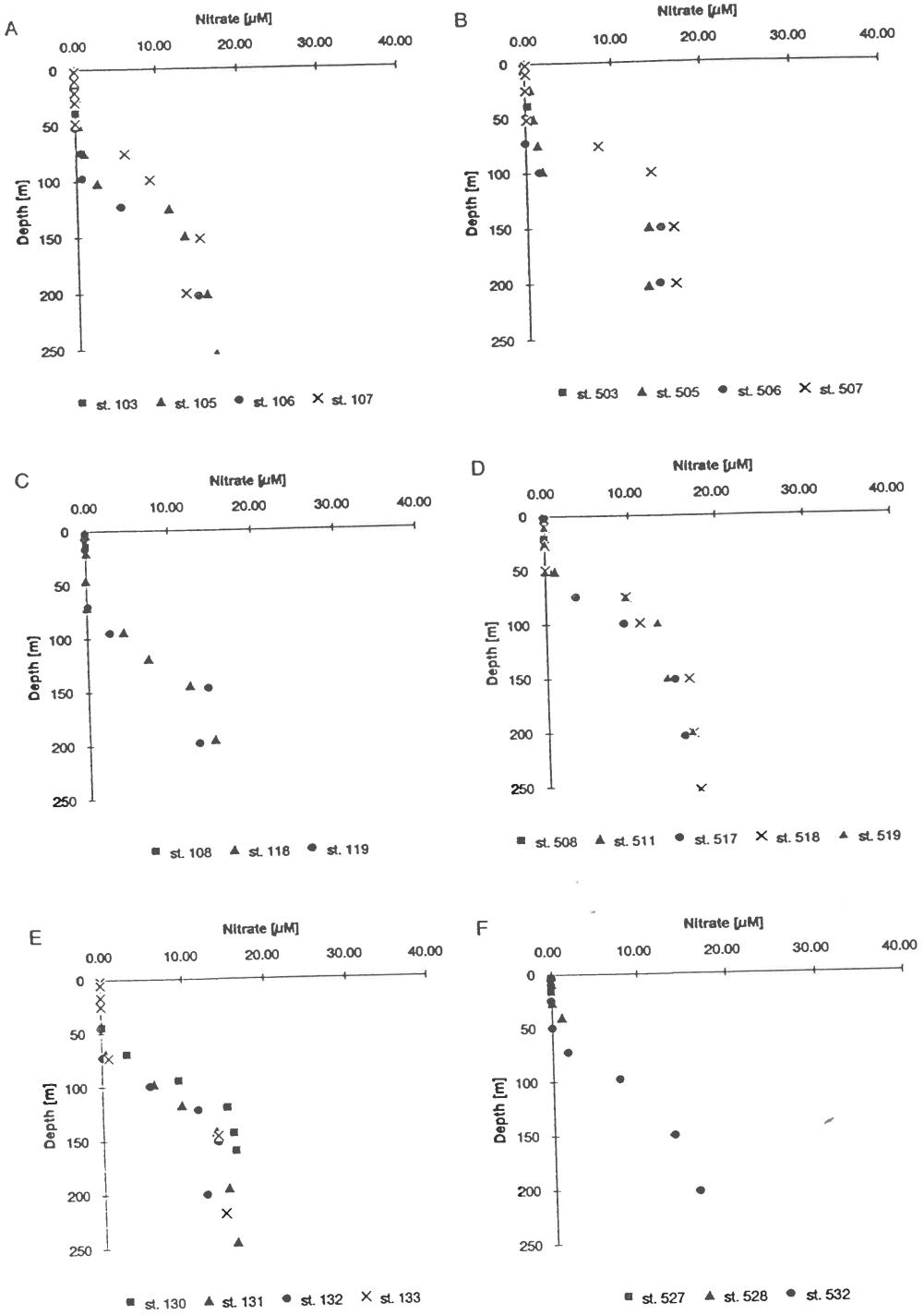

Fig. 4.2.2. Shallow nitrate-depth profiles. As in fig. 4.1.3.

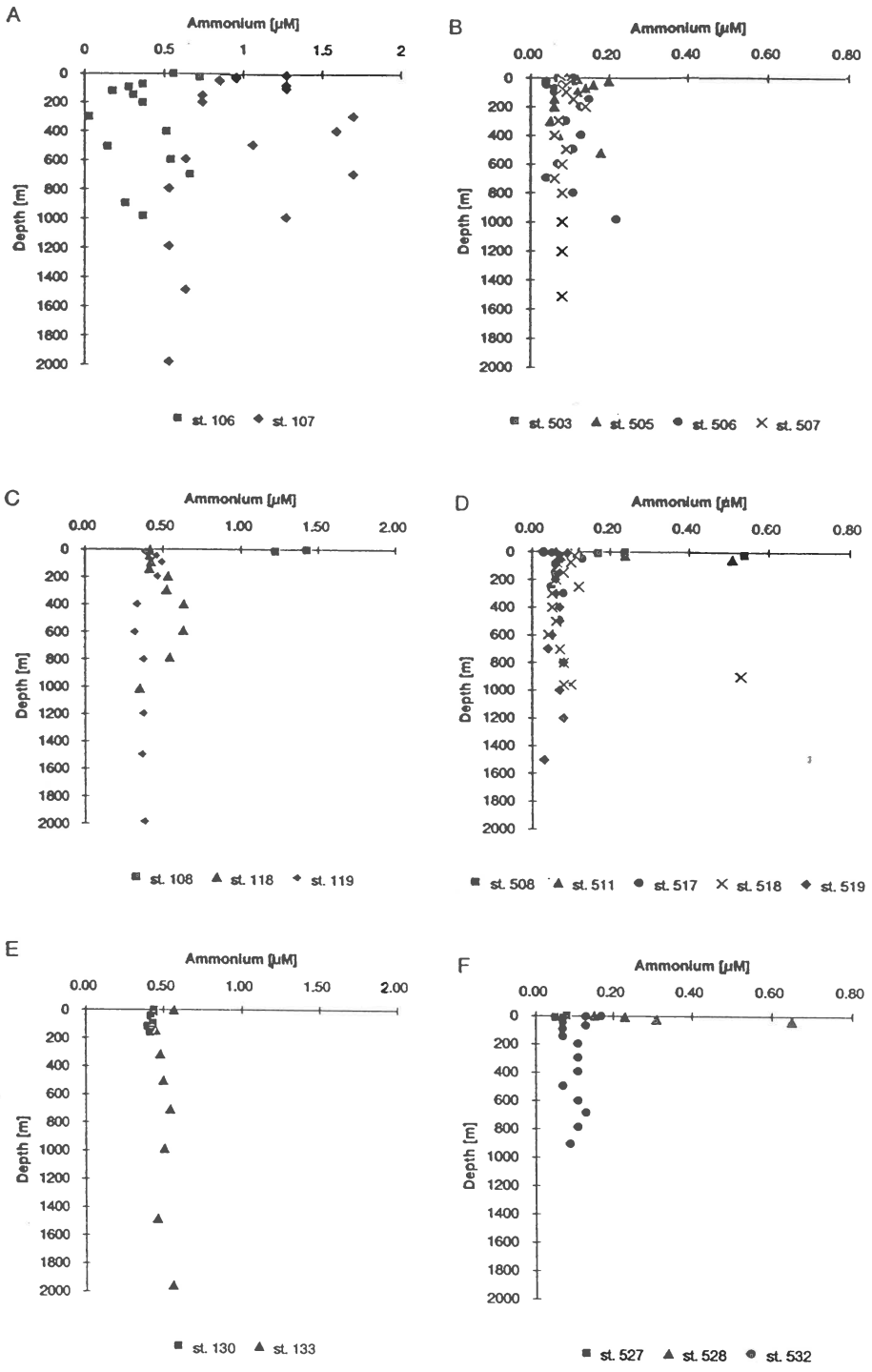

Fig. 4.2.3. Deep ammonium-depth profiles. As in fig. 4.1.3.

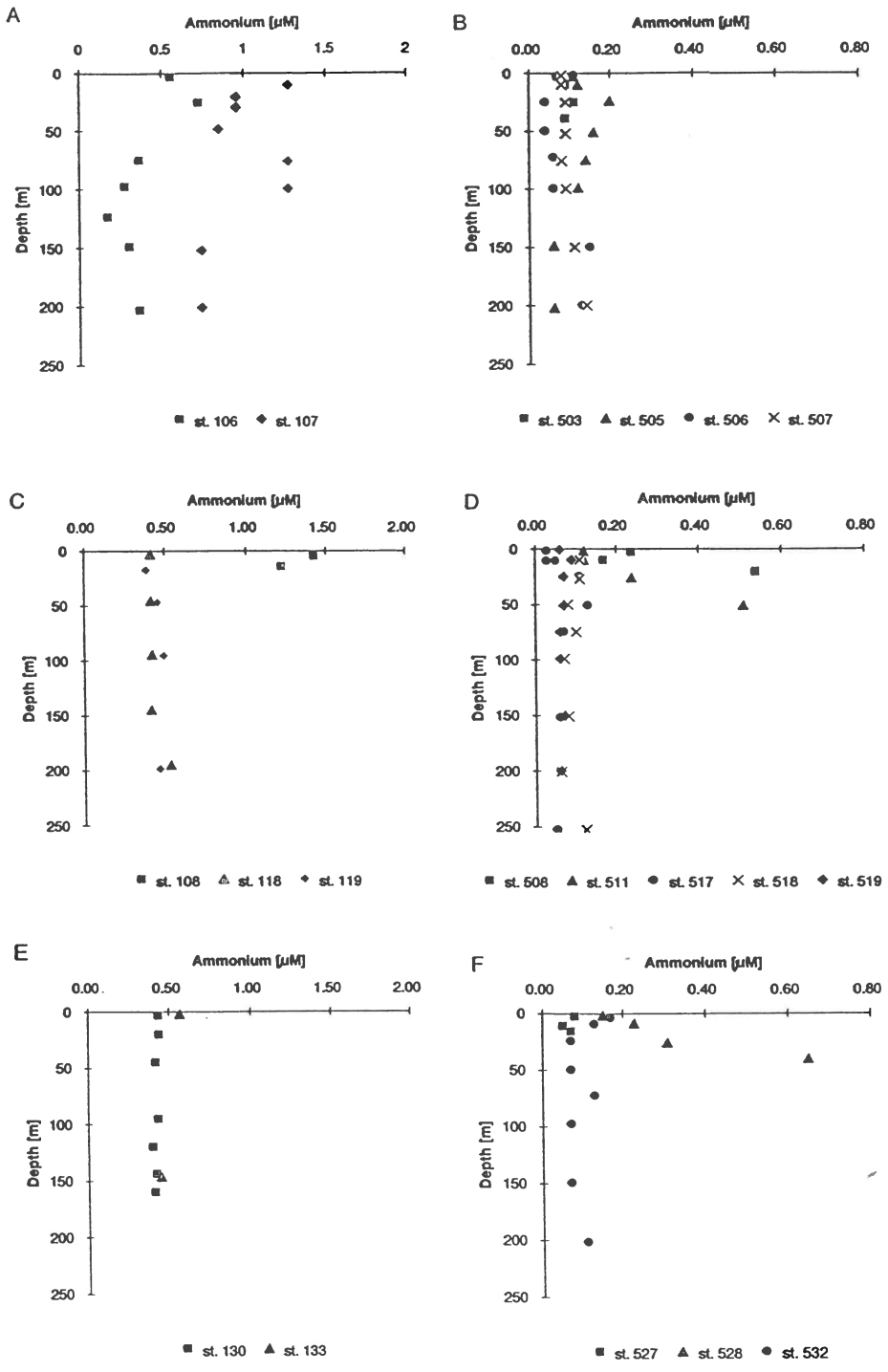

Fig. 4.2.4. Shallow ammonium-depth profiles. As in fig. 4.1.3.

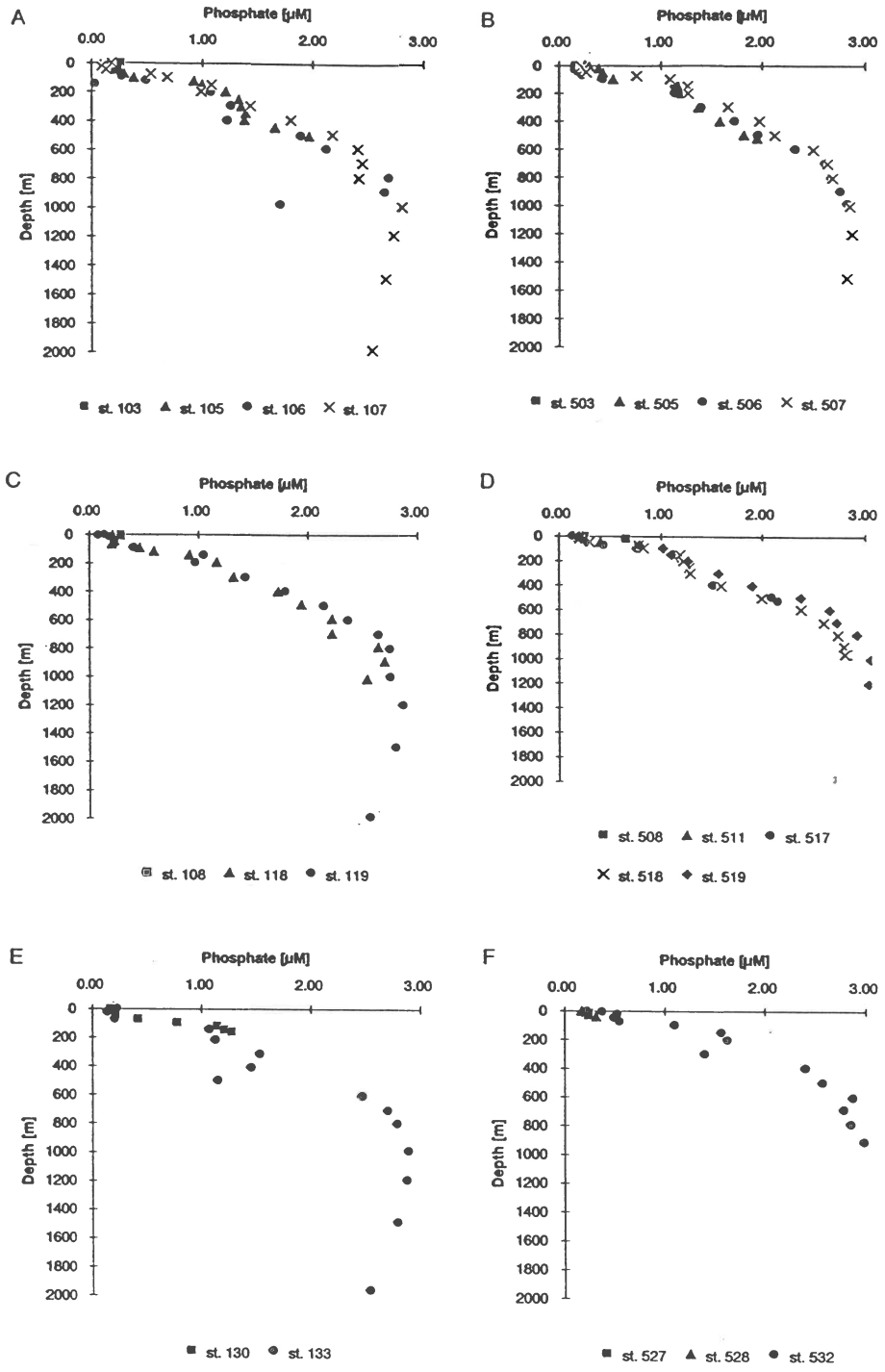

Fig. 4.2.5. Deep phosphate-depth profiles. As in fig. 4.1.3.

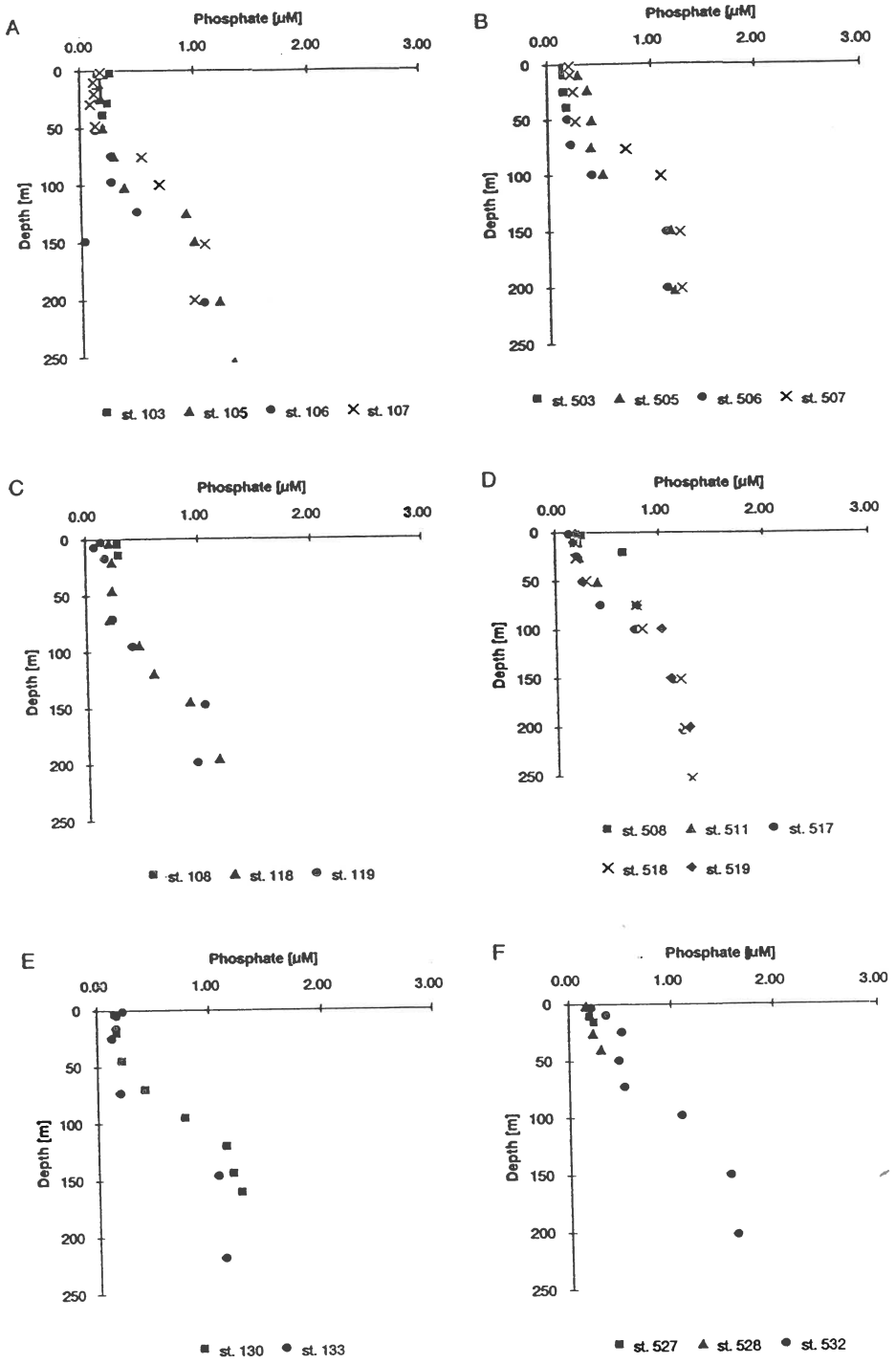

Fig. 4.2.6. Shallow phosphate-depth profiles. As in fig. 4.1.3.

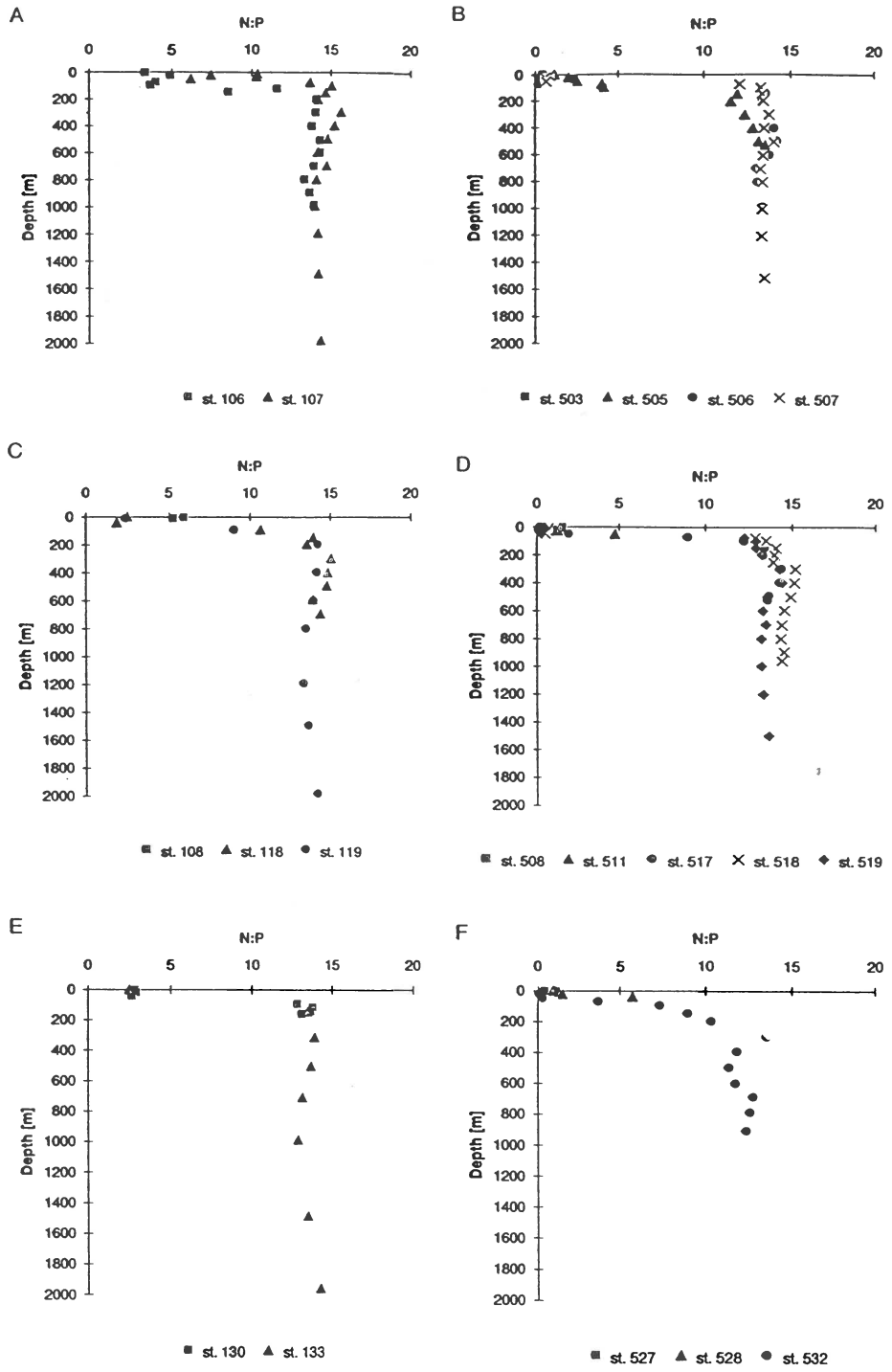

Fig. 4.2.7. N:P ratios. As in fig. 4.1.3.

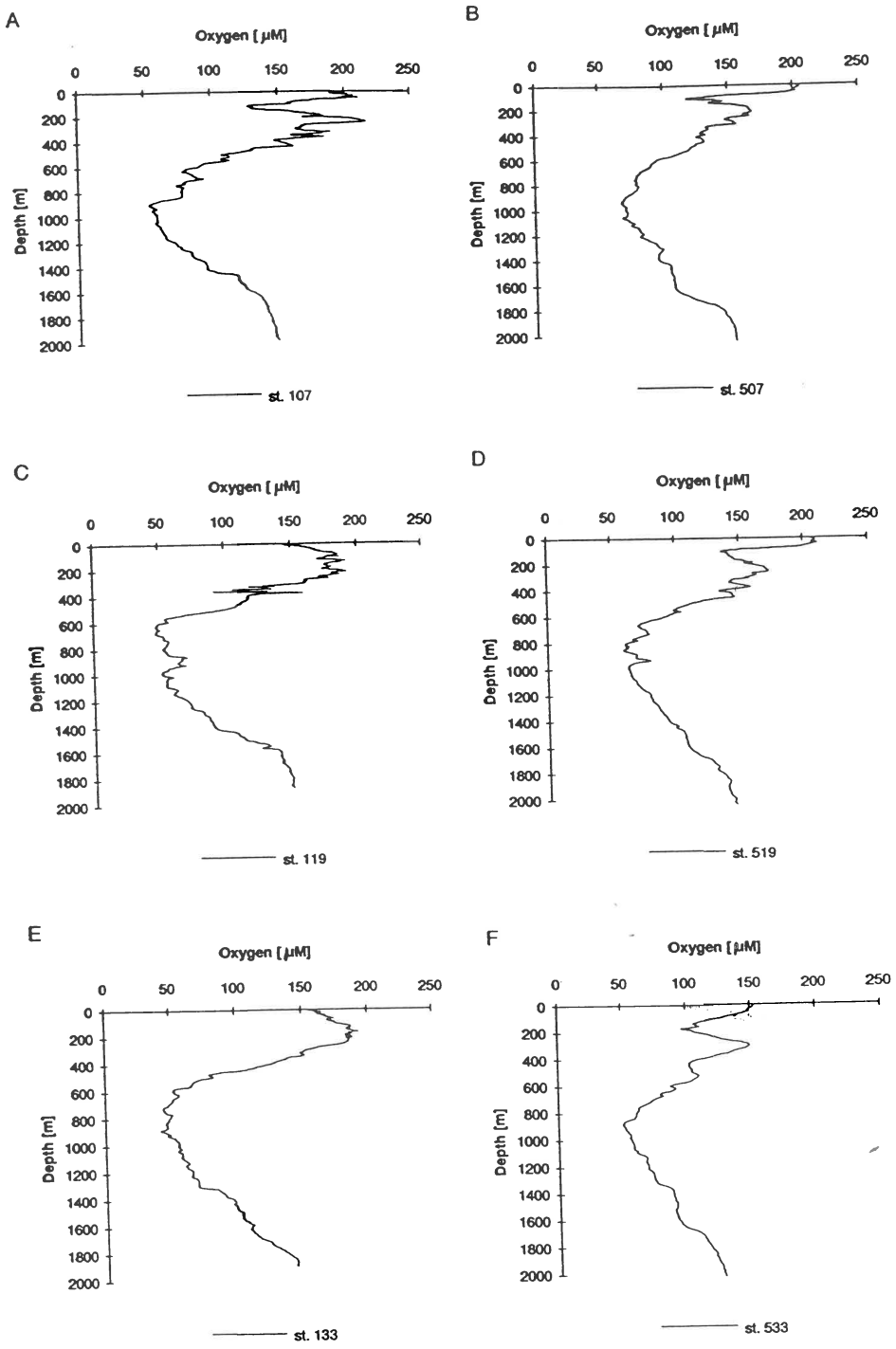

Fig. 4.2.8. Deep oxygen-depth profiles. As in fig. 4.1.3.

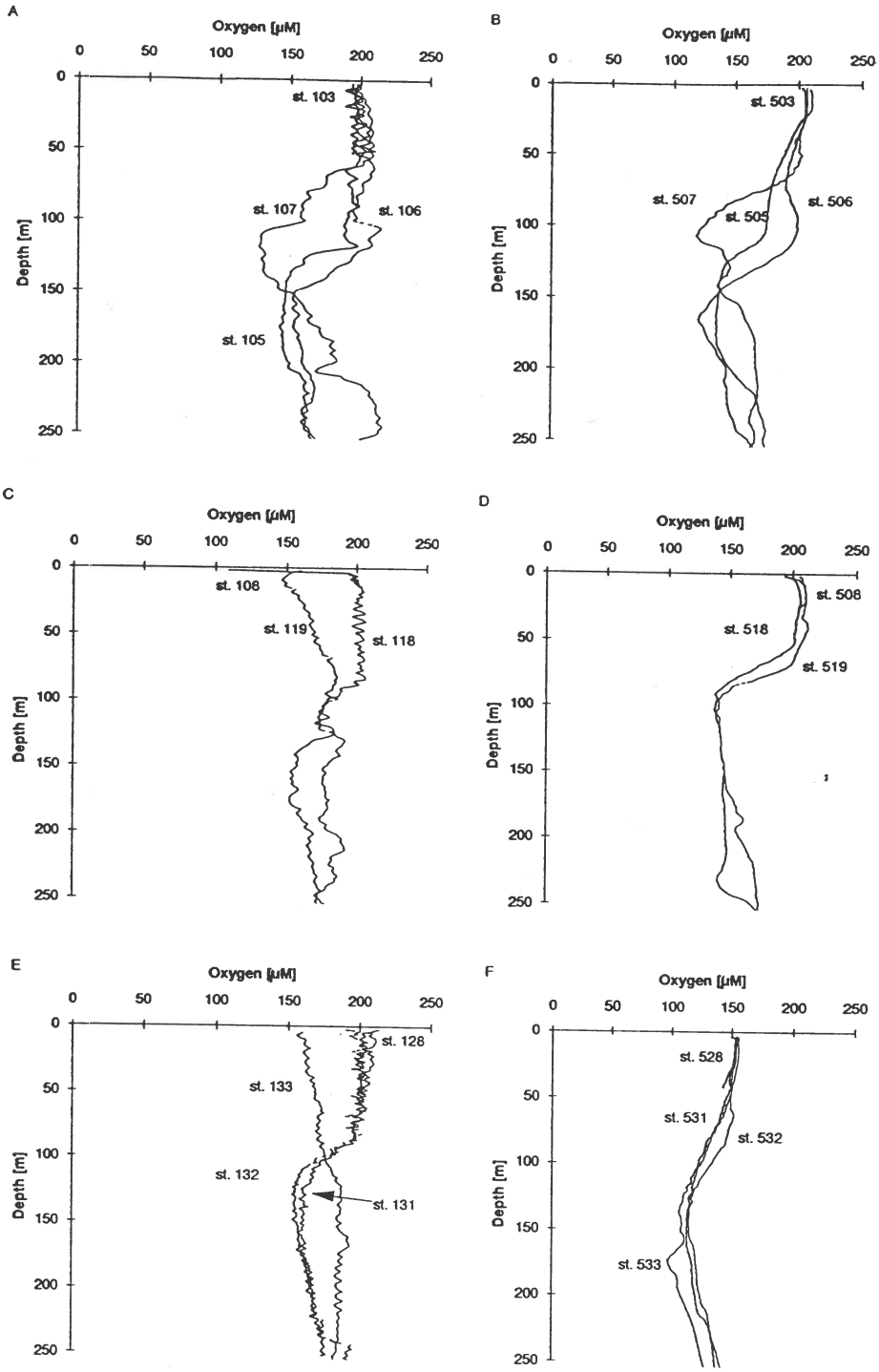

Fig. 4.2.9. Shallow oxygen-depth profiles. As in fig. 4.1.3.

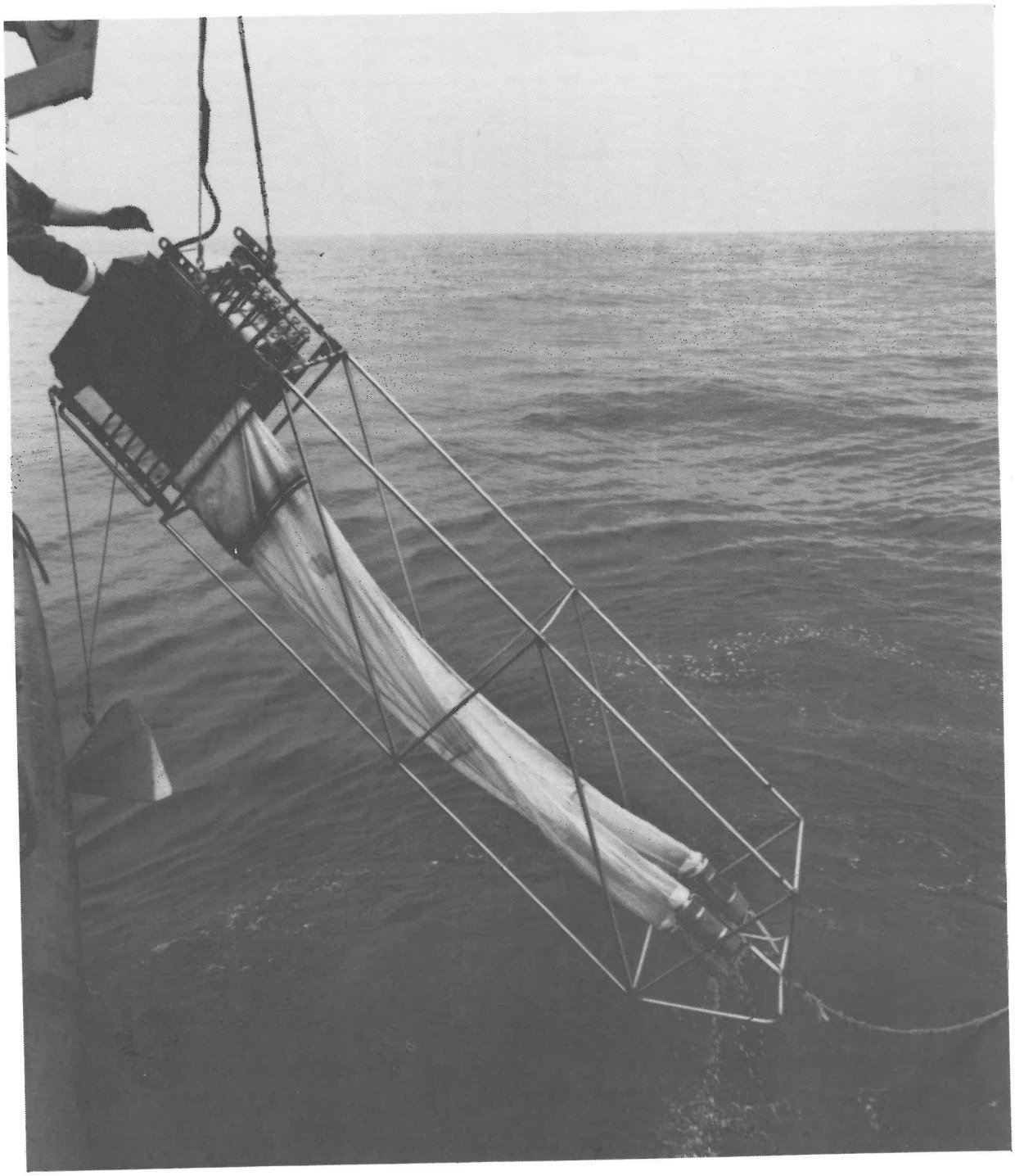

Multinet

4.3. PRIMARY PRODUCTION OF PHYTOPLANKTON IN THE COASTAL ECOSYSTEM OF KENYA

Jacco Kromkamp, Jan Peene, Pieter van Rijswijk, Jan Sinke & Nico Goosen
Centre for Estuarine and Coastal Ecology, Netherlands Institute of Ecology
Yerseke, The Netherlands

introduction

The primary production by phytoplankton along the coastal zone of Kenya is largely unknown, although phytoplankton blooms were occasionally observed by remote sensing using CZCS-data. It can be expected that the different monsoonal stages will influence phytoplankton production in different ways. The rains associated with the south-east monsoon will increase the river discharge and enrich the coastal ecosystem with nutrients. On the other hand, during this period the East African Current (EAC) is very active and large amounts of water from the open Indian Ocean are blown to the coast. Hence, the expected pulse in primary production due to the nutrient input will most likely only be observed close to the shore. During the second cruise in November/December (A2) the winds had changed inducing the North-East monsoon, although the EAC was still active, but water velocities were very much lower. Also, our second cruise was just after the small rain period, probably causing a second, minor nutrient input to the coastal ecosystem. We attempted to measure the influence of the different monsoonal periods on the primary production of phytoplankton along three transects perpendicular on the Kenyan coast. It will be shown that during the second cruise (A2) rates of primary production were higher than during the first cruise.

methods

Three transects were sampled: the Kiwayuu transect, the Sabaki transect and the Gazi transect (see Heip, Hemminga & De Bie, this volume, for more info). At most stations samples were taken near the surface, near the bottom of the mixed layer and at the fluorescence maximum, which was mostly located in the upper half of the thermocline.
Simulated *in situ* primary production was measured in a rotating incubator with a daylight light source. Samples, preferably taken during the morning, were incubated for 3-3.5 h at *in situ* temperature. Particulate production was measured using the ^{14}C-technique. In all cases the dark bottle uptake was subtracted from the light bottle values. On a number of occasions, 24h production was determined. Light in the incubator was measured with a spherical PAR sensor (Biospherical Instruments).
Incident irradiance (PAR) was measured with a cosine corrected sensor (MACAM, SD 101QW) connected to Keithley 175A multimeter. Readings were stored every 10 minutes. Under water light (460 nm) was measured with a sensor mounted on the CTD.
For size fractionated production and biomass determination, membrane filters were used with 0.45, 3.0 and 12.0 µm. Chlorophyll was determined using reverse phase HPLC. Samples for pigment analyses were frozen and lyophilized before extraction in 100% methanol.
At a number of stations, picoplankton algal cells were counted using epifluorescence microscopy. Colonies of the nitrogen fixing diazotroph *Trichodesmium* were counted on 12.0 µm membrane filters using a dissection microscope.
Nitrogen fixation was assayed by means of the acetylene reduction technique. It was assumed that 8 electrons were necessary to reduce molecular nitrogen to ammonia. The samples were incubated at an irradiance of 45 $\mu E.m^{-2}.s^{-1}$.

results

Watercolumn structure
During the A1 cruise in June/July, the EAC was very active, causing high water velocities. As a result, the mixed layer was extended to 80-100 m, after which the thermocline started. Nutrients were nearly all in the limiting range, but from nutrient ratio's nitrogen was likely the most limiting nutrient. Fluorescence was more or less constant in the mixed layer, but peaked in the upper thermocline. In general though, photosynthetic rates of thermocline samples were low in comparison to mixed layer samples. No clear temperature or salinity patterns were observed in the layer above the main thermocline, indicating that the upper 80-100 m were well mixed. This is in sharp contrast to the situation observed during the second cruise. Water velocities were much lower, and the thermocline started at 40-60 m. However, small temperature differences could be noted in the upper layer, indicating that microstratification did occur in the 'mixed layer'. This can be seen in Fig. 4.3.1. Again, the fluorescence in the thermocline increased, indicating a 'deep chlorophyll maximum'. However, the fluorescence values also increased with depth in the upper water layer. As the biomass did not increase in general, quenching of algal fluorescence due to high irradiance near the surface is most likely. This, together with the microstratification in temperature, indicates that mixing times in the upper 40-50 m are rather long. Such a 'stable' watercolumn is ideal for the cyanobacterium *Trichodesmium*, which is able to regulate its buoyancy. Ind-

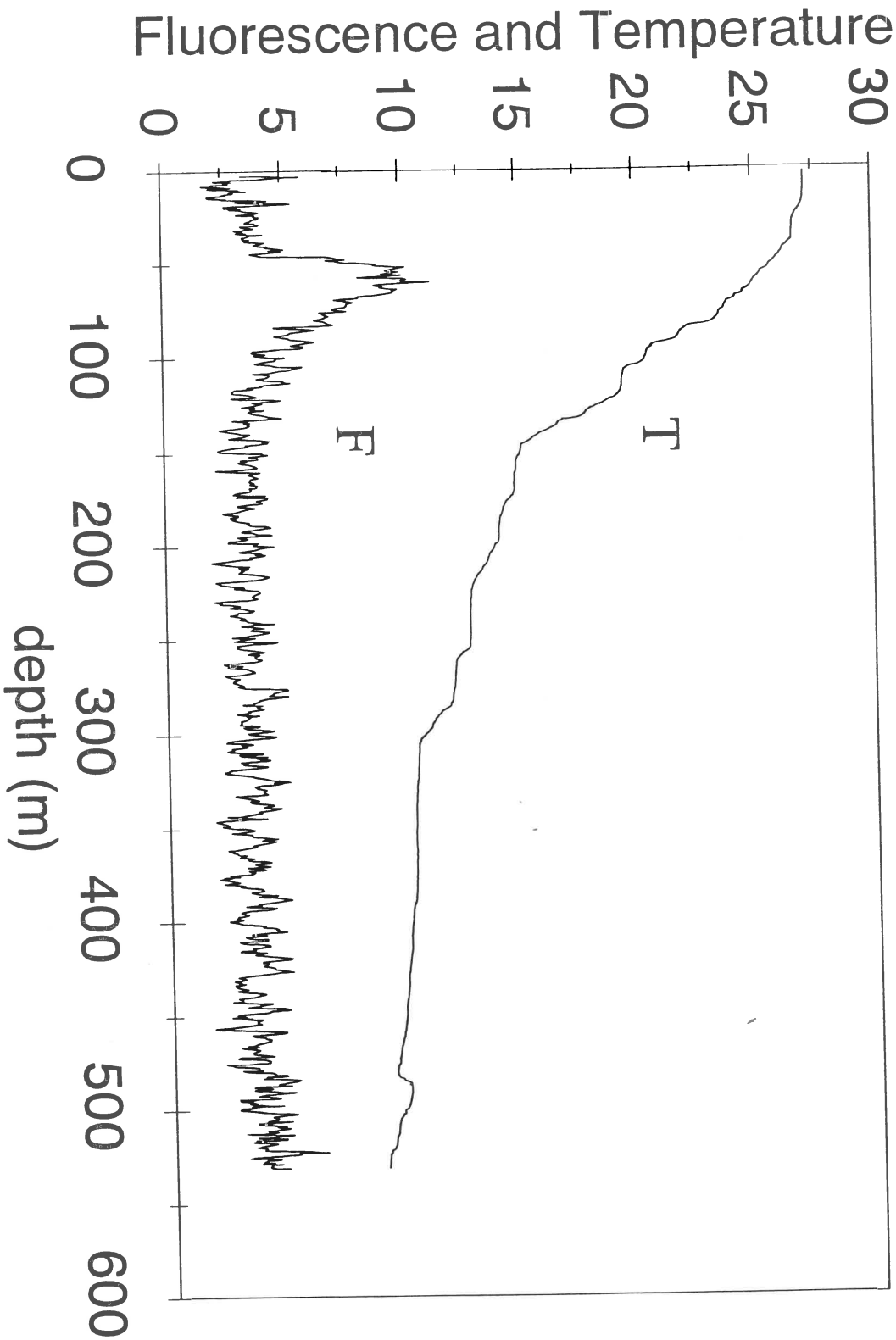

Fig. 4.3.1. Temperature (°C) and fluorescence (arbitrary units) of station 517.

eed, *Trichodesmium* colonies were observed, sometimes in very large numbers, especially at the shallower stations. This will be discussed later.

Biomass

During the A1 cruise, picoplankton was the dominant phytoplankton, at least at the deeper stations and in term of numbers. At the shallower stations some diatoms were seen. Of the *Synechoccocus*-type algae, approx. 75% passed a 1.0 µm filter. Cell numbers varied between 1 and 30 x 10^6 cells per liter. Cell numbers in the thermocline were less than 15% of those at the surface. As yet no results are available for the A2-cruise, although picoplankton cells still dominated the microscopic observations. However, the pigment analyses gave a different picture: in general, the chlorophyll-*a* fraction smaller than 3.0 µm comprises 30-50% of the total chlorophyll-*a*, whereas the fraction larger than 12 µm varies between 15-50%. Chlorophyll-*b* is the second most important pigment. The chlorophyll *a/b*-ratio varies between 1 and 30 and averages 3.9 ($\pm$ 6.9) indicating the presence of chlorophytes, most likely eukaryotic green picoplankters. Fytoplankton chlorophyll-*a* concentrations of surface samples were below 1 µg.l^{-1}, and decreased offshore to very low values (Table 4.3.1). Surprisingly, in general concentrations did not differ greatly during the two cruises, despite the fact that rates of primary production during the second A2 cruise were substantially higher (see below). This might be caused by the higher nutrient concentrations present during the second cruise.

Primary production

During both cruises rates of photosynthesis in the upper water layers (irradiance > I_k) were higher in the shallower stations close to the coast as compared to surface samples taken from the more offshore station. This suggested that the areal production would be higher in the near shore stations. This was indeed true for the Gazi transect during the first cruise, where areal primary production decreased sharply offshore and was hardly measurable at the deeper stations (Fig. 4.3.2a). However, loss of photosynthetic activity in the deeper stations was partly compensated by the deeper water column of the more offshore stations (Fig. 4.3.2 b,c). Note that the primary production at the deeper stations increases from south to north: whereas at the Gazi transect the primary production of the mixed layer (taken as 100 m deep) is below 100 mgC.m^{-2}.d^{-1} at the stations 1000 and 2000, at the Kiwayuu transect the primary production increased to more than 400 mgC.m^{-2}.d^{-1}.

Areal production rates have not been calculated for the second cruise yet. However, from a comparison of the subsurface rates of photosynthesis, it is clear that photosynthetic activities were much higher at the end of the South-East monsoon (second cruise). Especially the production in the two more southerly transects (Gazi and Sabaki) was substantially higher (Fig.4.3.3). Major differences disappeared and all transects showed similar rates of primary production. Because production was much higher during the A1 cruise at the Kiwayuu stations, differences between both cruises at the Kiwayuu stations were small (Fig. 4.3.4).

Trichodesmium: *buoyancy*

As mentioned before the upper water layer above the thermocline was physically rather stable since microstratification could be observed. This is the ideal type of physical environment for a colony forming algal species which can regulate its buoyancy and vertical migration. Although some diatoms have been observed to regulate their buoyancy (Villareal, 1988), the diazotrophic cyanobacterial genus *Trichodesmium* is well known for this (Carpenter, 1983; Walsby, 1978; Villareal & Carpenter, 1990). Because *Trichodesmium* can fix molecular nitrogen, this organism can be responsible, at least theoretically, for a substantial input of nitrogen in the photic zone and thus for the formation of new production. We encountered *Trichodesmium* mainly in the shallower stations (up to 500 m water depth, with a preference for the stations with shallower depths). At the 1000 and 2000 m stations it was nearly absent. Surface scums were noticed, especially around noon or later in the afternoon. Fig.4.3. 5 shows a strong positive buoyancy of most colonies at station 511 on November 29, resulting in a marked vertical distribution with a maximum at the surface. That night windspeeds rose (6 Beaufort), causing a

Table 4.3.1. Chloropohyll-*a* concentrations (µg.l^{-1}) in subsurface samples during the two cruises.

station depth	20	20 A1	500 A2	500 A1	1000 A2	1000 A1	2000 A2	2000 A1	A2
GAZI	0.79	0.73	0.22	0.29	0.33	0.36	0.05	0.32	
SABAKI		0.65	0.59	0.36	0.28	0.19	0.15	0.16	0.11
KIWAYUU		0.85	0.70	0.27	0.26	0.23	0.10	0.18	0.05

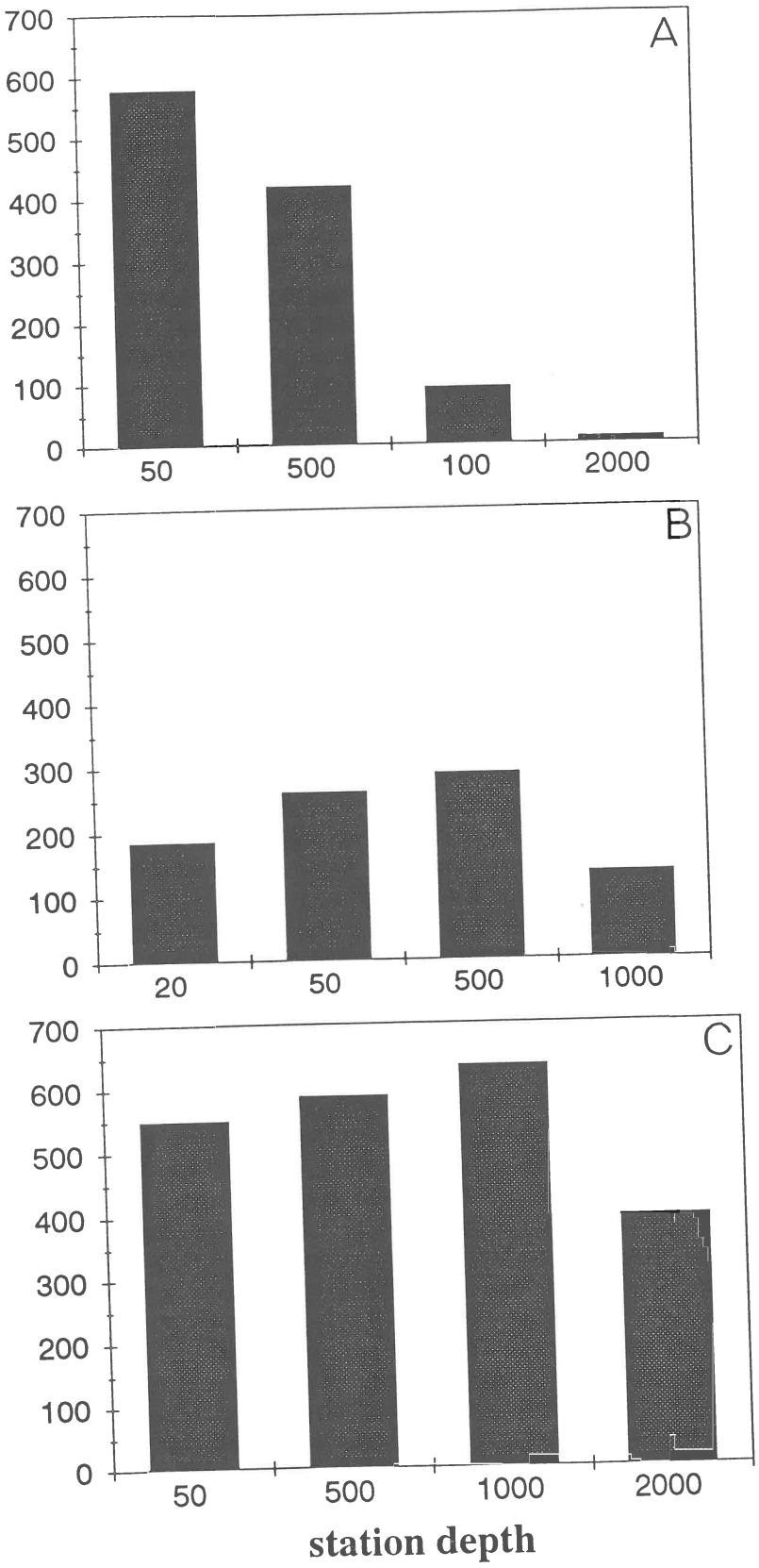

Fig. 4.3.2. Daily gross primary production along the stations of the three transects during the A1-cruise. (A) Gazi transect; (B) Sabaki transect; (C) Kiwayuu transect

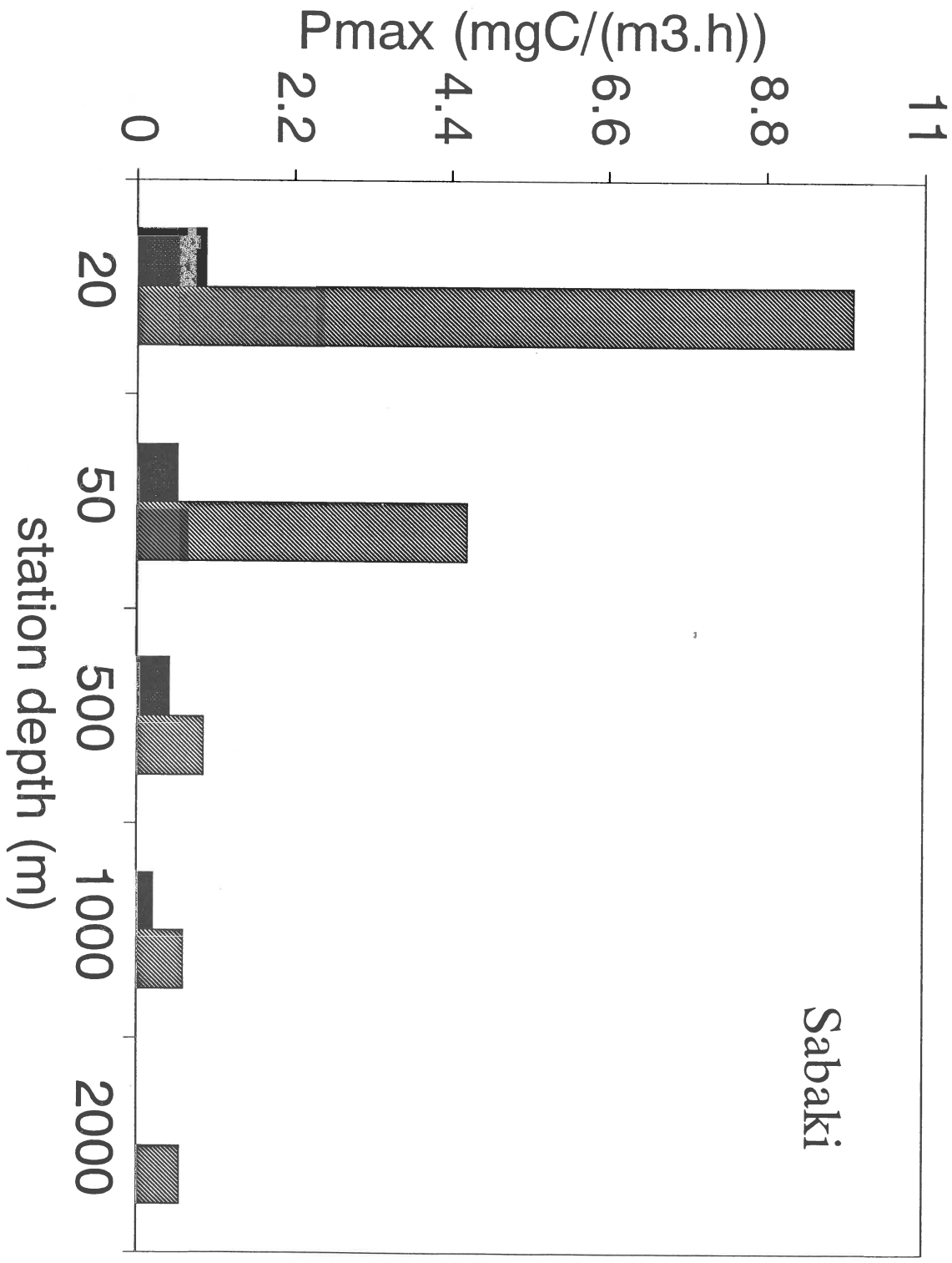

Fig. 4.3.3. Maximum rates of photosynthesis (Pmax) of surface samples for stations along the the Sabaki transect. Left bars: A1; right bars A2-cruise.

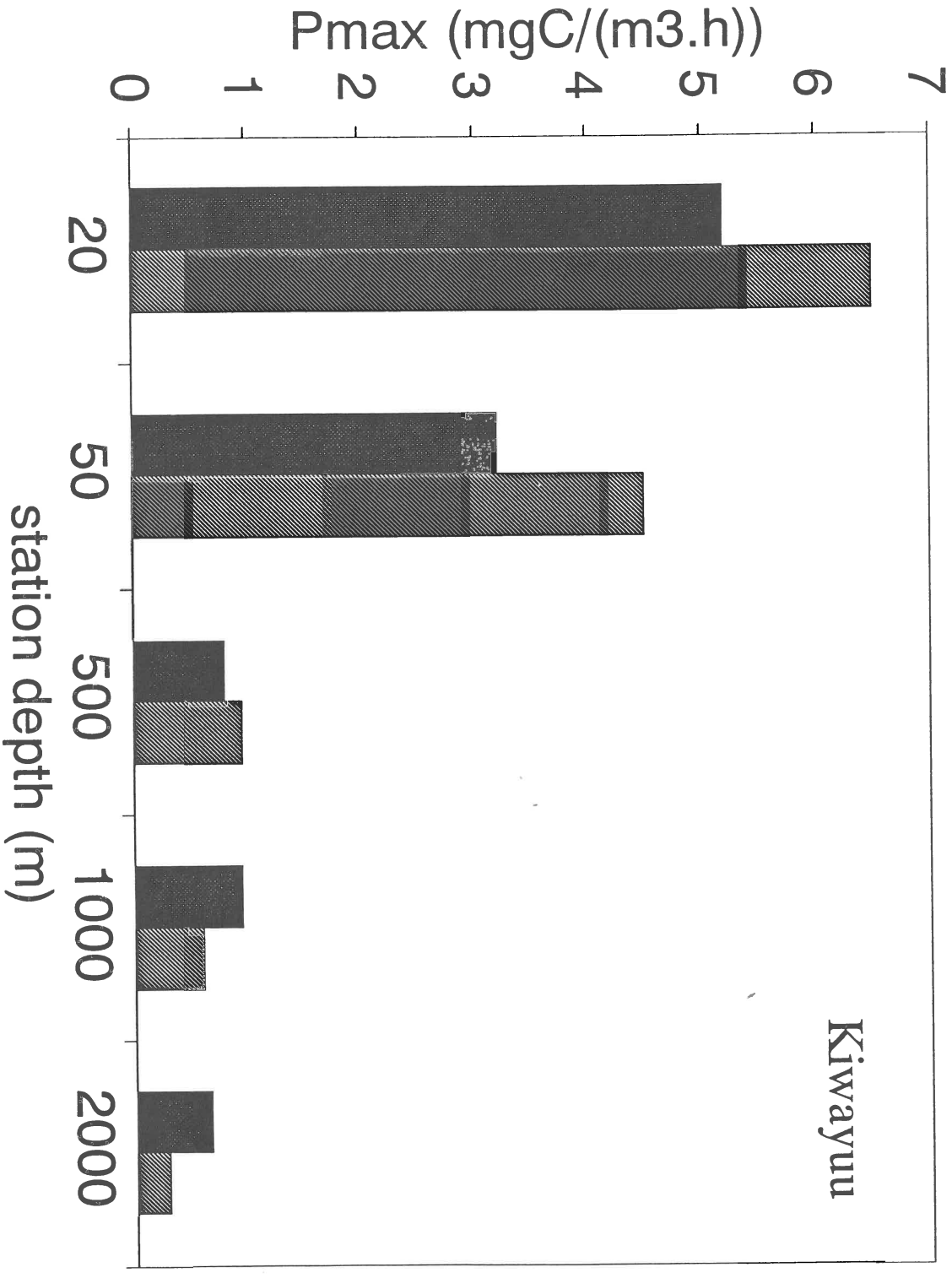

Fig. 4.3.4. Maximum rates of photosynthesis (Pmax) of surface samples for stations along the the Kiwayuu transect. Left bars: A1; right bars A2-cruise.

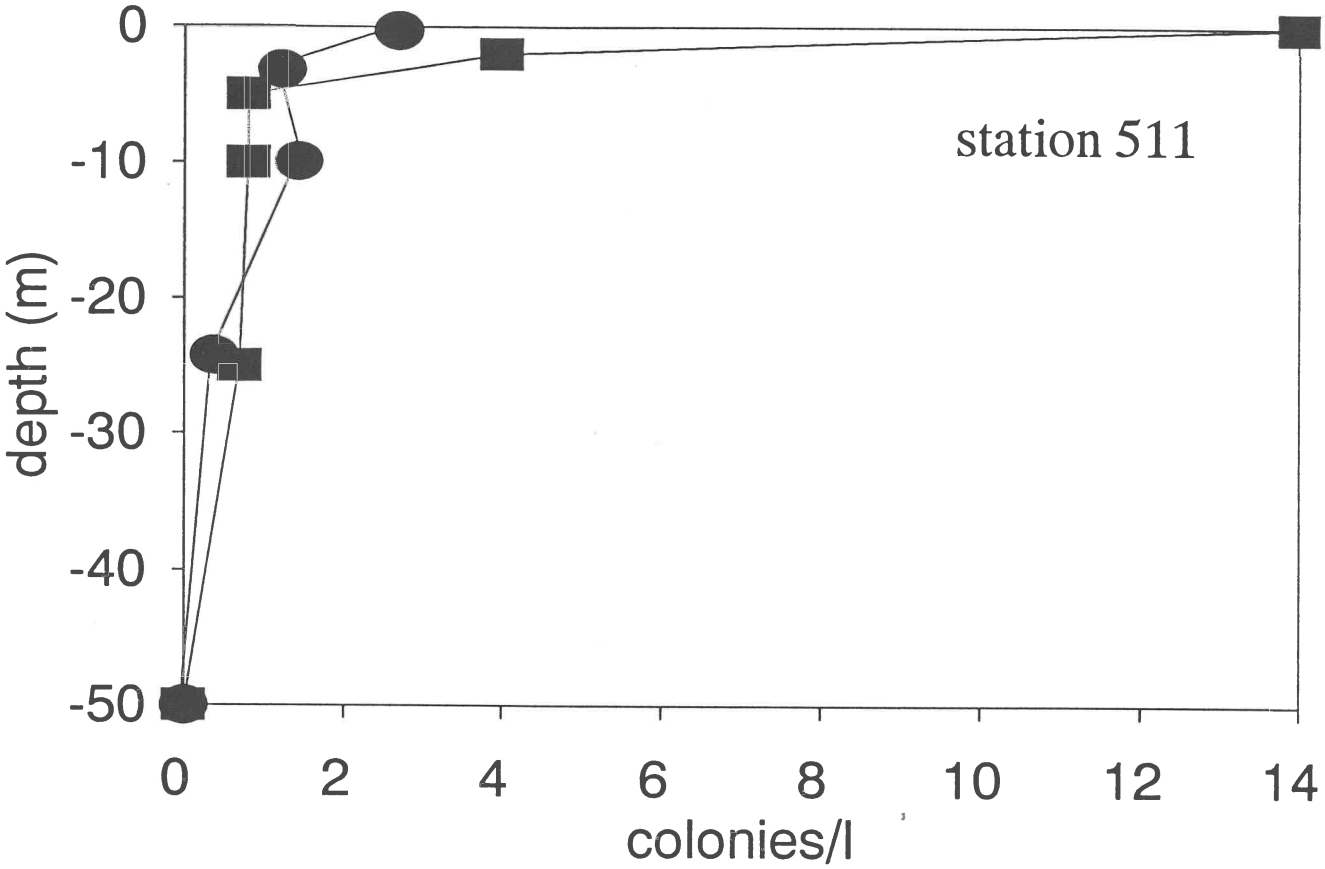

Fig. 4.3.5. Vertical distribution of *Trichodesmium* colonies. Circles: 28 November, squares: 29 November.

more homogenous distribution of *Trichodesmium* colonies. However, despite the fact that no temperature differences were found during the first 25 m the next day, the colonies had partly resisted entrainment by turbulent mixing. Due to the patchy distribution of the colonies, quantifying the total number of *Trichodesmium* filaments is very difficult. At station 527 we counted 25 colonies.l^{-1} at the surface, whereas at station 528 no colonies were found in the morning, but in the early afternoon a surface bloom developed with 268 colonies.l^{-1}. At station 517 we counted 152 colonies.l^{-1}. At station 505 a massive bloom was encountered. This bloom seemed to be associated with a front which was measured (a deepening of the mixed layer to 100 m). Large streaks with colonies were floating at the surface (we measured more than 99% floating colonies) in which more than 220 colonies.ml^{-1} (!) were counted.

Trichodesmium: *nitrogen fixation*

Although we have measured filament lengths in combination with nitrogenase activities at several stations, most results have to be calculated yet. Preliminary calculations on one occasion on a number of colonies gave a rate of N_2-fixation of $2x10^{-3}$ nmol N_2.colony^{-1}.h^{-1}. Nitrogenase activity dropped near the end of the day. Hardly any nitrogen fixation took place when the samples were incubated in the dark.

As mentioned above, a huge surface bloom of *Trichodesmium* was encountered at station 505 in the second half of the afternoon. Using the above rate of nitrogen fixation, we estimated that the bloom fixed 7.5 mg of $N_2.m^{-2}.day^{-1}$. This highly significant number demonstrates the important role of *Trichodesmium* in the Kenyan coastal ecosystem during this part of the monsoon period.

references

Carpenter, E.J., 1983. Physiology and ecology of marine planktonic *Oscillatoria (Trichodesmium)*. Mar. Biol. Lett. 4: 69-85.

Villareal, T.A., 1988. Positive buoyancy in the oceanic diatom *Rhizosolenia debyana* H. Peragallo. Deep-Sea Res. 35: 1037-1045.

Villareal, T.A. & E.J. Carpenter, 1990. Diel buoyancy in the marine diazotrophic cyanobacterium *Trichodesmium thiebautii*. Limnol. Oceanogr. 35: 1832-1837.

Walsby, A.E., 1978. The properties and buoyancy-providing role of gas vacuoles in *Trichodesmium* Ehrenberg. Br. Phycol. J. 13: 103-116.

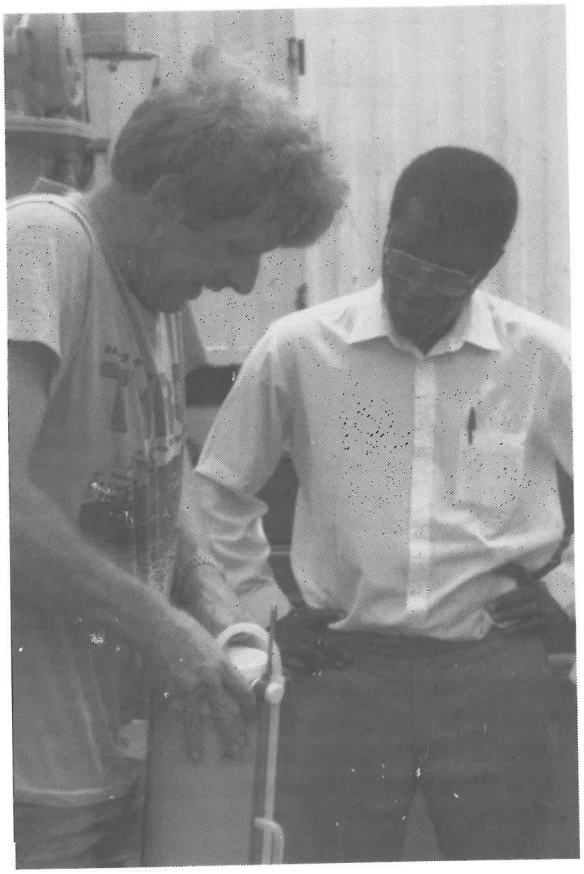

Dr. Ezekiel Okemwa, director of KMFRI, Mombasa, visiting r.v. Tyro.

4.4. UPTAKE OF NITROGENOUS NUTRIENTS BY PHYTOPLANKTON IN THE TROPICAL WESTERN INDIAN OCEAN (KENYAN COAST): MONSOONAL AND SPATIAL VARIABILITY

Mengesha Semeneh, Frank Dehairs & Leo Goeyens
Vrije Universiteit Brussel, Laboratory of Analytical Chemistry, Pleinlaan 2, B-1050 Brussel, Belgium.

introduction

The seasonal migration of the Inter-Tropical Convergence Zone leads to two different monsoon regimes in the Indian Ocean (McClanahan, 1988) : the Southeast (SE) and the Northeast (NE) monsoon. During the SE monsoon the westward flowing Southern Equatorial Current faces the African continent, splits and eventually forms the East African Coastal Current (EACC), a northward flowing water current which causes upwelling along the Somalia coast. This situation persists from May to September. During the NE monsoon (November to March) a switch in wind direction reverses the surface water circulation. The Somali current forms and flows southwestward to merge with the EACC (McClanahan, 1988; Swallow *et al.,* 1991; Burkill *et al.,* 1993).

Strong seasonal and spatial variability in primary production characterize the northwestern Indian Ocean (Burkill *et al.*, 1993; Mantoura *et al.*, 1993; Owens *et al.,* 1993). The region encompasses different biogeochemical provinces, especially with respect to nitrogen cycling (Mantoura *et al.,* 1993; Burkill *et al.,* 1993). High primary productivity values (up to 1.8 gC m^{-2} d^{-1}; Smith & Codispoti, 1980) along the Somali coast during the SE monsoon are mainly due to increased nutrient availability (NO_3 >19 µM) through deep mixing. Increased export of organic matter to the deep ocean and f-ratios of 0.92 were observed during this period (Nair *et al.,* 1989; Owens *et al.,* 1993). But off the coast of Somalia and south of this upwelling zone primary productivition is very low (0.3 gC m^{-2} d^{-1}; Smith & Codispoti, 1980; Owens *et al.,* 1993). In both, the northern central Indian Ocean (average NO_3 = 13.3 nM and f-ratio = 0.12) and northeastern Indian Ocean (NO_3 < 0.5 µM and f-ratio > 0.24) regenerated production is predominant (Gomes *et al.,* 1992; Mantoura *et al.,* 1993; Owens *et al.,* 1993).

results

Surface nutrient concentrations in the study area were very low throughout (Table 4.4.1). Temporal variability of nitrate was negligible, whereas ammonium increased significantly during the SE monsoon period. In order to assess nutrient availability for phytoplankton nutrition, we calculated integrated stocks of nitrate and ammonium for the total depth of the upper mixed layer. All nutrient stocks (Table 4.4.1) were very low, indicating that the state of nutrient impoverishment observed in the surface waters extended to the whole upper mixed layer. Nitrate and ammonium stocks in oceanic stations (> 200 m depth) were higher during the SE monsoon period.

Average surface POC concentrations were 8.71 and 7.22 µM and average surface PON concentrations were 0.82 and 0.75 µM during the SE and NE monsoon, respectively (Table 4.4.1). Significantly higher POC and PON values were observed in neritic waters (<200 m depth). The C:N ratios of particulate material (obtained by linear regression analysis) were close to the Redfield ratio of 6.6.

A significant difference in specific nitrate uptake rate was observed for both monsoon periods (Table 4.4.2). Values ranged from 0.0009 to 0.003 h^{-1}, with an average rate of 0.002 during the NE monsoon, whereas very low values (mean: 0.0001 h^{-1}) occurred during the SE monsoon. Inter- and intratransect variations in specific nitrate uptake rate were very small, implying little spatial variability. During both monsoon periods the specific ammonium uptake rates exceeded the specific nitrate uptake rates (Table 4.4.2), a common feature of oligotrophic areas. Specific ammonium uptake rates averaged to 0.014 and 0.008 h^{-1} during the NE and SE monsoon periods, respectively. The specific ammonium uptake rates in the oceanic stations exceeded the ones of the neritic stations by a factor of 3. Nitrate transport rates were extremely low during the SE monsoon, ranging from <0.02 to 0.36 nM h^{-1} with a mean value of 0.11 nM h^{-1}. These uptake rates are one order of magnitude lower than those observed during the NE monsoon (range = 0.53 - 3.75 nM h^{-1}, mean = 1.4 nM h^{-1}). Ammonium uptake rates during the SE monsoon ranged from 2.34 to 45.14 nM h^{-1}, with a mean value of 14.6 nM h^{-1}. Except for stations 127 and 128, these uptake rates are quite similar to those observed during the NE monsoon (range = 1.76 - 15.55 nM h^{-1}, mean = 5.0 nM h^{-1}). The f-ratios never exceeded 0.5 (Table 4.4.2), which indicates predominance of regenerated production. The f-ratio ranged from <0.01 to 0.03 during the SE monsoon, with an average value of 0.01, which is close to the estimates of Eppley & Peterson (1979) for oligotrophic oceans. During the NE monsoon, on the contrary, the f-ratios were significantly higher, ranging from 0.11 to 0.47 (mean value of 0.24).

discussion

Both the nutrient and uptake rate data indicate that the region is highly oligotrophic. The very low nutrient concentrations in the study area contrast with the

Table 4.4.1. Surface concentrations (0-25 m) and stocks of nitrogeneous nutrients, surface particulate carbon and nitrogen concentrations and C:N ratios in the study area; all concentrations are in µM; neritic stations are defined as less than 200 m deep.

		Monsoon	Neritic station	Oceanic stations	All stations
Surface concentration	Nitrate	SE	0.09 (<0.03 - 0.41)	0.05 (0.03 - 0.15)	0.06 (<0.03 - 0.41)
		NE	0.03 (0.03 - 0.12)	0.04 (<0.03 - 0.13)	0.03 (<0.03 - 0.13)
	Ammonium	SE	0.24 (0.03 - 0.51)	0.21 (0.06 - 0.45)	0.22 (0.03 - 0.51)
		NE	0.12 (0.07 - 0.21)	0.08 (<0.03 - 0.14)	0.10 (<0.03 - 0.21)
Stock	Nitrate	SE	0.14 (0.03 - 0.43)	0.49 (0.00 - 1.98)	0.33 (0.00 - 1.98)
		NE	0.14 (0.00 - 0.30)	0.18 (0.00 - 0.94)	0.17 (0.00 - 0.94)
	Ammonium	SE	0.22 (0.05 - 0.52)	0.19 (0.06 - 0.41)	0.21 (0.06 - 0.52)
		NE	0.16 (0.07 - 0.28)	0.10 (0.02 - 0.23)	0.12 (0.02 - 0.28)
Particulate matter	POC	SE	11.67 (9.09 - 20.67)	6.17 (3.91 - 6.76)	8.71 (3.91 - 20.67)
		NE	9.15 (6.81 - 12.59)	6.14 (5.00 - 8.66)	7.22 (5.0 - 12.59)
	PON	SE	1.19 (0.49 - 2.15)	0.50 (0.33 - 0.66)	0.82 (0.33 - 2.15)
		NE	1.08 (0.33 - 0.78)	0.56 (0.60 - 1.30)	0.75 (0.60 - 1.30)
	C:N	SE			8.21 + 0.81
		NE			6.40 + 0.84

nutrient rich monsoonal upwelling areas of the southeastern Arabia and Somalia coasts. Persistence of very low nitrate concentrations in the surface layer (Table 4.4.1) made the region largely dependent on regenerated production (maximum f-ratio = 0.47). The NE monsoon was characterized by reduced wind stress, shallower thermocline, lowest nitrate concentrations and predominance of regenerated production (mean f-ratio = 0.24). During the SE monsoon the upper mixed layer was deeper and nitrate as well as ammonium availabilities were higher. Nitrate uptake rates and new production ratios were extremely low (Table 4.4.2), however. Since the two monsoon periods were characterized by similar biomasses and C:N ratios, the monsoonal difference in specific uptake rate appeared to be physiological. The combined effect of increased ammonium concentrations and reduced stability of the water column led to considerable decreases in nitrate uptake rate. Very low nitrate uptake rates are not surprising as the phytoplankton exposure to higher surface nitrate concentrations was only to 0.41 µM. Moreover, inhibition of nitrate uptake by ammonium in oligotrophic regions can be effective at low ambient ammonium concentrations due to the high affinity (low K_s) of phytoplankton for the latter nutrient (Dortch, 1990; Eppley *et al.*, 1990; Parker, 1993). Furthermore, the population was largely dominated by picoplankton (J. Kromkamp, personal communication) which prefer the highly available, locally produced and energetically profitable ammonium (Owens *et al.*, 1993). Specific ammonium uptake rates in the neritic regions differed from the ones in the oceanic area (Table 4.4.2). During the NE monsoon phytoplankton in the oceanic region demonstrated a markedly higher specific ammonium uptake rate, while the ambient ammonium concentrations were similar. Large differences in ammonium to nitrate specific uptake ratios preclude that varying proportions of detritus in PON be responsible for the significant difference in specific ammonium uptake rate between the two regions. This indicates that phytoplankton in the oceanic region show greater capacity to utilize ammonium. The relative importance of nitrate was highest in the neritic region, but primary production was still predominantly based on regenerated production. This was especially more pronounced during the NE monsoon period (f-ratio = 0.36).

The differences in specific ammonium uptake rate during the two monsoon periods illustrate different strategies with respect to ammonium utilization of oceanic and neritic phytoplankton assemblages. The increase in ammonium concentration during the SE monsoon (Table 4.4.1) was accompanied by a significant increase in specific ammonium uptake rate in neritic stations only. This was not, however, observed in oceanic stations. The neritic assemblage demonstrated highest ammonium uptake rates when the ambient concentrations were highest. On the other hand, constancy of specific ammonium uptake rate in oceanic regions despite significant increase in ambient ammonium concentration indicates that the oceanic phytoplankton assemblage runs with an 'all time' high specific ammonium uptake rate strategy. Apparently, this strategy suites best with the mode of ammonium supply in the oceanic region, *i.e.* chiefly zooplankton excretion and microbial remineralization. Relatively

Table 4.4.2. Specific nitrogen uptake rates ($_{\upsilon}$(nu), h^{-1}), transport rates ($_{\rho}$(rho), nM h^{-1}) and f-ratios.

Monsoon	Transect	Station	υnitrate	υammonium	ρnitrate	ρammonium	f-ratio
SE	Sabaki	108	0.0001	0.0036	0.2	7.7	0.03
		114	<0.0001	0.0151	0.004	9.98	<0.01
		117	0.0001	0.0071	0.02	2.34	0.01
	Tana	120	0.0001	0.0108	0.07	9.98	0.01
	Kiwayu	127	0.0003	0.0309	0.36	45.14	0.01
		128	<0.0001	0.0205	0.03	20.48	<0.01
		132	0.0001	0.0101	0.06	6.66	0.01
NE	Gazi	503	0.0017	0.0045	1.66	4.39	0.27
		505	0.0025	0.0085	1.91	6.56	0.23
		506	0.0029	0.0090	1.29	3.97	0.24
		507	0.0015	0.0061	0.69	2.79	0.20
	Sabaki	508	0.0030	0.0034	3.75	4.24	0.47
		511	0.0014	0.0024	1.15	1.93	0.37
		517	0.0018	0.0077	0.74	3.14	0.19
		518	0.0012	0.0089	0.53	3.84	0.12
		519	0.0013	0.0086	1.00	6.59	0.13
	Kiwayu	527	0.0009	0.0029	1.13	3.82	0.23
		528	0.0014	0.0016	1.53	1.76	0.46
		531	0.0029	0.0236	1.88	15.55	0.11
		532	0.0023	0.0096	0.70	2.88	0.20
		533	0.0026	0.0103	2.01	8.02	0.20

high specific ammonium uptake rates under conditions of very low ambient ammonium concentration imply a dynamic equilibrium between uptake and supply. It offers the advantage for phytoplankton to exploit conditions of high ammonium concentrations, *e.g.* right after zooplankton excretion events. Ammonium production by heterotrophs (mainly microzooplankton) meets a substantial fraction of the phytoplankton's nitrogen requirement in oligotrophic oceanic systems (Jackson 1980), as also observed in oligotrophic tropical oceanic regions,1 where phytoplankton achieve a relatively high growth rate in an ambient nutrient concentration close to the detection limit (Jackson 1980, Glibert and McCarthy 1984, Eppley *et al.* 1990).

conclusion

The seasonal change in monsoon regime affected nitrogen uptake regime of phytoplankton. The study area was extremely oligotrophic and ammonium was consistently the predominant nitrogenous nutrient. However, neritic and oceanic regions exhibited marked differences of ammonium uptake rate and relative importance of new production. Neritic and oceanic phytoplankton assemblages evidenced different strategies with respect to ammonium utilization, being a physiological adaptation to the supply mode of ammonium in the euphotic zone.

acknowledgements

We are grateful to J. Sinke and J. Van Ooijen for nutrient analyses and to J. P. Clement for technical assistance. F. Dehairs is a research associate at the National Fund for Scientific Research, Belgium; M. Semeneh is on leave from Addis Ababa University, Ethiopia.

references

Burkill P.H., R.F.C. Mantoura & N.J.P. Owens, 1993. Biogeochemical cycling in the northwestern Indian Ocean: a brief overview. Deep-Sea Res. 40: 643-649.

Dortch Q., 1990. The interaction between ammonium and nitrate uptake in phytoplankton. Mar. Ecol. Progr. Ser. 61: 183-201.

Eppley R.W., C. Garside, E.H. Renger & E. Orellana, 1990. Variability of nitrate concentration in nitrogen-depleted subtropical surface waters. Mar. Biol. 107: 53-60.

Eppley R.W. & B.J. Peterson, 1979. Particulate organic matter flux and planktonic new production in the deep ocean. Nature 282: 677-680.

Glibert P.M. & J.J. McCarthy, 1984. Uptake and assimilation of ammonium and nitrate by phytoplankton : indices of nutritional status for natural assemblages. J. Plankt. Res. 6: 667-697.

Gomes H.R., J.I. Goes & A.H. Paruleker, 1992. Size-fractionated biomass, photosynthesis and dark CO_2 fixation of in tropical oceanic environment. J. Plankt. Res. 14: 1307-1329.

Jackson G.A., 1980. Phytoplankton growth and zooplankton grazing in oligotrophic oceans. Nature 284: 439-441.

Mantoura R.F.C., C.S. Law, N.J.P. Owens, P.H. Burkill, E.M.S. Woodward, R.J.M. Howland & C.A. Llewellyn, 1993. Nitrogen biochemical cycling in the northwestern Indian Ocean. Deep-Sea Res. 40: 651-671.

McClanahan T.R., 1988. Seasonality in East Africa's coastal waters. Mar. Ecol. Progr. Ser. 44: 191-199.

Nair R.R., V. Ittekkot, S.J. Manganini, V. Ramaswamy, B. Hakkel, E.T. Degens, B.N. Desai & S. Honjo, 1989. Increased particulate flux to the deep ocean related to monsoons. Nature 338: 749-751.

Owens N.J.P., P.H. Burkill, R.F.C. Mantoura, E.M.S. Woodward, I.E. Bellan, J. Aiken, R.J.M. Howland & C.A. Llewellyn, 1993. Size-fractionated primary production and nitrogen assimilation in the north-western Indian Ocean. Deep-Sea Res. 40: 697-709.

Parker R.A., 1993. Dynamic models for ammonium inhibition of nitrate uptake by phytoplankton. Ecological Modelling 66: 113-120.

Smith S.L. & L.A. Codispoti, 1980. Southwest Monsoon of 1979: chemical and biological response of Somalia coastal waters. Science 209: 597-599.

Swallow J.C., F. Schott & M. Fieux, 1991. Structure and transport of the East African Coastal Current. J. Geophys. Res. 96: 22245-22257.

4.5. BIOMASS AND PRODUCTION OF BACTERIA AND PROTOZOA IN COASTAL WATERS OF THE WESTERN INDIAN OCEAN

Nico Goosen, Pieter van Rijswijk & Monique de Bie
Netherlands Institute of Ecology, Centre for Estuarine and Coastal Ecology, Yerseke, The Netherlands

introduction

Bacterioplankton plays an important role in the oceans carbon cycle. It is the most important source of particle formation in surface waters of the oceans (Ducklow, 1986; Cole *et al.*, 1988). At the same time it acts as a 'sink' returning fixed carbon to CO_2 (Ducklow, 1991). In the oceans interior bacterioplankton oxidizes dissolved organic carbon (DOC; Toggweiler, 1989) and hydrolizes suspended particles (Cho & Azam, 1988).
To gain a better understanding of the importance of bacterioplankton in the carbon cycle, information is needed on depth profiles of the biomass and production rates of bacteria in different oceans. Until now there are very few reports on bacterial properties in the Indian Ocean (Sorokin *et al.*, 1985; Ducklow, 1993). In this paper we present data on bacterioplankton abundance and production and microzooplankton abundance during two cruises in the western Indian Ocean in June-July and November-December 1992.

material and methods

This work was carried out during two cruises, A1 (June-July 1992) and A2 (November-December 1992), aboard R.V. *Tyro* as part of the Netherlands Indian Ocean Program. Four transects were sampled along the Kenyan coast (see Heip & Hemminga, this volume). Each transect consisted of five stations with depths of 20 m, 50 m, 500 m, 1000 m, and 2000 m. During cruise A2 the Tana transect was not sampled. At each station samples were taken by a CTD rosette cast. Samples were taken above, in and beneath the thermocline.
Concentrations of bacteria and heterotrophic nanoflagellates (HNAN) were determined directly on board by epifluorescence microscopy after preservation with 2% glutaraldehyde, staining with DAPI and primulin respectively (Porter & Feig, 1980; Bloem *et al.*, 1986) and filtration on black polycarbonate filters. Bacterial production rates were estimated in triplicate by measuring the incorporation of methyl-^{3}H-thymidine (TdR, specific activity 82-86 Ci mmol^{-1}; Amersham, U.K.) into cold trichloroacetic acid (TCA)-insoluble material (Fuhrman & Azam, 1982; Ellenbroek & Cappenberg, 1991). The incorporation of tritiated thymidine was linear for at least two hours and saturation occurred at a final concentration of 2 nM. In the assays a final concentration of 10 nM thymidine and an incubation time of 60 minutes at *in situ* temperature was used. After filtration of samples the filters were dissolved in Filtercount (Packard) and counted in an LKB RackBeta scintillation counter.
Samples for the determination of dissolved organic carbon (DOC) were filtered through disposable PTFE Teflon filters with 0.2 µm pore size, preserved with $HgCl_2$ and stored at 4°C in acid rinsed polyethylene vials.

preliminary results

Both cruises were performed during the South-East (SE) monsoon. During cruise A1 high current velocities occurred (5 knots) and the depth of the upper thermocline was at 70-80 meters. Cruise A2 was almost at the end of the SE monsoon. Wind velocities were very low, the direction had already turned but in general the water current was still SE with velocities of about 2 knots. The upper thermocline was at 30-40 meters depth. However at the GAZI-transect the upper thermocline was at the same depth as in june-july. The temperature of the surface water during the cruise A1 and A2 was 26-27°C and 27-28°C respectively
Bacterial concentrations in the surface water ranged from 1 to 5×10^5 cells/ml. Cocci were the most abundant bacterial form present. In the surface water no change in bacterioplankton abundance was observed with increasing distance from the coast. At stations of 500 m depth or more the concentration of bacteria decreased with depth (fig. 4.5.1). The main decrease took place in the thermocline. Below 250 m bacterial concentrations were up to a factor 10 lower than in the surface water. During cruise A1 bacterioplankton abundances in the surface water were consistently higher than during cruise A2.
The concentration of heterotrophic flagellates in the surface water was between 100-600 cells.ml^{-1}. In general the concentration of flagellates decreased with depth to concentrations below 100 cells.ml^{-1} (fig. 4.5.1). No ciliates were found.
The Thymidine incorporation rates in the surface water decreased with the distance from the coast on all four transects (fig. 4.5.2). At stations with a depth of 20 and 50 meters the thymidine incorporation rate was between 1.5 and 9 pmole TdR l^{-1} h^{-1} with significantly higher incorporation rates during cruise A2, specially at the Gazi and Kiwayuu tyransects. The thymidine incorporation rate in the surface water at stations with a depth of 500 to 2000 meters was between 1 and 2 pmole TdR l^{-1} h^{-1} and the differences in incorporation rate between cruise A1 and A2 were very small. A vertical profile of thymidine incorporation is shown in

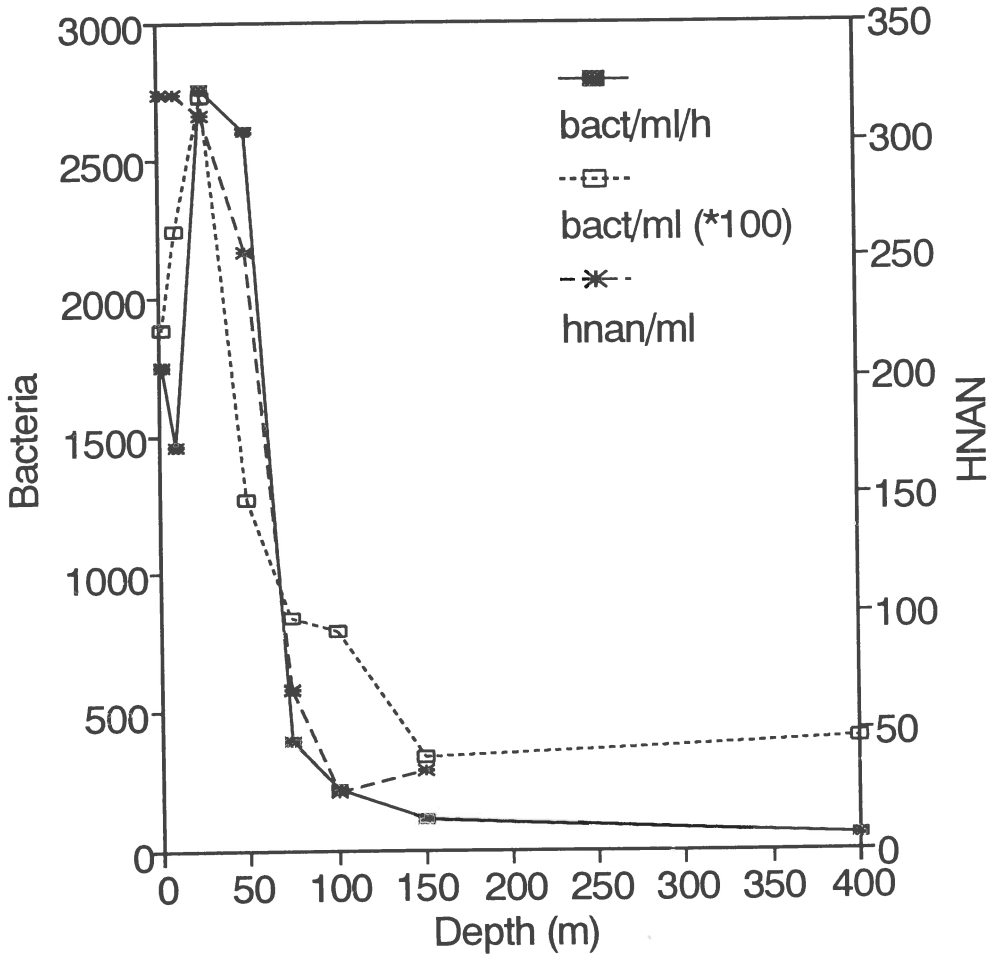

Fig. 4.5.1. Bacterial production and concentration of bacteria and heterotrophic nanoflagellates (HNAN) at station 517, Sabaki-transect.

fig. 4.5.3. Incorporation rates decreased with depth. The main decrease in incorporation rate occurred in the thermocline. At the stations where a more detailed depth profile was measured one or two subsurface peaks in thymidine incorporation were observed in the upper 75 m (fig. 4.5.3). Duplicate measurements of the same station during one day showed that the thymidine incorporation rate can be variable.
DOC concentrations ranged from 0.4 to 1.3 ppm and generally a gradual decrease with increasing depth occurred. At some stations an increased concentrations was found at 250-500 m depth.

discussion

Only few modern studies on bacterioplankton in the Indian Ocean have been reported (Sorokin *et al.*, 1985; Ducklow, 1993). These studies were performed in the central and north western part of the Indian Ocean respectively. The objective of our research was to describe the distribution of bacterial abundance and production rates in the western Indian Ocean, specially the Kenyan coastal areas. Samples were studied from surface water to depths of 1000 m. Most samples were from the upper 250 m. For deeper samples it was not possible to maintain ambient temperatures, pressures or oxygen levels during sample recovery and subsequent processing. Although for thymidine incorporation studies samples were incubated at the ambient (± 2°C) temperature. The above lack to maintain ambient conditions for especially oxygen and pressure may have consequences for reliability of the measured thymidine incorporation rates. For samples from water layers with low oxygen levels the effect of aeration is probably low (Ducklow, 1993). According to Carlucci *et al.* (1986) effects of hydrostatic pressure on samples from 0 to 2000 m are minimal. As our samples came from a maximam depth of 1000 m we presume that they are not affected by pressure.

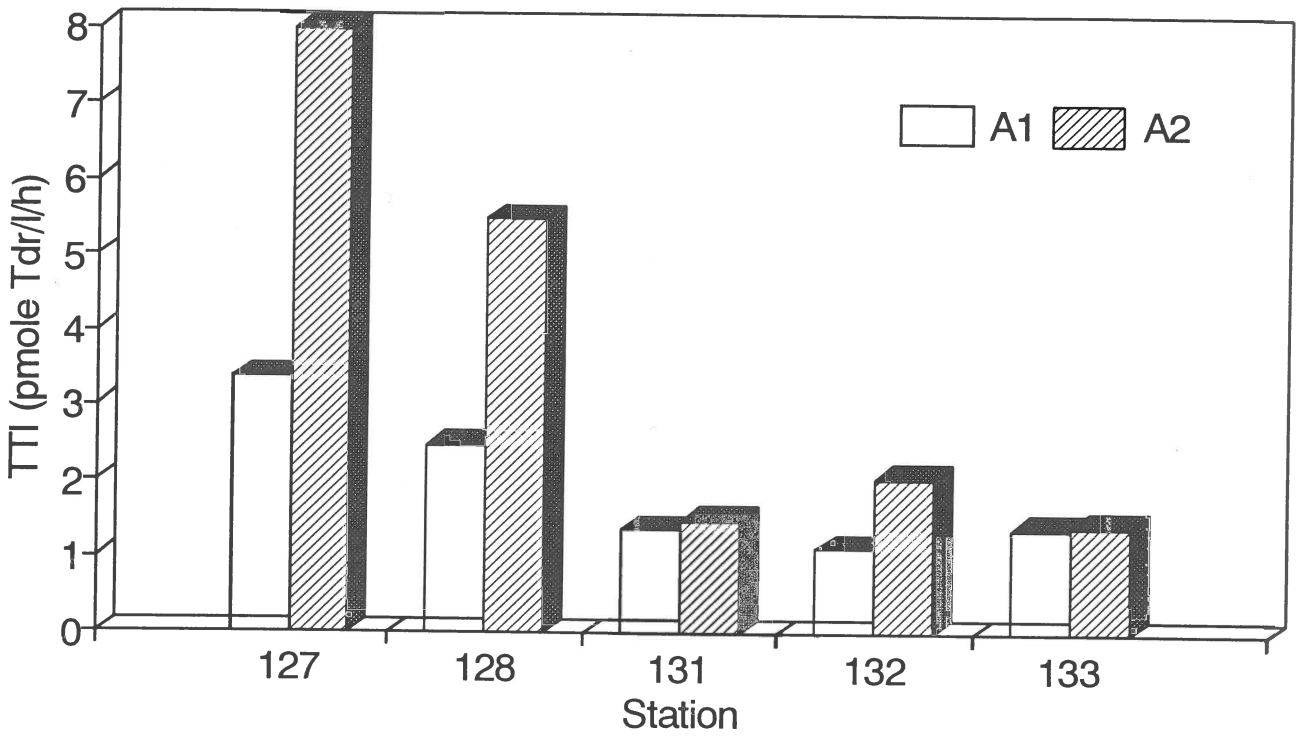

Fig. 4.5.2. ^{3}H-thymidine incorporation (TTI) rate in surface water (2 m depth) of the Kiwayuu-transect during cruises A1 and A2.

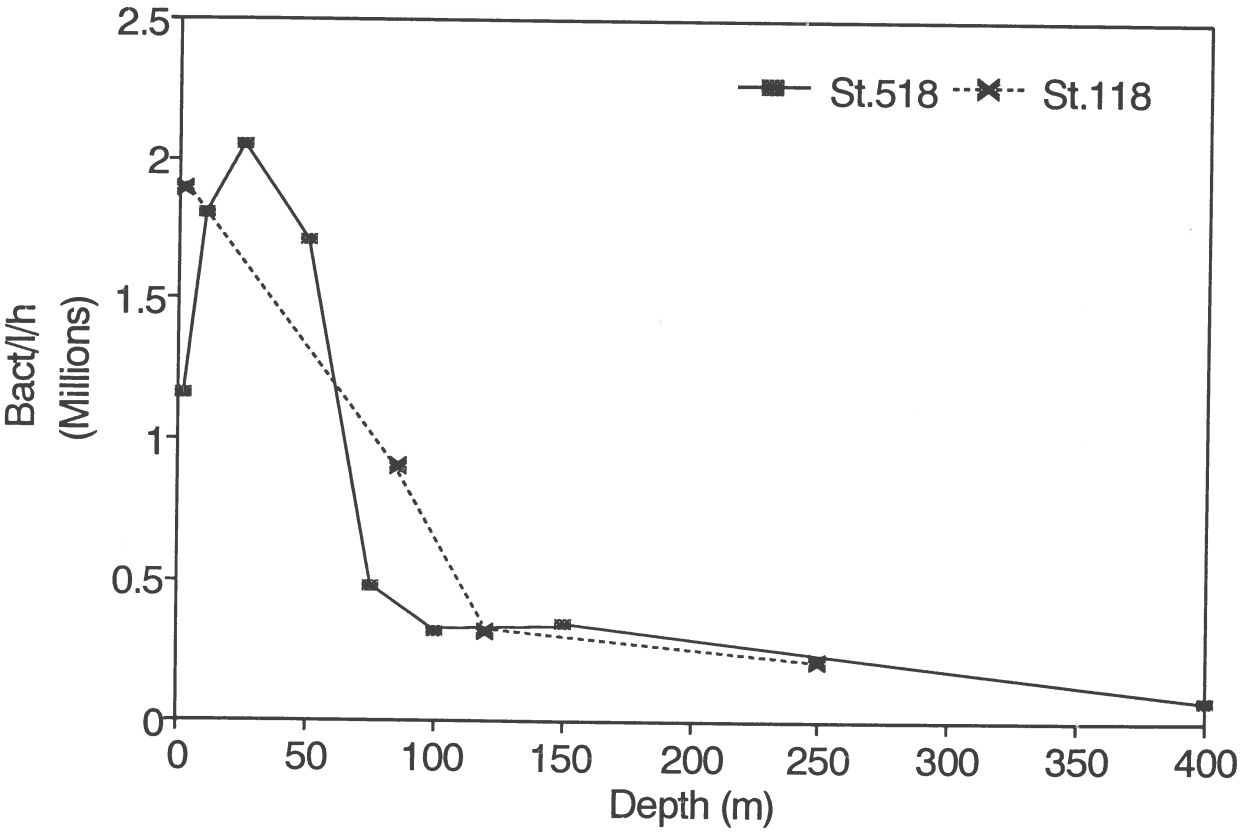

Fig. 4.5.3. Depth profiles of bacterial production at station 118 during cruise A1 and A2.

For calculation of bacterial biomass and production (BP) expressed in carbon units, conversion factors have to be determined or assumed. During this study conversion factors were not determined. To ensure a good comparison with the only other reported study on bacterioplankton in this area of the Indian Ocean (Ducklow, 1993) we assumed the following factors: 2×10^{-14} gC cell^{-1}; 1.18×10^{18} cells mole^{-1} (Riemann & Bell, 1990).

The thymidine incorporation rates we measured in the coastal zone of Kenya (2-4.5°S, 39.5-41°E) were clearly lower than Ducklow (1993) found for the north western part of the Indian Ocean and the Gulf of Oman. From the measured thymidine incorporation rates in the surface water bacterial production rates of 35-200 ngC l^{-1} h^{-1} for the near coastal stations (20-50 m depth) can be calculated. In the stations with a depth of 500-2000 m bacterial production rates in the surface water were 24-47 ngC l^{-1} h^{-1}. While the bacterial concentrations in the surface water are rather constant the production rates are clearly higher near the coast. This may indicate a higher productivity and more intensive grazing by heterotrophic flagellates in near coastal waters. In fact we did found in some near coastal stations an increased abundance of heterotrophic flagellates.

references

Bloem, J., M.-J.B. Bär-Gilissen & T.E. Cappenberg, 1986. Fixation, counting, and manipulation of heterotrophic nanoflagellates. Appl. Environ. Microbiol. 52: 1266-1272.

Carlucci, A.F., D.B. Craven, K.J. Robertson & S.M. Henrichs, 1986. Microheterotrophic utilization of dissolved free amino acids in depth profiles off Southern California. Oceanologica Acta 9: 89-96.

Cho, B.C. & F. Azam, 1988. Major role of bacteria in biogeochemical fluxes in the ocean's interior. Nature 332: 441-443.

Cole, J.J., M.L. Pace & S. Findlay, 1988. Bacterial production in fresh and saltwater ecosystems: a cross-system overview. Mar. Ecol. Progr. Ser. 43: 1-10.

Ducklow, H.W., 1986. Bacterial biomass in warm core Gulf Stream ring 82B: Meso scale distribution, temporal changes, and production. Deep-Sea Res. 33: 1789-1812.

Ducklow, H.W., 1991. The passage of carbon through microbial foodwebs: results from flow network models. Mar. Microb. Foodwebs 5: 1-16.

Ducklow, H.W., 1993. Bacterioplankton distribution and production in the northwestern Indian Ocean and Gulf of Oman, September 1986. Deep-Sea Research II 40: 753-771.

Ellenbroek, F.M. & T.E. Cappenberg, 1991. DNA synthesis and tritiated thymidine incorporation by heterotrophic freshwater bacteria in continuous culture. Appl. Environ. Microbiol. 57: 1675-1682.

Fuhrman, J.A. & F. Azam, 1982. Thymidine incorporation as a measure of heterotrophic bacterioplankton production in marine surface waters: evaluation and field results. Mar. Biol. 66: 109-120.

Porter, K.G. & Y.S. Feig, 1980. The use of DAPI for identifying and counting aquatic microflora. Limnol. Oceanogr. 25: 943-948.

Riemann, B. & R.T. Bell, 1990. Advances in estimating bacterial biomass and growth in aquatic systems. Arch. Hydrobiol. 118: 385-401.

Sorokin, Y.I., A.I. Kopylov & N.V. Mamaeva, 1985. Abundance and dynamics of microplankton in the central tropical Indian Ocean. Mar. Ecol. Prog. Ser. 24: 27-41.

Toggweiler, J.G., 1989. Is the downward dissolved organic matter (DOM) flux important in carbon transport. In: W.H. Berger, V.S. Smetacek & G. Wefer (eds), Productivity of the oceans: present and past: 65-83. Wiley & Son.

4.6. ZOOPLANKTON COMMUNITIES OFF THE KENYAN COAST

Melckzedeck Osore, Lin Zhu, Michele Tackx & Nanette Daro
Ecology Laboratory, Free University of Brussels, Pleinlaan 2, 1050 Brussels, Belgium

introduction

As part of the Project A2 of the Kenya-Dutch expedition to the Indian Ocean, the zooplankton community structure of the Kenya coastal waters was studied. Sampling stations along three parallel transects located off Kiwayuu, the Sabaki mouth and Gazi Bay were considered. The aim of the study was to quantify the abundance and diversity of zooplankton in the nearshore and offshore waters off the Kenya coast during the South-East monsoon period.

material and methods

Zooplankton was sampled at each station using vertical net hauls (mesh size of 200 µm). Samples were preserved in 4% formalin. Laboratory analysis involved identification of zooplankton to species level and counting using a stereo microscope. For the purpose of studying spatial distribution, the Two Way Indicator SPecies ANalysis technique TWINSPAN (Hill, 1979) was employed, based on the zooplankton abundance data. Margalef's (1951) index was used to calculate diversity. For details on the methodology, the reader is referred to Osore (1994).

results and discussion

The Sabaki transect had the highest average zooplankton density (836 ind./m^3), followed by the Gazi transect (686 ind./m^3) and Kiwayuu had the lowest (463 ind/m^3). Fig. 4.6.1. shows the results of the TWINSPAN on the averaged abundance data.
The nearshore stations (less than 200 m depth), 503 (Gazi) and 508 (Sabaki), are clustered together with *Clausocalanus* spp. as indicator species. The Kiwayuu transect stations 531, 532, 533 and the Sabaki transect station 517, all which lie within the 1000 m depth line, are clustered together. The indicator species is the euphausiid *Calyptopis* sp. The Sabaki transect stations 518 and 519 located beyond the 1000 m depth line, are clustered together (indicator species: bivalve larvae). Finally, the Gazi transect stations located beyond the 200 m depth line cluster together. The geographical locations of the clusters identified by TWINSPAN are given in fig. 4.6.2.
Fig. 4.6.3. shows the diversity of the zooplankton along the three transects. For all transects, the diversity was high near shore (3.86 to 4.50) and decreased offshore (1.77 to 3.55). The diversity gradient in the Gazi transect was compared with diversity of the zooplankton measured at three stations inside Gazi Bay during the same season (stn 3 near the mangroves, stn 2 over the seagrass beds in the middle of the bay and stn 1 at the seaward entrance of the bay). As can be seen in Fig. 4.6.4, diversity tends to decrease from the mangrove station (3) towards the open sea (stn 507), with the exception of station 503, where diversity peaks.

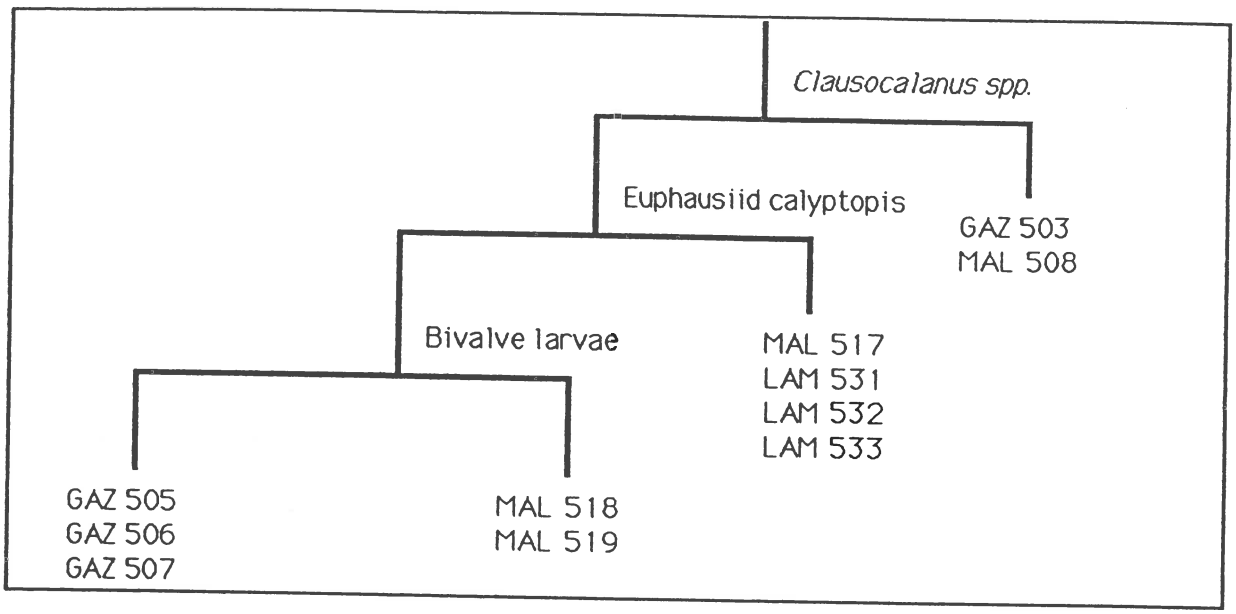

Fig. 4.6.1. Dendrogram of stations following TWINSPAN analysis.

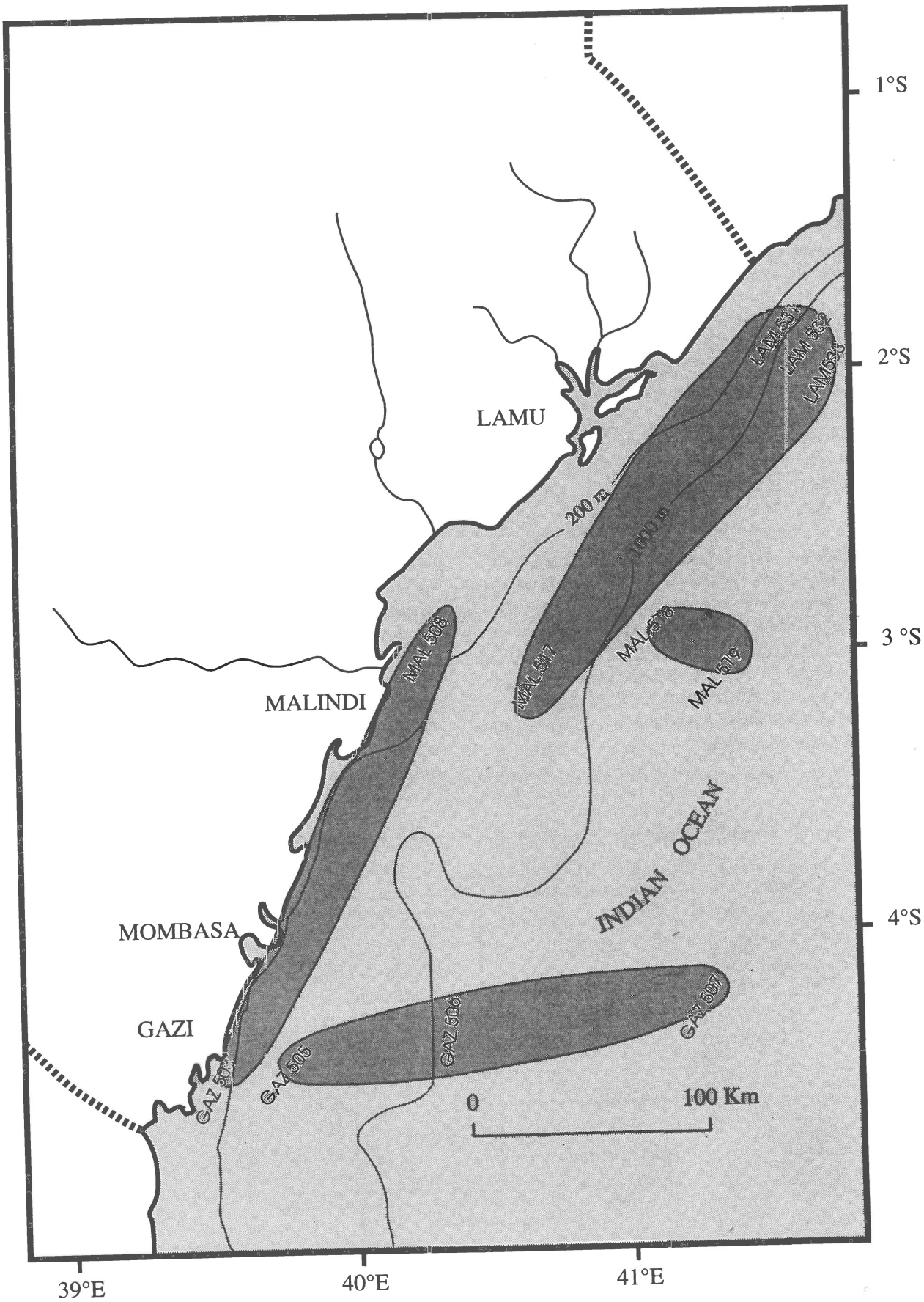

Fig. 4.6.2. Geographical locations of the clusters identified by TWINSPAN

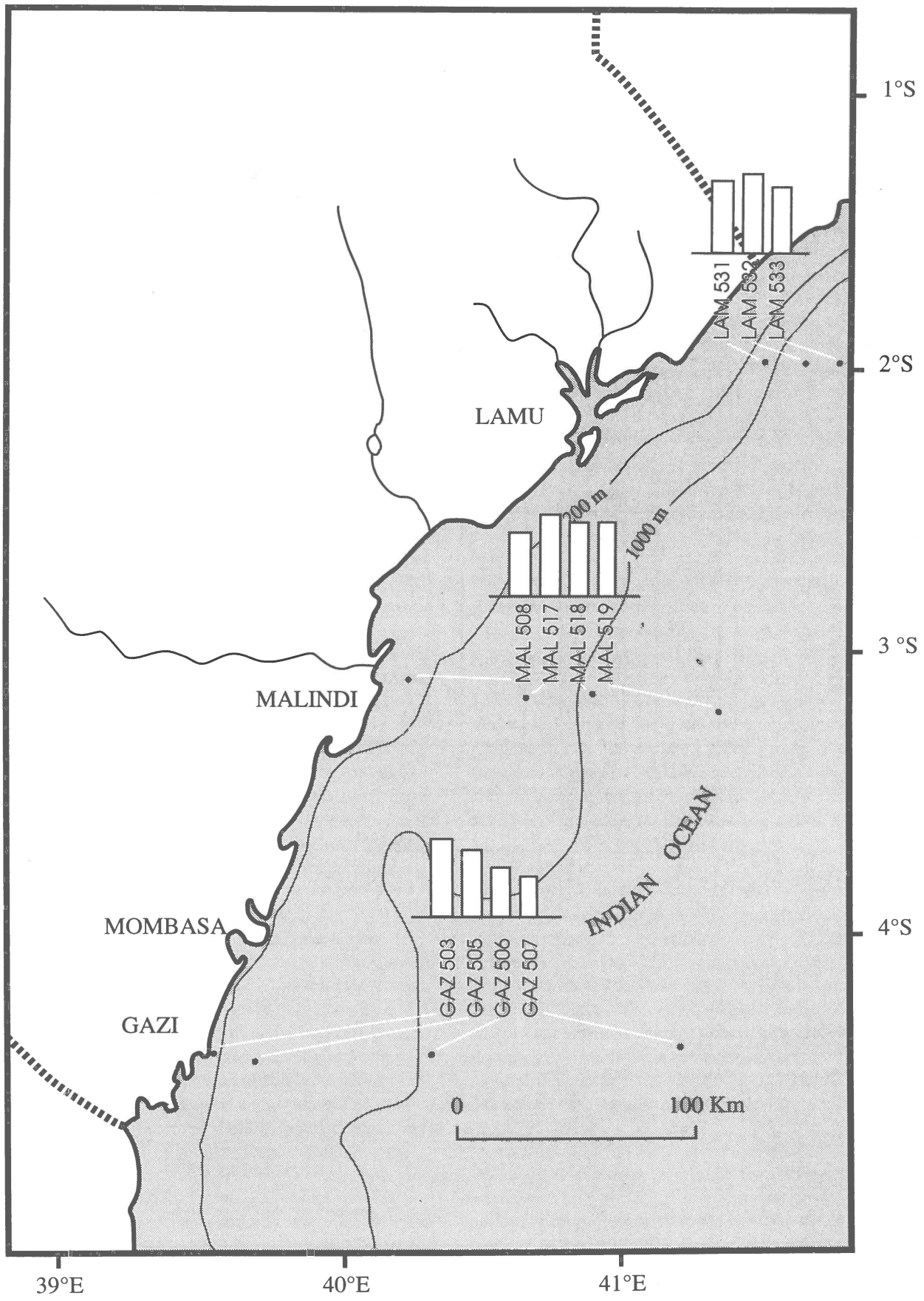

Fig. 4.6.3. Diversity (Margalef's index) of zooplankton along the three transects.

The tendencies in abundance and diversity of zooplankton will further be analyzed in relation to the particulate matter concentration and composition. For this purpose, gut fullness of deep-frozen organisms collected at each station will be analyzed by image analysis (Tackx *et al.*, manuscript). This will further be combined using multivariate techniques with microscopic data on phytoplankton species composition and abundance (Wawiye, in progress) and environmental variables measured by CTD.

references

Hill, M.O., 1979. TWINSPAN, A computer programme for arranging multivariate data in an ordered two-way classification of the individuals and attributes. Cornell Univ., Ithaca, New York.

Margalef, D.R., 1951. Diversidad de especies en les communidades naturales. Publnes Inst. Biol. Apl. Barcelona 9: 5-7.

Osore, M.K.W. , 1994. A study of the zooplankton of Gazi, Kenya and the adjacent waters: community structure and seasonal variation. MSc. Thesis (F.A.M.E.). 104 pp.

Tackx, M.L.M., L. Zhu, W. De Coster, R. Billones & M.H. Daro (manuscript). Measuring selectivity of feeding by estuarine copepods using image analysis combined with microscopic- and Coulter counting. Submitted to ICES J. Mar. Sc.

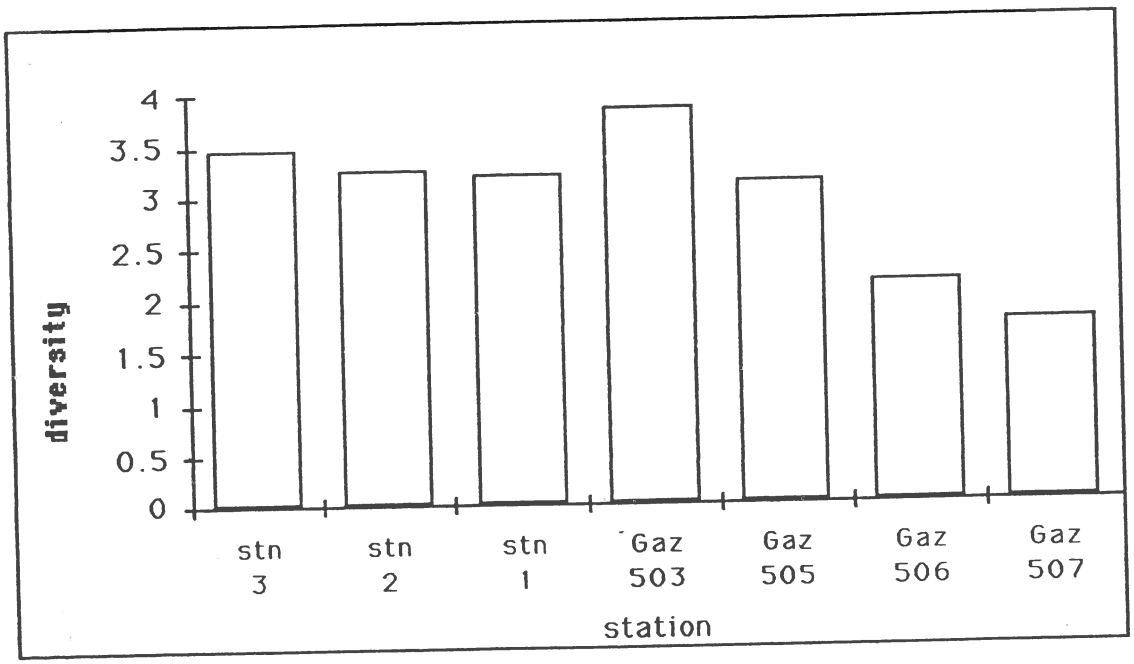

Fig. 4.6.4. Diversity (Margalef's index) of zooplankton from Gazi bay and the coastal transect in front of Gazi.

4.7. ZOOPLANKTON SPECIES DISTRIBUTION AND ABUNDANCE DURING THE MONSOONS OFF THE KENYAN COAST, 1992

James Mwaluma
Kenya Marine and Fisheries Research Institute, P.O Box 81651, Mombasa, Kenya

introduction

Studies carried out on board R.V. *Tyro* were aimed at studying the effects of the monsoons on the functioning of the ecosystem of the Kenyan shelf. Along the Kenya coast, the NE monsoon season is between November and March and the SE monsoon season between April and October. The SE monsoons are usually characterised by high clouds, rain, wind energy and decreased temperatures and high light intensity. During the NE monsoons, the situation is reverse. Interactions between off-shore and coastal areas and the impact of the monsoons on the shelf are virtually unknown. Hence samples were collected with the aim to study the distribution, taxonomy and abundance of zooplankton in the coastal waters, the dominant species and how they vary with the different monsoons. Such investigations are necessary to explain the essence and mechanisms of functioning of ecosystems and for processes of organic matter production as well as for understanding the principles of forming the productive aggregations of plankton (Petipa, 1985).
Three transects perpendicular to the coast were made (i) Kiwayuu transect to the north (ii) Gazi transect to the south and (iii) Tana transect where the river Tana drains into the sea. The Gazi transect was linked to the land-based programme the aim of which was to study the coastal processes. This was to provide information as to whether the productivity of the coastal waters was dependent on export of organic matter from rivers, seagrass meadows and mangrove areas.
Each transect had 3 or 4 stations starting from shallow stations of 50 m to deep ones of 2000 m. Depth stratified sampling was done by towing horizontally a multiplankton sampler (m.p.s.) fitted with a 200µm and 55µm mesh size plankton net. A deck pump using 200µm and 55µm mesh, was also used to collect surface (0-3 m) zooplankton on each station. For shallow stations (50 m), only one shallow cast was made. For deeper stations, 500-2000 m, three to four deep casts were made. Conductivity, temperature and depth were measured simultaneously as the multinet was cast. Collected samples were analysed for species composition, biomass, density and species diversity. Biomass estimations were made by dry-weight and ash-weight measurements. Results so far cover only 50 m and 500 m stations.

results

The upper surface layers had a water temperature ranging between 26 and 29°C. At the thermocline, which was at around 80 m deep, temperature dropped rapidly to around 15°C.
Zooplankton biomass was greatest during the NE monsoon. The highest recorded biomass was 18.6 mg/m^3 at the 50 m station in the Gazi transect (fig 4.7.1). The Kiwayuu transect (50 m) also indicated a high biomass of 10.1 mg/m^3. During the SE monsoon highest recorded biomass was 7.8 mg/m^3 (see fig 4.7.1) at the Kiwayuu transect (50 m). The shallower 50 m stations recorded 5.2 and 5.6 mg/m^3 at the Gazi and Sabaki transects respectively. In deeper stations (500 m), the upper surface layers (0-100 m) yielded higher biomass as compared to the deeper layers. This is due to light limitation which hinders productivity beyond the euphotic zone. A greater zooplankton diversity exist especially in the shallower (50 m) stations for both seasons. Of all zooplankton groups recorded, copepods were the most dominant group which formed up to 80% of the total zooplankton population.
Calanoid copepods outnumbered all other plankton groups in numerical abundance and species diversity and this group is respdnsable for most of the secondary productivity (Stephen, 1984).

Species composition above the thermocline.
The shelf during the SE monsoon was dominated by *Paracalanus* sp, *Acrocalanus gibber, Acrocalanus* sp, *Undinula vulgaris, Oithona* sps, *Eucalanus attenuatus, E. subcrassus, Acartia danae, Temora discaudata, T. turbinata, T. stylifera, Oncaea venusta, Candacia* sp, *Corycaeus* sps, *Centropages orcinii, C. furcatus, Rhinecalanus cornutus*, and copepod nauplii. Others were, *Macrosetella* sps, *Saphirina* sps, *Corycaeus* sps, *Copila mirabilis* and *Clytymnestra scutellata* amongst others.
In the NE monsoon dominant copepod species were *Paracalanus* sp, *Undinula vulgaris, Temora turbinata, Calanus elliptica, Oncaea conifera, O. venusta, Oithona* sps, and copepod nauplii. Others were *Acartia* sps, *Pontillopsis armata, Pontillopsis* sps, *Labidocera pavo, Calocalanus pavo, Corycaeus* sps and *Eucalanus attenuatus* amongst others.

Species composition below the themocline.
Below the thermocline dominant copepod species were *Eucalanus crassus, Pleuromamma gracilis, P. xiphias, Haloptilus mucronatus, Haloptolus* sps, *Neocalanus* sp, *Lucicutia flaviconis, L. clausii, Scottocalanus longispinus, Euchaeta marina, Aetideus armatus* and *Candacia* sps amongst others. This was the case in both seasons.

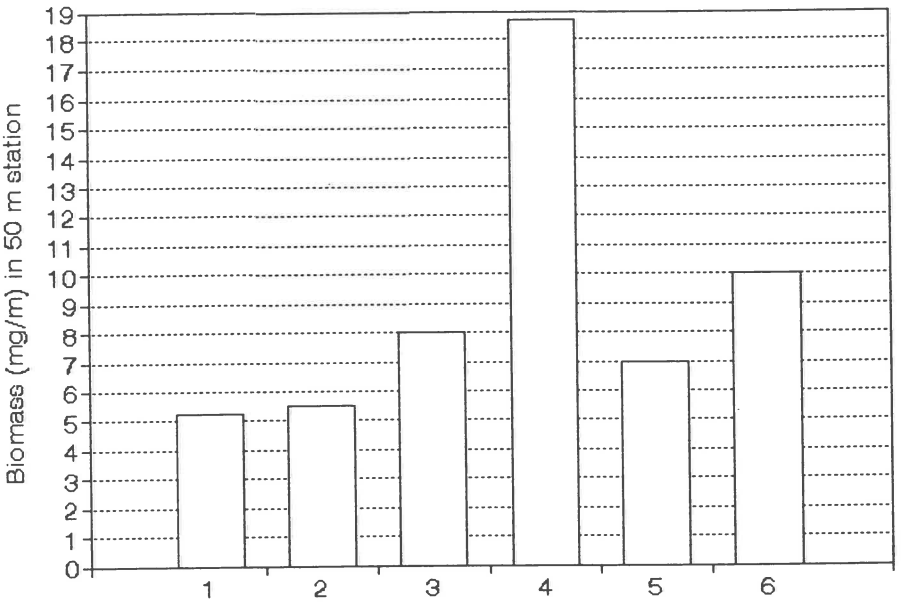

Fig. 4.7.1. Zooplankton biomass in three 50 m stations during A1 (1-3) and A2 (4-6)

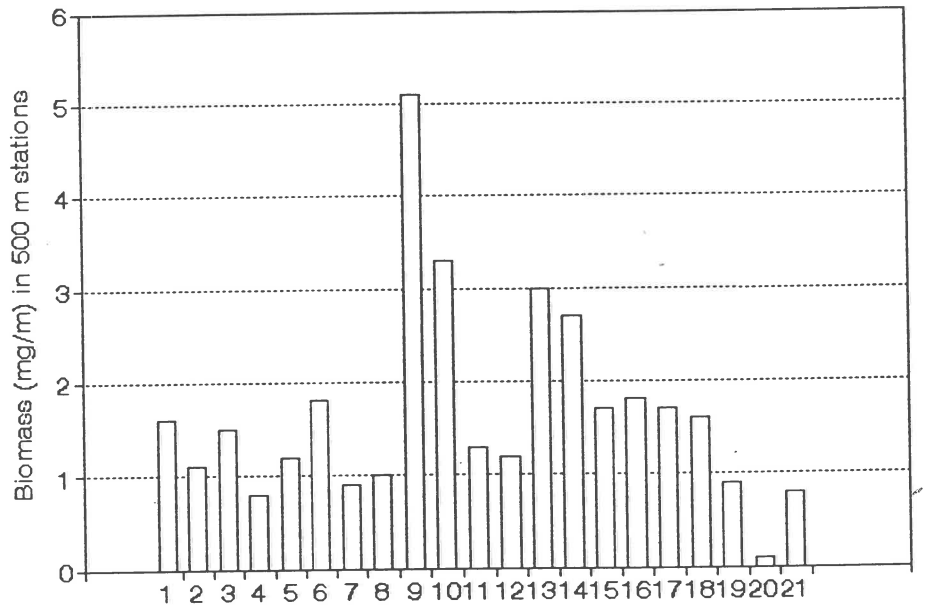

Fig. 4.7.2. Zooplankton biomass in 500 m stations during A1 (1-12) and A2 (13-21)

The copepod species aggregated at different depth levels depending on the physico-chemical properties of the water layers.

Considerable change in fauna occurs below the surface waters. The single most dominant copepod species over the shelf was *Undinula vulgaris* which occurred during the NE monsoon at Sabaki transect (50 m). The population in numbers reached 11,872 per m^3.

Other zooplankton groups which were of equal importance were chaetognaths *(Sagitta* sps), mysiids, gastropod larvae, appendicularians and polyzoans amongst others (see table 4.7.1). Most of these occurred on the continental shelf during the NE monsoon. Typically oceanic species included salps, ctenophores, Foraminifera, heteropods, pteropods and polyzoans. Fish eggs and larvae were abundant during the NE monsoon in the Gazi transect. brachyuran larvae, Caridea and cha-

Table 4.7.1. Dominant zooplankton groups over the continental shelf during the 1992 monsoons.

North East monsoons	South East monsoons
Chaetognaths	Chaetognaths
Appendicularians	Salps
Gastropod larvae	Ostracods
Fish eggs and larvae	Branchyuran larvae
	Caridea

etognaths were abundant in th SE monsoon in Kiwayuu transect (see table 4.7.1). Other groups identified were molluscan larvae made up of gastropod larvae and bivalve larvae, Sergestidae (*Lucifer* protozoa and adults), amphipods (gamariids and hyperiids), anomuran larvae, cladocerans, isopods, polychaete larvae and cephalopod larvae (squids) which were only found on the shelf areas. The high zooplankton production in the NE monsoons can be probably explained by high organic matter transported into the system by river run-off and also due to reversal of the currents which may cause upwelling and recycling of nutrients. Biomass values for oceanic waters were quite low because nutrients get assimilated by phytoplankton and microbacteria in their transport from the land input resources at the shelf before they get to the oceanic province. Hence there is no immediate food energy to be passed on to higher trophic levels. There is increased productivity over the continental shelf due to greater mixing of nutrients, especially during the rainy season, and good light penetration which boosts primary productivity. Analysis for numerical abundance is still going on, especially for the deeper stations as well as samples for diurnal vertical migration.

references

Saraswathy, M. & H. Krishnaiyer, 1986. Ecology of *Pleuromamma indica* Wolfenden in the Indian Ocean. Indian Journal of Marine Sciences 15: 219-227.

Tamara, S.P., 1985. Aims, materials and results of economically active zones of the Indian Ocean (14th complex expedition on the R/V "Proffesor Vodyanitsky"). Pol. Arch. Hydrobiol. 32: 209-230.

Wickstead, J.H., 1962. Plankton from the E. African area of the Indian Ocean. Nature 196: 1224-1225.

Wickstead, J.H., 1963. Estimate of total zooplankton in the Zanzibar areå of the Indian Ocean with a comparison of the results with two different nets. Proc. Zool. Soc. Lond. 141: 527-608.

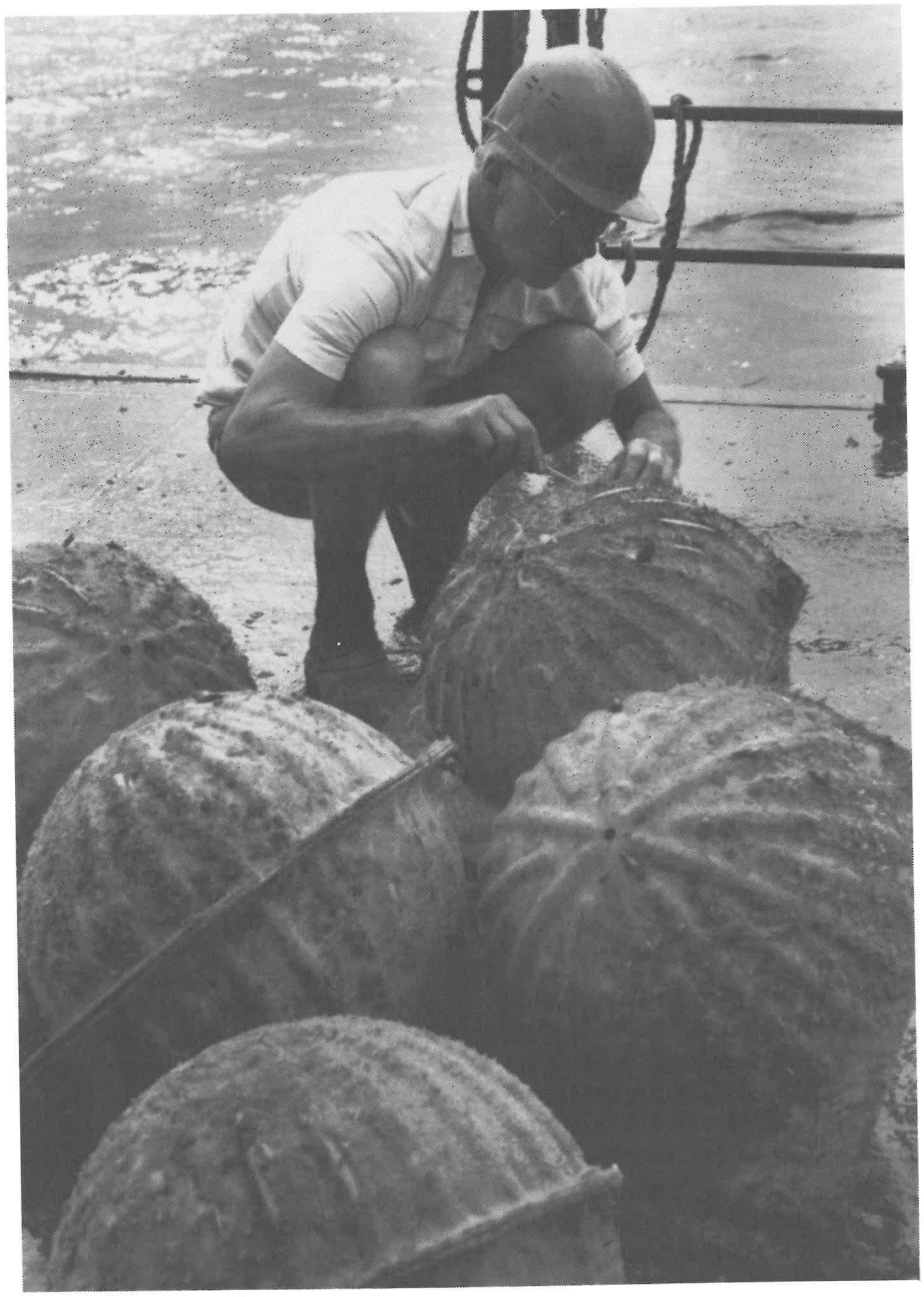

Benthologist Peter de Wilde.

4.8. DISTRIBUTION AND ACTIVITY OF THE BENTHIC INFAUNA ALONG THE KENYAN SHELF

Gerard C.A. Duineveld, Eilke M. Berghuis, Tom Tahey & Peter A.W.J. de Wilde
Netherlands Institute for Sea Research, P.O. Box 59, 1790 AB Den Burg, Texel.

introduction

In the framework of the NIOP project on the Monsoonal influence on the marine ecosystem along the Kenyan coast, two cruises with RV. *Tyro* were made in order to study the carbon and nutrient cycles in the pelagic and benthic communities. The cruises took place in the periods June and November/December which supposedly covered the SE and NE Monsoon respectively. As river-input and current pattern are different during the two monsoons, associated benthic and pelagic processes were assumed to change as well. The present contribution discusses the results obtained in a study of the benthic metabolism and the structure of the benthic fauna.
Two main groups of animals were selected for studying the structure of the benthic community, *viz.* the meiofauna and macro-infauna. Because of the relatively long life span of metazoan animals, compared to unicellular organisms, their biomass represents an integrated measure for food availability over time scales exceeding months. The biomass of the benthic microbial community was not determined separately, but will be incorporated in an estimate of the sediment DNA biomass. The metabolic activity of the benthic community was studied by measuring the oxygen uptake of intact sediment cores. This was carried out *in-situ* on the sea-floor as well as on board of the ship. The consumption estimates from these measurements give direct insight into the prevailing availability of labile organic material at the seabed. Concurrently with the measurements of oxygen consumption, sediment-water fluxes of nutrients were determined, to evaluate the role of the seabed in nutrient recycling. Additional sediment samples were collected to assess its carbon, nitrogen and phytodetritus content.

methods

Study area
In both periods, measurements and sampling were carried out along three principal transects perpendicular to the coastline. The southernmost Gazi-transect was situated near a stretch of coast with a longshore reef and an inshore creek bordered by mangroves. The middle Sabaki-transect was located near the mouth of the river Sabaki whereas the northernmost Kiwayu transect near the Somali border had no river in the immediate vicinity.
Each transect encompassed four major stations at 50, 500, 1000 and 2000 m depth. Along the Sabaki-transect a 200 m station was sampled as well. Only during the June-cruise some supplementary stations were visited near the mouth of the river Tana (50 and 150 m depth).

Sediment sampling
At each station, a minimum of one box-core sample (30 cm diameter) was washed over a 0.5 mm sieve for the macrofauna and one subcore of 10 cm depth and 7 cm^2 was collected for meiofauna. All samples were preserved in buffered formalin. At the 50 m stations an additional set of five macro- and meiofaunal samples was taken as part of a global study on the faunal diversity on continental shelves, a current project of the Plymouth Marine Laboratory (UK).
Subcores for the analysis of the grainsize, carbon and phytopigment content of the sediment were taken from sediment cores used in respiration experiments (see below). For the purpose of comparing phytopigments in the sediment and overlying water, a sample of bottom-water (2-20 liter) was filtered at every station. Samples for phytopigments were deep immediately frozen (-80°C). Chlorophyll-*a* and phaeopigments were separated by means of HPLC and detected with a fluorimeter.

Oxygen and nutrient flux measurements
Fluxes of oxygen and nutrients were measured *in situ* as well as on board. One instrument for *in-situ* measurements was a free-falling benthic lander, able to carry out a programmed series of operations at great depths. The lander holds two corers which after being driven into the sediment and sealed off, serve as incubation chambers. The oxygen decrease in the chambers is recorded by micro-electrodes. At three preset times during the incubation, 30 ml samples are drawn from inside (and outside) the chamber for determination of nutrient fluxes (Si, PO_4, NH_4, NO_x). Initial and final concentrations of oxygen and nutrients were determined in samples taken by respectively two Niskin bottles attached to the lander frame and a special cuvette inside the incubation chambers. Other operations comprise taking photographs from the sediment within the chambers, opening and closing of sediment traps mounted on top of the lander, and taking small subcores which are taken to the surface. Upon acoustic release of the ballast weights on the lander, flotation spheres bring the lander to the ocean surface.
The second instrument deployed for *in-situ* respiration measurements, is a modified box corer ('bell-jar') which is lowered onto the sea-bed by cable. Weights

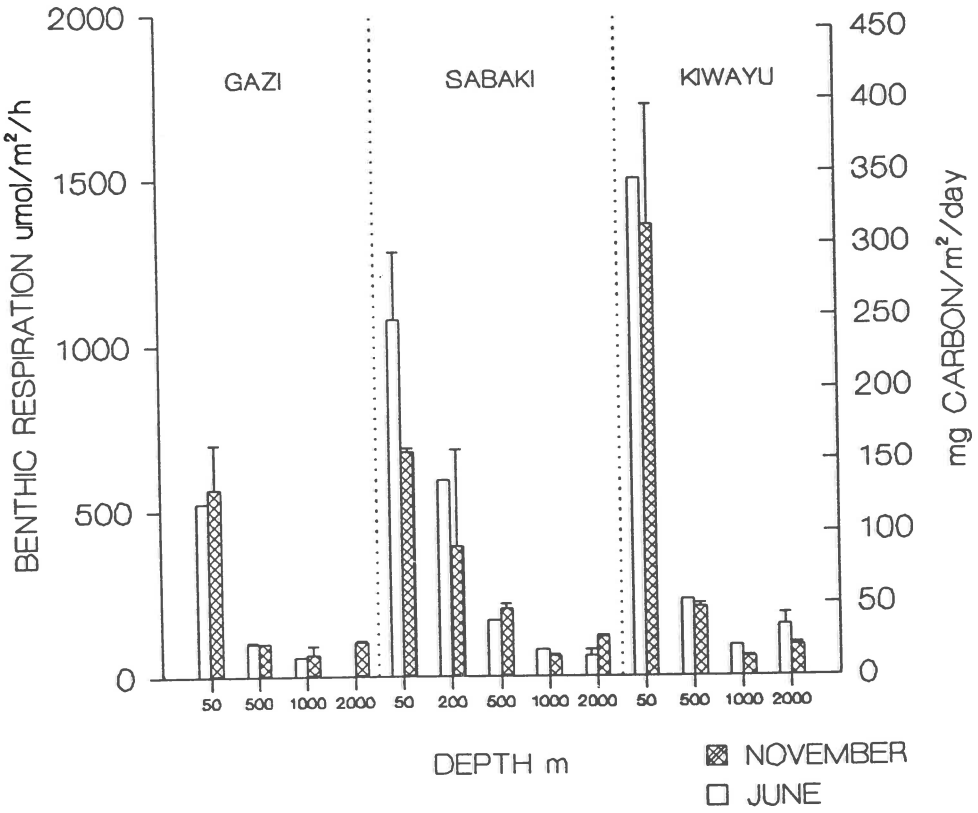

Fig. 4.8.1. Comparison of benthic respiration rates measured in shipboard incubated cores in June and November (NIOP-A1 resp. A2). Units in lefthand scale are µmoles m^{-2} h^{-1}; the righthand scale provides the equivalent in mg Carbon day^{-1}. Gazi is the southernmost, Sabaki the middle, and Kiwayu the northernmost transect.

drive the core tube into the sediment and a lid holding electrodes, strirrer and data memory subsequently closes the core tube. After deployment the instrument is detached from the ship and left to stand-alone. The device is recovered from the seafloor by the inflation of floatation 'parachutes'. The maximum operation depth of the 'bell-jars' is 120 m.

Finally, sediment oxygen consumption and nutrient fluxes were measured in incubated sediment cores on board the ship. Sediment cores (50 cm diameter) were taken with a box corer equipped with a valve to ensure retrieval of *in-situ* bottom water and undisturbed samples. On deck a 30 cm wide perspex chamber was inserted into the boxcore sample and sealed with a lid holding an electrode and stirrer. The entire arrangement was placed into a dark, thermostatted incubator for the duration of the measurements. Ensuing data from the electrodes were recorded on a PC. At regular time intervals small volumes were drawn from the headspace of the core for the assessment of nutrient fluxes.

At the 2000 m stations visited during the first cruise, incubation experiments were, for logistic reason, performed in 10 cm wide chambers, but otherwise always the 30 cm wide chambers were used. The smaller diameter and the more severe manipulation of the small chambers render the data less reliable and moreover do not allow measurement of nutrient fluxes.

results

Sediment oxygen consumption

Fig. 4.8.1 compares the sediment oxygen-fluxes at the major stations during both cruises. Both cruises produced a roughly similar pattern with respect to the respiration rates at 50 and 500 m stations, *viz.* lowest values at the southern Gazi transect and the highest ones at the northern Kiwayu transect. While in June intermediate rates were found at 50 and 500 m stations of the middle Sabaki transect, the November rates at the 50 m Sabaki station were more close to the 50 m Gazi values and concurrent rates at the 500 m station were the same as the 500 m Kiwayu values.

Only one 200 m station was sampled twice in both cruises, one off Sabaki. The one rate measured in June was halfway in between the ones at 50 and 500 m rate.

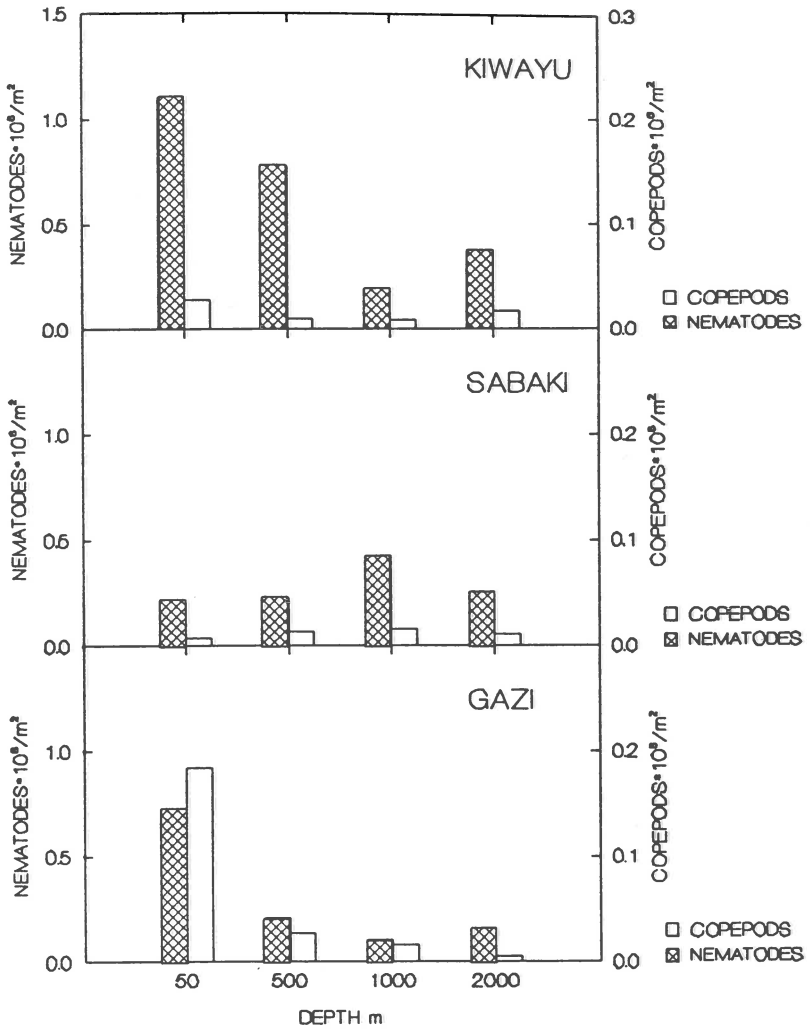

Fig. 4.8.2. Abundances of the principal meiofaunal taxa, *i.e.* nematodes and copepods, in the upper 5 cm of the sediment in June 1992 (NIOP-A1). Units along left- and righthand scale are millions per m^2.

The two November incubations yielded widely diverging values (185 and 590 µmol/m^2/h). The two boxes, however, did contain different sedimenttypes which are apparently patchy distributed along the shelfbreak. The 1000 m rates from June expose the same trend as the ones from shallower depths, *i.e.* an increase to the north. Because of reasons mentioned in the Method Section, the 2000 m values from June are less reliable, but they likewise show an increase towards the Kiwayu transect. In November, however, the differences between corresponding 1000 and 2000 m stations of all three transects are marginal.

Fig.4.8.1 does not show the June data from the stations near the Tana river (50 m and 200 m). Respiration rates at 50 m and 200 m Tana stations (995 and 590 µmol/m^2/h) equalled the ones found in June off Sabaki.

A marked result, particularly in the dataset of November, is the depressed respiration rate at the 1000 m stations in comparison to the 2000 m stations. It could be demonstrated that this difference was partly due to oxygen minimum present at 1000 m along the entire continental slope off Kenya. By raising the oxygen content in the headspace of the incubations enhanced uptake rates were obtained.

Nutrient fluxes

So far only the nutrient flux data from the June cruise have been processed. Both the silicate and nitrate efflux at depths of 50-500 m were highest off the river Sabaki. Fluxes along the southern Gazi and northernmost Kiwayu transect were of the same magnitude. Comparison between silicate fluxes measured on shipboard and the few *in-situ* data indicate that deck-incubations may produce a serious overestimate of the flux rate.

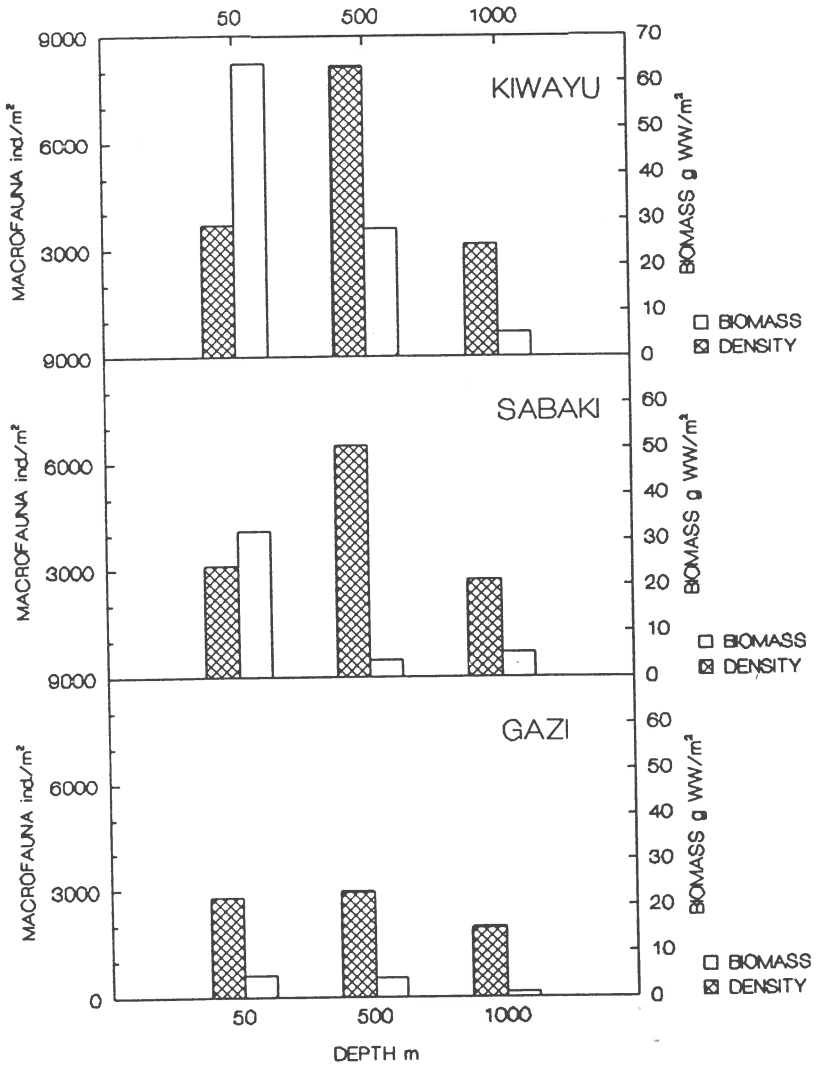

Fig. 4.8.3. Abundance and biomass distribution of macrofauna (> 0.5 mm) in June 1992 (NIOP-A1). Abundance is expressed in numbers of individuals per m^2; biomass in g Wet Weight per m^2.

Faunal analysis

Only samples taken in June for the meio- and macrofauna have been sorted and counted. The overall Nematode abundance (fig. 4.8.2) is highest at the northernmost transect while their density distribution closely reflects the pattern in respiratory activity of the sediment. Meiofaunal abundances along the Sabaki show in this respect a deviating pattern, with exceptionally low numbers at 50 m and comparatively high densities at 1000 m. At the southernmost Gazi the distribution pattern was again in line with sediment respiratory activity of the seabed. High densities, especially of copepods, were found at the shallow station and low densities deeper down.

Fig. 4.8.3 shows the abundance and biomass (wet weight) of the macrofauna at the 50-1000 m stations in June. The 2000 m samples have not been included because of the smaller size of the cores used. On average, biomass and abundance were highest on the northern Kiwayu transect and lowest on the southernmost Gazi transect. In contrast to biomass, which shows a decline with increasing depth, abundances seem to be highest at the 500 m stations.

Sediment phytopigments

Fig. 4.8.4 shows the distribution of chloroplastic pigments (chlorophyll-*a* + phaeopigments) in the top 1 cm of the sediment in June. Concentrations were lowest on the southern Gazi transect and highest on the northern Kiwayu transect. The share of chlorophyll-*a* in the sum of chloroplastic pigments was invariably maximal at the 50 m stations of each transect. There were, however, considerable differences among the 50 m stations. The 50 m station off the Sabaki had a markedly low percentage of chlorophyll-*a*, while at the 50 m station of the Kiwayu this percentage was

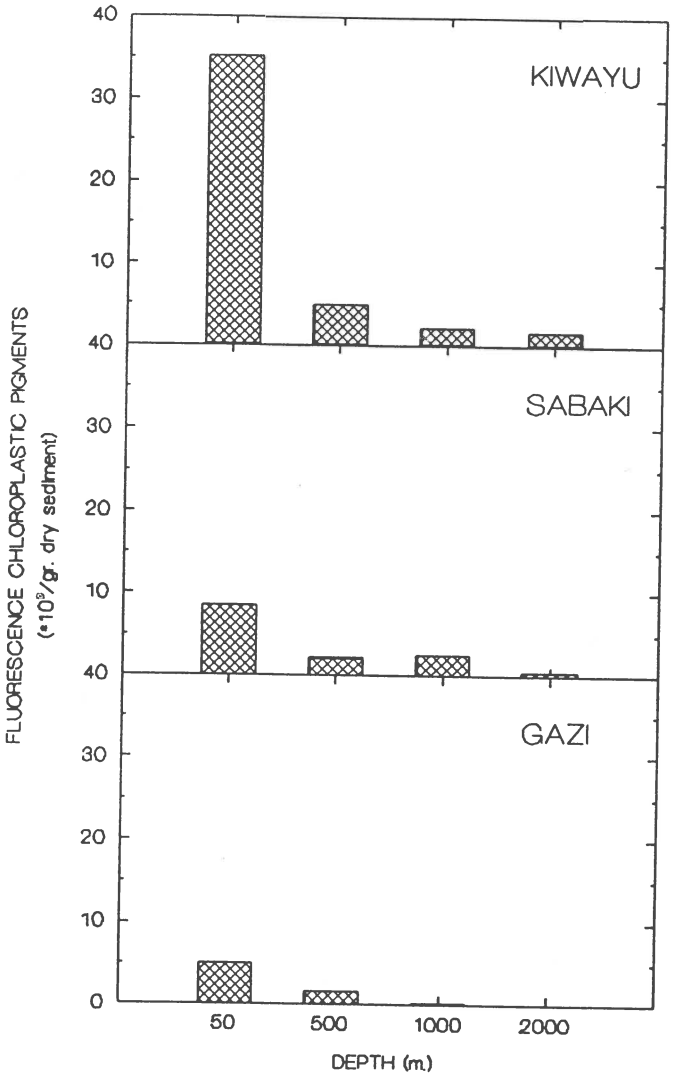

Fig. 4.8.4. Relative concentrations of chloroplastic pigments in the upper 1 cm of the sediment in June 1992 (NIOP-A1). Height of bars corresponds to the summed fluorescence of all chlorophyllous pigments and their derivatives.

extremely high. Below depths of 1000 m, chlorophyll-*a* could only be detected at the northern Kiwayu transect.

discussion

The available data from both cruises point at an enrichment of the benthic community at shallower depths (50 and 500 m) of the northern Kiwayu transect relative to the more southern ones. The respiration and phytopigment data from June indicate that also at greater depths, the northern transect receives a greater input of organic material. The respiration values from November, in contrast, did not reveal a substantial difference between the deeper stations of the transects. The fact that the gross pattern of benthic respiration remained constant during the period of investigation is not all that surprising since the current pattern along the coast had not yet changed in November as would have been the case with the onset of the NE Monsoon. This still leaves the differences between the transects to be accounted for. In view of the absence of rivers in the vicinity of the northern Kiwayu transect, the high benthic activity and standing stock on the northern transect is rather unexpected. One explanation could be that organic material and nutrients derived from the Sabaki and Tana flow close to the coast in northward direction, being the prevailing current direction in June and November. At the point where the continental shelf is narrowest, *i.e.* at the Kiwayu transect, the effect of this riverload may become apparent in the form of extra input of allochtonous organic material and/or enhanced primary production. At this stage, the

only evidence for extra input of terrestrial or coastal particulate material at the Kiwayu transect is the abundance of plant rhizomes in the box-core samples from 50 m. The high contents of chlorophyll-*a* in the Kiwayu sediments, on the other hand, strongly suggest that most of the phytodetritus is derived from local primary production. It is unlikely that algae produced near the southern rivers remain intact during transport. The high phaeophorbide content in the top 1 mm of the shallow Sabaki sediments, for instance, points at deposition of highly degraded detritus and thus high grazing pressure. Forthcoming data on deposition rates and carbon-isotopes in combination with primary production estimates (NIOO/CEMO, Yerseke) will hopefully shed light on the sources of the organic material at the three transects.

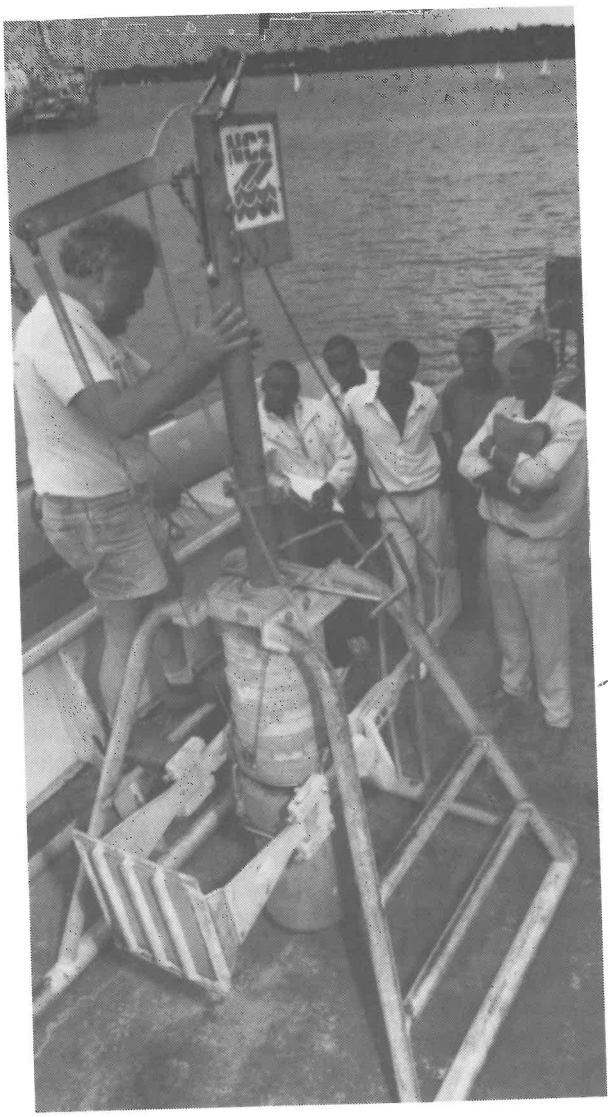

Before the cruise chief-technician Jack Schilling explains the operation of the box corer to Kenyan counterparts.

NETHERLANDS INDIAN OCEAN PROGRAMME

CRUISE REPORTS

CHIEF-EDITOR:
J. VAN DER LAND

Vol. 1:	Monsoons and Pelagic Systems *editor*: M.A. Baars ISBN 90-73239-24-9; 1994
Vol. 2:	Oceanic Reefs of the Seychelles *editor*: J. van der Land ISBN 90-73239-25-7; 1994
Vol. 3:	Geological Study of the Arabian Sea *editors*: W.J.M. van der Linden & C.H. van der Weijden ISBN 90-73239-26-5; 1994
Vol. 4:	Tracing a Seasonal Upwelling *editors*: J.E. van Hinte, S.R. Troelstra & Tj.C.E. van Weering ISBN 90-73239-27-3; 1995
Vol. 5:	Monsoons and Coastal Ecosystems in Kenya *editors*: C.H.R. Heip, M.A. Hemminga & M.J.M. de Bie ISBN 90-73239-28-1; 1995
Complete Set:	ISBN 90-73239-29-X

These cruise reports (each about 150 pp.) can be obtained from: The Librarian, National Museum of Natural History, P.O. Box 9517, 2300 RA Leiden, The Netherlands.
Prepayment of Dfl. 20,- (US$ 12) per volume is necessary by the following options.
Otherwise prices will be increased with Dfl. 10,- for accountfees.
I have deposited the required amount on:
❒ bankaccount nr. 45.12.21.907 of ABN-AMRO, stating 'Cruise Reports vol. x'.
Please charge my:
❒ American Express
❒ MasterCard
❒ Visa
Cardnr. Expiry Date

Date Signature